WATER ELECTROLYSIS SATELLITE PROPULSION SYSTEM

R. Carl Stechman, et al

Marquardt Company

Prepared for:

Air Force Rocket Propulsion Laboratory

January 1973

AFRPL-TR-72-132

WATER ELECTROLYSIS SATELLITE PROPULSION SYSTEM

R. C. Stechman Jr.
J. G. Campbell

THE MARQUARDT COMPANY
VAN NUYS, CALIFORNIA

TECHNICAL REPORT AFRPL-TR-72-132
JANUARY 1973

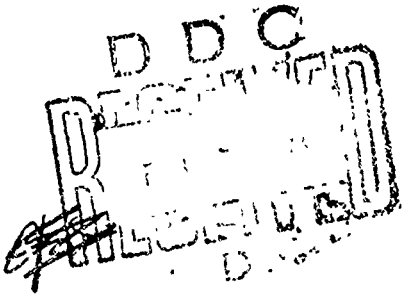

AIR FORCE ROCKET PROPULSION LABORATORY
AIR FORCE SYSTEMS COMMAND
EDWARDS AIR FORCE BASE, CALIFORNIA 93523

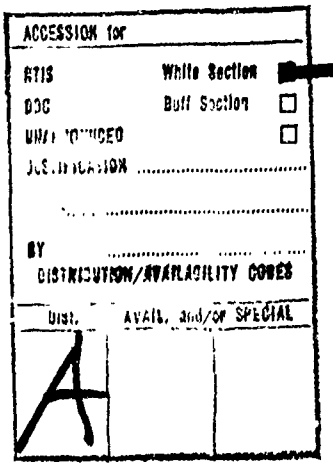

When U.S. Government drawings, specifications, or other data are used for any purpose other than a definitely related Government procurement operation, the Government thereby incurs no responsibility nor any obligation whatsoever, and the fact that the Government may have formulated, furnished, or in any way supplied the said drawings, specifications, or other data, is not to be regarded by implication or otherwise, or in any manner licensing the holder or any other person or corporation, or conveying any rights or permission to manufacture, use, or sell any patented invention that may in any way be related thereto.

UNCLASSIFIED
Security Classification

DOCUMENT CONTROL DATA - R & D

(Security classification of title, body of abstract and indexing annotation must be entered when the overall report is classified)

1. ORIGINATING ACTIVITY (Corporate author)	2a. REPORT SECURITY CLASSIFICATION
The Marquardt Company 16555 Saticoy Street Van Nuys, California 91409	UNCLASSIFIED 2b. GROUP

3. REPORT TITLE

Water Electrolysis Satellite Propulsion System

4. DESCRIPTIVE NOTES (Type of report and inclusive dates)

Final Report covering period July 1971 to October 1972

5. AUTHOR(S) (First name, middle initial, last name)

R. Carl Stechman, John G. Campbell

6. REPORT DATE	7a. TOTAL NO. OF PAGES	7b. NO. OF REFS
January 1973	242	4

8a. CONTRACT OR GRANT NO.	9a. ORIGINATOR'S REPORT NUMBER(S)
F04611-71-C-0055 b. PROJECT NO. 3058 c. d.	Marquardt Report S-1247 9b. OTHER REPORT NO(S) (Any other numbers that may be assigned this report) AFRPL-TR-72-132

10. DISTRIBUTION STATEMENT

Approved for Public Release: Distribution Unlimited

11. SUPPLEMENTARY NOTES	12. SPONSORING MILITARY ACTIVITY
	Air Force Rocket Propulsion Laboratory Edwards Air Force Base, California 93523

13. ABSTRACT

A water electrolysis satellite propulsion system capable of providng 100,000 pound-seconds of impulse during a seven year life was fabricated and tested in three modes of operation -- simple blowdown, helium repressurization and repressurization by oxygen in a feedback mode. The tests verified the systems predicted capabilities in all three modes at generation rates of 0 to 2.3 lbs/day of propellant, with an electrical energy conversion efficiency of up to 82%. 5.0 pound thrust and a 0.1 pound thrust GO_2/GH_2 engine were tested as separate components with measured specific impulses of 345 and 330 seconds, respectively, at a mixture ratio of 8. The 0.1 pound engine accumulated 14,330 seconds of burn time and 151,263 ignitions, while the 5 pound thrust engine attained 10,031 seconds of burn time and 69,700 ignitions. The demonstrated overall performance of the system and engines shows its applicability to satellite and spacecraft which require high performance, reliable operation, and long life capabilities.

DD FORM 1 NOV 68 1473

I

UNCLASSIFIED
Security Classification

14 KEY WORDS	LINK A		LINK B		LINK C	
	ROLE	WT	ROLE	WT	ROLE	WT
Water Electrolysis						
Satellite						
Rocket Engine						
Propulsion						
Oxygen						
Hydrogen						
System						
Electrical						
Mission Analysis						
3-Axis Stabilized						
Spin-Stabilized						

AFRPL-TR-72-132

WATER ELECTROLYSIS SATELLITE PROPULSION SYSTEM

R. C. Stechman Jr.
J. G. Campbell

THE MARQUARDT COMPANY
VAN NUYS, CALIFORNIA

TECHNICAL REPORT AFRPL-TR-72-132
JANUARY 1973

AIR FORCE ROCKET PROPULSION LABORATORY
AIR FORCE SYSTEMS COMMAND
EDWARDS AIR FORCE BASE, CALIFORNIA 93523

II b

FOREWORD

This is the final report submitted in fulfillment of Contract F04611-71-C-0055 with the Air Force Rocket Propulsion Laboratory. The Air Force Project Engineers were Paul C. Erickson and Melvin V. Rogers.

The contract effort was conducted by the engineering division under R. C. Stechman, Jr., Program Manager; J. G. Campbell, Project Engineer; and R. V. Loustau, Design Engineer. The Electrolysis Unit was supplied by the General Electric Company, Lynn, Massachusetts. A. Erickson and W. A. Titterington of General Electric were the principals concerned with the design and test of the subject unit.

The report has been prepared in accordance with MIL-STD-847 (USAF) dated 25 February 1965. The period of the report is July, 1971 through October, 1972.

This technical report has been reviewed and is approved.

Melvin V. Rogers
Project Engineer
AFRPL/LKDA

TABLE OF CONTENTS

LIST OF ILLUSTRATIONS

LIST OF ILLUSTRATIONS (CONTINUED)

LIST OF ILLUSTRATIONS (CONTINUED)

LIST OF TABLES

SECTION I

INTRODUCTION

The water electrolysis propulsion system shown conceptually in Figure 1 combines the desirable characteristics of inert propellant storage with high energy propellant combustion.

The system consists of an electrolysis unit, electrical power system, tankage and thrusters. Energy is supplied to the electrolysis unit from the satellite electrical power supply. The electrolysis unit converts the water to separated gases of hydrogen and oxygen which are then burned, as required, in the rocket engine thrusters. Separation of the generated gases avoids the flame propagation and detonation problems observed in previous mixed gas systems.[1] The gas generation rate can be matched to the mission requirements such that the power required at any point in time is minimized. The electrolysis unit also has the capability to generate gas at a higher rate for critical time constrained maneuvers such as orbit repositioning when additional power is available. The rocket engine's high specific impulse capabilities, along with the storability of water, hydrogen and oxygen make this system a prime candidate for satellite systems in the near future.

A program was conducted by Marquardt to develop a separated gas electrolysis system and two rocket engines in the thrust range applicable to satellites with 7 year life spans and 100,000 pound seconds of total impulse. Some of the significant anticipated advantages of the water electrolysis satellite propulsion system are:

- Lighter weight system due to high specific impulse and low impulse bit capability
- High reliability
- Non-toxic, non-corrosive propellants
- Lower average power consumption
- Multi-operational mode flexibility to accomplish various satellite mission propulsive requirements in the most efficient and effective manner.

In particular, the water electrolysis satellite propulsion system has significantly higher performance when compared to a monopropellant or earth storable

1. Rollbuhler, R. J., "Experimental Performance of a Water Electrolysis Rocket", NASA TMX-1737, February 1969.

bipropellant system. System weight studies of typical missions for both spin stabilized and 3 axes stabilized satellites show the advantages of the electrolysis system. For instance, a 3000 pound/10 year life satellite for a 3 axis stabilized system with north south station keeping results in a >1000 pound propulsion system with monopropellants, and 850 pounds using earth storable bipropellants while the water electrolysis system weight is less than 700 pounds. This weight advantage combined with all of its previously discussed characteristics makes this system a highly competitive candidate for future satellites.

Based on the weight and mission/system analysis, this program was conducted to:

a. Demonstrate the feasibility of a separated gas water electrolysis system

b. Develop 0.1 and 5.0 pound thrust rocket engines which would operate on the gaseous hydrogen and oxygen generated by the system.

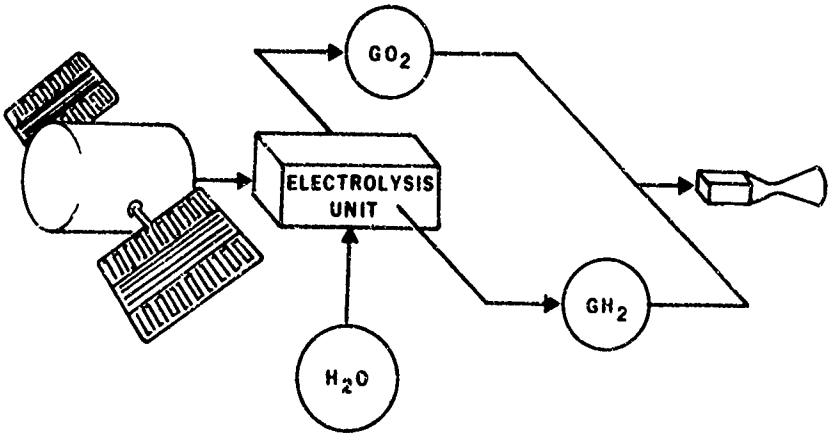

FIGURE 1. WATER ELECTROLYSIS SYSTEM PROPULSION CONCEPT

SECTION II

SUMMARY

A water electrolysis satellite propulsion system was designed, fabricated and tested to demonstrate its feasibility and capabilities to meet Air Force mission and system objectives. The system consists of a propellant supply system and two rocket engines of 0.1 and 5 pounds thrust.

The program conducted consisted of a mission and system analysis phase, design and fabrication phase, and a test program. At the conclusion of the test program a flightweight system was designed which exhibited no single point failure mode. A reliability analysis was also conducted in support of the flightweight system design.

1. MISSION SYSTEM ANALYSIS

The design of both the system and the engines was based on satisfying the basic criteria shown in Table 1.

Based on these requirements, a mission analysis was conducted which indicated the amount of propellant required, the engine duty cycles, and the average power requirements for the mission.

As shown in Table 2, the majority of the propellant is required for station keeping and the generation rate of gases is less than 0.1 pounds/day or about 16-20 watts of power. For repositioning and initial position and velocity, a generation rate of 2.3 pounds/day of gases (230 watts) was assumed. This rate was based on the capabilities of the electrolysis unit and obviously can be varied according to specific requirements. The total amount of water required for this point design mission is less than 300 pounds. These two tables provided the basis for the design concept which was evaluated.

2. PROPELLANT SUPPLY SYSTEM

The propellant supply system consists of a pressurized water tank, an electrolysis unit for separating water into gaseous hydrogen and oxygen, plenum tanks to store the generated gases until used by the rocket engines and the system controls.

a. Electrolysis Unit

The basic function of the electrolysis unit, supplied by the General Electric Company of Lynn, Massachusetts, is to separate water into gaseous hydrogen and gaseous oxygen with electrolysis by ion exchange and is the result of passing an electrical current through a plastic membrane which is saturated with water. The rate of electrolysis of water is proportional to the amount of electrical current.

TABLE 1

MISSION AND PROPULSION REQUIREMENTS

Criteria and Assumptions

ITEM		REQUIREMENTS	
		SPIN STABILIZED	3 AXES STABILIZED
Mission	ORBIT	24 Hour Synchronous Orbit	
	LIFE REQUIREMENT	7 Years	
	SPIN RATES	60 to 120 RPM	360° in 24 Hours
Propulsive Requirements	ATTITUDE CONTROL	±0.5°	±0.1°
	TIP-OFF RATE	Assumed Zero	1 Degree/second (All Axes)
	ΔV REQUIREMENTS Booster Injection Errors Repositioning Station Keeping Total	50 FPS 200 FPS 157 FPS/YR 1,400 FPS	
	TOTAL IMPULSE Attitude Control Total Mission	3,000 LBF-Sec. 100,000 LBF-Sec.	
	SPIN-UP	Assumed Accomplished Prior to Ejection from the Upper Stage by Other Propulsive Means	None Required
Configuration	MOMENT ARMS	3 Feet	
	Ixx Ixx Iyy Iyy Izz Izz	800 Slug-Ft.^{2} 650 Slug-Ft.^{2} 350 Slug-Ft.^{2}	
	POWER REQUIREMENTS On-Orbit Operation Orbit Correction and Repositioning	100 Watts Probably Higher than 100 Watts	

TABLE 2

POINT DESIGN MISSION REQUIREMENTS

Maneuver or Mission Event	RFQ Requirement	Satellite Weight (lbs.)	Operational Mode	Time	Electrolysis Power (Watts)	Total Impulse (lb.-sec.)	Est. Avg. Specific Impulse (sec.)	Required Propellants (lbs.)
Booster Injection Errors • Tip-off Rate	1.0 Degree/sec. (in all Axes)	2460	Blowdown (Generated Prior to Launch)	26 min.	0	10 - 12	320	0.035
• Position & Velocity	ΔV = 50 fps	2420	Blowdown (Generated After Launch at a Rate of 2.3 lbm/day)	5 days	220	3,000	350	19.9
Station-Keeping	ΔV = 157 fps/yr. E-W/N-S In. ≥ 8.9 x 15 NM Ellipsoid	2290 (Avg.)	Generated as Required (Avg. Requirement ≈ 0.08 lbm/day)	7 years	10	78,000	346	231.9
Attitude Control Requirements	I_p = 3000 lb.-sec. Spin: ±0.5° D.B. 3 Axes: ±0.1° D.B.	2290 (Avg.)	Generated as Required (Avg. Requirement 0.0037 lbm/day)	7 years	10	3,000	275	30.9
Repositioning	ΔV = 200 fps	2290	Repeated Blowdown (Generated at a Rate of 2.3 lbm/day)	16 days	220	14,300	350	40.9
Contingency		2290	Generated as Required	As Required	10	300	320	1.22
TOTALS	ΔV = 1400 fps					100,000	330 (Avg.)	294.85

The plastic membrane acts as a solid polymer electrolyte (SPE) without requiring any other electrolytic agent such as acid or alkaline fluids. Figure 2 shows the electrolysis process as pertains to the unit tested in this program, while Figure 3 is a schematic diagram of the physical construction of a single electrolysis cell.

Figure 4 shows the 6 cell electrolysis unit fabricated and tested during this program. Table 3 shows the basic characteristics of the unit while Figure 5 shows the power required to electrolyze various amounts of water. A single cell unit similar to the 6 cell system accumulated nearly 4000 hours of testing during the program.

TABLE 3. ELECTROLYSIS CELL CHARACTERISTICS

Design Parameter	Design Data
Number of Cells	6
High H_2O Rate (maximum)	2.3 lbs H_2O day
Low H_2O Rate (adjustable)	0.1 to 0.6 lb H_2O/day
Cell Stack Characteristics @70°F Mean Temperature	
Stack Current	22 amps
Stack Voltage	10.7 VDC
Stack Input Power @2.3 lb H_2O/day	235 watts
Stack Heat Loss	44 watts
Current Density	100 Amps/ft^2

b. Feed System

The propellant supply system fabricated is designed to operate in three modes of water pressurization; i.e., simple blowdown, repressurized blowdown or oxygen pressurized blowdown. The system shown in Figure 6 is assembled on a frame structure and has many valves and alternate flow paths provided for ground testing.

c. System Tests

Tests were conducted on the system to determine its characteristics and performance during various modes of operation. During the test sequence the water pressure and system power was varied while the system was subjected to both standby and propellant blowdown operations. Power input to the system varied from zero to 255 watts while the tank pressure was varied between 225 and 254 psia. All subsystems operated in a normal manner.

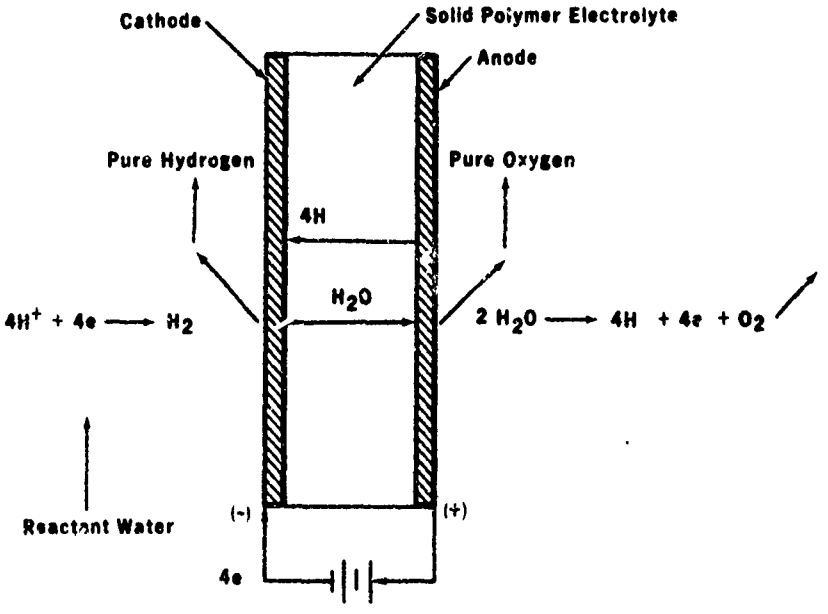

FIGURE 2. ELECTROLYSIS PROCESS

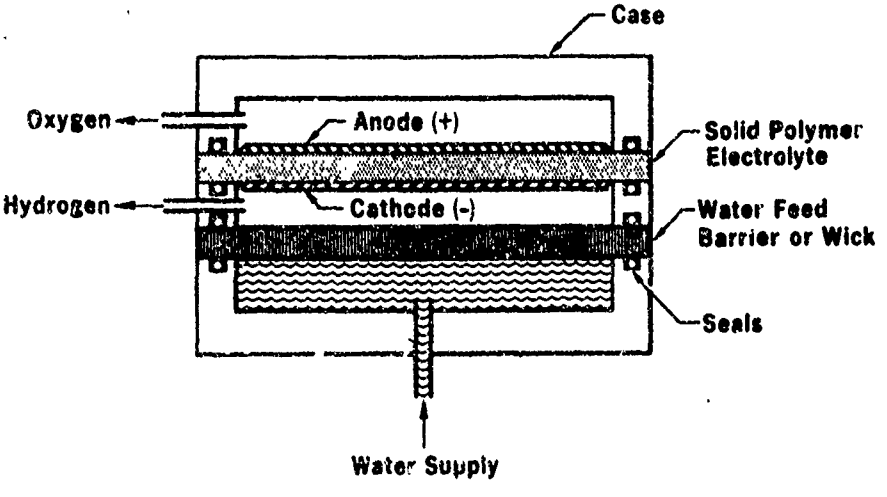

FIGURE 3. WATER ELECTROLYSIS CELL SCHEMATIC

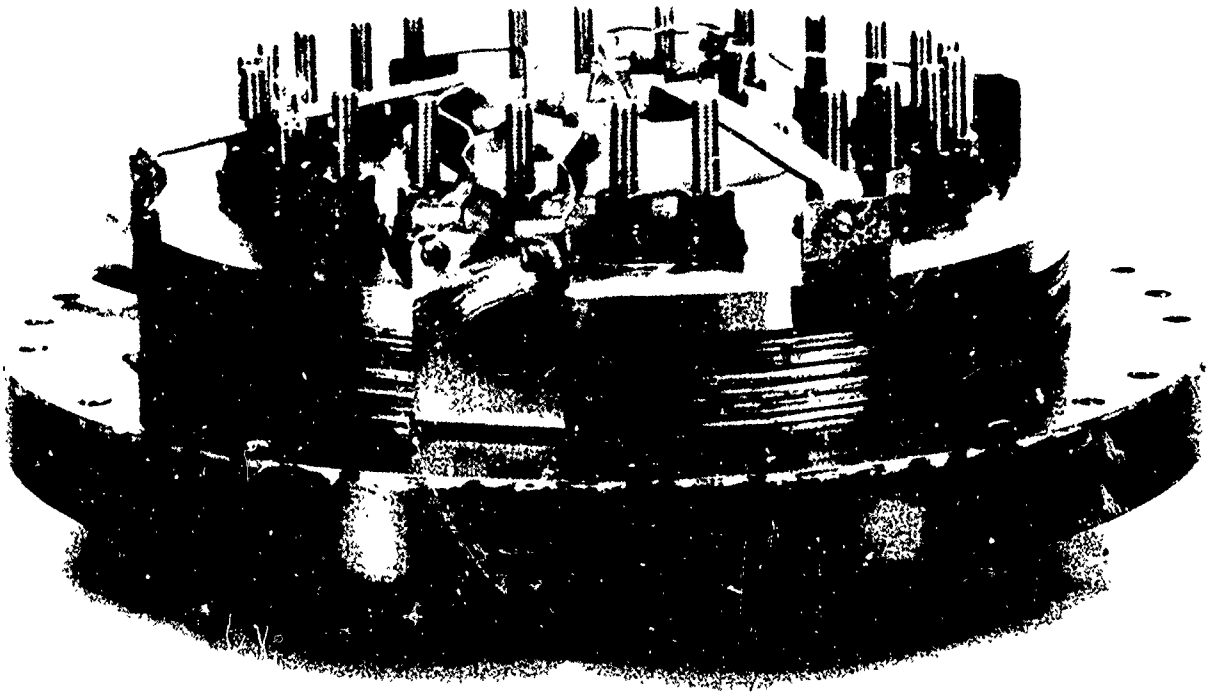

FIGURE 4. SIX CELL ELECTROLYSIS UNIT

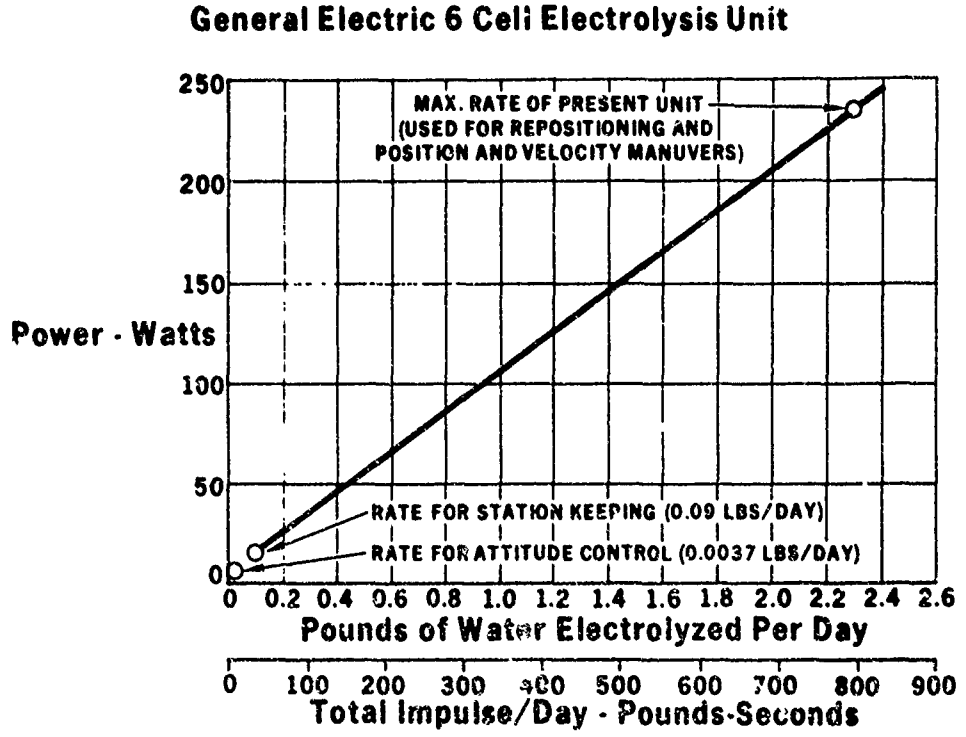

FIGURE 5. POWER REQUIREMENTS

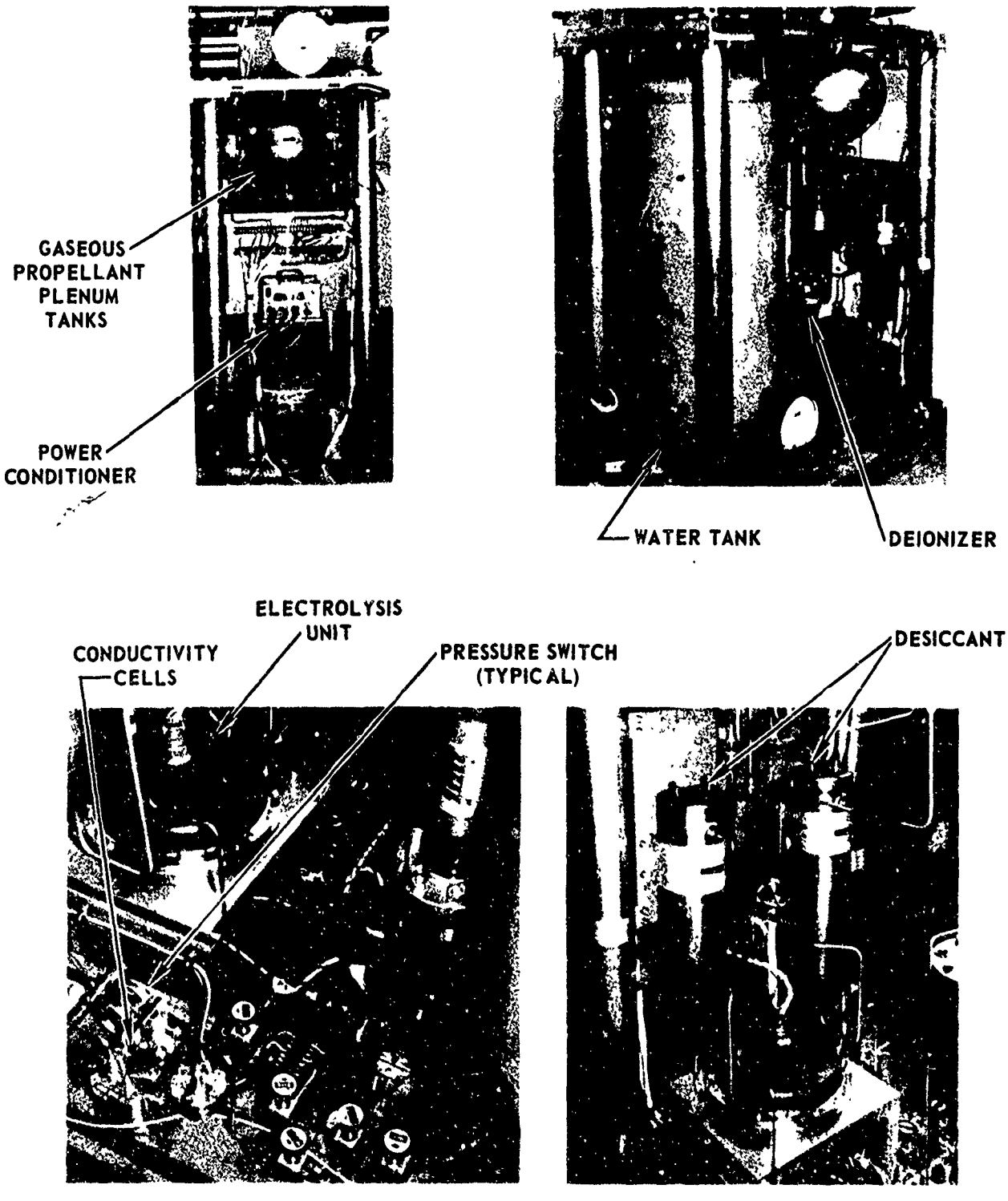

FIGURE 6. WATER ELECTROLYSIS FEED SYSTEM

3. ROCKET ENGINES (Thrusters)

Two rocket engines which are capable of being utilized with the water electrolysis satellite feed system were developed. The design criteria for the engines were based on mission/system studies and are thus applicable to both spin stabilized and 3-axis stabilized systems. The goal of the development program undertaken was to provide the basic design criteria for flightweight engines and to verify the performance and reliability estimates which have been previously proposed. The two thrust ranges chosen - 0.10 and 5.0 pounds - are representative of engines which are used or will be used in satellites.

The thrusters operate directly off the H_2 and O_2 storage tanks in a blowdown mode of operation and are sized to burn at a mixture ratio of 8. (The exact mixture ratio is 7.934 based on the electrolysis of water into 2 moles of H_2 and one mole of oxygen.) Sonic orifices located just upstream of the propellant valves are used to meter the flow to the thrusters and minimize the system/engine dynamic interaction. Variations in system temperatures and inaccuracies in orificing are automatically compensated for in the system by a minor variation in storage tank pressure between the H_2 and O_2 tanks.

The 0.1-pound and 5.0-pound thrust rocket engines are designed to operate using up to 100 percent water saturated GO_2 and GH_2 which is delivered from the electrolysis system and both are ignited by capacitance spark discharge. Both engines were basically boilerplate in design but certain aspects were to eventually approach that of a prototype or flightweight version.

a. 5-Pound Thruster

The 5-pound thrust engine shown on Figure 7 is composed of two high response Marquardt R-4D coaxial solenoid valves (identical to those used in the Apollo SM/RCS and LM/RCS engines), a nickel 6 element premix injector with integral H_2 film cooling for the combustor. The combustion chamber and exit nozzle is constructed of $MoSi_2$ coated molybdenum.

A modified Champion FHE 231 spark plug is located in the center of the injector face. The valves are thermally isolated from the combustion chamber and injector by the use of thin tube and structural membrane.

b. 0.1-Pound Thruster

The basic design of the 0.1-pound thruster is essentially identical to that of a 5.0-pound thruster, but due to its small size specific design characteristics have been incorporated which result in an efficient and responsive system at some sacrifice in weight. The engine shown in Figure 8 (less valves) is boilerplate in design except for the molybdenum combustor.

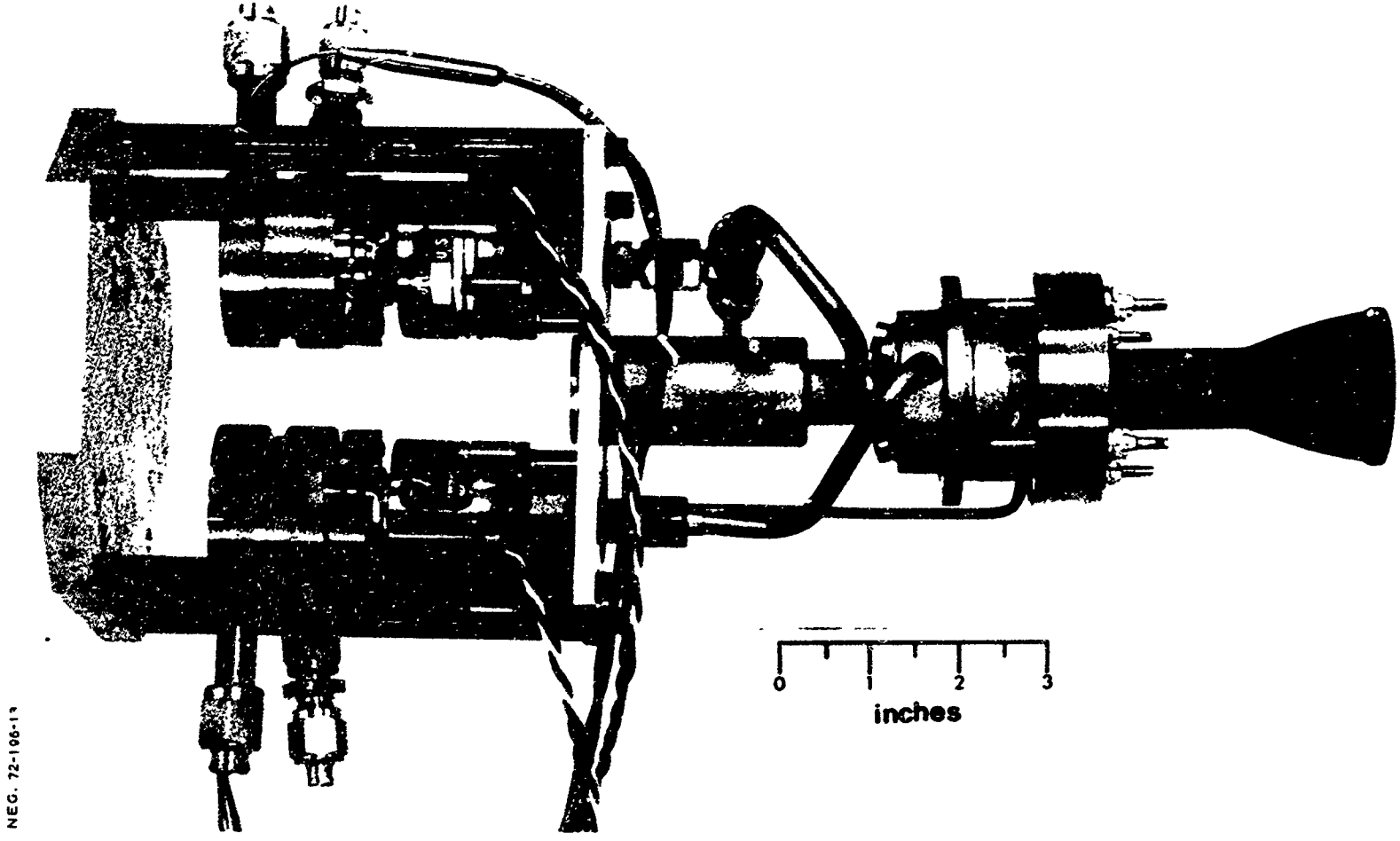

FIGURE 55. 5 LB_f THRUSTER PRIOR TO INITIAL TESTS

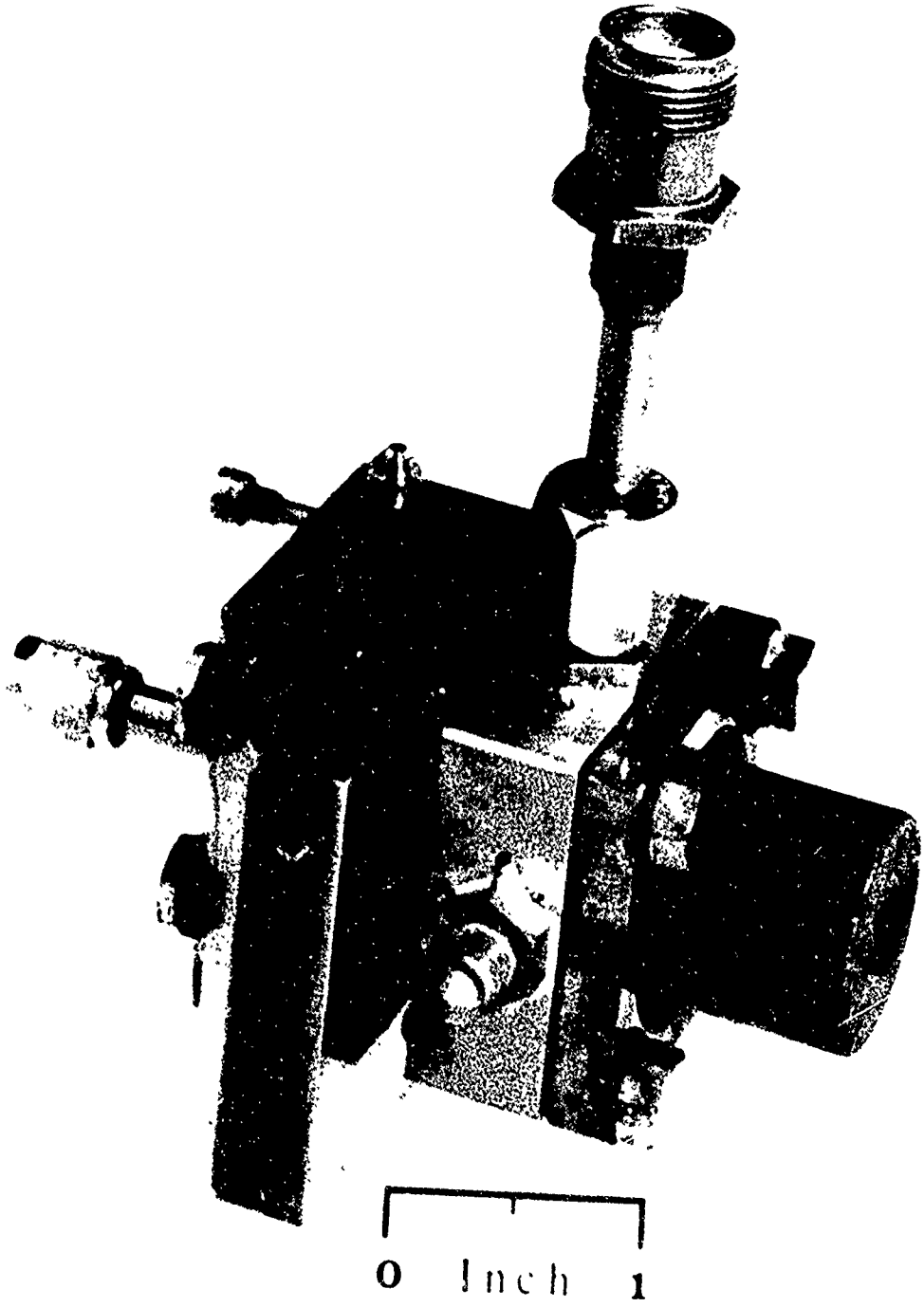

NEG. 72-230-11

FIGURE 8. 0.1 LB_f GO_2/GH_2 ROCKET ENGINE (THRUSTER)

c. Igniter Characteristics

A capacitive discharge igniter control system for spark plug excitation (Figure 9) consists of an Igniter Control Unit (ICU) with its high voltage cable assembly and the power input cable. The ICU can be adjusted for variable spark delay and delivers 50 or 100 millijoules per spark at 28 volts dc. The system (less cable) weighed less than 10 oz. even though the system is boilerplate in nature.

d. Test Program

A series of tests were conducted on both engines to demonstrate the life and performance characteristics of the design under both pulsing and steady state conditions. Table 4 shows the duty cycles and test program for each engine which was designed to demonstrate each engine's capabilities. The results of the tests are shown in Table 5 where, as shown, nearly all requirements were met.

Figures 10, 11, and 12 show the specific impulse of the 5 lbf and 0.1 lbf engines as a function of electrical pulse width, thrust, and percent fuel film cooling.

The specific impulse of 345 seconds at steady state for the 5 lb thrust engine is 1.5% below the design goal and the pulsing performance at 50 ms is 5% better than the design goal. Termination of the 5 pound thrust engine tests after nearly 70,000 cycles of the 75,000 cycle goal was caused by an injector premix orifice weld failure and subsequent combustor erosion due to interaction of the melted nickel with the coating of the combustor.

The specific impulse of 325-330 seconds at steady state for the 0.1 lbf engine is ~10% better than the design goal of 300 seconds. The 0.1 lb engine completed the programmed test series with no significant anomalies.

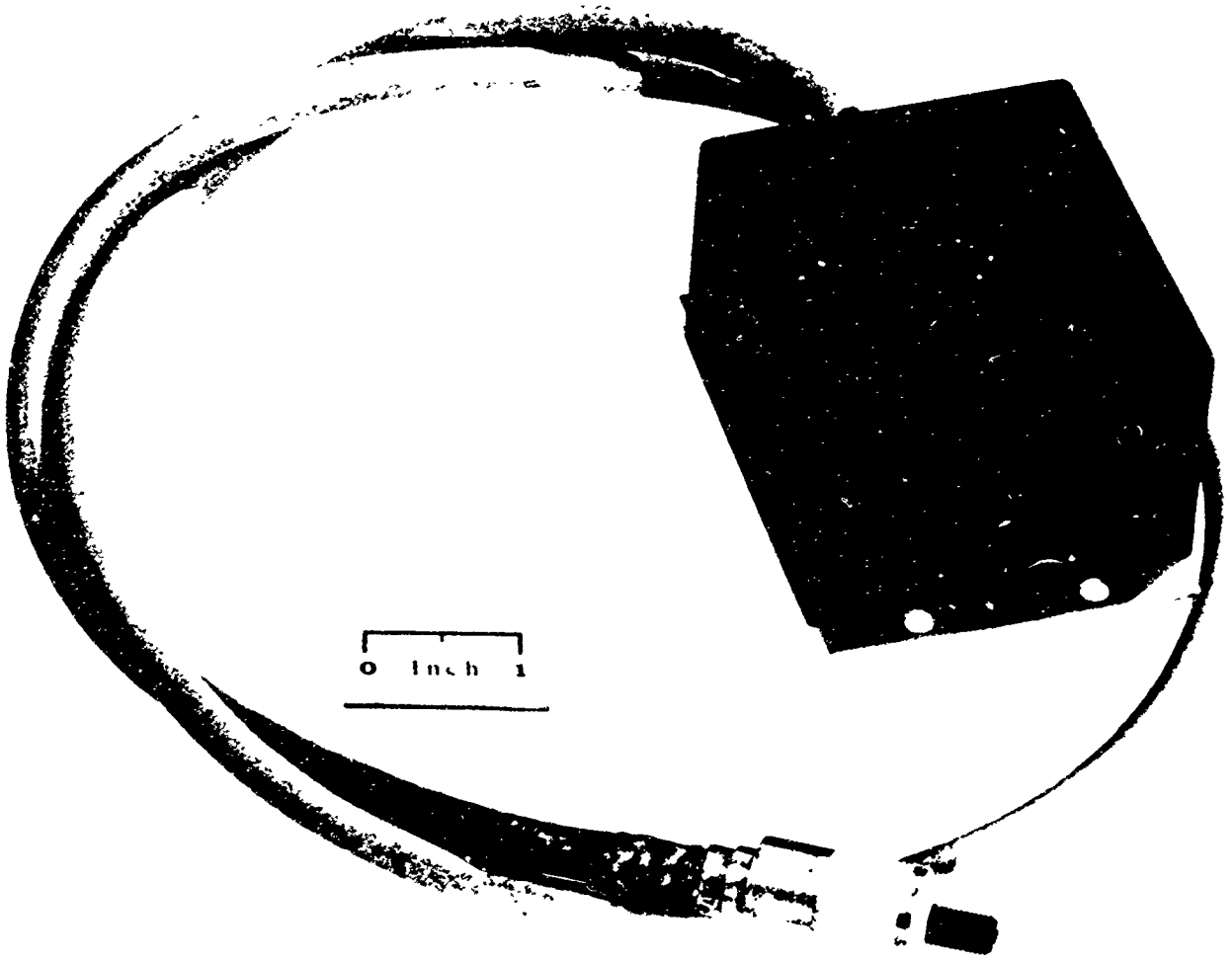

NEG 72-196-14

FIGURE 9. IGNITER CONTROL SYSTEM

TABLE 4 TEST PROGRAM

5.0 LB. THRUST ENGINE	
SEQUENCE	DUTY CYCLE
ENGINE CHARACTERIZATION	0.020 SEC. TO STEADY STATE INLET PRESSURES--200 TO 70 PSIA
DUTY CYCLE TESTS	25 PULSE TESTS AT 1000 PULSES/TEST AT EACH OF THE FOLLOWING CONDITIONS: ON TIME(SEC) OFF TIME(SEC) 0.050 0.450 0.100 0.900 0.250 0.750
STEADY STATE BLOWDOWN	50 CYCLES
0.1 LB. THRUST ENGINE	
ENGINE CHARACTERIZATION	0.012 SEC. TO STEADY STATE INLET PRESSURES--200 TO 70 PSIA
DUTY CYCLE TESTS	1000 0.020 SEC. FIRINGS AT 1 PULSE/MIN. 150000 0.020 SEC. PULSES AT 2 HZ.
STEADY STATE THERMAL TESTS	50 STEADY STATE FIRINGS

TABLE 5 TEST RESULTS SUMMARY

THRUST (POUNDS)	5.0	0.1
CHAMBER PRESSURE (PSIA)	50	80
SPECIFIC IMPULSE (SEC.)	345 at 40:1	330 at 100:1
MINIMUM PULSE WIDTH DEMON.	0.020 SEC.	0 012 SEC.
IGNITIONS DEMONSTRATED	69,700	151,263
BURN TIME DEMONSTRATED	10,031 SEC.	14,320 SEC.

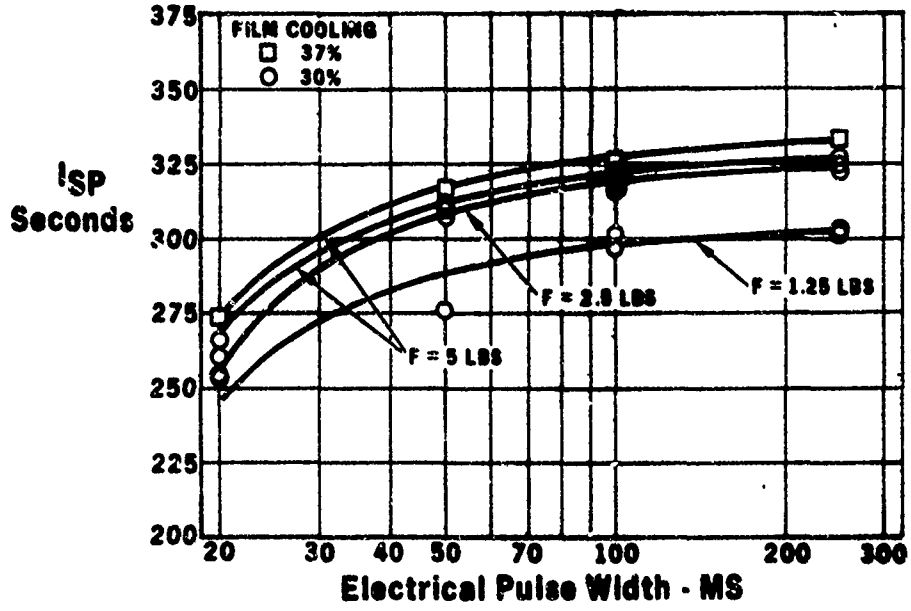

FIGURE 10. SPECIFIC IMPULSE VS ELECTRICAL PULSE WIDTH AT O/F = 8, 5LB$_f$ THRUSTER

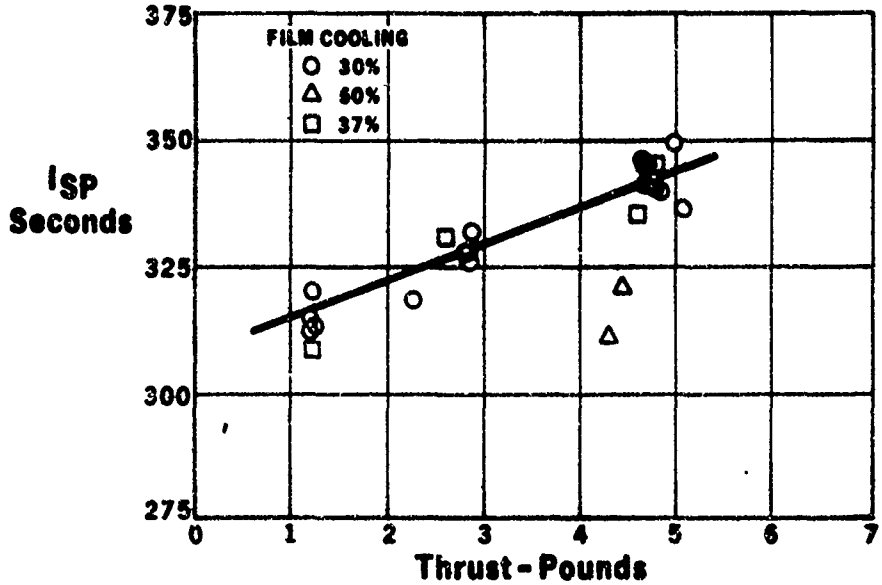

FIGURE 11. SPECIFIC IMPULSE VS THRUST AT O/F = 8, 5 LB$_f$ THRUSTER

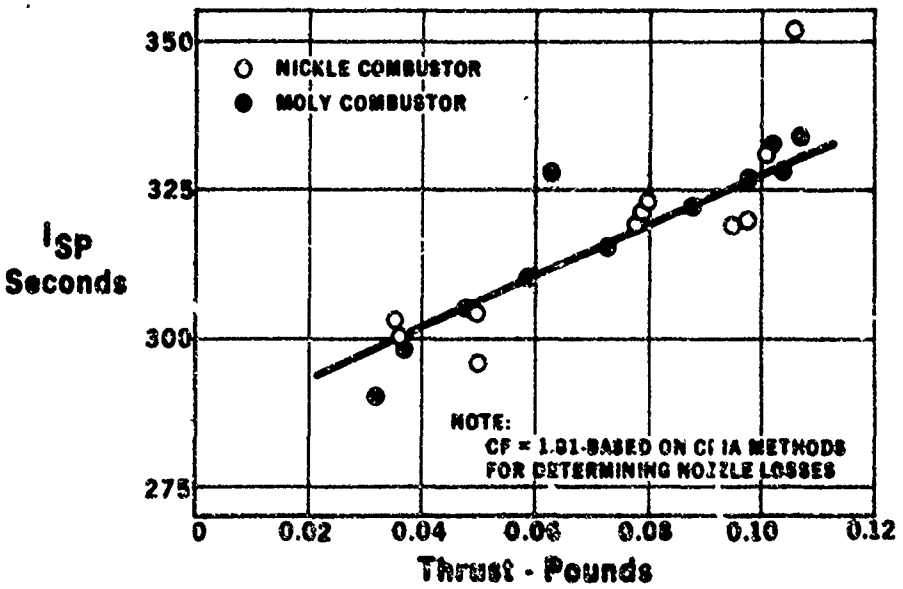

FIGURE 12. SPECIFIC IMPULSE VS THRUST AT O/F =8, 0.1 LB$_f$ THRUSTER

5. SUMMARY OF CONCLUSIONS

The results of the Water Electrolysis Satellite Propulsion System program have shown that a separated gas electrolysis system which generates propellant for gaseous oxygen/gaseous hydrogen rocket engines will result in a satellite propulsion system which is characterized by:

1. A high specific impulse (up to 350 seconds) and low impulse bit capability (4×10^{-5} lb-sec demonstrated).

2. An ability to provide a wide range of impulse rates and thrust levels at low power consumption rates as demonstrated by the system tests conducted at propellant generation rates from 0.1 to 2.3 pounds/day.

SECTION III

MISSION/SYSTEM ANALYSIS

An analysis of the mission requirements is presented in Table 6 to determine point design criteria for the system. Since the water electrolysis sytem is constrained by the available power (the unit can generate about one pound of propellant per day/ 100 watts of power), the determination of the impulse profile for the mission is a key factor in determining the optimum propulsion system approach.

Primary mission events and maneuvers were analyzed for both 3-axis and spin-stabilized satellites. Alternate methods for the conduct of critical maneuvers were investigated and the trade-off impact of these alternates on the mission, vehicle, and propulsion system design were evaluated. The propulsion requirements of both of these missions were subsequently overlayed to establish the composite point design propulsion system requirements. In defining the point design requirements, prime consideration was given to the following factors.

- The system must be capable of being used in either a spin-stabilized or a 3-axes stabilized system.
- The system must have the inherent flexibility to provide alternate modes of accomplishing the various mission events or maneuvers.
- The system should have the inherent flexibility and growth capability to provide for a wide spectrum of mission requirements (i.e., increased total impulse, smaller impulse bits, variable generation rates, etc).
- The system should have the capability to operate at off-design and safety margin conditions.

The analyses presented herein are based upon the gross criteria and assumptions defined in Table 6 . Of particular importance are such factors as time constraints for specific mission events, or the orbit injection techniques (i.e., is the satellite spun up prior to ejection from the upper stage). These factors, as well as significant change in the satellite configuration (moment of inertia, moment arms) could result in modification of the selected point design requirements. However, since the assumptions used herein are based upon previous application approaches and studies, such modifications should be minor and serve as a competent baseline for subsequent iterations.

TABLE 6. MISSION REQUIREMENTS

ITEM		REQUIREMENTS	
		SPIN STABILIZED	3 AXES STABILIZED
Mission	ORBIT	24 Hour Synchronous Orbit	
	LIFE REQUIREMENT	7 Years	
	SPIN RATES	60 to 120 RPM	360° in 24 Hours
Propulsive Requirements	ATTITUDE CONTROL	±0.5°	±0.1°
	TIP-OFF RATE	Assumed Zero	1 Degree/second(All Axes)
	ΔV REQUIREMENTS Booster Injection Errors Repositioning Station Keeping Total	50 FPS 200 FPS 157 FPS/YR 1,400 FPS	
	TOTAL IMPULSE Attitude Control Total Mission	2,000 LBF-Sec. 100,000 LBF-Sec.	
	SPIN-UP	Assumed Accomplished Prior to Ejection from the Upper Stage by Other Propulsive Means	None Required
Configuration	MOMENT ARMS	3 Feet	
	Ixx Ixx Iyy Iyy Izz Izz	800 Slug-Ft.^{2} 800 Slug-Ft.^{2} 350 Slug-Ft.^{2}	
	POWER REQUIREMENTS On-Orbit Operation Orbit Correction and Repositioning	100 Watts Probably Higher than 100 Watts	

TABLE 7. POINT DESIGN MISSION REQUIREMENTS

Maneuver or Mission Event	RFQ Requirement	Satellite Weight (lbs.)	Operational Mode	Time	Electrolysis Power (Watts)	Total Impulse (lb.-sec.)	Est. Avg. Specific Impulse (sec.)	Required Propellants (lbs.)
Booster Injection Errors • Tip-off Rate	1.0 Degree/sec. (in all Axes)	2400	Blowdown (Generated Prior to Launch)	20 min.	0	10 - 12	320	0.035
• Position & Velocity	ΔV = 50 fps	2400	Blowdown (Generated After Launch at a Rate of 2.3 lbm/day)	5 days	220	3,000	360	10.9
Station - Keeping	ΔV = 157 fps/yr. E - W/N - S in. ≥ 0.9 x 15 NM Ellipsoid	2290 (Avg.)	Generated as Required (Avg. Requirement ≃ 0.00 lbm/day)	7 years	18	78,500	340	231.0
Attitude Control Requirements	I_z = 2000 lb. - sec. Spin: ±0.5° D.B. 3 Axes: ±0.1° D.B.	2290 (Avg.)	Generated as Required (Avg. Requirement: 0.0037 lbm/day)	7 years	12	2,000	275	10.9
Repositioning	ΔV = 200 fps	2290	Repeated Blowdown (Generated at a Rate of 2.3 lbm/day)	15 days	220	14,300	340	40.5
Contingency		2290	Generated as Requi	As Required	18	300	320	1.22
TOTALS	ΔV = 1400 fps					100,000	320 (Avg.)	294.65

1. 3-AXES STABILIZED MISSION

The primary factors and options that were considered in accomplishing the required maneuvers for the 3-axes stabilized mission are as follows:

a. Booster Injection Errors (Tip-Off Rate)

Cancellation of the tip-off rate of 1°/sec in all axes is normally a time-critical maneuver, since precise tracking and status assessment of the satellite must be effectively accomplished as soon as possible. Also, position and velocity correction of the satellite cannot be made until this tip-off rate is cancelled and the satellite stabilized. Because of this time constraint, the system should be designed to have sufficient propellant generated and stored prior to launch for immediate accomplishment of this maneuver. The relatively small amount of total impulse required for this maneuver does not have any significant impact on system weight or design.

b. Booster Injection Error (Position and Velocity Errors)

Since a relatively large total impulse (i.e., ≈ 3800 lbf-sec) is required for this maneuver, there are several basic options for accomplishing it.

- Generate and store the required propellant for this maneuver prior to launch. Figure 13 shows the required gaseous propellant volumes required for this approach as a function of storage pressure. For any reasonable storage volumes, extremely high pressure storage would be required with a significant weight penalty and safety considerations occurring as well as increased development risk.

- Generate the propellant in orbit. Figure 13 shows the required generation time as a function of input power available. If the constraint of 100 watts of power is imposed, the fastest this maneuver could be accomplished is 10 days. However, as is very likely, additional power would probably be available from other nonoperating satellite systems during this phase of the mission and, therefore, this maneuver could be accomplished in significantly shorter time periods.

The final selected approach for individual systems will involve the trade-off of such primary factors as:

- Power available
- Effect of maneuver time on mission time constraints, objectives and cost effectiveness
- Criticality of system weight and volume.

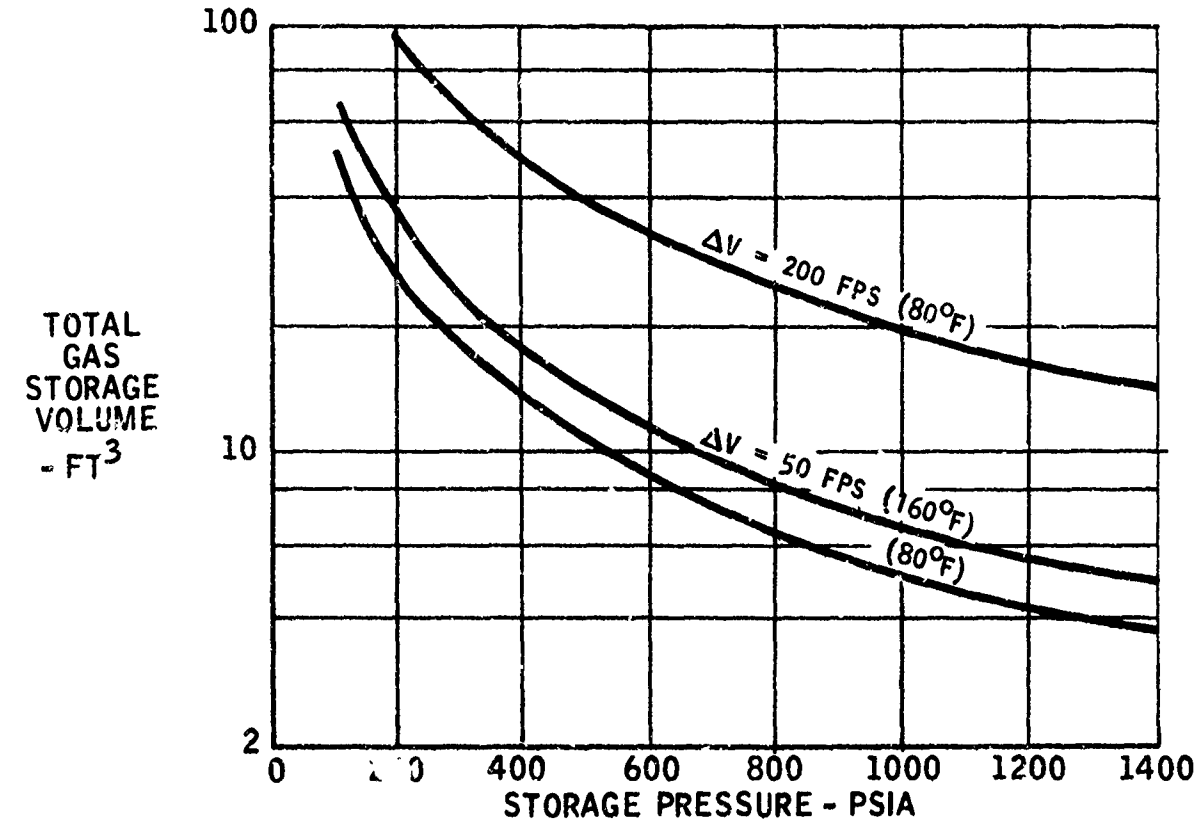

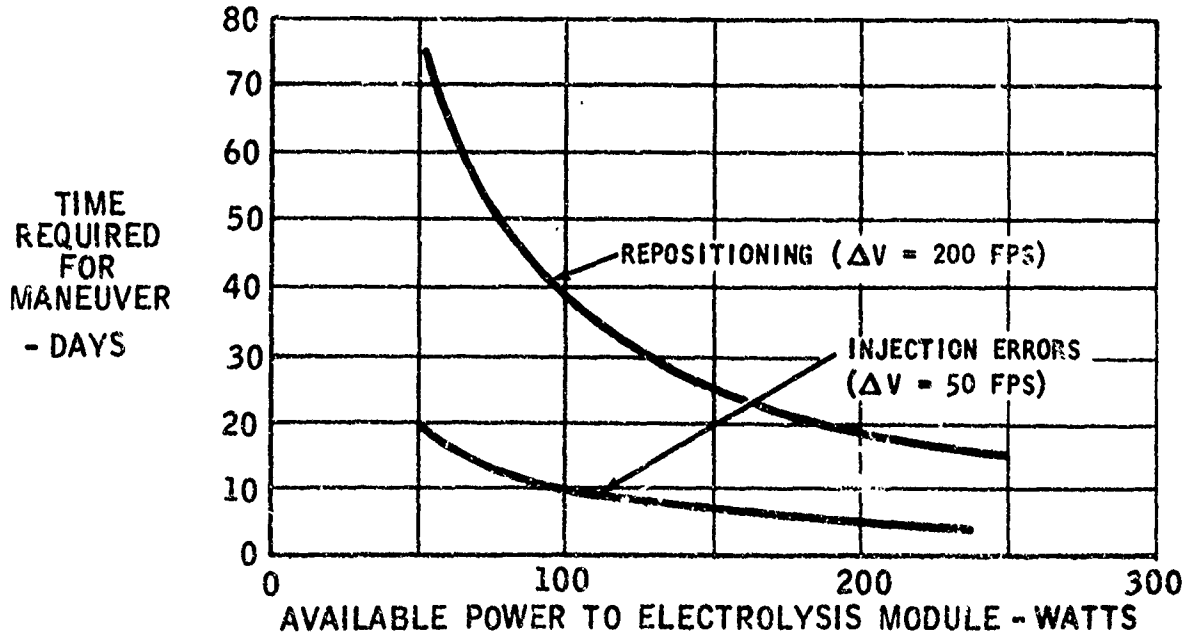

FIGURE 13. ELECTROLYSIS SYSTEM DESIGN CHARACTERISTICS

The optimum approach will probably involve a combination of the above options and will vary for specific missions.

c. Station-Keeping

The predominant requirement for station-keeping impulse is for cross-track ΔV corrections, with subsequent minimal requirements for in-plane ΔV, cross-track coupling, and in-plane coupling. The total ΔV requirement of 157 fps per year results in an average generation rate of approximately 0.09 lbm/day being required even for the worst case conditions.

d. Repositioning

The ΔV requirement of 200 fps requires a large total impulse ($\approx$ 14,300 lb-sec). Conduct of this maneuver in a single continuous burn is not practical since either of the following concepts results in unrealistic system requirements.

(1) Continuous generation of propellants by the electrolysis module for the continuous burn would require approximately 120 kilowatts of power.

(2) Storage of the required propellant (by operating the electrolysis module over a long period at a higher generation rate than required for station-keeping and attitude control and accumulating the residuals) results in extremely large storage and high pressure requirements. Per Figure 13, over 20 ft^3 would be required at a storage pressure of 1000 psia.

Figure 13 shows the required maneuver time as a function of power available to the electrolysis module. If the constraint of 100 watts of power is imposed, the fastest repositioning time would be approximately 37 days. However, since additional power would probably be available from other nonoperating systems during this phase of the mission, significantly shorter repositioning times would be required.

e. Attitude Control

Attitude control comprises limit cycle control requirements provides an interesting insight into the many interrelationships and variables involved. For the purposes of this analysis, it is assumed that mission and vehicle factors (moment of inertias, moment arms, required limit-cycle dead-bands, satellite weight, nature and magnitude of disturbance torques, etc.) are fixed and consistent with the basic criteria of Table 6, so that the primary trade-offs involving the propulsion system can be evaluated. Of primary importance from limit cycle operation is the minimum impulse bit that is achievable and this is dependent on such factors as:

- Thrust level
- Mode of operation

  Hot gas
  Cold gas (both propellants)
  Cold gas (GO_2 only)
  Cold gas (GH_2 only)

- Number of thrusters operating (for this study, it is assumed that they were operated in a coupled mode)
- Thruster on-time.

Figure 14 presents a plot of impulse bit as a function of valve open time for various modes of operation for both the 5-lbf and 0.1-lbf thruster. Valve open time (VϕT) is the time that propellants are following through the thruster and is define as:

VϕT = (Electrical Pulse Width) - (Valve Opening Time) + (Valve Closing Time)

The data is presented in this manner to provide for a direct comparison without being complicated by the difference in response time for various candidate valves.

The minimum impulse bit to be used for limit-cycle operation has a very significant effect on the total impulse, propellant, and valve cycle requirements for the mission. Provided that the minimum impulse bit is adequately above that required for the minimum angular rate limit, the lower the minimum impulse bit requirement, the lower the total impulse propellant and valve cycles, as shown on the following figures.

(1) Total Mission Impulse Requirements (Figure 15)

An impulse bit of 0.0012 lbf-sec or less will be required to maintain the total mission attitude control impulse below 3000 lbf-sec. (It should be noted that the impulse bit requirement will be even lower if the total impulse requirement of 3000 lbf-sec includes that required for such factors as solar pressure disturbance torque correction.)

(2) Total Mission Starts (Figure 16)

Since the reliability of the thrusters is a primary function of the number of starts required, it is imperative that required number of starts be restricted to the minimum possible. As shown, the combined total mission starts for all thrusters for limit-cycle operation is a reasonable 260,000 if the impulse bit is 0.0012 lbf-sec or less.

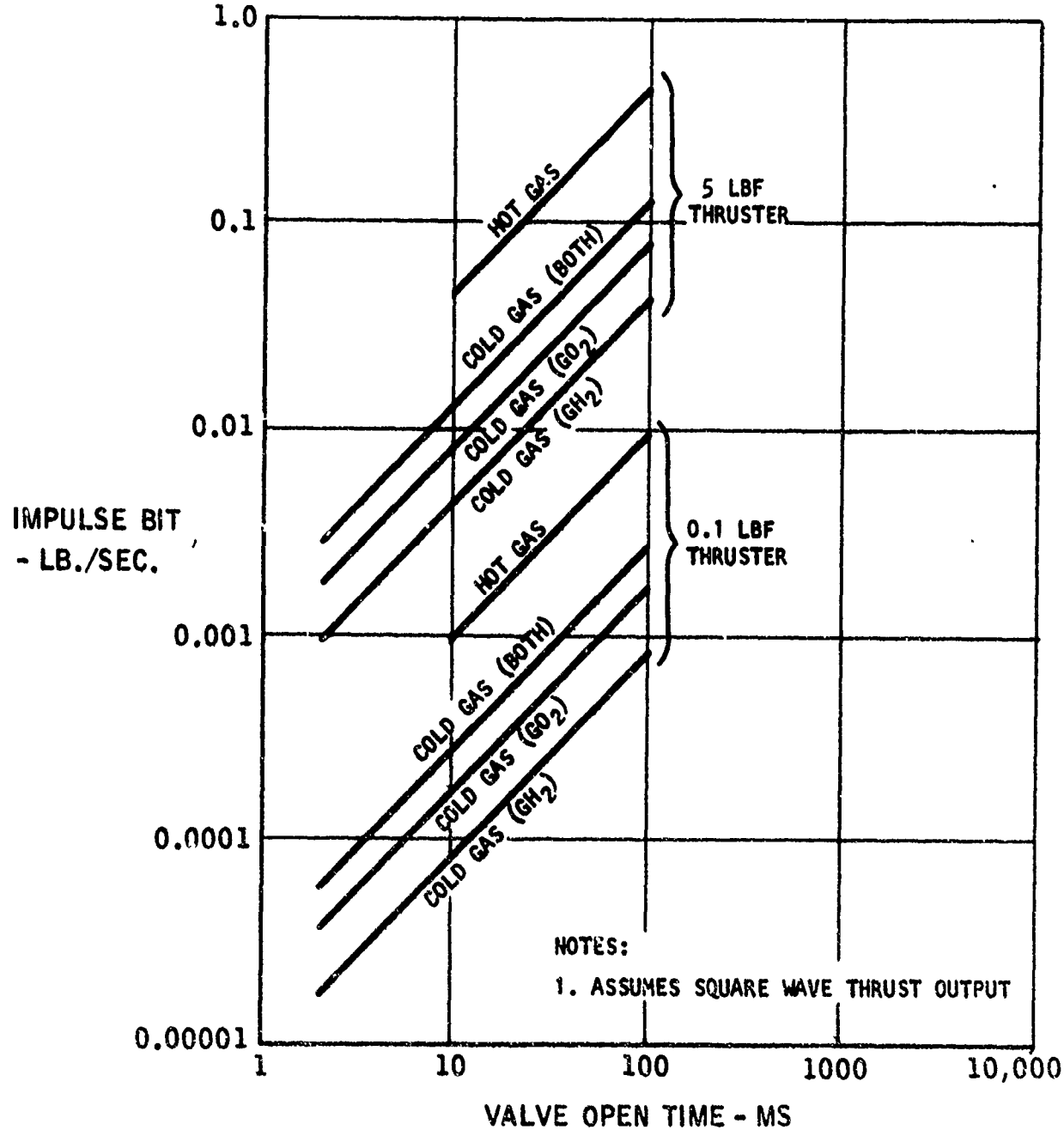

FIGURE 14. IMPULSE BIT VS VALVE OPEN TIME (PER ENGINE)

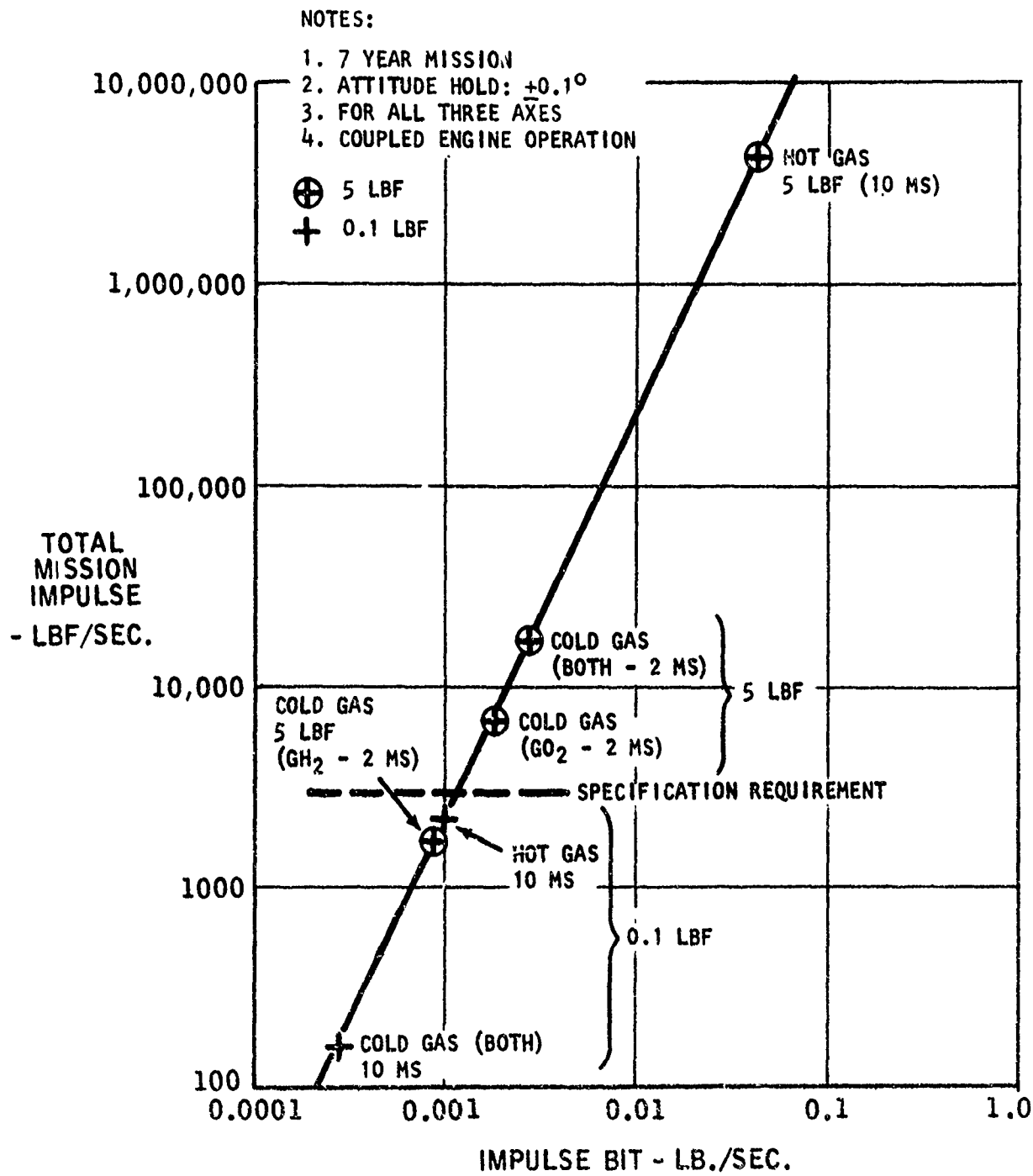

FIGURE 15. TOTAL MISSION IMPULSE VS IMPULSE BIT (LIMIT CYCLE OPERATION)

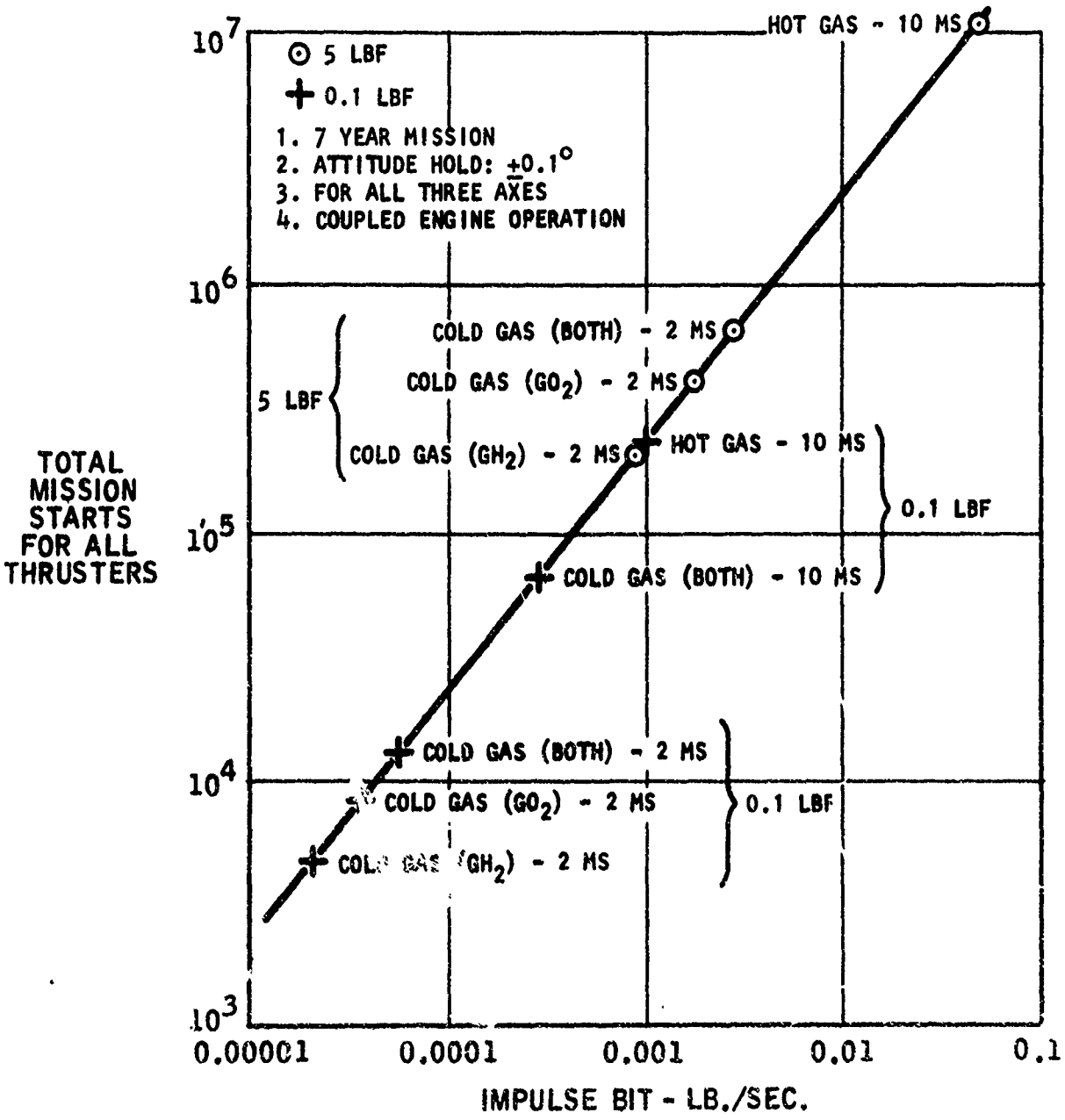

FIGURE 16. TOTAL MISSION STARTS VS IMPULSE BIT (LIMIT CYCLE OPERATION)

(3) Total Mission Propellant Requirements (Figure 17)

Since propellant consumption for limit-cycle operation is proportional to I_t^2/I_{sp}, tremendous propellant savings can result by operating at the small impulse bits available from cold-flow operation even though the specific impulses are significantly lower.

2. SPIN-STABILIZED MISSION

The spin-stabilized mission, in general, presents less severe propulsive system requirements than the 3-axes stabilized mission. For instance, fewer thrusters are required and the inertial forces generated by the spinning satellite are usually helpful from a propellant expulsion and feed-system viewpoint. Relative to the individual mission events and maneuvers, the following comments apply.

a. Booster Injection Errors (Tip-Off Rate)

This error would probably not be applicable to a spin-stabilized satellite. Normal procedure for spin-stabilized satellite. Normal procedure for spin-stabilized satellites is to spin them up prior to ejection from upper-stage vehicle.

b. Booster Injection Error (Position and Velocity Errors)

The same comments and requirements apply as discussed for the 3-axes stabilized mission.

c. Station-Keeping

Essentially the same comments and requirements apply as discussed for the 3-axes stabilized mission.

d. Attitude Control

The attitude control requirements would be significantly less for the spin-stabilized mission than for the 3-axes stabilized mission because it has a wider attitude control deadband (±0.5°) as well as being spin-stabilized.

The only potential mission requirement which could present an additional complexity to the spin-stabilized mission is if the water electrolysis system was required to provide the propulsive energy for spin-up of the satellite. Normally, for spin-stabilized satellites, this is accomplished prior to separation from the upper-stage and includes spin-up of the combined satellite and apogee engine. The apogee engine is required for transfer of the satellite from the elliptical transfer orbit to the synchronous orbit. This spin-up is usually accomplished by upper-state systems or small solid engines. In one case, the on-board propulsion system has also been used. However, for this application, it appears that this is not the required or desired approach.

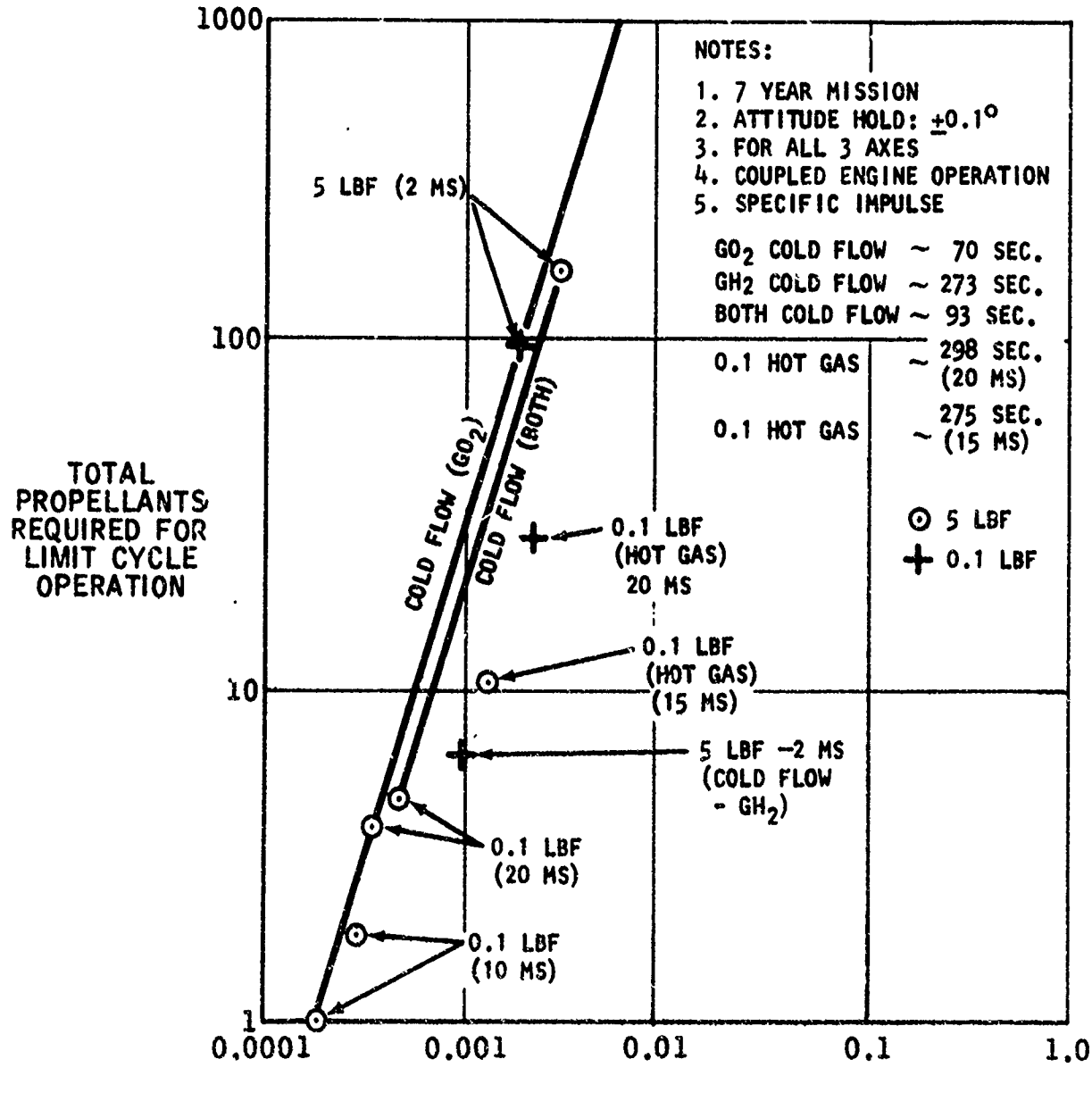

FIGURE 17. TOTAL MISSION PROPELLANT REQUIREMENTS FOR LIMIT CYCLE OPERATION

3. POINT DESIGN MISSION REQUIREMENTS

The following composite point design mission and propulsion system requirements were generated for both a spin-stabilized and a 3-axes stabilized mission.

- Mission Profile and Operational Modes - The mission impulse profile and operational modes are defined in Table 7. The estimated average specific impulses for each event are based on the predicted perfor mance characteristics of the thrusters and an estimated duty cycle for the specific event.

- Require Propellants H_2O - ≈295 lbm for the above mission profile. This number assumes 100% utilization of the propellant; however, there are other factors which must be taken into account (expulsion efficiency, vapor must be taken into account; vapor losses, etc.).

- Required Initial Ullage Gas Capacity - For correction of the tip rate booster injection errors, only ≈ 0.036 lbm of propellants is required. However, in order to conduct efficiently the subsequent position and velocity error corrections, an adequate gas storage capacity should be provided in order that reasonable length burn durations can occur. Therefore, a minimum initial ullage gas capacity of slightly greater than 0.4 lbm is required for the point design mission.

- Life Requirement - Seven years

- Generation Rate - For the combined station-keeping and attitude control requirements of the mission, a gas generation rate of 0.1 lbm/day is more than adequate. This results in a water electrolysis power demand of only 17 watts. For the large ΔV maneuvers (repositioning and booster errors), a generation rate of 2.3 lbm/day was selected since it appeared to be a reasonable compromise between the time required for the maneuvers at this generation rate and the power that one might expect to have available during these particular mission phases. This generation rate requires 230 watts power which is somewhat more than the defined constraint. However, it appeared reasonable to assume that during both those maneuvers, many satellite systems are not required to operate and at least 230 watts should be available. It should be noted that the electrolysis sytem proposed herein has the inherent capability to operate anywhere between 0 watts (no generation) and 230 watts (2.3 lbm/day) in the event some other power level is more compatible with the actual power availability of the satellite during these mission phases.

- Environmental Considerations - The propellant feed system (electrolysis module, tankage, and expulsion system) should be capable of operating on either a spin-stabilized (effects of inertial forces) or a 3-axes stabilized (essentially zero-g) mission.

SECTION IV

DESIGN, FABRICATION AND TEST

Based on the mission/system analysis and contractual requirements, a water electrolysis propulsion system was designed, fabricated and tested to characterize the capabilities of this concept as to its capabilities to meet the mission requirements. The testing was conducted on two basic systems composed of electrolysis unit, system component (propellant supply system) tests and thruster tests.

1. PROPELLANT SUPPLY SYSTEM

The propellant supply system is composed of the electrolysis unit and power conditioner which was supplied by the General Electric Company of Lynn, Massachusetts and the tankage, valves, switches and lines necessary to store water and the resultant hydrogen and oxygen. The details of this portion of the program are contained in Section IVA and the Appendix.

2. ROCKET ENGINES (Thrusters)

Two rocket engines producing 0.1 lbs and 5 lbs of thrust were developed and tested during this program. The engines were both ignited by a spark ignition device and were evaluated with water saturated hydrogen and oxygen simulating the products resulting from the electrolysis of water. Section IVB contains the details of the program concerned with the development of the 5 pound thrust rocket engine while Section IVC documents the 0,1 pound rocket engine program results. Section IVD contains the data concerned with the spark plug and igniter control circuitry.

SECTION IVA

PROPELLANT SUPPLY SYSTEM

The propellant supply system consists of a pressurized water tank, an electrolysis unit for separating water into gaseous hydrogen and oxygen, plenum tanks to store gaseous oxygen and hydrogen until used by the rocket engines, and system controls.

1. ELECTROLYSIS UNIT

The basic function of the electrolysis unit, separating water into gaseous oxygen and gaseous hydrogen by ion exchange, is accomplished by passing electrical current through a plastic membrane which is saturated with water. The rate of electrolysis of the water is proportional to the amount of electrical current. The plastic membrane acts as a solid polymer electrolyte (SPE) without requiring any other electrolytic agent such as acid or alkaline fluids. High purity deionized water is supplied to the electrolysis unit.

The electrolysis process is shown schematically in Figure 18. The ion exchange membrane (SPE) is a perfluorinated sulfonic acid developed specifically to meet the stability and performance requirements of a long-lived electrolysis module. Chemically, the polymer approximates:

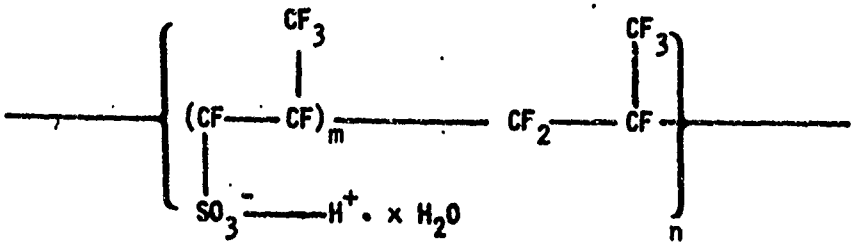

Ionic conductivity is provided by the mobility of the hydrogen ions (H^+). These ions move through the polymer sheet by passing from (SO_3^-) to (SO_3^-). The sulfonic acid groups (SO_3^-) are fixed and do not move, thus the concentration of the acid must remain constant within the SPE.

The reactant water is supplied to the cathode (hydrogen) side of the cell. It is transferred to the anode side by diffusion across the SPE to supply the water required for electrolysis. The generated hydrogen and oxygen leaving the cell contain only that amount of water vapor necessary to saturate the gases at the selected operating temperature and pressure level, thus no free liquid water leaves the cell. For water to diffuse from the cathode (where it is supplied) across the SPE to the anode, a water gradient must exist. This gradient slightly increases the SPE electrical resistance and lowers the water activity at the anode. If water were added directly to the anode, no water gradient across the SPE would result. However, free liquid water would leave with the generated hydrogen as it would be transferred electrochemically across

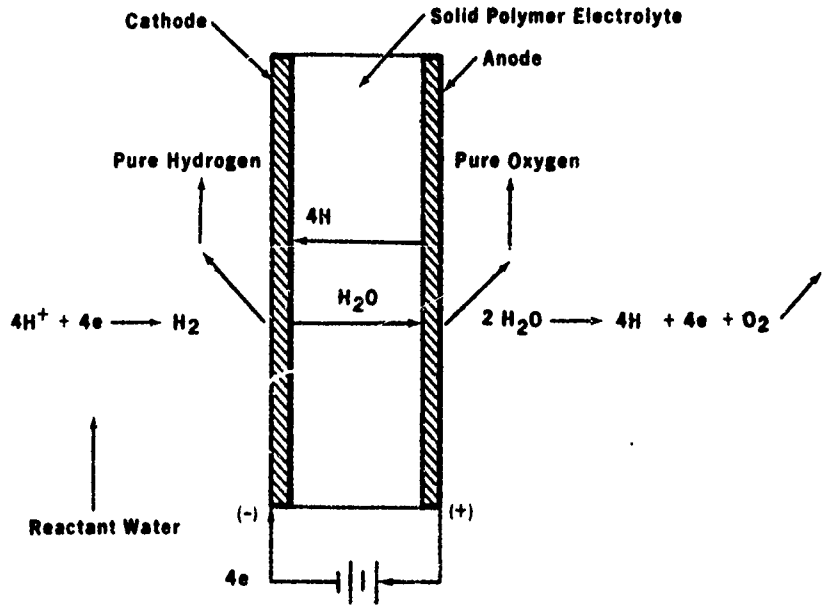

FIGURE 18. ELECTROLYSIS PROCESS

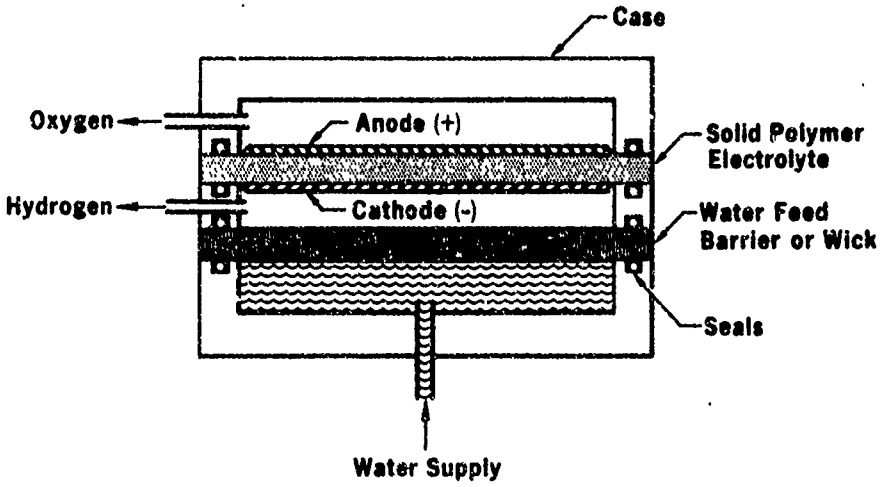

FIGURE 19. SCHEMATIC DIAGRAM OF ELECTROLYSIS CELL

the membrane with the protons ($H^+ \cdot x H_2O$). Cathode feed water mode of operation eliminates this phenomena, thus providing generated hydrogen and oxygen gas without free liquid water. The slightly lower performance of the cell resulting from the cathode mode of operation is more than compensated for by the elimination of the gas/water phase separation requirement.

A schematic diagram of the physical construction of a single electrolysis cell is shown in Figure 19. A manifold adjoining the anode side of the SPE, the site of the oxygen release, is connected to the oxygen plenum tank. The manifold adjoining the cathode side of the SPE, the site of hydrogen release, is connected to the hydrogen plenum tanks. The water is supplied to the hydrogen manifold by diffusion across the water feed barrier, another solid polymer membrane not carrying electrical current. The rate of water flow across the water feed barrier (WFB) into the hydrogen manifold is proportional to the pressure drop between the water supply manifold and the hydrogen manifold and is also influenced by the temperature of the WFB.

Any water diffusing across the WFB which is not consumed by the electrolysis process will collect in the hydrogen manifold and eventually pass into the hydrogen tanks. Therefore, the pressure drop from the water supply to the hydrogen manifold must not exceed that value which will transport water at the electrolysis rate associated with the electrical current supplied.

The water passing across the WFB will diffuse as water vapor into the hydrogen manifold, with a concentration gradient within the WFB and across the hydrogen manifold, a 0.006-inch gap between the WFB and the SPE. The hydrogen will, therefore, be about 95% saturated with water. An additional concentration gradient across the SPE will provide about 85% water vapor saturation in the oxygen.

The water feed barrier has approximately the same area as the active area of the electrolysis cell. The gas gap between the water feed barrier and the cell electrode is made as small as practical without impeding the flow of gas evolving from the electrode. The water feed barrier (WFB) utilizing a solid polymer electrolyte has the special property of allowing the rapid transfer of water through the barrier by evaporation, providing the pressure gradient across the WFB is not excessive.

a. Water Transfer Characteristics of an SPE Membrane

The solid polymer electrolyte (SPE) which has cation exchange properties also has unusual physical properties which facilitate the use of the material as a water transport medium. These same properties are also important to attaining good performance in an electrochemical cell utilizing the SPE.

The properties of the SPE as related to water content are summarized as follows:

(1) Equilibrium Water Content

The SPE has a characteristic equilibrium water content which is primarily dependent on the ion exchange capacity of the SPE and the temperature at which the SPE is initially equilibrated.

(2) Constant Water Content Characteristic

The SPE may be equilibrated at a high equilibration temperature with a resulting high water content and still maintain the same water content at a lower environmental temperature. The SPE has the property of maintaining an essentially constant equilibrium water content even though the actual water content of the SPE may be reduced for extended periods of time due to drying or other stimuli which will be described later.

(3) Vapor Suppression Effect

If evaporation occurs at the surface of the SPE or any other effect or stimulus reduces the water content at the surface below that of the equilibrium water content the relative humidity will be less than 100% (activity of less than unity). If any effect causes the surface of the SPE to have an activity of less than 1.0, vapor diffusion of water in close proximity to the site will tend to restore the water content in the SPE to the equilibrium value.

(4) Electro-osmotic Water Transfer Effect

Each hydronium ion tends to transfer liquid water from the anode (oxygen) electrode to the cathode (hydrogen) electrode during the operation of an electrolysis cell that utilizes an acid electrolyte (cation exchange SPE). Each hydronium ion is surrounded by water and it tends to carry along 5 to 8 water molecules as the ion is transported to the cathode (hydrogen side) by an electrical potential difference between the electrodes. The dissociation of water takes place at the anode of an electrolysis cell which utilizes a cation exchange SPE. If no water is directly supplied to the anode, the water content of the SPE will tend to be depleted until steady state water content gradients are established within the SPE which will permit some other source (such as an evaporative surface or a flooded cathode) to supply the water at the anode by passage through the membrane at a rate equal to the rate of electrolysis.

(5) Hydraulic Permeability

If water is supplied to one surface of the SPE at a pressure higher than the other surface, liquid water will permeate the SPE at a rate proportional to the differential pressure and increasing with an increase in the temperature and the water content of the SPE.

Figure 20 shows the hydraulic permeability effect for an equilibrium temperature of 160° F and a water content of 0.22 gm water/gm dry SPE for a

No. Cells: 6
Cell Area: 33.2 sq in.
SPE Thk.: 0.01 in.
Equil. Temp.: 160°F
Water Content
0.24 gm/gm SPE
0.326 cc/cc Tot.

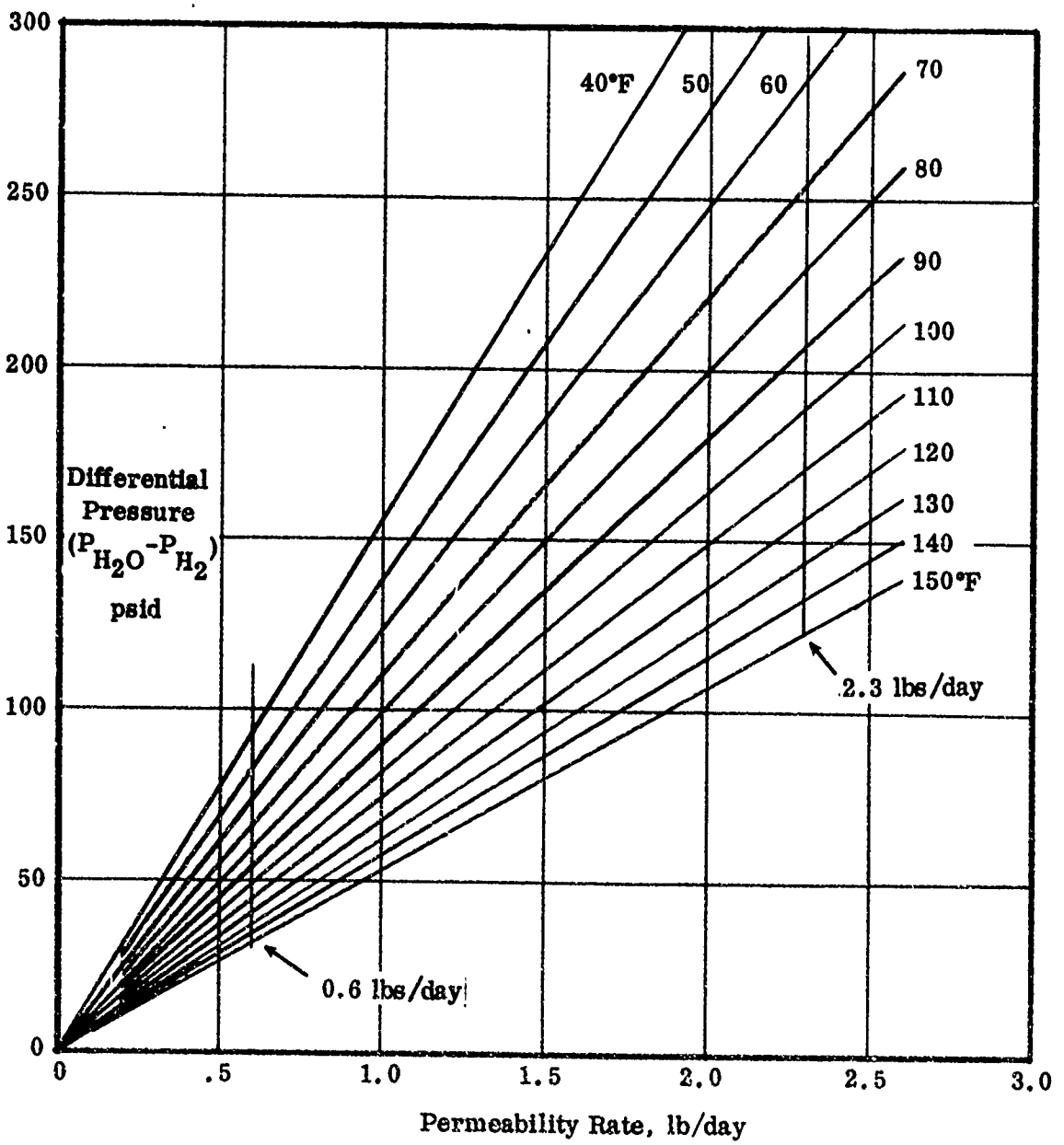

FIGURE 20. PERMEABILITY OF WATER FEED BARRIER FOR 160°F EQUILIBRIUM TEMPERATURE

total WFB area of 199.2 in.^{2} (6 cells of 33.2 in.^{2} each). For an equilibration temperature of 275°F and a water content of 0.38 gm H_2O per gm dry SPE, the permeability would be about four times greater.

(6) Osmotic Water Transfer

The experimental data for the hydraulic permeability data is used to predict the osmotic water transfer that takes place within the SPE in the presence of water content gradients.

(7) Gas Permeability

Gas permeates through the SPE in proportion to the difference in partial pressure of a given gas across the SPE and increasing with an increase in the temperature and water content of the SPE. Each species of gas has individual permeability characteristics. The gas permeation results from the gas going into solution on the surface having the highest partial pressure, diffusing through the liquid content of the membrane, and coming out of solution on the low pressure side of the membrane.

(8) Electrical Conductivity

The SPE is electrically conductive but the electrical conductivity decreases as the water content of the SPE is decreased. An increase in the electrical resistance of the SPE causes an increase in the cell voltage which may be estimated from the following equation:

$$\Delta E = I \cdot \Delta R \qquad \text{(Eq. 1)}$$

where ΔE = increase in cell voltage

I = current

ΔR = change in SPE resistance due to some physical effect

The resistivity is determined by an AC resistance measured at 1000 to 2000 Hz, rather than by a DC resistance measurement due to the DC polairzation characteristics of the SPE which are also typical of electrolyte solutions. A low water content in the SPE of the electrolysis cell can result in an increase in the operating voltage penalty as evaluated from Equation 1. As the water content approaches 0.434 gm/gm SPE, the SPE resistance increases rapidly for an SPE which has an equilibrium water content of 0.38 gm/gm SPE.

(9) Water Content Gradients in an Electrolysis Cell

Figure 21 shows the water content gradient in an electrolysis cell operating with a flooded cathode as a dashed line. The data shown is specifically for the following operating conditions of the electrolysis cell:

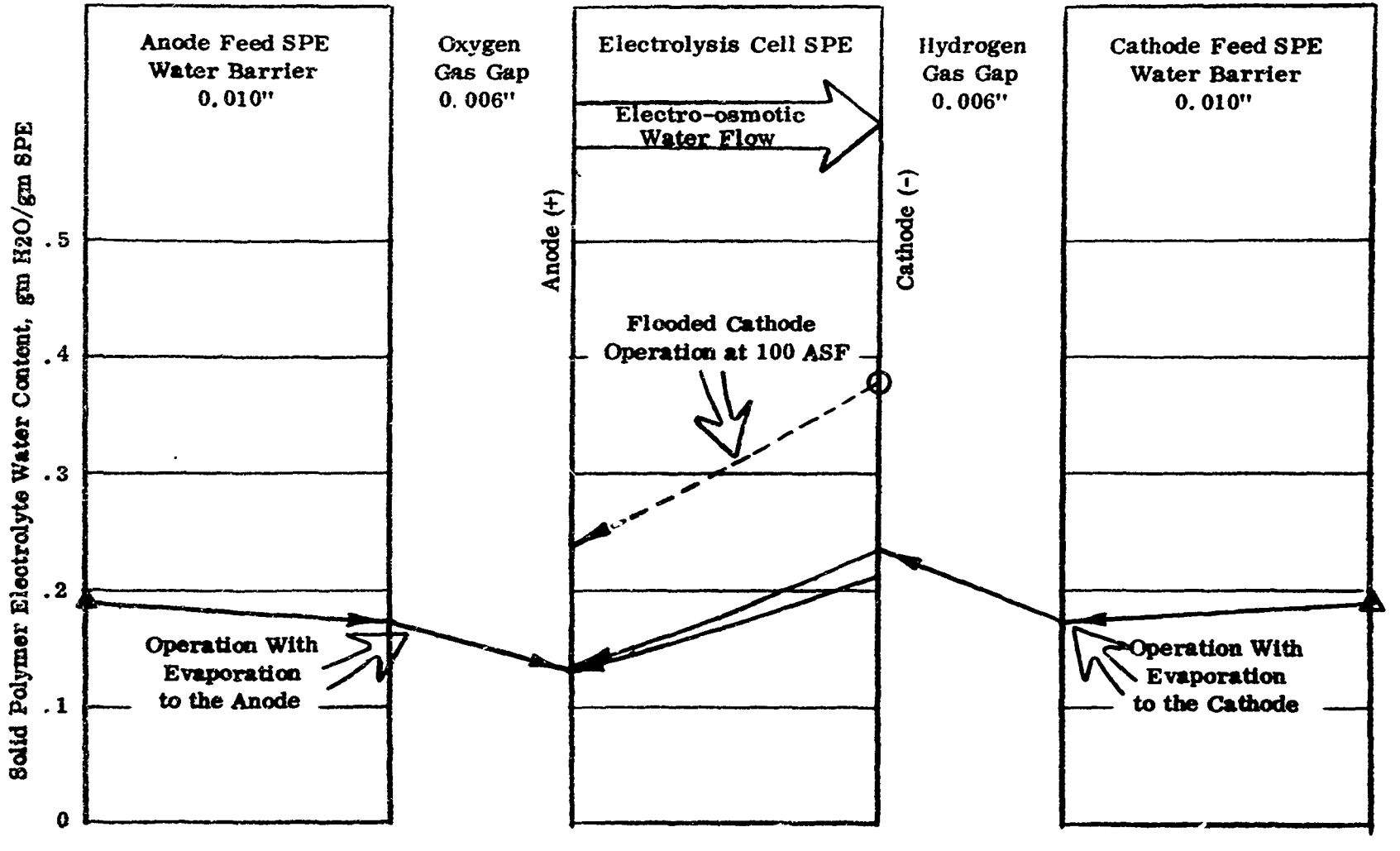

SPE Equilibrium Water Contents: Electrolysis Cell 0.377 gm/gm SPE
Water Feed Barriers 0.189

FIGURE 21. WATER CONCENTRATION GRADIENTS IN AN ELECTROLYSIS CELL

Current density	100 ASF
Temperature	100°F
Pressure	200 psia
Water content	0.38 gm/gm SPE

When the electrolysis cell operates in the flooded cathode mode, the electro-osmotic effect tends to deplete the water content at the anode until the water content gradient is sufficient to cause osmotic diffusion of water through the membrane at the electrolysis rate and evaporation rate occurring at the anode. Evaporation of water occurs at both the anode and cathode due to the convection of water vapor with the generated gases leaving the cells.

b. Water Supply Pressurization Analysis

The problem of dissolved gas transfer to the water compartments and gas transport across the water feed barrier was reviewed. It was concluded that any pressurant gas other than hydrogen presents essentially no problems with a positive or zero pressure differential across the water feed barrier. A negative differential pressure can exist for short periods using a tentative criterion of the product differential pressure and time being 10 psid-hr.

If the pressurant gas is hydrogen, a positive pressure differential pressure ($P_{H_2O} > P_{H_2}$) should exist across the water feed barrier for long periods of operation. The differential pressure should be at least +1 psid for each 100 psia of water supply pressurization with hydrogen to cause dissolved hydrogen to be driven through the water feed barrier. This criterion assumes that hydrogen comes out of solution as the water is evaporated from the water compartment. If the dissolved gas stays in solution there is a possibility that the dissolved hydrogen will be convected through the water feed barrier with the water transport.

c. Six-Cell Electrolysis Unit

A six-cell electrolysis unit was designed and fabricated by General Electric Company to provide the following rates of water electrolysis:

Maximum electrolysis rate: 2.3 lb/day
Minimum electrolysis rate: 0.10 to 0.60 lb/day
(rate adjustable)

The design of the six cell electrolysis unit is shown in Figure 22. The six cells are compressed between end plates with 24 tie rods to provide a seal for ring-type rubber gaskets between the internal oxygen, hydrogen, and water compartments. One end plate together with a dome-shaped head form an enclosure for the stack as shown in Figure 23. Four fluid ports which communicate with the internal compartments are located in the base or enclosure plate. Feed water for electrolysis is delivered through a manifold to the water compartment of each cell. Similarly, when generated, oxygen is delivered through a manifold from the oxygen compartment of

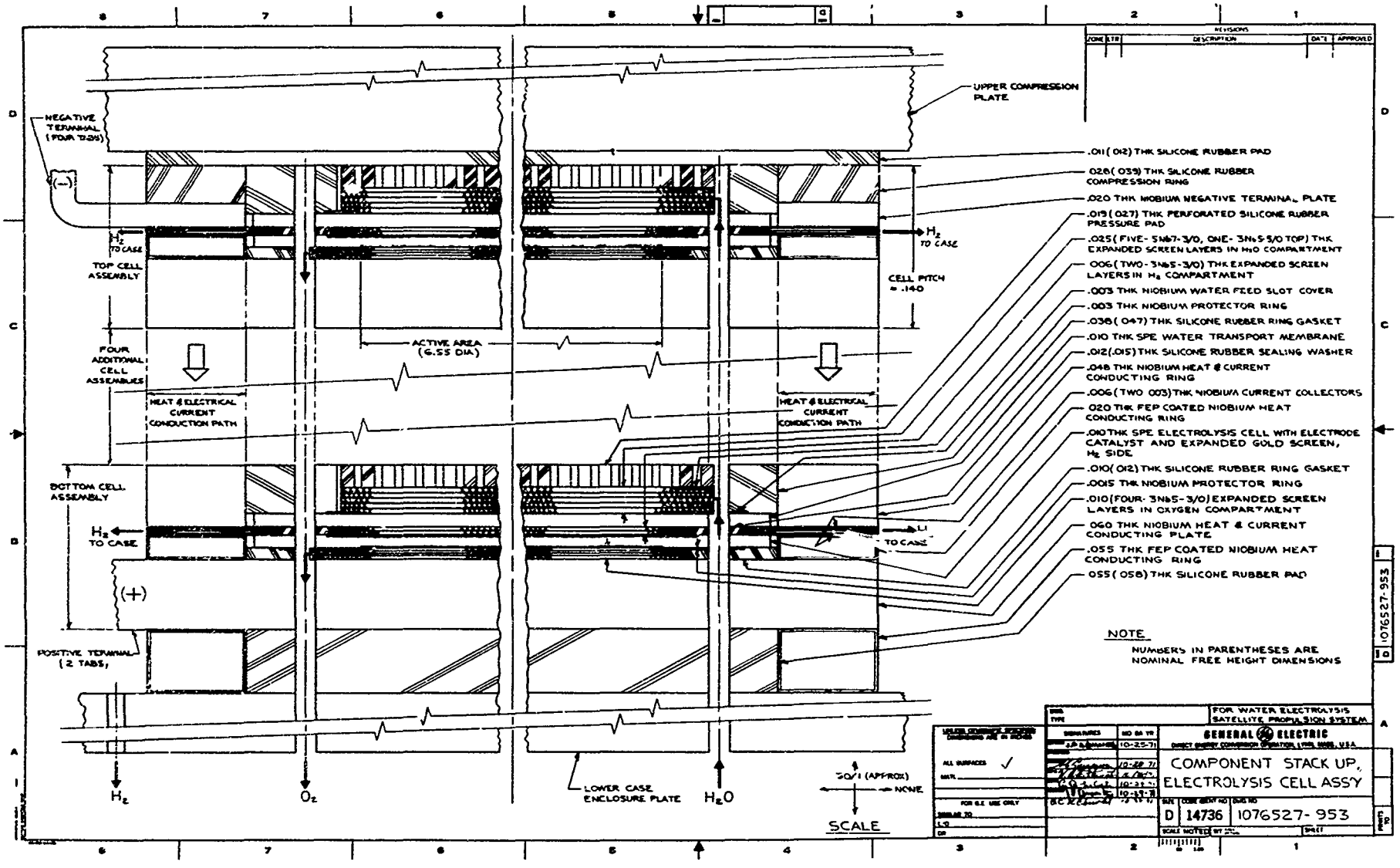

FIGURE 22. COMPONENT STACK UP, ELECTROLYSIS CELL ASSEMBLY

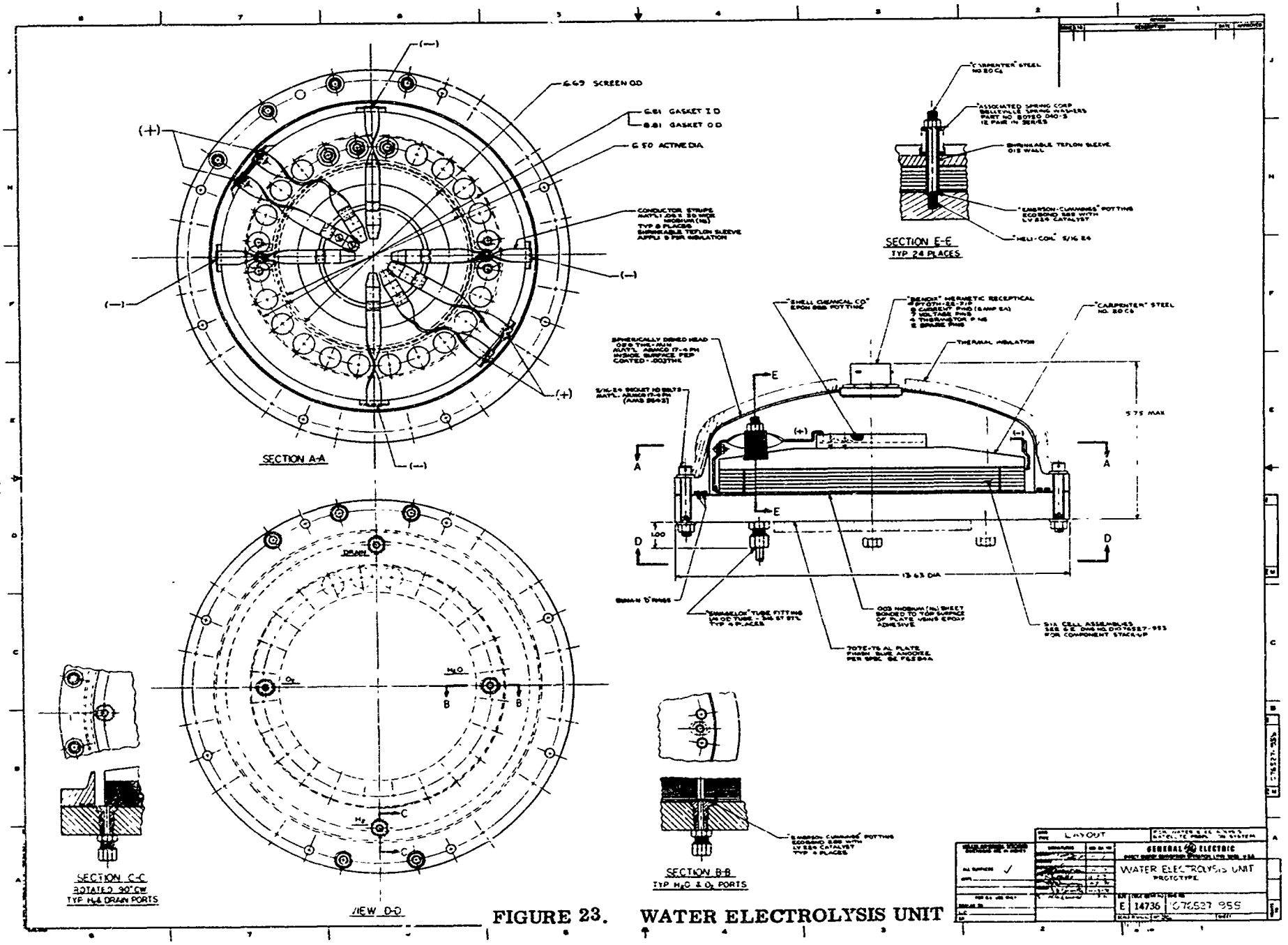

FIGURE 23. WATER ELECTROLYSIS UNIT

each cell. The hydrogen, however, is radially exhausted into the domed enclosure through multi-ply screens which form the hydrogen compartment. Multi-ply screens are also used in the water and oxygen compartments to support the compressive load of the stack assembly and provide fluid distribution, respectively, to and from the active cell area.

Water is transported across a 0.010-inch thick solid polymer electrolyte (SPE) membrane by hydraulic permeability caused by total pressure differential and/or by a differential of water vapor pressure (humidity difference) on the two sides of the water transport membrane. One side is maintained at 100 percent relative humidity by the supply of water, whereas the other side faces the hydrogen compartment with its relative humidity established by cell current or water consumption rate, operating pressure and operating temperature. Water vapor is transported across the hydrogen screen gap of 0.006 inch to the cathode of the electrolysis cell where hydrogen is generated. Liquid water can be transported across the membrane according to the hydraulic permeability characteristics shown in Figure 20. It is important to control (P_{H_2O}-P_{H_2}) pressure differential such that permeability rate is maintained less than electrolysis rate to avoid liquid water entrainment with the generated hydrogen.

Each electrolysis cell consists of a 0.010-inch thick solid polymer electrolyte with a thin layer of catalyst on the cathode and anode surfaces. Water is transported across the cell to the anode or oxygen side. A schematic representation of this process is shown in Figure 18. An input DC voltage of at least 1.46 volts is required for the electrolysis process of a single cell with voltage increasing approximately proportional to cell current or water electrolysis rate. At a given current, cell voltage is also increased by increased hydrogen pressure but is decreased by elevated temperature. The six cells of the electrolysis module are connected electrically in series with typical performance demonstrated by the voltage-current plot shown in Figure 24. Power is supplied to the electrolysis module through a centrally located electrical connector on the top of the enclosure and current is regulated by the power conditioner to standby, low-power, and high-power current operating levels which will be described more fully later.

Voltage leads are also brought through the same connector for monitoring individual cell performance as well as stack terminal voltage. Two copper-constantan thermocouples are attached to the center, top surface of the upper end plate and leads are carried through pins in the power-input connector. The heat generated by the cells is transferred by conduction to the enclosure plate which is bolted to a frame acting as a heat sink. The uppermost cell (No. 1) is therefore the hottest during operation and the thermocouple measurements will reflect this temperature level.

Some of the design parameters of the water electrolysis module/power conditioner are provided in Table 8. The maximum current output capacity of the power conditioner is 25 amperes. The design and proof pressures of the water electrolysis module are also cited. The internal design is such that water compartment pressure should always equal or exceed hydrogen and oxygen compartment pressures. It is

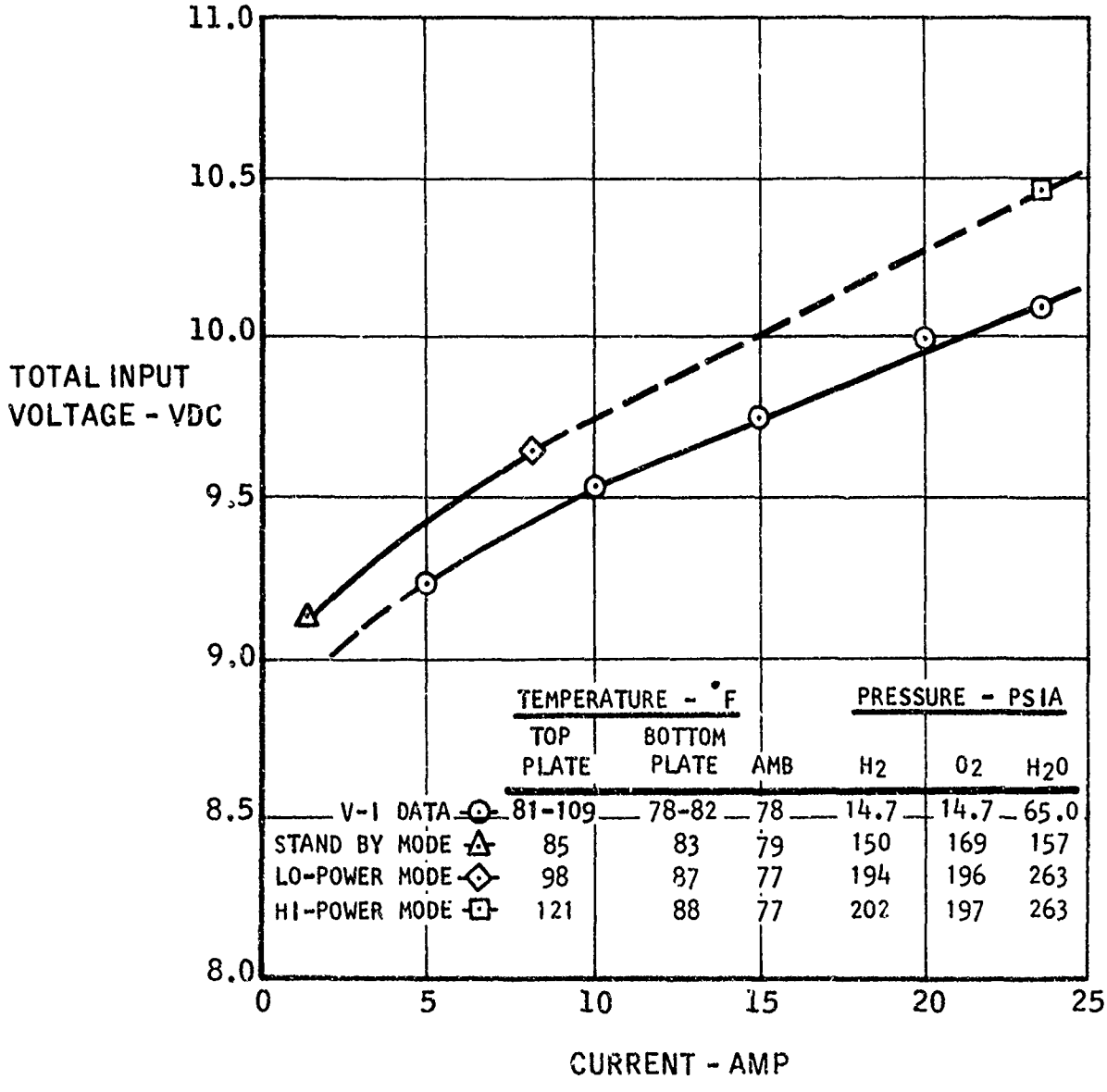

FIGURE 24 VOLTAGE CURRENT DATA FOR SIX CELL ELECTROLYSIS UNIT

TABLE 8

WATER ELECTROLYSIS UNIT DESIGN PARAMETERS

Item No.	Design Parameter	Design Data	
1	Water Electrolysis Rate		
	High Rate	2.3 lb/day	
	Low Rate	0.1 to 0.6 lb/day	
2	Stack Operating Data, 70°F Mean Cell Temp.	High Rate (2.3 Lbs./Day)	Low Rate (0.1 Lbs./Day)
	Stack Current	22 amps	1.76 Amps
	Stack Voltage	10.7 VDC	9.55 VDC
	Stack Input Power	235 watts	16.8 watts
	Stack Heat Loss	44 watts	8 watts
3	Number of Cells	6	
4	Compartment Operating Pressures		
	Max. Oxygen	250 psia	
	Min. Oxygen at Blowdown	67 psia	
	Max. Hydrogen	200 psia	
	Min. Hydrogen at Blowdown	67 psia	
	Max. Water	250 psia	
	Min. Water	200 psia	
	Max. $(P_{H_2O} - P_{H_2})$ Steady State	70 psid	
	Max. $(P_{H_2O} - P_{H_2})$ Blowdown Transient	183 psid	
	Max. $(P_{O_2} - P_{H_2})$	70 psid	
	Max. $(P_{H_2} - P_{O_2})$ at Open Circuit	200 psid	
5	Proof Pressures		
	Container	500 psi	
	Water Membrane Differential	250 psid	
	Cell Membrane Differential	250 psid	

TABLE 8 (Cont')

Item No.		
6	Container End Plate	
	Total Load at Proof Pressure	54,100 lb
	Fastening Screws	17-4 PH SS, 16, 5/16 - 18 Thd.
	End Plate	7075-T6 Al, 1.00 thk x 13.63 in. dia.
7	Stack End Plate	
	Total Load at Proof Pressure	28,500 lb
	Fastening Screws	Carpenter 20 Cb, 24, 5/16 - 24 Thd.
	Belleville Washers	SS, Assoc. Spring Corp., B 0750-040S 12 doublets compressed solid.
	End Plate	Carpenter 20 Cb, .75 thk x 10.6 in. dia.
8	Container Dome	Torospherical Head Material 17-4 PH, .060 in. thk
	Cell Design Parameters	
1	Electrode Diameter	6.5 in.
2	Active Area	33.2 sq in. or 0.23 sq ft
3	Ion Exchange Membrane	GE Spec. A50GN340
4	Nominal Cell Membrane Thickness	.010 in.
5	Nominal Water Transport Membrane Thickness	.010 in.
6	Cathode (H_2 Side) Catalyst Support	Expanded Gold Screen .003 in. thk, 6.75 dia.
7	H_2 Gap Screening	Two Layers - 3 Nb5 - 3/0 Expanded Screen
8	O_2 Gap Screening	Four Layers - 3 Nb5 - 3/0 Expanded Screen Pressed to .010 in. thickness
9	Water Gap Screening	Five Layers - 5 Nb7 - 3/0 Expanded Screen One - 3 Nb5 - 5/0 Top Expanded Screen Pressed to .025 in. thickness
10	Gasket Seal	6.81 ID x 8.81 OD GE Silicone Rubber SE-4404 O_2 Gap .012 in. thk H_2O Gap .047 in. thk

TABLE 8 (Cont')

Item No.			
11	Pressure Pad		.027 in. thk x 6.68 in. dia. perforated sheet. GE Silicone Rubber SE-4404
12	Cell Pitch		0.140 in.
13	Operating Mode		Cathode Water Vapor Feed
14	Max. Current at High Electrolysis Rate		23 amps
15	Max. Current Density		100 amps/sq ft
16	Max. Current at Low Electrolysis Rate		7.5 amps
	Power Conditioner Design Parameters		
1	Input Voltage		28 ± 3 VDC
2	Output Voltage		0-23.5 VDC Max.
3	Output Current		Two Output Levels 23 amps (fixed) 1-10 amps (adjustable)
4	Signal Input	Logic Format	"Low Rate" - Closure to Common "High Rate" - Closure to Common "Off" - Neither of Above
5	Signal Outputs	Logic	28 VDC, 1 amp capability to customer circuitry for Water Electrolysis Unit Voltage ≥ preset value TBD.
6	Max. Input Power		270 watts
7	Max. Power Loss		32 watts
8	Max. Heat Loss		32 watts

expected that pressure differential between the oxygen and hydrogen compartments will be less than 70 psid in either direction.

d. Single-Cell Prototype

A single-cell electrolysis unit was fabricated and tested by General Electric early in the program to gather performance data for validation of the six-cell electrolysis unit design which was subsequently fabricated and delivered to Marquardt. The single cell, with an area of 33.2 in.^{2}, was designed with the same dimensions as each of the cells in the six-cell electrolysis unit. The components of the single-cell unit are shown in Figure 25. The single cell was tested initially at low pressures using a plexiglass case, which was soon replaced by a steel case for high pressure testing.

The single-cell unit with the cover removed is shown in Figure 26. 24 stack studs are shown which apply a compressive load to the cell assembly. Four tabs and current leads are connected to the negative terminal, whereas two tabs and current leads are connected to the positive terminal of the cell. The assembled unit with the stainless steel cover, which replaced the plexiglass cover, and lucite sealing ring forming the enclosure is shown in Figure 27.

e. Single-Cell Testing

Initial single-cell testing was done with water recirculating through the water manifold to maintain isothermal conditions. A total of 4196 hours of operation was accumulated during the single-cell testing which is summarized in Table 9.

(1) Tests Nos. 1 Through 11

The first 11 tests were made at low pressures to check out the cell and gather data on water permeability of the water feed barrier. The results, in general, verified the analytical predictions of water transport characteristics.

(2) Tests Nos. 2 Through 18

The next series of tests, with the exception of Test No. 15, were made to evaluate the behavior of the electrolysis unit during alternating periods of off and on operation. Tests were also made to determine the quantity of water formed during the shutdown of the unit. A so-called "hydrogen takeover" occurs on the oxygen side when the oxygen compartment of the cell is isolated by a valve which permits the gradual gaseous diffusion of hydrogen stored in the unit pressure test case to combine with all the oxygen present to form water. On restarting the unit, all of the residual hydrogen in the oxygen compartment is electrochemically pumped across the electrolysis cell membrane to the hydrogen compartment before electrolysis can begin. A cell voltage-time trace of this startup, which took less than two minutes, and subsequent shuddown or discharge, which took over seven hours, is shown in Figure 28. The length of these periods depend upon the gas pressure conditions and applied current. It was discovered that water is expelled from the unit out the oxygen side on startup. The amount

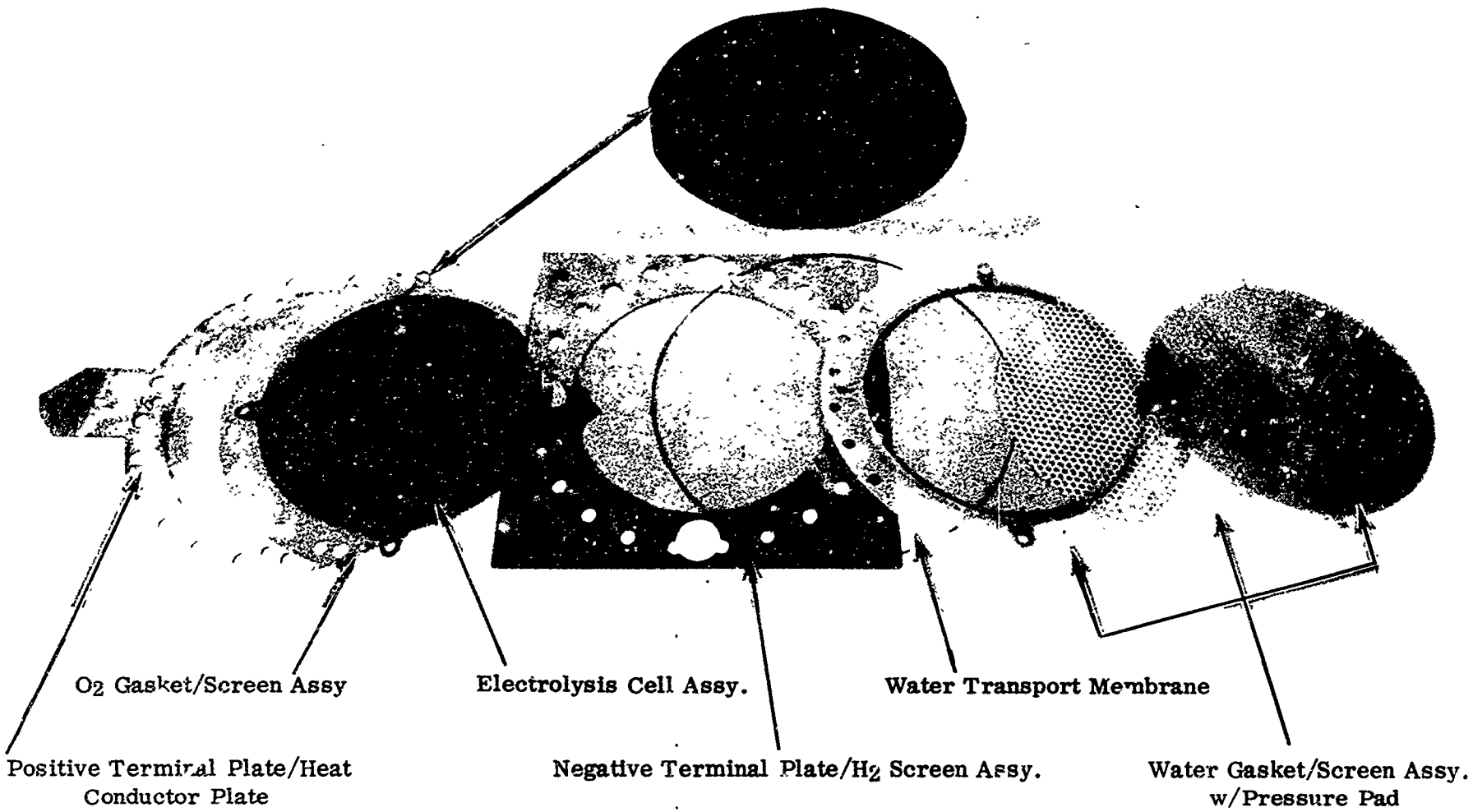

FIGURE 25. Electrolysis Single-Cell Components (Water Transport Membrane Design)

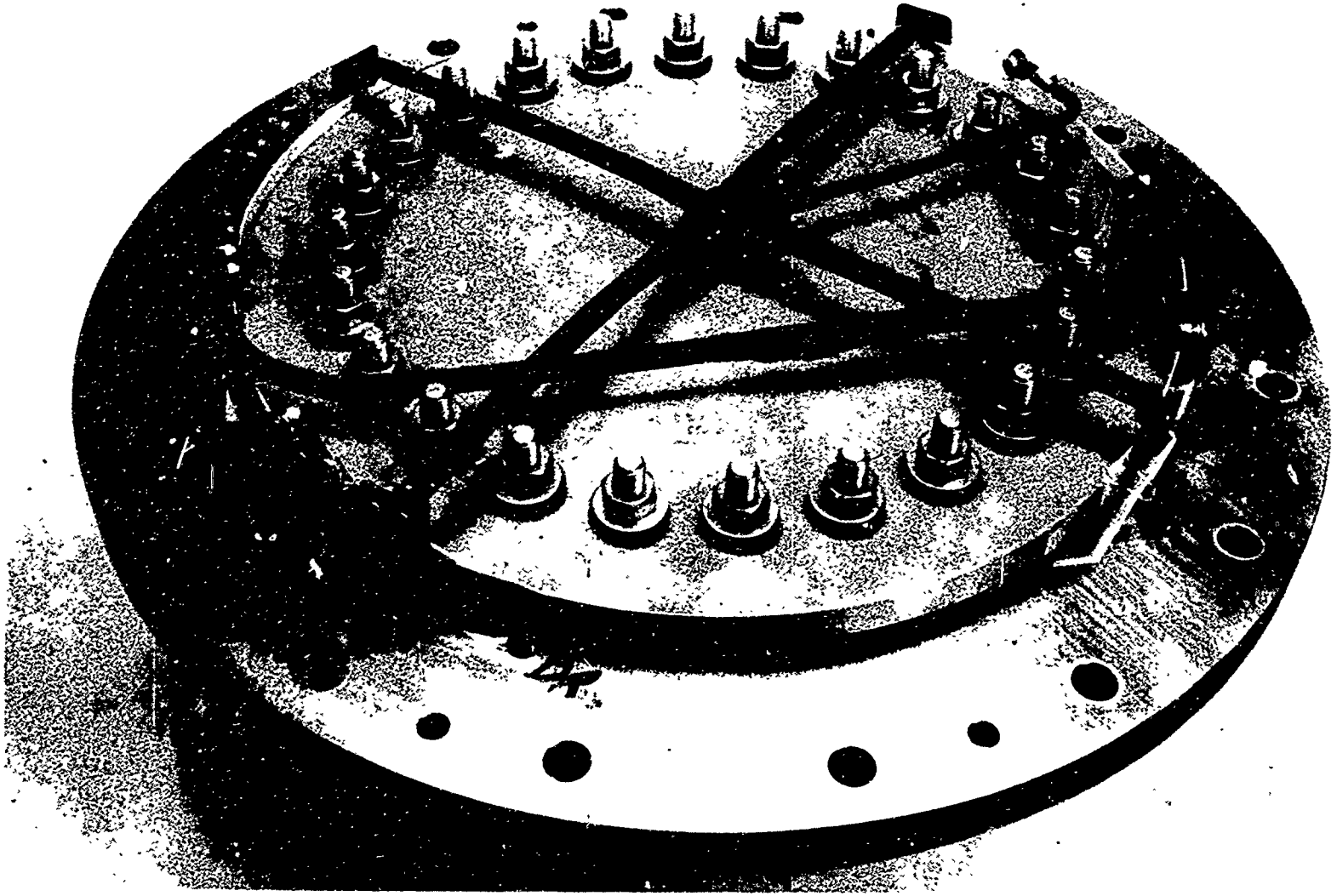

FIGURE 26. ELECTROLYSIS CELL WITHOUT COVER

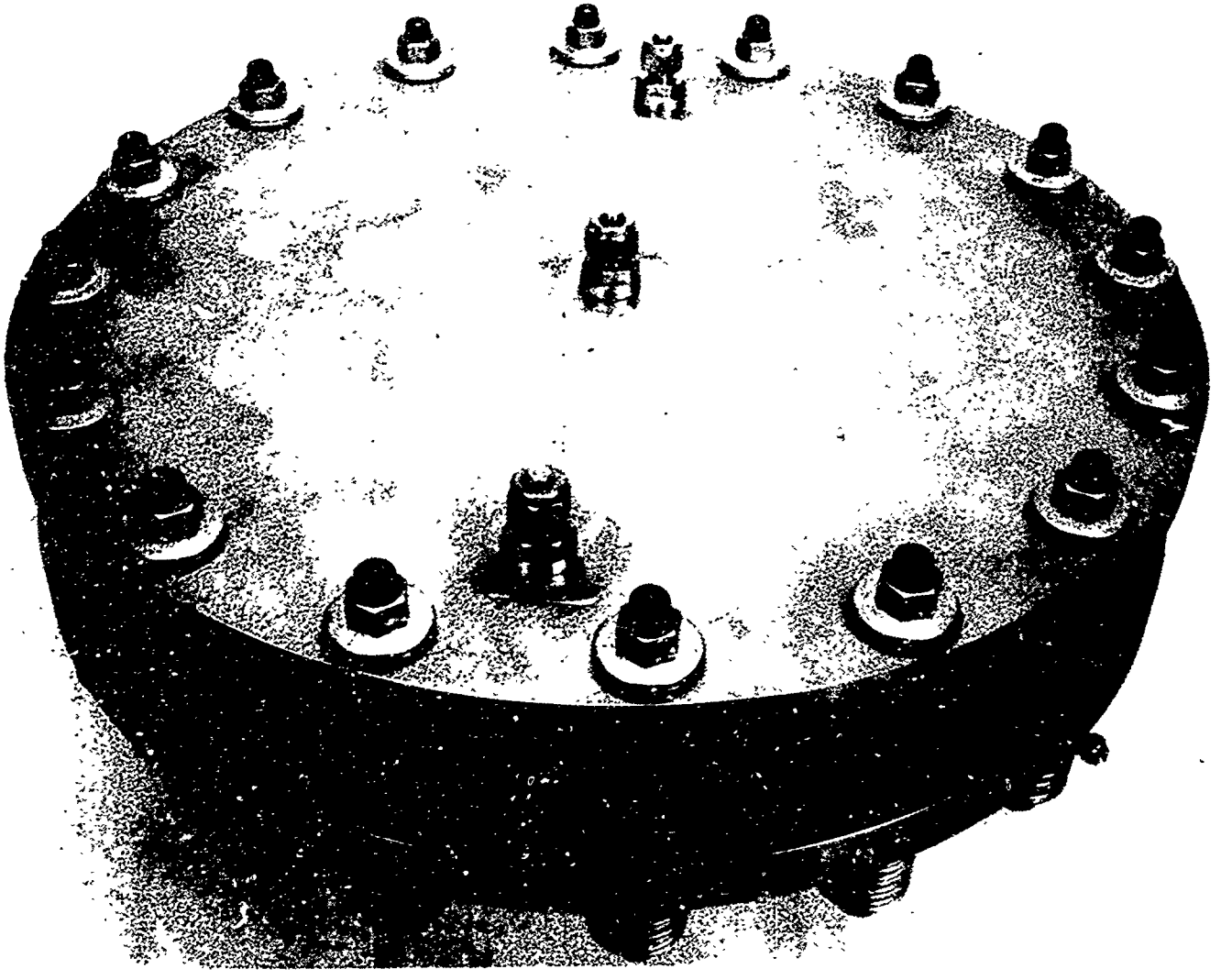

NEG. 374465

FIGURE 27. SINGLE ELECTROLYSIS CELL WITH COVER

TABLE 9

WATER ELECTROLYSIS SATELLITE PROPULSION SYSTEM

Test History of Single Prototype Electrolysis Cell

Test No.	Test Purpose	Test Conditions: Current Amps	Voltage vdc	H_2 Press. psig	O_2 Press. psig	H_2O Press. psig	Cell Temp. °F	Elapsed Time, hr	Comments
1	Performance Checkout	0 to 23		0	0	0 to 20	70 to 80	28.7	
2	Low Pressure Checkout	0 to 23		44	40	50		5.6	
3	H_2O ΔP Test	1.6		0	0	50		24.3	No H_2O on H_2 side
4	H_2O ΔP Test	1.6		0	0	70		16.2	25 cc H_2O on H_2 side
5	H_2O ΔP Test	1.6		0	0	40		29	13 cc H_2O on H_2 side
6	H_2O ΔP Test	1.6		0	0	10		72.3	No H_2O
7	H_2O ΔP Test	1.6		0	0	20		98.9	No H_2O
8	H_2O ΔP Test	0		0	0	20		64.7	21.5 cc H_2O on H_2 side
9	H_2 Δ P Test	23		8	0	1		8.2	Unit shutdown - high cell voltage
10	H_2 Δ P Test	23		8	0	14		45.9	No H_2O - unit stable
11	H_2O ΔP Test	23		8	0	9		33.1	No H_2O - unit stable
12	H_2 Takeover Test	0		50 to 40	40 to 0 to 40	50		87.4	0.5 cc H_2O on O_2 side
13	H_2 Takeover Test	0		40 to 37	20 to 0 to 37	47		22	0.96 cc H_2O on O_2 side
14	Open Circuit Test	0		43	40 to 20	46		39.8	5.5 cc H_2O on O_2 side
15	0.5 lb/day Test	4.7		0	0	50		113.4	No H_2O
16	H_2 Takeover Test	0		10	Not Measured	50		24	O_2 side down 7.5 cc H_2 on O_2 side
17	H_2 Takeover Test	0		10	Not Measured	50		26	O_2 side down 7.5 cc H_2 on O_2 side
18	H_2 Takeover Test	0		10	Not Measured	50		95	O_2 side up 3 cc H_2O on O_2 side
19	Pressure Mapping	1 to 23		0 to 120	0 to 220	50 to 260	66 to 75	70.5	
20	Temperature Mapping	6.4 to 23		185 to 193	213 to 230	225 to 260	70 to 120	234.3	Drained 95 cc H_2O out H_2 side
21	Temperature Mapping	1 to 23		180 to 230	210 to 230	212 to 290	99 to 110	61.4	Added more insulation. No H_2O out H_2O side

TABLE 9 (CONTINUED)

WATER ELECTROLYSIS SATELLITE PROPULSION SYSTEM

Test History of Single Prototype Electrolysis Cell

Test Conditions

Test No.	Test Purpose	Current Amps	Voltage vdc	H_2 Press. psig	O_2 Press. psig	H_2O Press. psig	Cell Temp. °F	Elapsed Time, hr	Comments
22	H_2O ΔP Test	6.9		183 to 185	218 to 230	245 to 247	102 to 105	72.3	Approximately 63 psid ΔP maintained. No H_2O out H_2 side
23	Pressure/voltage Decay and Buildup	0 to 6.9		196 to 231	106 to 232	196 to 250	98 to 106	25.8	
24	Parasitic Current Measurements	0.44 to 0.30		207 to 217	168 to 232	189 to 205	67 to 103	29.8	Unit deactivated after completion for test setup alterations
25	Parasitic Current Measurements	0.42 to 0.88	1.53/1.56	118 to 207	187 to 235	118 to 198	65 to 70	161.7	Unit shutdown temporarily to install pressure switch and water trap in O_2 outlet line
26	Standby Cycling	0/1 to 10	0.4/1.64	100 to 190	0 to 230	100 to 200	58 to 78	440 160 cycles	Total H_2O out O_2 side 23 cc only on severe discharges below $P_{O_2} < 50$ psig
27	Warm-up and Standby Cycling	0/1 to 15	1.35/1.68	180 to 192	63 to 219	186 to 220	84 to 105	48 5 cycles	No H_2O drained out O_2 of H_2 sides
28	Blowdown/Pump-up	23.0	1.69/1.75	186 to 47 to 170	182 to 50 to 180	240 to 235	102 to 109	2.6	10 min blowdown No H_2O out H_2 side
29	Cooldown and Standby Cycling	0/1.0	0.7/1.53	152 to 172	66 to 216	135 to 187	109 to 60	148.0 39 cycles	0.8 cc out O_2 side No H_2O out H_2 side
30	Blowdown/Pump-up	23.0	1.91/1.75	187 to 34 to 193	181 to 18 to 184	241 to 200	~70	104	Refilled H_2O storage tank and measured H_2O resistivity
31	Low power mode (continuous)	6.4	1.66/1.6	190	180	240	70 to 100	282	No H_2O out of H_2 side
32	H_2O ΔP capability	6.4 to 4.0	1.6/1.54	185	180	250	100 to 123	297	Drained 80 cc H_2O at 4.0 amp level and 123°F operation
33	Low power mode vs temperature	6.4	1.57/1.63	185	180	256	122 to 82	23	No H_2O out of H_2 side

TABLE 9 (CONCLUDED)

WATER ELECTROLYSIS SATELLITE PROPULSION SYSTEM

Test History of Single Prototype Electrolysis Cell

Test Conditions

Test No.		Current Amps	Voltage vdc	H_2 Press. psig	O_2 Press. psig	H_2O Press. psig	Cell Temp. °F	Elapsed Time, hr	Comments
34	V-1 Data	1 to 16	1.576/1.800	174 to 182	175 to 186	222 to 255	61 to 63	47	Low temperature, voltage-current data
35	Low Power Mode Low Temperature	6.40-6.42	1.667/1.682	182 to 183	176 to 181	253 to 255	59 to 65	89	No H_2O out H_2 or O_2 sides
36	Low Power Mode High Temperature	6.40-6.42	1.604/1.614	182 to 192	178 to 187	254 to 255	92 to 107	95	No H_2O out H_2 or O_2 sides
37	H_2O ΔP capability	5.00	1.59/1.61	190 to 191	185 to 187	254 to 255	98 to 104	72	ΔP = 65 psid. Drained 16 cc H_2O out H_2 side, 0.1 cc H_2O out O_2 side
38	H_2O ΔP capability	6.39-6.47	1.608/1.613	180 to 193	177 to 186	254 to 255	94 to 109	168	ΔP = 65-70 psid. Drained 23 cc H_2O out H_2 side, 1 cc H_2O out O_2 side
39	H_2O ΔP capability	8.44-8.57	1.615/1.634	184 to 193	178 to 186	254 to 256	95 to 109	272	ΔP = 60-70 psid. No H_2O out H_2 side, drained 1 cc H_2O out O_2 side
40	H_2O ΔP capability	8.40-8.65	1.615/1.683	180 to 194	181 to 190	253 to 255	71 to 120	686	ΔP ~65 psid. No H_2O out H_2 side, drained ~0.5 cc O_2 side

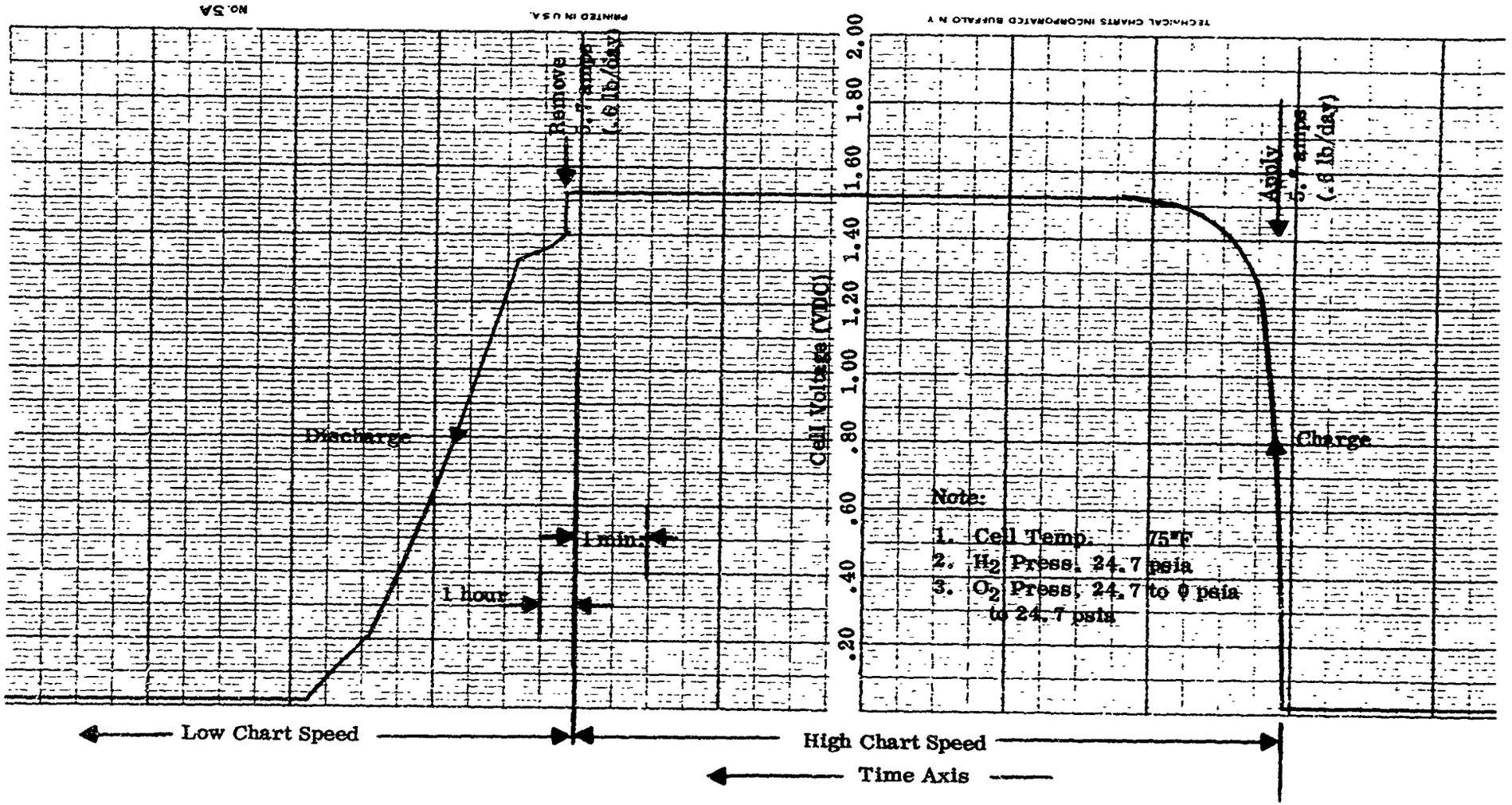

FIGURE 28. SINGLE CELL SHUTDOWN TEST CELL VOLTAGE VS. TIME

calculated as 2 cc of water per cell is primarily all due to the water formed by reduction of metallic oxide and adsorbed oxygen on the anode catalyst rather than that from the free oxygen in the cell oxygen compartment side.

(3) Test No. 19

During Test No. 19, the single-cell unit was tested at room temperature to determine cell performance at normal maximum and minimum operating pressures. The results are shown in Figure 29. The higher voltage at the higher operating pressure was predicted and is caused by the lower diffusivity of water vapor transported to the cell across the hydrogen gap at higher gas density.

(4) Tests Nos. 20 and 21

Cell performance was evaluated at elevated temperatures during Tests Nos. 20 and 21, while essentially constant high-pressure conditions were maintained. The results are shown in Figure 30. Substantially better unit performance is caused by both improved cell electrochemical reaction rates and increased diffusivity of water vapor at higher temperature. Control of cell temperature was obtained by setting the unit on a hot plate with thermal Variac control. After applying 3 to 4-inch thickness of fiberglass blanket and aluminum foil insulation around the unit, water condensation in the hydrogen-side enclosure was minimized during operation over 100°F. Thermocouples were attached to the center and edge of the bottom plate and on the top compression plate for the cell within the enclosure. Temperature readings, top and bottom, were usually within 2 to 3°F even at 110°F. No water condensate was drained from the hydrogen enclosure after a total of 134 hours' operation at 100°F.

(5) Test No. 22

A 72-hour test at 6.9 amps (0.6-lb O_2/day) and 100°F with a nominal water barrier (P_{H_2O} - P_{H_2}) differential pressure of 63 psid was performed after which no water was observed from the hydrogen enclosure.

(6) Test No. 23

Test No. 23 was made to measure cell voltage decay and oxygen pressure decay with time when the unit was shut down. Hand valves were closed which isolated the H_2, O_2 and H_2O cell volumes as an open circuit condition was maintained. Oxygen pressure decreased much more rapidly than hydrogen pressure because of the small oxygen compartment volume. Both oxygen pressure and cell voltage decay approximately linearly with time, as shown in Figure 31. After reopening the isolation valves for normal unit electrolysis operation following the shutdown period shown in Figure 26, no water was expelled with the oxygen gas or drained from the hydrogen enclosure. Hydrogen is exhausted out the top of the enclosure, as a separate drain line is provided for measuring any water accumulation within the hydrogen enclosure outside the cell hydrogen cavity.

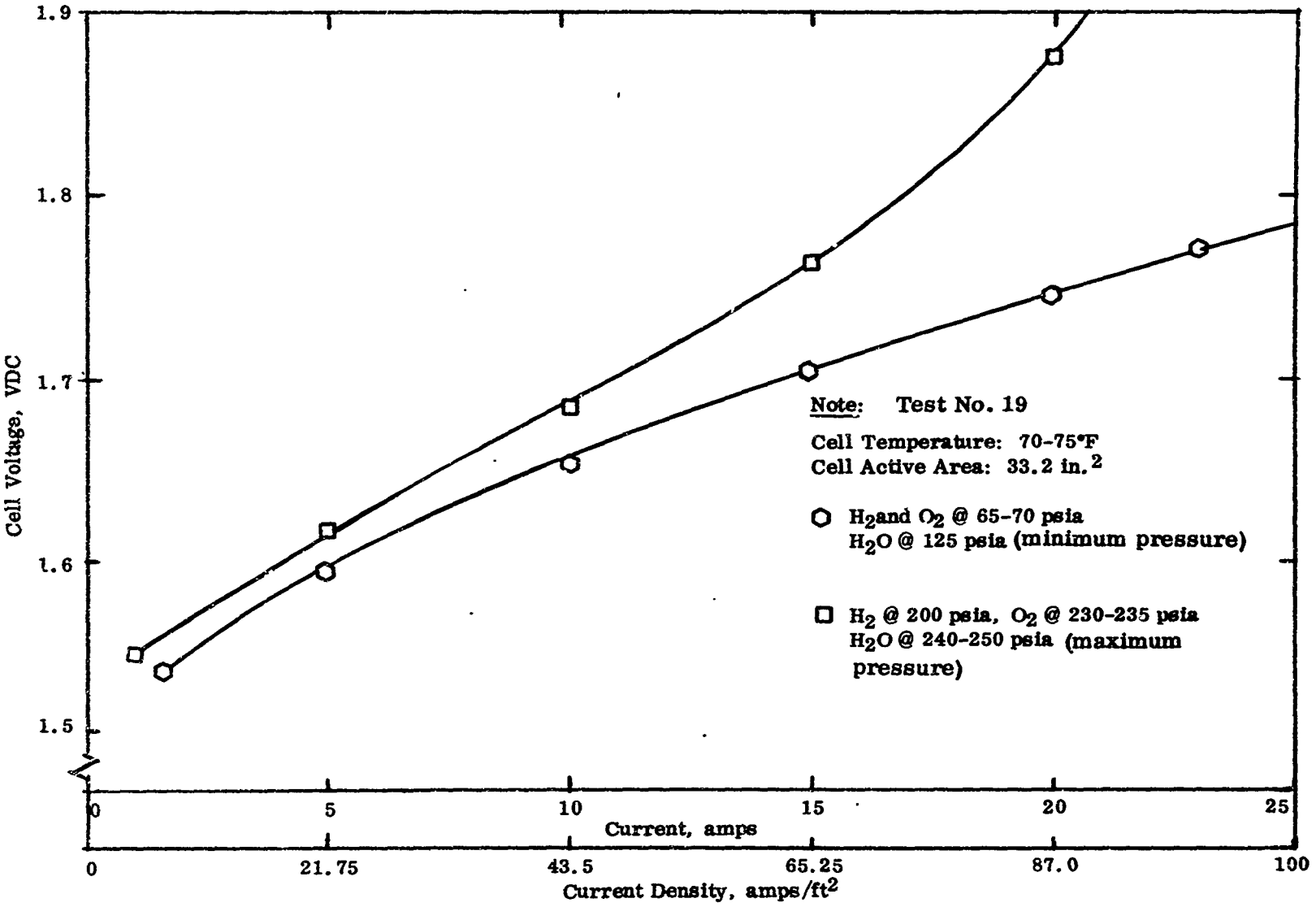

FIGURE 29. SINGLE CELL PERFORMANCE TEST AT PRESSURE EXTREMES, TEST NO. 19

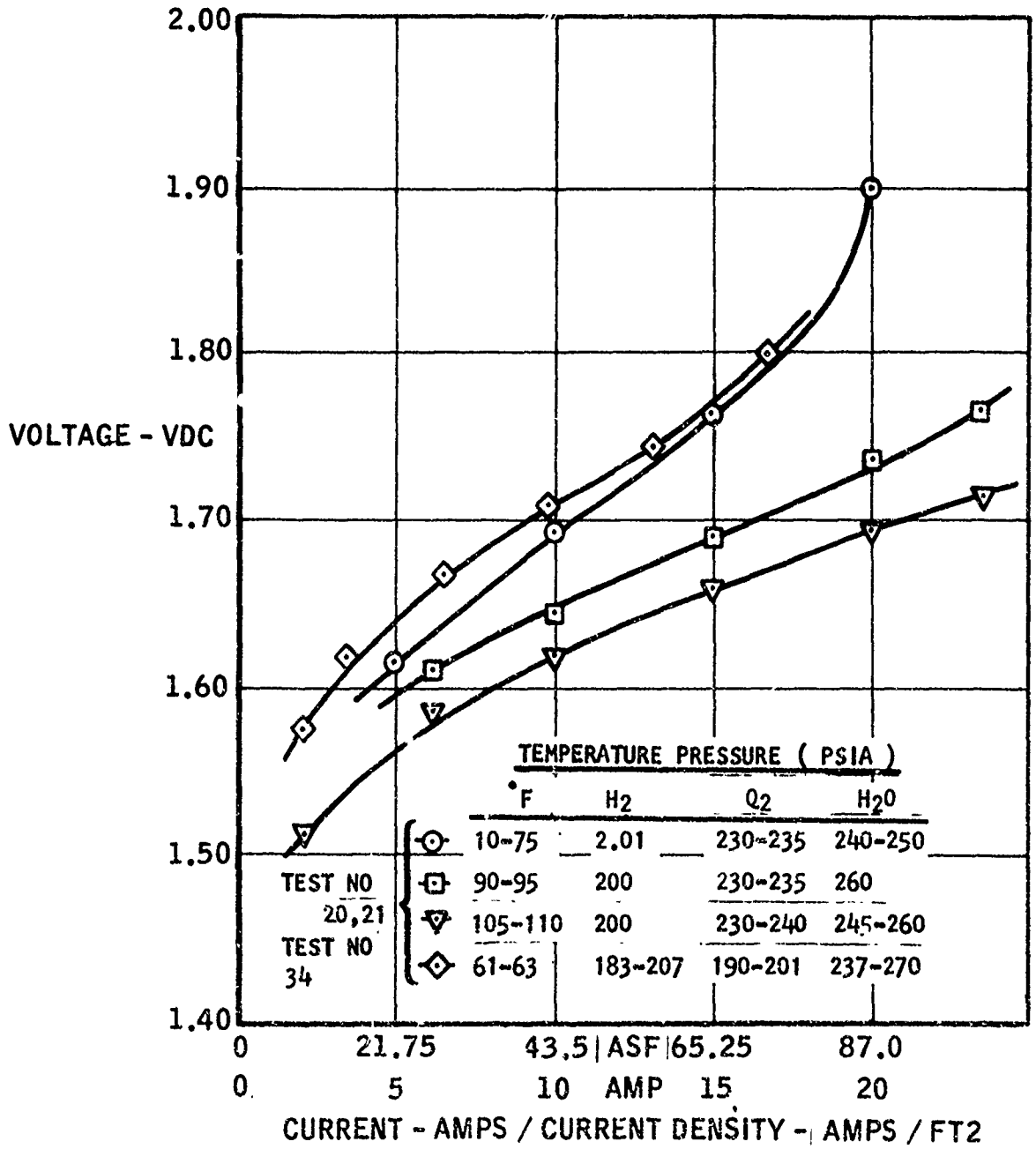

FIGURE 30. SINGLE CELL PERFORMANCE AT ELEVATED TEMPERATURES,

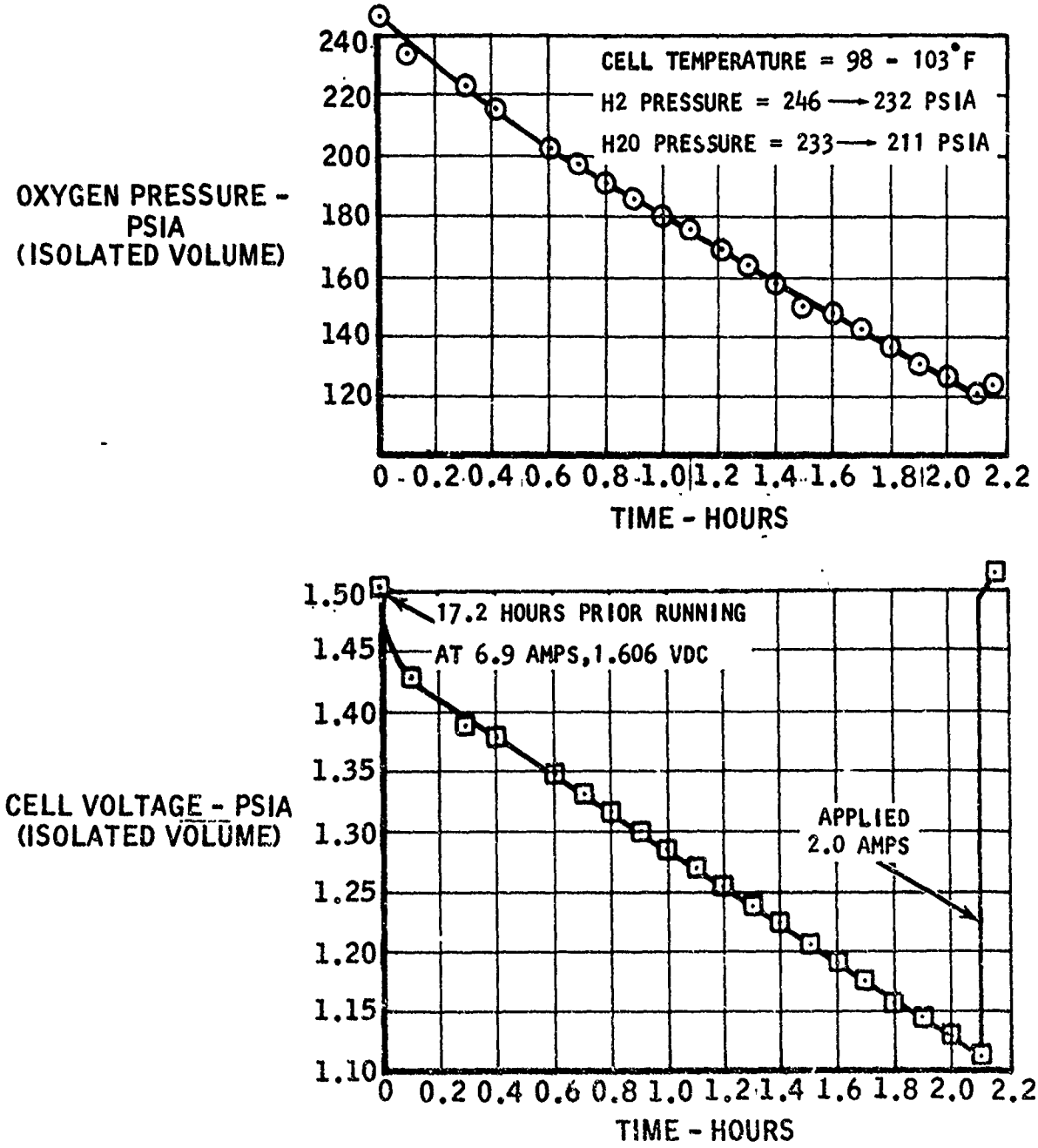

FIGURE 31. CELL VOLTAGE/OXYGEN PRESSURE DECAY DURING SHUTDOWN OF SINGLE CELL

(7) Test No. 24

Test No. 24 was conducted to establish what trickle current would be necessary to compensate for parasitic hydrogen and oxygen diffusion losses. This was performed by setting a cell current which maintained constant oxygen compartment pressure when hand valves were closed to isolate the H_2, O_2 and H_2O cell compartment volumes. The results are provided below.

Cell Parasitic Current, Amp	Avg Cell Temp, °F	O_2	H_2	H_2O
0.85	99	185	228	218
0.58	68	197	223	205

(8) Tests Nos. 25 Through 27

Tests 25 through 27 were performed with the objective of finding the most optimum pressure and voltage condition for the water electrolysis unit when subjected to a shutdown mode of zero gas output to the system gas storage tanks. This was accomplished by conducting unattended, automatic cycling tests on the single cell in a standby mode which alternated between an open-circuit condition and a powered condition at a trickle current of one amp or more with the oxygen and hydrogen outlet valves and water inlet valve closed. Current was removed by a pressure switch when oxygen cell pressure reached about 200 psig, whereas the load was reapplied by a voltage relay at a preset minimum open-circuit voltage adjusted between 0.4 to 1.4 volts. After several days of automatic cycling operation, the electrolysis cell was returned to a continuously-powered mode with all valves open to measure any entrained liquid water in the discharged gases. It was discovered that water formation on the anode or water entrained in the oxygen gas could be essentially eliminated if oxygen pressure during the open circuit period did not fall below 50 psig within the cell compartment. A voltage trace selected from the recorder and illustrated in Figure 32 shows the variation in voltage during the powered and open circuit period with a complete standby cycle of about 8-3/4 hours for the settings established. Pressure variation, not shown, would be linear increasing and decreasing ramps with respective powered and open-circuit periods which form a triangle over the complete cycle. A one-amp trickle current was found sufficient to overcome the maximum parasitic loss of oxygen and hydrogen diffusion at a temperature of 100°F. The period of one complete cycle varied with cell temperature as well as the pressure switch and voltage relay settings.

As the result of system modifications for standby operation of the prototype water electrolysis unit were made, they include modification of the power circuit for inclusion of an oxygen cell pressure switch and the use of oxygen and hydrogen check valves to replace the latching solenoid isolation valves. An oxygen cell pressure switch was selected to provide both electrolysis "on" and "off" switching functions at respective minimum and maximum oxygen cell pressure during the standby mode. Since there would be six cells in the prototype unit, the detection of a common

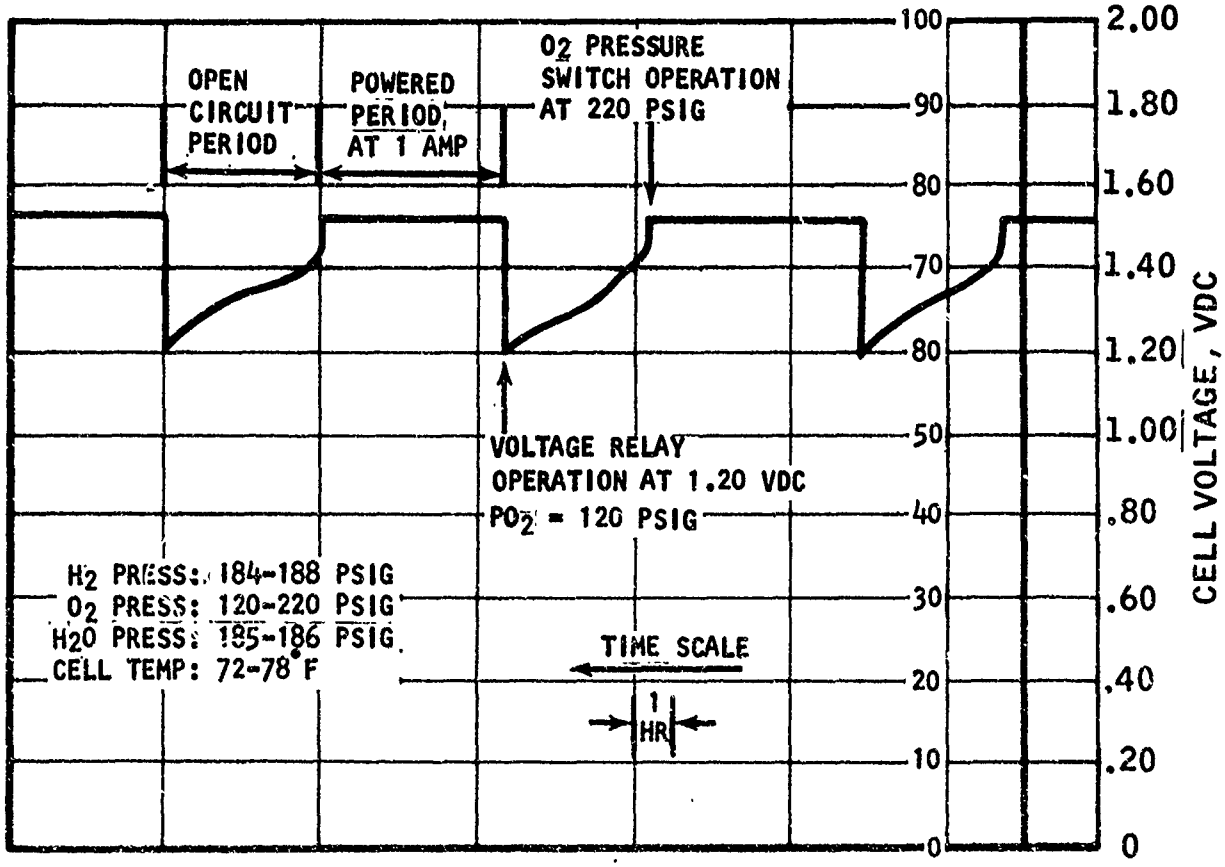

FIGURE 32. SINGLE CELL VOLTAGE DURING STANDBY CYCLING

oxygen cell pressure was more meaningful and reliable in maintaining the desired individual cell and stack condition than total stack voltage measurements in the standby mode.

(9) Test No. 28

A simulated blowdown and subsequent pump-up test was performed on the single cell with the results shown in Table 8. The blowdown time was longer (due to flow restriction of the H_2 test facility valve) and the pump-up time shorter (small H_2 volume) than expected in the prototype system.

(10) Test No. 29

Additional testing was performed during Test No. 29 to investigate the performance of the cell during standby cycling. After 39 cycles, no water was found during venting of the hydrogen manifold, and only 0.8 cc was found on the oxygen side.

(11) Test No. 30

A manually controlled blowdown and subsequent pump-up test was performed successfully at room temperature (~70°F) at 100 ASF, thus demonstrating stacks capability to sustain stable operation below the nominal cell design temperature of 100°F.

(12) Tests Nos. 31 Through 33

Continuous operation in the low power mode (0.6 lb/day rate) at various cell temperatures was conducted on the electrolysis unit to evaluate long-term operation in this mode with particular attention to detection of any water accumulation on the H_2 side. No water was observed during these tests except when the low power mode was reduced to approximately 0.4 lb/day rate at a cell temperature of 120° F. The tests to date have verified the predicted water differential pressure capability of the water feed barrier membrane concept.

(13) Test No. 34

Cell voltage vs current data was obtained at an operating temperature of 61 - 63° F with resultant performance plotted in Figure 25. Since the test points were sustained for only a few minutes, the voltage particularly at low-current settings is slightly higher than an equilibrium value established by steady cell water content and water partial pressure gradients.

(14) Tests Nos. 35 Through 39

Continuous operation in the low power mode was continued at a cell temperature of about 100°F to determine differential pressure capability of the

water feed barrier. A cell current of 8.5 amp was required to prevent liquid water transport to the hydrogen side at sustained operation of 100°F and 70 psid differential pressure. This required electrical input current of 8.5 amps is in agreement with a predicted permeability rate of 0.8 lb H_2O/day (7.5-amp equivalent) per Figure 20, plus approximately 1-amp parasitic current for diffusion losses.

(15) Test No. 40

A long (686-hour) test in the low power mode was at essentially the same conditions for the entire test period. No free liquid water was evident in the generated hydrogen with a pressure differential of ~65 psid which is in agreement with the predicted permeability rate for these cell test conditions. A total of 4196 hours of operation had been accumulated on the single cell with the completion of Test No. 40.

f. Six-Cell Unit Checkout Testing

The six-cell electrolysis unit was tested initially at General Electric Co. to check out functional integrity and basic performance characteristics. Table 10 summarizes the types of tests accomplished by General Electric on the six-cell unit. Total operating time was 22.8 hours.

(1) Test No. 1

Cell No. 3 failed during the initial checkout tests. Subsequent disassembly and inspection of the six-cell unit led to the conclusion that the probable cause of failure had been overheating caused by the heat of reaction from a hydrogen leak to the oxygen side of Cell No. 3. The leak was attributed to inadequate compression of the rubber sealing gasket between the hydrogen and oxygen, which was then redesigned. The burned-out Cell No. 3 was replaced by the single cell which had completed testing.

(2) Test No. 2

A series of corrective actions were taken during the second series of checkout tests, including an increase in the thermal conductance from the cells to the aluminum base plate and elimination of several electrical shorts.

During Test No. 3, water flow to Cells 1, 2, and 3 was found to be blocked. Examination during disassembly showed that the rubber gaskets had deflected enough under compression to block the access ports. The protruding rubber was reamed out, allowing adequate water flow.

(3) Test No. 4

The six-cell module, power conditioner and pressure switch successfully completed checkout testing and were successfully gas leak checked at 200 psig, O_2 and $H_2O > H_2$ to demonstrate unit integrity. The unit enclosure was proof

TABLE 10

SIX-CELL ELECTROLYSIS UNIT TESTING AT GENERAL ELECTRIC CO.

Test No.	Test Purpose	Current Amps	Voltage vdc	H_2 Press. psig	O_2 Press. psig	H_2O Press. psig	Cell Temp. °F	Elapsed Time Hr	Comments
1	Ambient Pressure Test	0-23	Various	0	0	30-57	72-91	7.1	Cell No. 3 failed due to lack of gasket compression
2	Ambient Pressure Test	0-3	Various	0	0	50	72	.5	Cells No. 2 and 6 showed electrical shorts
3	Ambient Pressure Test	0-23	Various	0-192	0-184	55-280	75-134	7.0	Water blockage occurring in Cells Nos. 1, 2 and 3
4	Open Circuit, Standby, Low and High Power Mode at Pressure	0-23	Various	0-192	0-184	50-250	81-120	8.0	All operating modes satisfactory
					Total Gas Time			22.8	

tested to 250 psig by pressurizing the manifolded O_2, H_2O and H_2 sides concurrently. The hydrogen manifold dome was proof tested separately to 400 psig. The six-cell electrolysis unit was then shipped to Marquardt for testing in the ground system tests.

2. POWER CONDITIONER

The power conditioner supplied by the General Electric Company controls the electrical current through the electrolysis unit to either 23 amps for the maximum electrolysis rate, and adjustable current between 1 and 10 amps for the minimum electrolysis rate, or a trickel current of 1 amp to maintain separation of hydrogen and oxygen within the electrolysis unit when the unit is turned off.

A functional diagram of the power conditions is shown in Figure 33. The basic principle is that of a step down regulator which will control input current to the stack over a range of input voltages from 25 to 31 volds dc, thereby compensating for changes in electrical resistance caused by cell temperature variations. The power conditioner supplied by General Electric Company is shown in Figure 34.

The power conditioner operates on a 28-volt power supply with a maximum input power of 270 watts and a maximum power loss of 32 watts (107 Btu/hr). The heat losses, electrical power consumption and water electrolysis rates for the electrolysis unit and power conditioner are shown in Figure 35. The power conditioner unit provided by General Electric Company is a breadboard unit which dissipates its heat loss by free convection from aluminum heat exchanger fins. Therefore, this unit must be operated in a sea level ambient environment. A conduction/radiation cooling surface would be designed for a flight system.

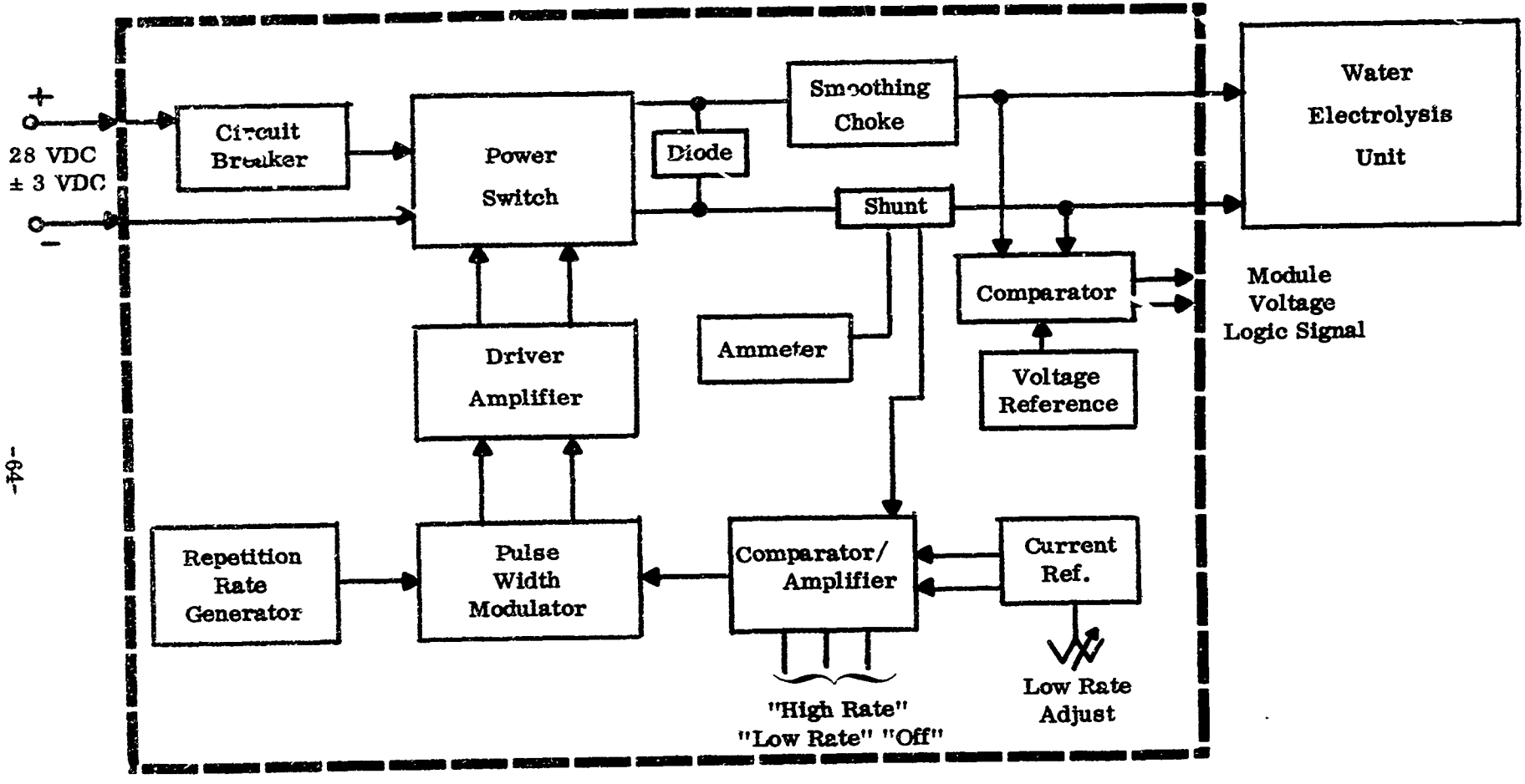

FIGURE 33. POWER CONDITIONER FUNCTIONAL DIAGRAM

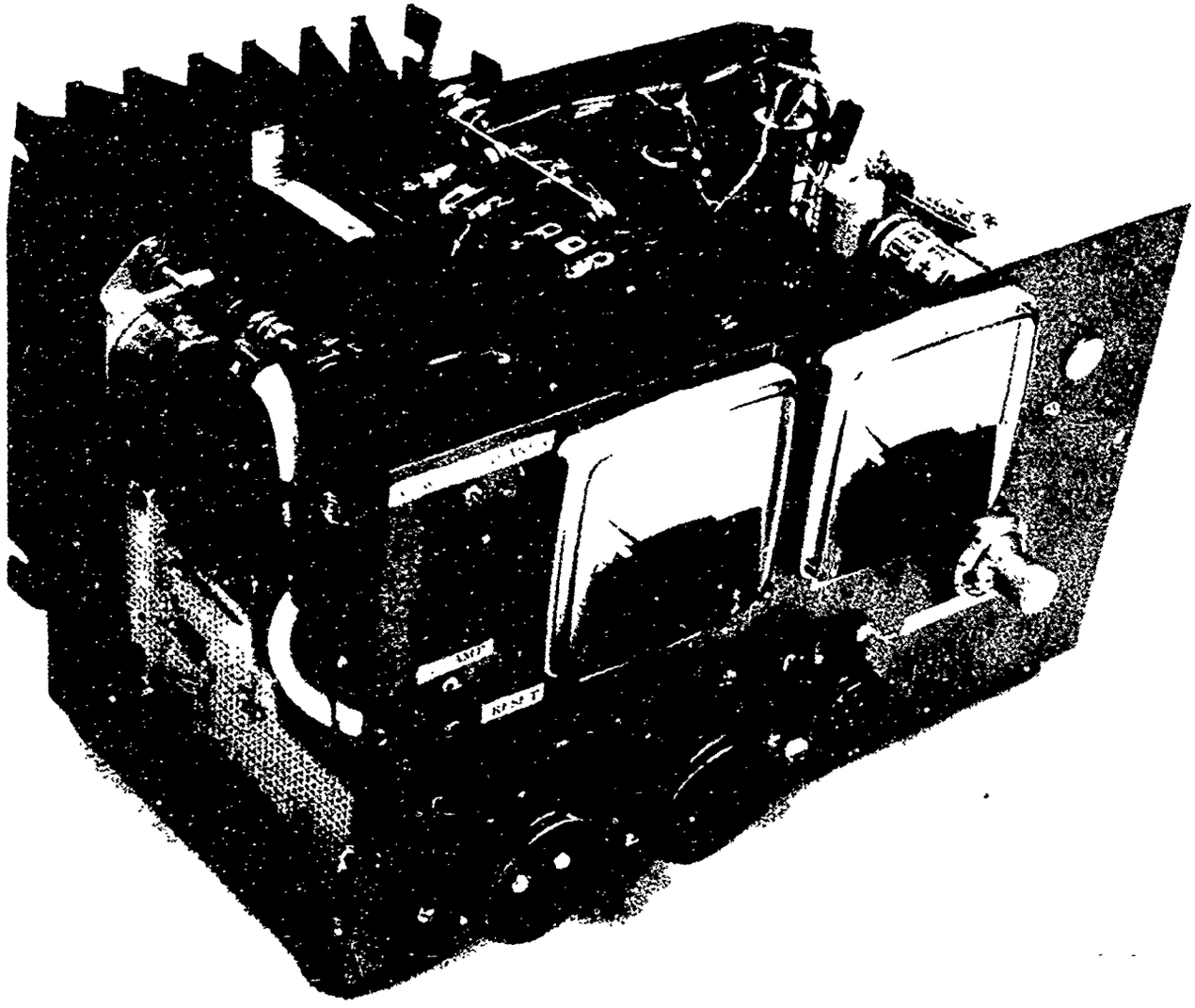

NEG. 376346

FIGURE 34. POWER CONDITIONER

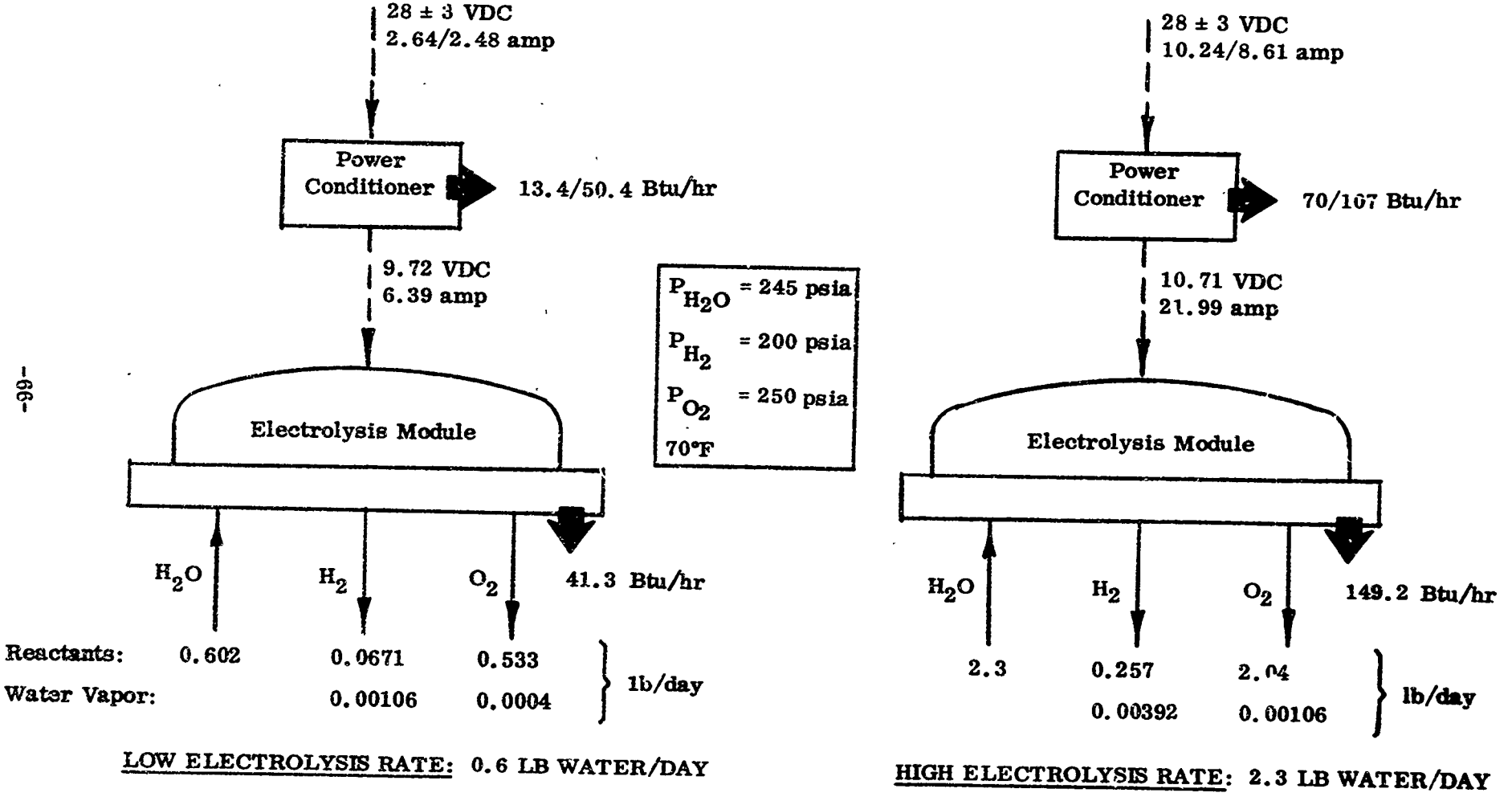

FIGURE 35. ELECTROLYSIS SUBSYSTEM - HEAT/MASS FLOW DIAGRAMS

3. SYSTEM STUDIES

A variety of methods for storing and delivering water to the electrolysis unit and storing gaseous hydrogen were studied. The basic design criteria used in developing water subsystems were as follows:

• Ambient Temperature:	40° F to 120°F
• Ambient Pressure:	Sea Level to Vacuum
• Water Purity:	Deionized, 2 Megohm Electrical Resistance Free of Fungus
• Water Quantity:	300 lbs
• Maximum Water Consumption:	2.3 lbs/day
• Minimum Water Consumption:	0.1 lbs/day
• Maximum Gaseous Propellant Pressures:	200 psia
• Minimum Gaseous Propellant Pressures:	67 psia
• Stored Hydrogen Volume:	2 ft^3
• Stored Oxygen Volume:	1 ft^3
• System Life:	7 Years

The above criteria were developed during preliminary system and mission analysis reported in Section III.

It was assumed that the delivery of water to the electrolysis unit and on-off control of the electrolysis unit should be controlled automatically by pressure switches on the hydrogen and oxygen tanks to the maximum possible extent.

Two optional components, a water deionizer and gaseous propellant desiccants, were included in the system studies, although their need was not definitely established.

The requirement for maintenance of deionized water for seven years raised the possibility that a mixed bed deionizer might be required in the system. Desiccants for drying the generated hydrogen and oxygen to avoid freezing in the gaseous propellant subsystem were also added to the system.

a. Pressure Balanced System

The first system concept evaluated was based on the use of a wick for supply of water to the solid polymer electrolyte. This system could be considered only for a water pressure identical to that within the electrolysis system and gaseous propellant tanks.

A schematic diagram of a pressure balanced system is shown in Figure 36. In a simple pressure balanced system, all water storage volumes would be connected by open passages and therefore would be isostatic. Oxygen would be stored in one or more tanks which would also contain water, with a bladder in each tank separating the oxygen from the water. The hydrogen and additional water would be stored in other tanks in a similar arrangement. Since electrolysis of water produces 2 moles of hydrogen for 1 mole of oxygen, the hydrogen volume in a pressure balanced system should be twice the oxygen volume. If this were the case, repetitive cycles of stoichiometric propellant usage and replenishment by electrolysis would always maintain equal pressure in the gas storage areas. If the initial hydrogen volume was twice the initial oxygen volume, and if two thirds of the water were initially stored in the hydrogen/water tank(s), with the other third of the water initially stored in the oxygen/water tank(s), stoichiometric consumption and replenishment of the H_2 and O_2 in a zero gravity, isothermal system would automatically force two thirds of the water consumed by the electrolysis unit to come from the hydrogen/oxygen tanks and would maintain equal pressure throughout the system.

The effects of gravity, temperature differences and nonstoichiometric engine firings on the pressure balanced system were evaluated. The following conclusions were reached.

(1) ΔV accelerations could transfer water from one hydrogen/water tank into another if multiple hydrogen/water tanks were used. This could be eliminated by using only one hydrogen/water tank or by using a check valve to allow water flow out of each tank but not in. A similar situation exists with the oxygen tanks. ΔV acceleration could also cause a slight shift of water from one propellant/water tank(s) to the other propellant/water tank(s) but this shift would be automatically reversed by the gas pressures as soon as the acceleration ceased.

(2) Unequal tank temperatures could cause unequal expansion or contraction of hydrogen and oxygen in any of the tanks, causing transfer of water between connected tanks. Check valves on the water outlet could prevent water transfer between tanks but would allow gaseous propellant pressures to become unequal. It was assumed that the hydrogen and oxygen pressures would not balance each other through the electrolysis unit, and this assumption has been confirmed by further study of the characteristics of the electrolysis unit.

(3) Nonstoichiometric engine firings followed by electrolysis replenisment would cause an accumulation of more of one gaseous propellant than could be stored in the idealized pressure balanced system. The gaseous propellant being accumulated would tend to push water from its tank(s) into the other propellant/water tank(s) in order to maintain equal water pressure. This shift in mass

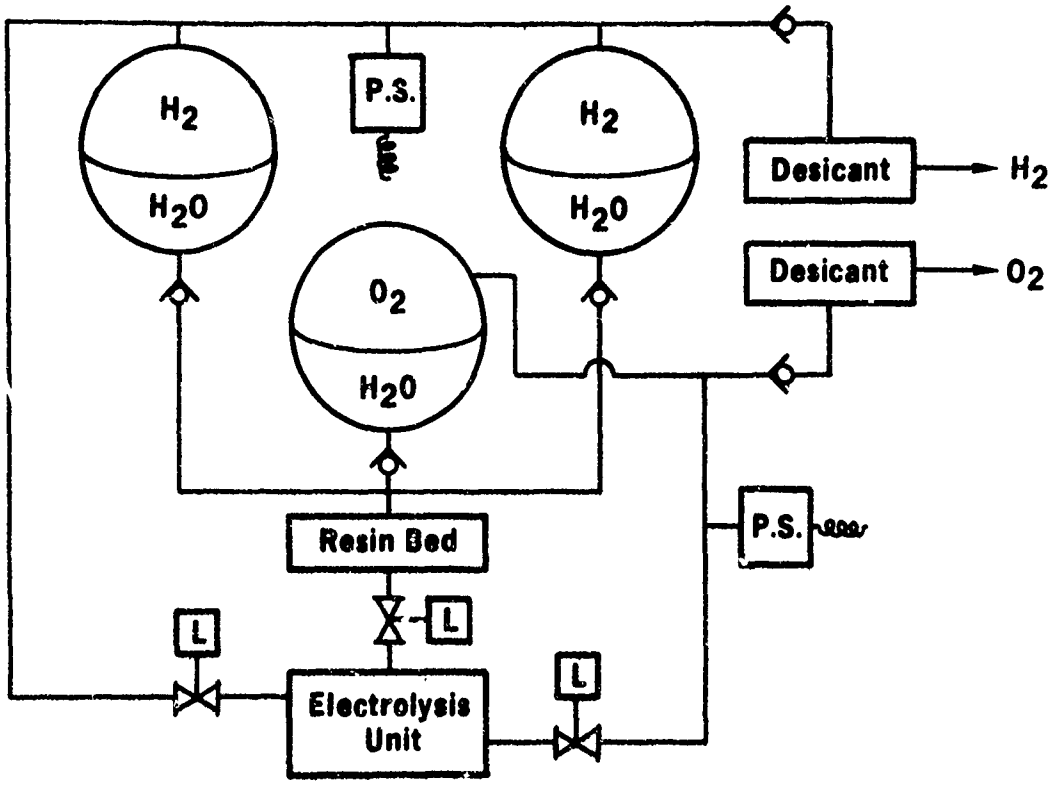

FIGURE 36. PRESSURE BALANCED SYSTEM

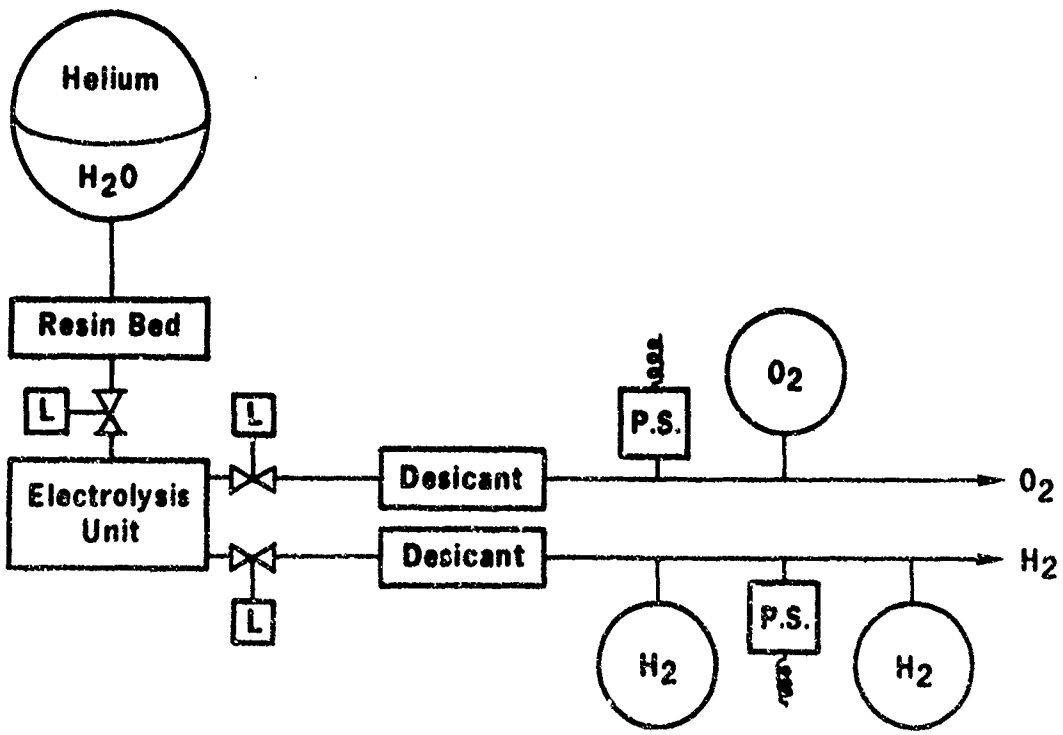

FIGURE 37. SIMPLE BLOWDOWN SYSTEM

is probably not a serious matter for a 3-axis stabilized vehicle but could well be a very serious problem for a spin stabilized vehicle. An exact evaluation of the effects of mass unbalance on wobble and orbit maintenance of the satellite would require a detailed analysis of a specific satellite and mission.

The mass shift caused by nonstoichiometric engine firings could be reduced in severity by check valves allowing water flow out of but not into each tank. However, there could still be a significant mass shift since check valves would allow the electrolysis water to be drawn unequally from the various tanks.

The major advantages of the pressure balanced system are that no pressurization system is required, and an open-close valve is not required between the water supply and the electrolysis unit.

The major disadvantage of the pressure balanced system is the shift of the center of gravity of water whenever the engine firings are not exactly at the stoichiometric mixture ratio.

The two causes of nonstoichiometric engine operation with the pressure balanced system are as follows:

(1) Nonstoichiometric ratio of O_2 and H_2 sonic orifice discharge coefficients

(2) Unequal temperatures of O_2 and H_2.

A two percent error in engine mixture ratio could cause significant mass balance shifts. It is not considered practical to achieve more than 1 percent accuracy in manufacturing sonic orifices. Temperature nonuniformities could easily produce more than a 1 percent shift in engine mixture ratios on a 3-axis stabilized vehicle, but would not be likely on a spin stabilized vehicle. The effects of nonstoichiometric sonic orifices would be reduced somewhat by statistical variability among a number of engines.

An additional disadvantage of the pressure balanced system is that the desiccant would have to be isolated from the gaseous propellants by check valves. Otherwise, water could continually diffuse across the bladders to keep the gaseous propellants saturated with water vapor. The design of a desiccator in this position would be rather difficult, since the gaseous propellants would pass through the desiccant very rapidly during blowdown operation.

b. Simple Blowdown System

The simple blowdown system is shown in Figure 37. In this system, all of the water is contained in one tank, which has a bladder and holds a volume of

pressurization gas initially at a comparatively high pressure. The feasibility of this system was made possible by General Electric's development of the use of a solid polymer membrane for controlled delivery of water to the electrolysis unit under relatively high pressure drop from water to hydrogen cell. As the water is removed, the pressurization gas expands and drops in pressure, falling to 200 psia when all of the water has been removed. The gaseous hydrogen and oxygen are stored in separate tanks after electrolysis.

The size and weight of the water tank depends on the initial pressure in a manner shown in Figure 38. If the initial pressure could be 600 psia, a 2.45-foot diameter tank would be sufficient to hold 5 ft^3 of water and enough pressurization gas to achieve 200 psia pressure when the water was all consumed.

The principal advantage of the simple blowdown system is that the center of gravity of the water would not shift because of nonstoichiometric engine firings, since all of the water would remain in the same tank.

Other advantages of the simple blowdown system would be that a pressurization system would not be required, and the gaseous propellants could be dried in desiccants before being stored in the O_2 and H_2 tanks.

The principal disadvantage of the simple blowdown system is that the pressure drop between the water tank and the hydrogen tank would be too high except for a very large water tank with a low initial gas pressure. This limitation arises from the fact that the solid polymer WFB which has been developed by General Electric Co. to supply water to the electrolysis unit under higher pressure drops between water and hydrogen than feasible with a wick feed is still somewhat limited in its current state of the art to tolerate very high pressure drops.

Almost all of General Electric's experience with the solid polymer membrane to date has been with a 0.010-inch thick membrane. GE has some evidence that the chemical and permeability characteristics of the membrane are not exactly linear, so that the performance of a WFB thicker than 0.010 inch would require test evaluation.

The maximum allowable pressure drop between water supply and hydrogen tank, using a single WFB, increases with the current being supplied to the electrolysis unit, which must be sufficient to electrolyze all of the water being transmitted across the WFB. For the electrolysis unit designed by General Electric using current WFB technology, the maximum pressure drop is only 12 psi for a current which electrolyzes 0.10 lb/day, increasing to 280 psi for a current which electrolyzes 2.3 lb/day. Therefore, the critical limitation of water to hydrogen pressure drop occurs at the minimum electrical current condition. Additionally, it would be necessary to close a valve between the water tank and the electrolysis unit whenever the electrolysis unit was turned off. Otherwise, water would slowly pass through the electrolysis unit into the hydrogen tank.

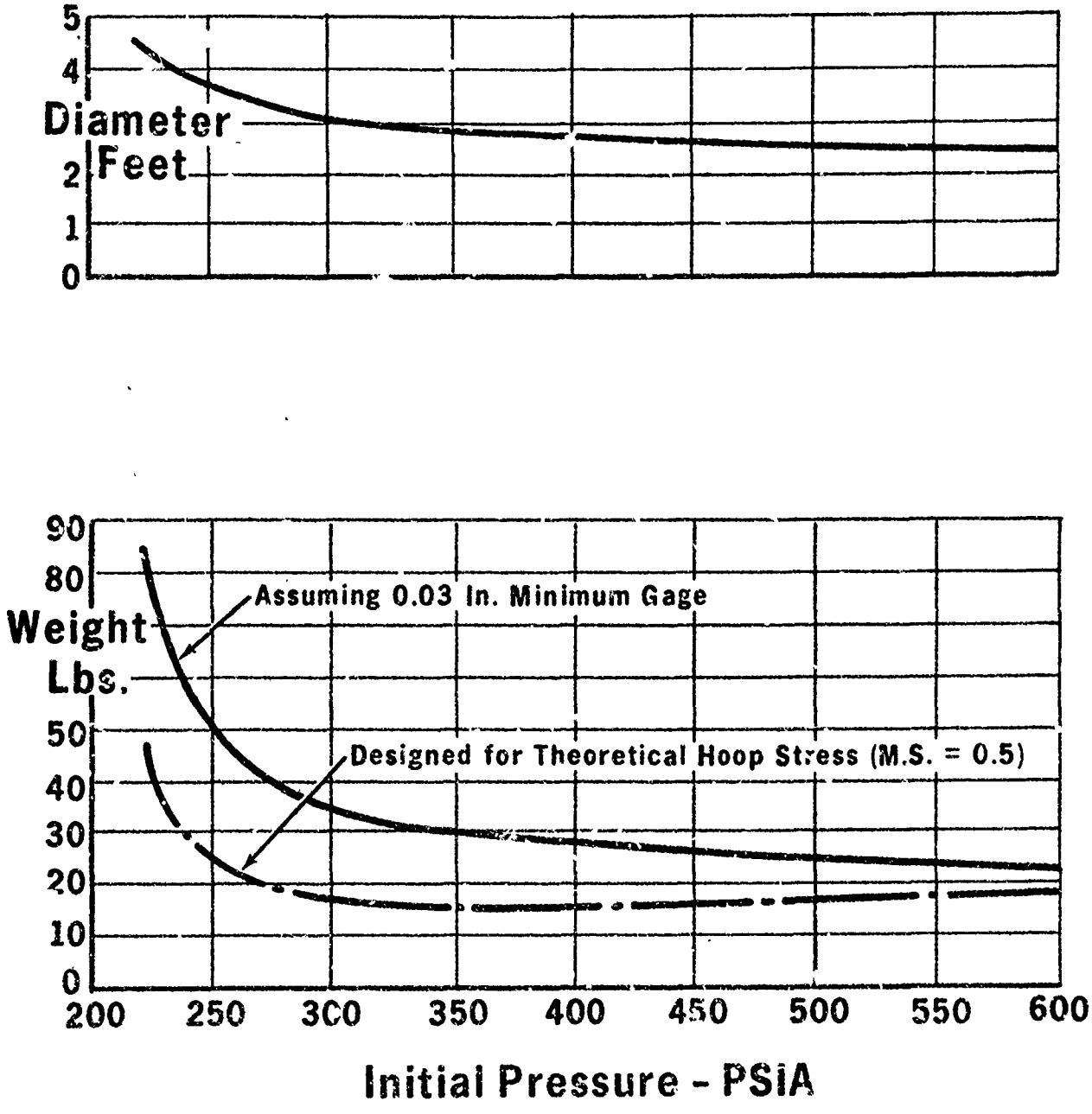

FIGURE 38. BLOWDOWN TANK DESIGN PARAMETERS

It was assumed that during engine blowdown when the gaseous propellant tanks drop from 200 psia to 67 psia, the electrolysis unit could operate in the high power mode. This would occur only during ΔV maneuvers.

c. Regulated Blowdown Systems

Two ways to modify the simple blowdown system so as to eliminate the problem of excessive water-to-hydrogen pressure drop would be to use a water pressure regulator or a hydraulic accumulator between the water tank and the electrolysis unit. The only disadvantage with the pressure regulator is the question of reliability and leakage. The combination of a pressure regulator and a valve which would close whenever the electrolysis unit was turned off might be a satisfactory system.

A hydraulic accumulator would operate with a limit switch which would open the upstream valve when the hydraulic accumulator had contracted to a minimum travel position and would close the upstream valve when the hydraulic accumulator had filled with enough water to extend to the maximum travel position. The two valves upstream and downstream of the hydraulic accumulator would be closed whenever the electrolysis unit was turned off, in order to eliminate any leakage of water through the electrolysis unit into the hydrogen tank. A small hydraulic accumulator which would hold 0.10 lb of water would experience about 3000 cycles during a seven-year mission. More engineering design and analysis would be required to establish the hydraulic accumulator design, and the reliability of this system would be questionable.

d. Repressurized System

Another way to avoid excessive water-to-hydrogen pressure drop would be to periodically repressurize the water tank. A large number of pressurization techniques could be considered, including the use of a high pressure gas bottle, a pulsing valve (or alternatively, a pressure regulator) and a relief valve to avoid overpressurization, as shown in Figure 39. A valve between the water tank and the electrolysis unit would be closed whenever the electrolysis unit was turned off.

The disadvantages of the repressurization system depend on the characteristics of the pressurization system. The system shown in Figure 39 appears to be a reliable system. Helium would be an excellent choice for the pressurization gas, since the weight of gas is very light. Any pressurization gas other than hydrogen could be used with the solid polymer WFB, since only H_2 would tend to be accumulated upstream of the WFB.

The amount of helium leakage to be expected in seven years through a valve from a 2000 psi bottle has been calculated to be 1/3 of the total volume of the water tank. The helium leak rate was assumed to be 0.1 scc/hr. Therefore, the relief valve would be activated only in the case of unusual leakage or extreme temperature increase.

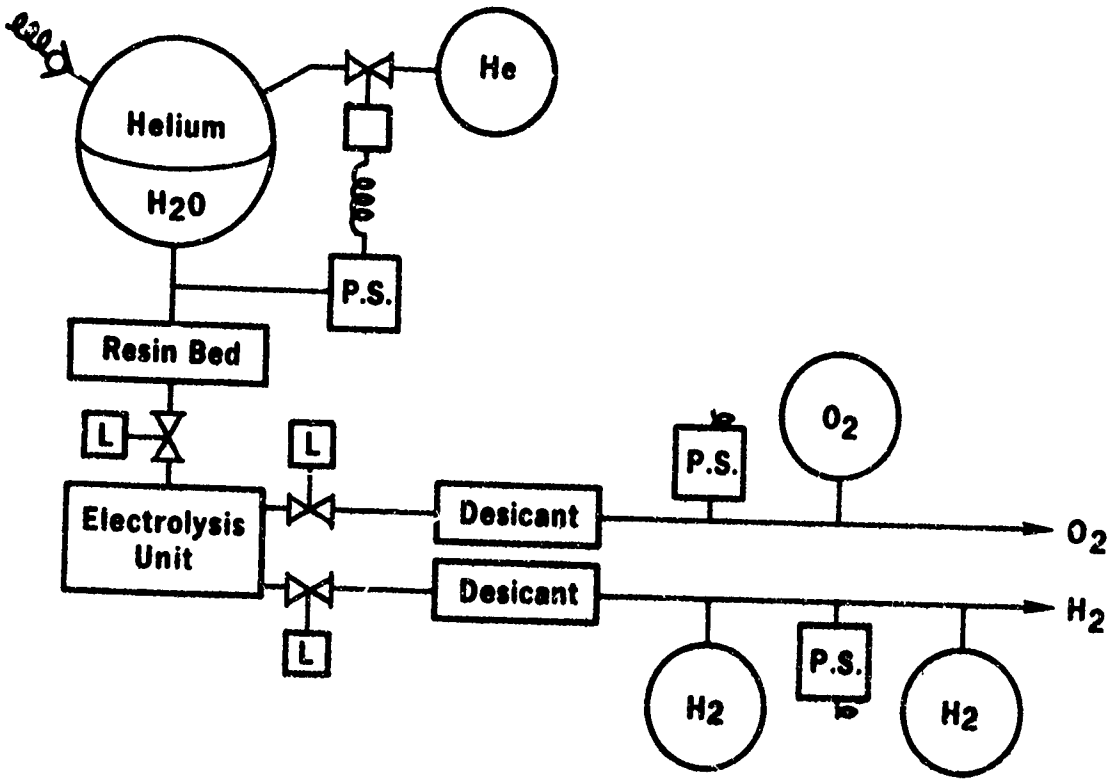

FIGURE 39. REPRESSURIZED SYSTEM

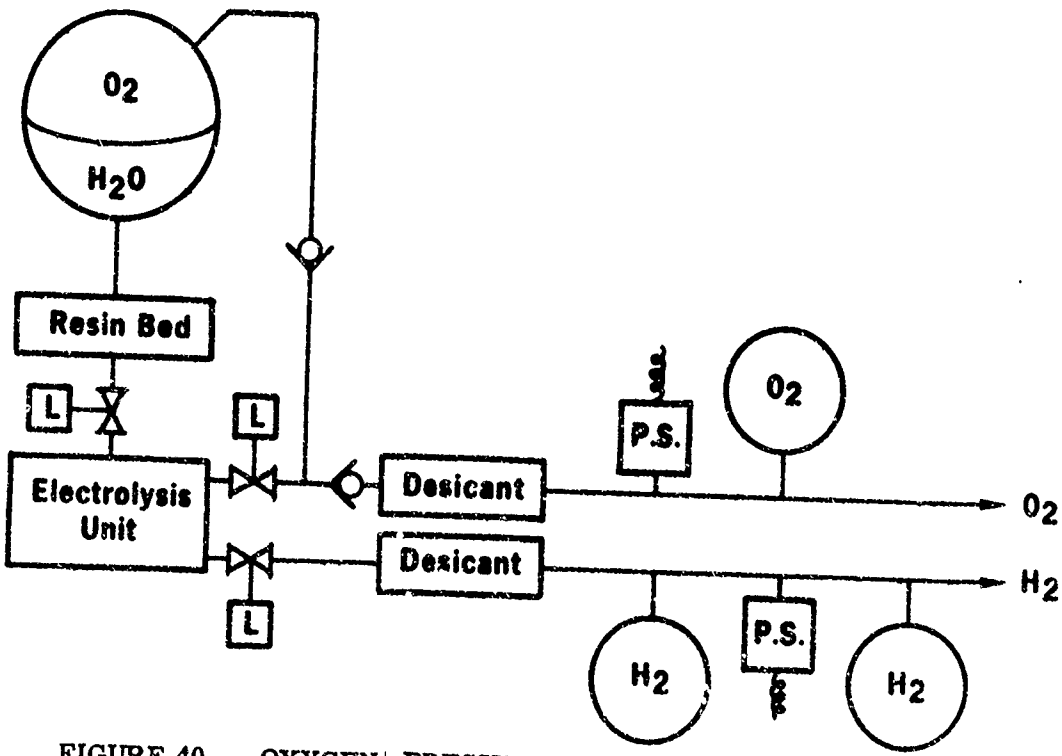

FIGURE 40. OXYGEN PRESSURIZED SYSTEM

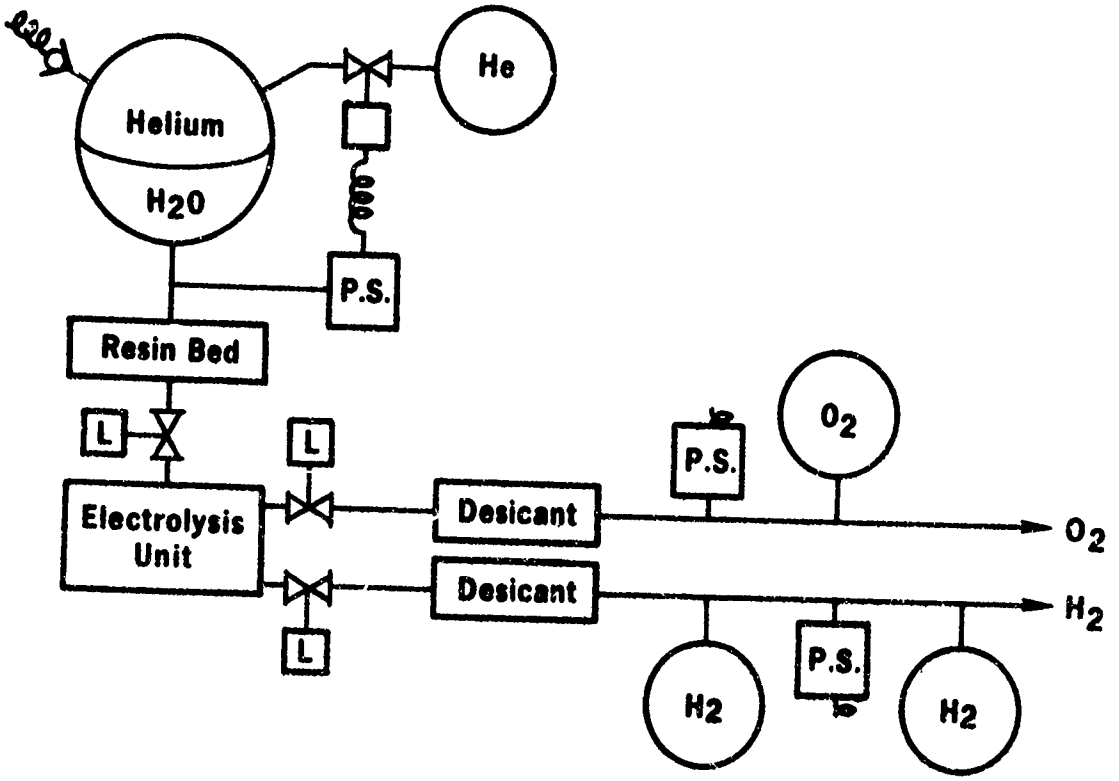

FIGURE 39. REPRESSURIZED SYSTEM

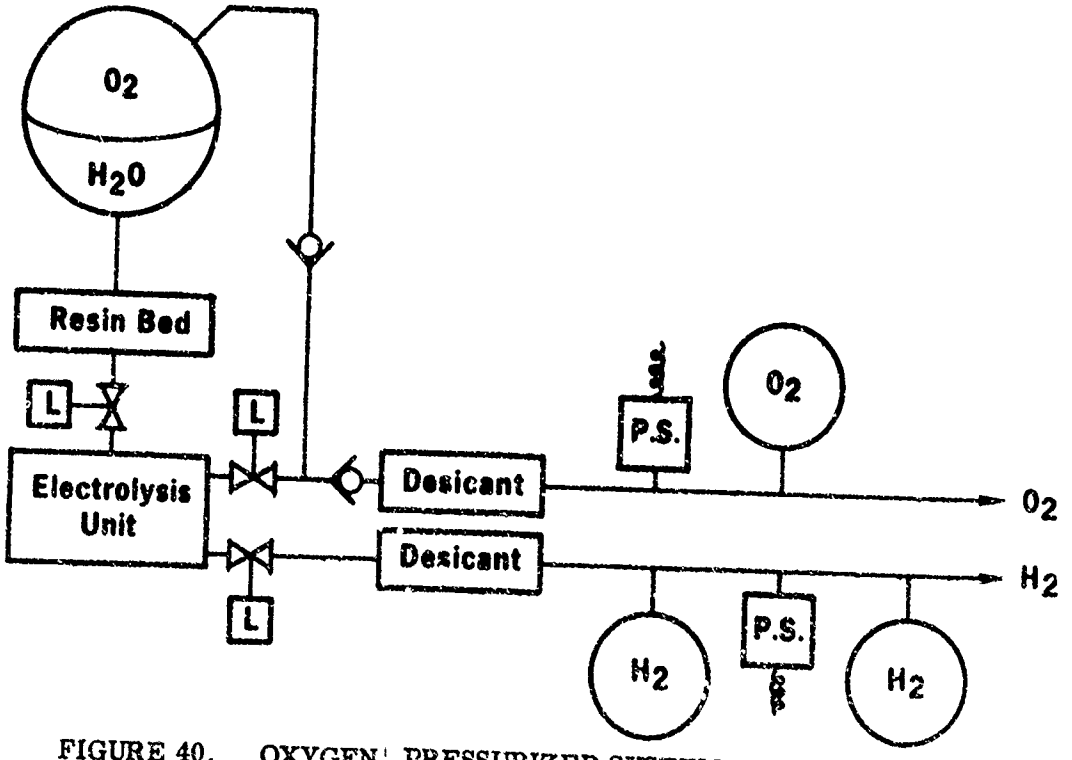

FIGURE 40. OXYGEN PRESSURIZED SYSTEM

One of the important characteristics of the helium repressurization system is the fact that leakage through the helium valve would not in itself cause a serious problem. On the other hand, leakage of water through a water pressure regulator, a hydraulic accumulator, or water valves would permit water flow into the hydrogen tank which would be a serious problem.

Elimination of the water-to-hydrogen pressure drop during blowdown by venting off pressurization gas would not be desirable because of the large weight of pressurization gas required for the several hundred engine blowdown cycles.

e. Oxygen Pressurized System

A water supply system based on self-pressurization by oxygen output from the electrolysis unit is shown schematically in Figure 40.

The pressure in the water tank is maintained by placing a check valve in a line between the oxygen outlet from the electrolysis unit and the water tank. The cracking differential pressure of this check valve can be some small value such as 5 psid. Another check valve is placed in the line going to the oxygen storage tank. If this check valve has a cracking differential pressure of 20 psid, the electrolysis oxygen outlet pressure would vary during blowdown from 220 psia down to 87 psia for oxygen tank pressures of 200 psia to 67 psia, respectively. The maximum water tank pressure would therefore be 215 psia. During portsions of a blowdown cycle, the water tank would not receive oxygen pressurization and would therefore slowly drop. All of the generated oxygen would then go into the storage tank until the storage tank pressure rose somewhat above 185 psia. At this point oxygen could pressurize the water tank if the water pressure were down to 200 psia. The 5 ft^3 of O_2 at 200 psia required to pressurize the water tank would not be usable as propellant. This amount of O_2 is 2% of the total O_2 generated from 5 ft^3 of H_2O.

The time required to empty and refill the O_2 and H_2 tanks during blowdown is shown in Figure 41. These tanks will have to be small enough in the oxygen repressurized system that the water tank pressure will not drop below 200 psia during the refill cycle, but this does not place any significant restriction on the system.

The water will be saturated with dissolved oxygen, unless a metalized impervious bladder were used. The dissolved oxygen will readily pass through the water feed barrier into the H_2 screen manifold (about 0.010-inch thick) adjacent to the SPE cathode. General Electric believes that practically all of the O_2 dissolved in the H_2O will react with H_2 along the catalytic cathode surface, forming a small amount of H_2O vapor which will then enter the normal electrolysis process of the SPE. However, there is a possibility that some small amount of O_2 could pass into the H_2 tank. This can only be explored in tests of the system in the oxygen pressurized mode.

The oxygen pressurized system could be simplified by eliminating the check valves on the oxygen side and using much larger O_2 and H_2 tanks. Analysis of a system with O_2, H_2 and H_2O tank volumes of 2.5 ft^3, 7.5 ft^3 and 5 ft^3, respectively,

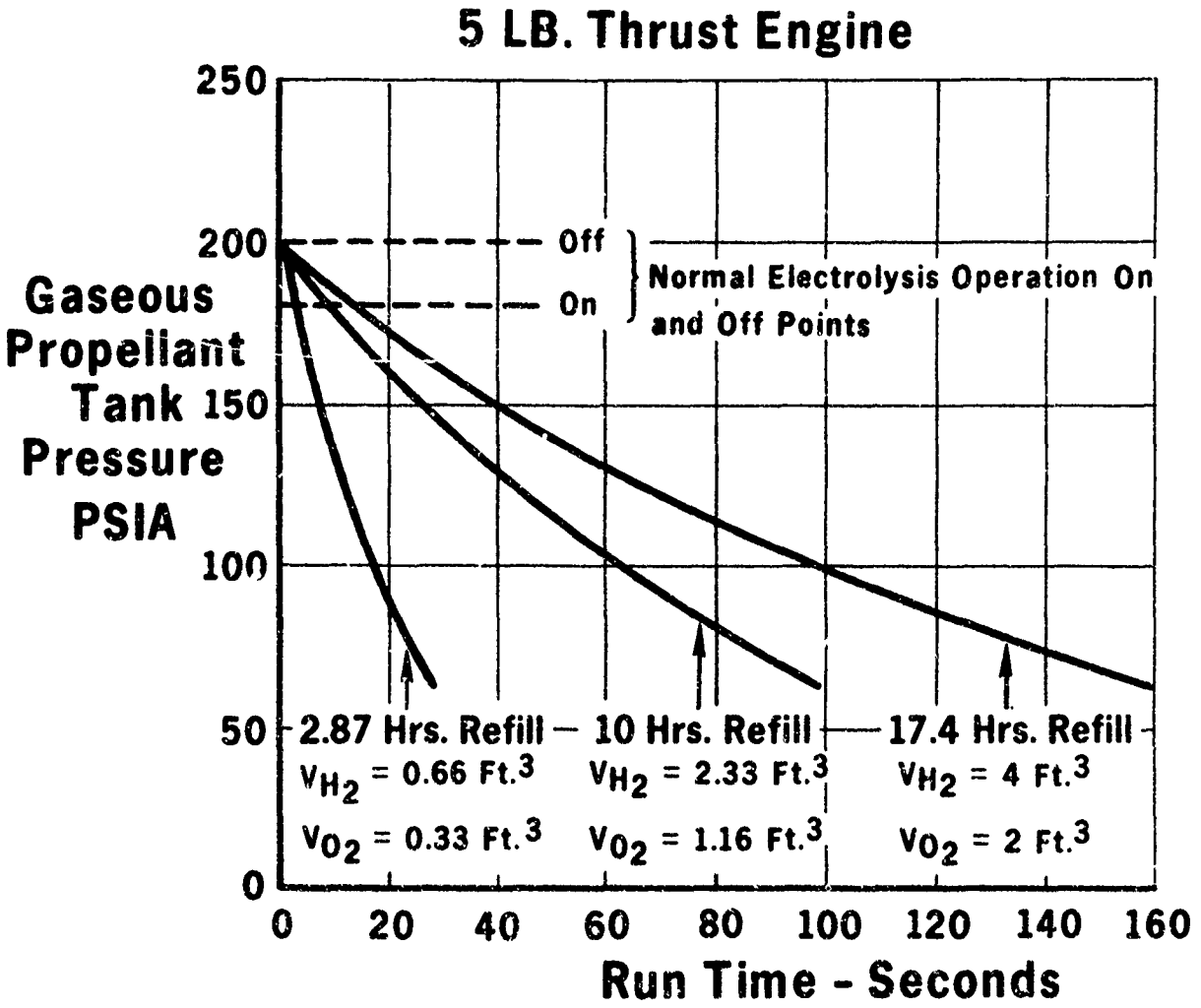

FIGURE 41. GASEOUS PROPELLANT TANK PRESSURE VS RUN TIME

shows that a system could be devised which would have a maximum pressure of H_2 of 180 psia, a maximum pressure of O_2 of 200 psia, and could operate without check valves. The total O_2 volume would vary from 2.5 ft^3 to 7.5 ft^3 during the mission. The O_2 pressure drop for a blowdown impulse of 100 lb/sec would vary from 18 psia at the start of a mission to 6 psia at the end. The H_2 pressure drop during each blowdown would be a constant 12 psia.

The disadvantages of this system are the additional weight of the larger tanks, and the fact that the engine O/F would shift on the order of 4% during a blowdown. The major advantage would be the low pressure drop (about 20 psia) between the water tank (O_2 pressure) and the H_2 tank at all times. A computer program analysis would be required to fully evaluate the cumulative effects of O/F variation.

4. SYSTEM COMPARISON

A comparison of various types of propellant supply systems was made in order to establish the design for the ground test system.

The weights of those components which would be unique to each of the systems are given in Figure 42. The heaviest system would be the simple blowdown system with a water-to-hydrogen pressure drop capability in the low power mode of 70 psia. This system, which would have a maximum water pressure of 250 psia, would be 25 to 30 pounds heavier than the other systems. An increase of H_2O to H_2 pressure drop capability of the electrolysis unit to allow a water pressure of 400 psia would reduce the simple blowdown system weight to about the same as other systems considered.

The oxygen pressurized blowdown system without check valves would minimize the H_2O - H_2 pressure drop limitation and appears to be feasible even with the existing electrolysis unit. The principal disadvantage, in addition to the O/F variation, would be an additional weight of O_2 and H_2 tanks of about 20 pounds (not included in Figure 42).

A comparison of the principal features of the various systems is shown in Figure 43. It was concluded that some form of blowdown system is preferable to a pressure balanced system for the purposes of the present program, primarily because of the mass unbalance problem with a pressure balanced system. However, the solid polymer water feed barrier, which G. E. considers much more reliable than a wick feed, would not be feasible with a pressure balanced system because of dissolved hydrogen blockage, and was therefore another reason for choosing the blowdown system.

5. GROUND TEST SYSTEM

A ground test system, which is described in detail in the appendix, and whose end view is shown on Figure 44, was designed and fabricated for this program. The system includes a six-cell electrolysis unit, a water supply system, and a gaseous propellant storage system which is capable of three modes of operation. Flow schematics of the three modes are shown in Figure 45.

SYSTEM	SYSTEM WEIGHT
SIMPLE BLOWDOWN (250 PSIA) H_2O TANK (250 PSIA MAX.)...49.5 LBS. HELIUM GAS (250 PSIA MAX.)... 3.3 LBS.	52.8 LBS.
SIMPLE BLOWDOWN (400 PSIA) H_2O TANK (400 PSIA MAX.)...27.2 LBS. HELIUM GAS (400 PSIA MAX.)... 1.3 LBS.	28.5 LBS.
REPRESSURIZED BLOWDOWN H_2O TANK .....17.0 LBS. HELIUM TANK ..... 4.0 LBS. HELIUM GAS..... 0.8 LBS. SOLENOID VALVE..... 0.3 LBS. PRESSURE SWITCH ..... 0.2 LBS. RELIEF VALVE ..... 0.2 LBS.	22.5 LBS.
OXYGEN REPRESSURIZED BLOWDOWN H_2O TANK .....17.0 LBS. OXYGEN GAS ..... 5.5 LBS. 2 CHECK VALVES ..... 0.4 LBS.	22.9 LBS.
PRESSURE BALANCED 1 OXYGEN/WATER TANK..... 9.4 LBS. 2 HYDROGEN/WATER TANKS...18.8 LBS. 5 CHECK VALVES ..... 1.0 LBS.	29.2 LBS.

FIGURE 42. SYSTEM INCREMENTAL WEIGHT COMPARISONS

System	Mass Unbalance	$P_{H_2O} \cdot P_{H_2}$ Limitation		Dissolved Gas Blockage	Other Disadvantages
		Current	Future		
Pressure Balanced, Wick Feed	Yes	No	No	No	Wick Reliability, Desicant Location, 5 Check Valves
Pressure Balanced, WFB	Yes	No	No	Yes	Desicant Location, 5 Check Valves
Simple Blowdown, WFB	No	Yes	No	No	Current Weight Ponalty
Repressurized WFB	No	Marg.	No	No	H_e Pressurization System Reliability
Hydrogen Repressurized WFB	No	Marg.	No	Yes	O/F Variation
Oxygen Repressurized WFB	No	Marg.	No	No	O/F Variation, Trace O_2 in H_2

FIGURE 43. SYSTEM COMPARISON

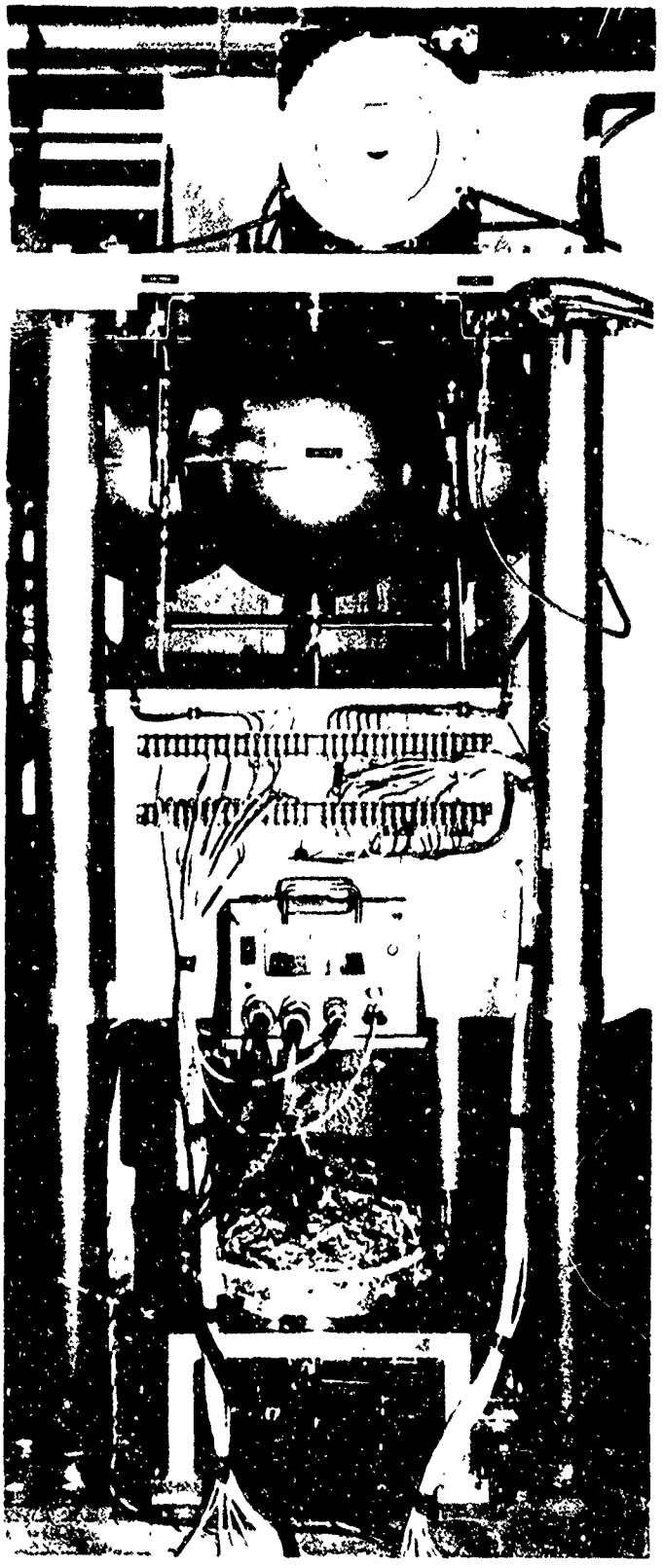

NEG. 72-2264

FIGURE 44. END VIEW OF GROUND TEST SYSTEM

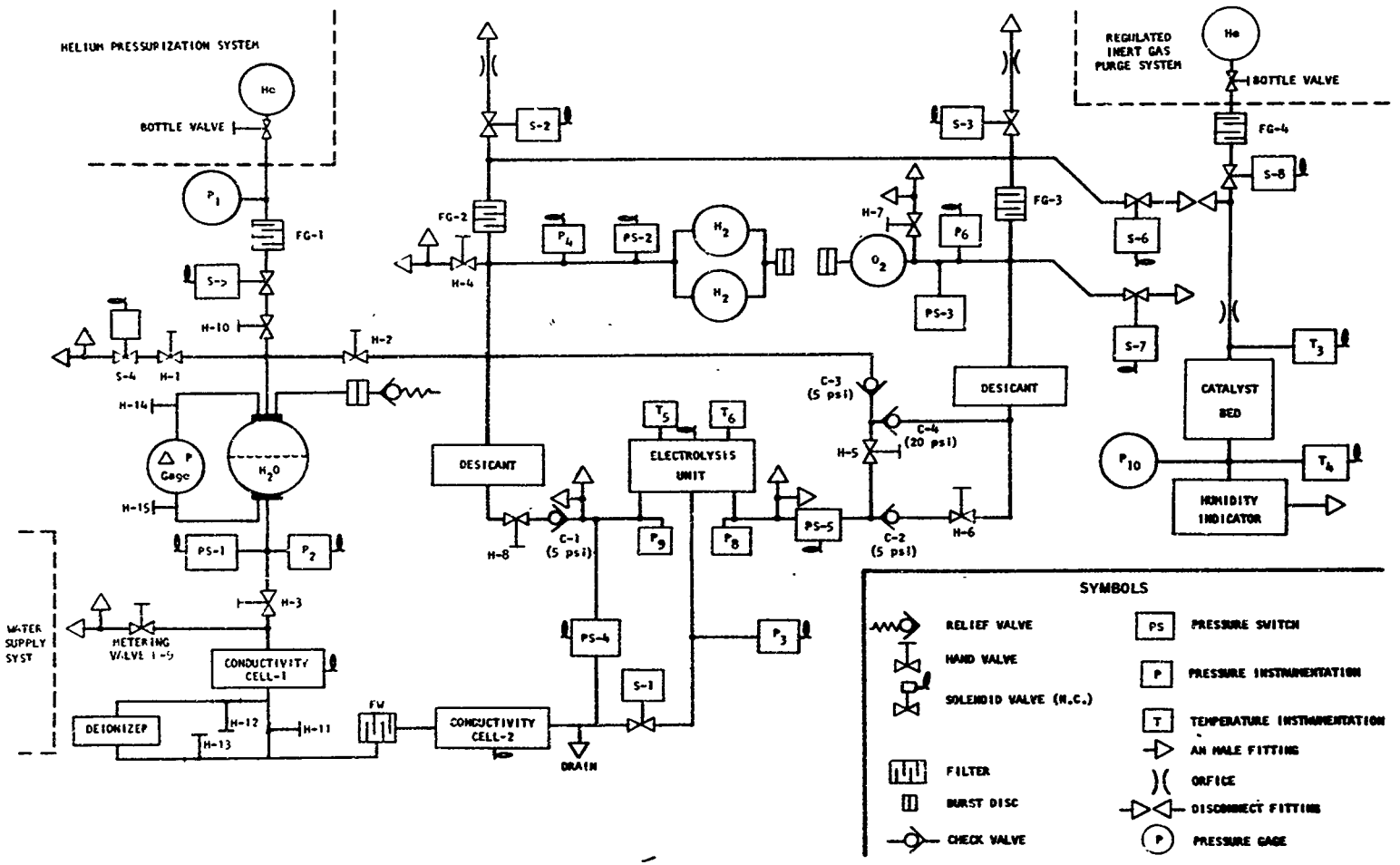

FIGURE 45. GROUND TEST SYSTEM

- Simple Blowdown
- Repressurized
- Oxygen Pressurized

For operation in the simple blowdown mode, hand valves H-10 and H-5 are closed and the water tank is pressurized with helium to the desired level.

For operation in the repressurized mode, hand valve H-10 is opened and helium is periodically added to the water tank through solenoid valve S-5 actuated by pressure switch PS-1.

For operation in the oxygen pressurized mode, hand valves H-6 and H-10 are closed, and H-2 and H-5 are opened.

6. SYSTEM TESTING

a. July 12, 1972

The ground test system was assembled and checkout tests were performed in Marquardt precision rocket laboratory Pad E. The water tank was filled with 45 gallons of ultra pure deionized water with an electrical resistance of 14 megohms or greater. The top of the water tank was connected to a vacuum system during the four-hour period required to load the water to remove most of the dissolved air from the water. The hydrogen system was evacuated, filled with helium, and evacuated again before loading with gaseous hydrogen.

b. July 13, 1972

The power conditioner was turned on with a low water tank pressure so that initial operation was in the low power mode. The water tank pressure was then gradually increased over a period of one hour to a pressure of 195 psig, giving a pressure drop from water to hydrogen greater than 70 psi, but the power conditioner would not switch into the high power mode. It was concluded that the test cell power supply did not have adequate current to switch the power conditioner.

c. July 14, 1972

A larger power supply was installed in Pad E with a capacity of 50 amps at 40 volts. The power conditioner was turned on with low water pressure. The electrolysis unit was then operating in the low power mode, but the current was 10 amps and could not be manually adjusted any lower. The water pressure was then increased to 220 psig and the power conditioner switched into high power mode.

d. July 19, 1972

A summary of the system testing on July 19 is given in Table 11. The electrolysis cell was activated in the high power mode with gas tanks at 155 psig and the water tank at 210 psig. Some rusty water was drained from the oxygen cell during the activation procedure.

The electrolysis unit switched to the low power mode when the hydrogen cell reached 153 psig, with a water-to-hydrogen pressure drop of 57 psid, compared with the desired val ue of 70 psid. The low power current was successfully adjusted with the manual adjustment over the range of 1 to 15 amps, contrary to the experience of the previous day. The current was then adjusted to 15 amps in the low power mode to speed up the rate of gas generation.

The hand valve H-10 was opened and the helium pressurization system opened until the water tank reached 240 psig, showing that pressure switch PS-1 and solenoid valve S-5 were working properly. The water tank pressure dropped to 238 psig during cooling after the pressurization.

The power conditioner shut off current when the oxygen pressure reached 191 psig, at which time the hydrogen pressure was 189 psig. This compared with a nominal maximum gas pressure of 185 psig.

The power conditioner switched to standby mode after being off for 18 minutes, during which time the oxygen cell pressure P_8 had dropped to 144 psig, the hydrogen cell pressure had dropped to 177 psig, and the water inlet pressure (between the isolation valve S-1 and the WFB) had dropped from 238 psig to 198 psig. The power conditioner was then on in the standby mode for 38 minutes and turned off when the oxygen cell pressure reached 177 psig, at which time the water inlet pressure had dropped still further to 159 psig. After 10 minutes off, the power conditioner switched to standby, at which time the oxygen cell pressure had dropped to 144 psig, and the water inlet pressure had also dropped to 144 psig, lower than the hydrogen cell pressure of 156 psig.

This series of standby cycling tests revealed that the water inlet pressure drops below the hydrogen cell pressure during standby operation. This raises the possibility of diffusion of hydrogen across the WFB, creating bubbles of hydrogen which might block the WFB during subsequent operation. Further testing will be required to understand this behavior.

A blowdown of the hydrogen and oxygen tanks was made at the end of the day. It was found that the oxygen tank pressure did not drop as rapidly as the hydrogen tank pressure. Subsequent investigation showed that the oxygen valve S-3 was malfunctioning and it was replaced.

TABLE 11

ELECTROLYSIS SYSTEM TEST RESULTS, JULY 19, 1972

Date	Time	Tank/Inlet PH_2O (psig)	(Cell) PO_2 (psig)	(Cell) PH_2 (psig)	(Tank) PH_2 (psig)	(Tank) PO_2 (psig)	Volts vdc	Amps	T_{Cell} °F	V1 vdc	V2 vdc	V3 vdc	V4 vdc	V5 vdc	V6 vdc	Resist. H_2O (megohm)	Power (watts)	
July 19	0945	210 / 210	0	0	156	153	10.14	22.00	70	-	-	-	-	-	-	-	236	High power at start
	1027	210 / 210	114	153	156	154	11.18	23/14	84	1.726	1.682	1.714	1.744	1.694	1.712	-	156	Switch to low power setting
	1205	238 / 210	175	173.5	167	165	10.90	14.62	76	1.729	1.694	1.722	1.758	1.699	1.717	-	160	Check repressurization circuit
	1308	238 / 238	183	180	175	173	10.90	14.62	82	1.727	1.693	1.722	1.760	1.699	1.718	-	160	
	1405	238 / 238	190	186.4	181	180	10.90	14.62	82	1.725	1.693	1.722	1.759	1.699	1.718	-	160	
	1414	238 / 238	191	189	182	182	10.90	14.6/0	82	-	-	-	-	-	-	-	160/0	Standby
	1432	238 / 198	144	177	183	182	8.90	0/.95	78	1.531	1.525	1.534	1.533	1.528	1.527	1.0-1.8	0/8.5	
	1510	238 / 159	177	159	183	182	9.85	0.90/0	72	-	-	-	-	-	-	-	9.0/0	
	1520	238 / 144	144	156	183	182	9.05	0/0.80	74	1.526	1.520	1.527	1.523	1.521	1.522	-	0/7.2	
	1542	238 / 238	174/143	156/128	183/125	182/162	9.80	0.80/23	70	-	-	-	-	-	-	-	225	Blowdown & switch to high power
	1600	238 / 238	175	128	125	162	11.0	23.2	92	1.721	1.707	1.726	1.740	1.702	1.729	-	255	Shutdown

e. July 24, 1972

The 316 stainless lines and fittings attached to the oxygen cell outlet were disassembled. Rust was found throughout these lines, including check valve C-2. The rest of the oxygen system was examined for rust and was found to be clean except for the threaded cap on the mild steel oxygen desiccant cylinder which had been electroless nickel plated on the inside. An investigation into the cause of the rust revealed that the four swagelok fittings on the access ports of the electrolysis unit had not been annealed after being welded to a machined stainless part before assembly in the electrolysis unit.

The mixture of oxygen and condensed water is very corrosive and will attack the heated zone near the weld unless the carbide precipitation resulting from weld heat is removed by annealing.

The weld joint on the four access fittings was covered with a 1-inch long section of ABS cycolac plastic tube bonded in place with Shell 828 epoxy to prevent rust from entering the system.

7. DEIONIZED WATER TESTS

A literature survey was made to locate data on electrical resistivity of deionized water stored for long periods of time. Although there is a large amount of data on corrosion of various metals in deionized water, such as that in References 2 and 3, the emphasis has been on the effects on the metal rather than the effects on the water. However, some information was obtained on water resistivity. For example, it was noted in Reference 3 that the resistivity of deionized water flowing in a stainless steel line was 10 megohms but was only 1 megohm when quiescent.

The ultra pure was loaded into the ...or tank on July 12, 1972 by flowing through a mixed resin bed. The resistance of the water was a minimum of 14 megohms leaving the deionizer and was 18 megohms for most of the time. The deionizer in the ground test system was isolated from the rest of the water system by keeping hand valves H-12 and H-13 closed. On July 18, both conductivity cells in the system indicated resistance much less than 1 megohm. Some water was flushed out of the system past conductivity cell No. 2, and the resistance rose immediately to 4 megohms. After turning off the water flow, the resistance drifted slowly downward, reaching 1.8 megohms after several hours.

On July 19, Cell No. 1 recorded 0.96 megohm and Cell No. 2 recorded 1.8 megohms. On July 24, the readings were 0.18 and 0.65 megohms on conductivity cells Nos. 1 and 2, respectively. On July 26 the same readings were 0.13 and 0.46 megohms, and on July 31 the readings were 0.09 and 0.26 megohms.

---

2. Johnson, Barbara A., Corrosion of Metals in Deionized Water at 38°C (100°F), NAS A-TM-X-1791, May 1969.

3. Symposium on High Purity Water Corrosion, ASTM Spec. Pub. No. 179, June 1955

On September 6, water was flushed out of the system past both conductivity cells, which immediately recorded 2 megohms. By September 12, with no water flow in the interim, Cell No. 1 had fallen to 0.3 megohm and Cell No. 2 was 0.7 megohm.

The above behavior indicates that the indicated electrical resistance of the water is very sensitive to the presence or absence of water velocity. Inquiries to Beckman Instruments and Balsbaugh were made, but no explanation of this phenomenon is presently available, since practically all water deionization work is done with flowing systems. However, it is believed that the resistance of 2 megohms measured in flowing water which had been stored in the stainless steel system for nearly two months is the correct indication of water ion level. Therefore, it is expected that the deionizer in the ground test system will not be required during future long term system testing.

SECTION IV-B

5-POUND THRUST ROCKET ENGINE

The objective of the 5-pound thrust engine program was to develop a gaseous oxygen-gaseous hydrogen rocket engine which operates at a mixture ratio of approximately 8 and will ignite 100% of the time. The design goal specific impulse for the engine was 350 seconds at steady state and 300 seconds at 50 milliseconds electrical pulse width. In addition, the engine should have the capability of igniting up to 150,000 times and a steady state burn capability in excess of five hours.

1. SUMMARY OF RESULTS FROM PROGRAM

During this program, over 69,700 ignitions and 10,031 seconds of burn time were attained on the 5.0-pound thrust engine shown in Figure 46 during a test firing. Termination of the 5-pound engine tests prior to the steady state documentation tests was caused by an injector premix orifice weld failure and subsequent combustor erosion due to the interaction of the melted nickel with the $MoSi_2$ coating on the molybdenum combustor. The performance of the engine with a 40:1 exit nozzle expansion area ratio during steady state was 345 seconds (see Figure 47) as documented by thrust measurements. The performance at 1/3 of the nominal thrust was approximately 315 seconds. Pulsing performance was higher than the design goal of 300 seconds (310-315 seconds at 50 ms) as shown in Figure 48. Ignition was documented at electrical pulse widths down to 20 ms.

Duty cycle verification tests were conducted at 50, 100 and 250 ms to accumulate 75,000 cycles. Prior to the duty cycle verification tests, a series of performance characterization tests and one steady state thermal test was run to obtain performance.

2. ENGINE DESIGN

The design of the 5-pound thrust rocket engine was based on prior experimental work at Marquardt and related contractor studies which showed that performance efficiencies up to 95% of theoretical could be obtained with present injector concepts. Since the design of the ignitor and injector was to be based on prior studies, the analytical effort was oriented toward thermal management. As will be shown later, the inclusion of this area significantly affected the injector concept.

a. Basic Design Criteria

The basic design characteristics of the 5-pound thrust rocket engine are shown in Table 12 for the initial engine configuration. The only characteristics to change during the program were the type of injector element and the energy source.

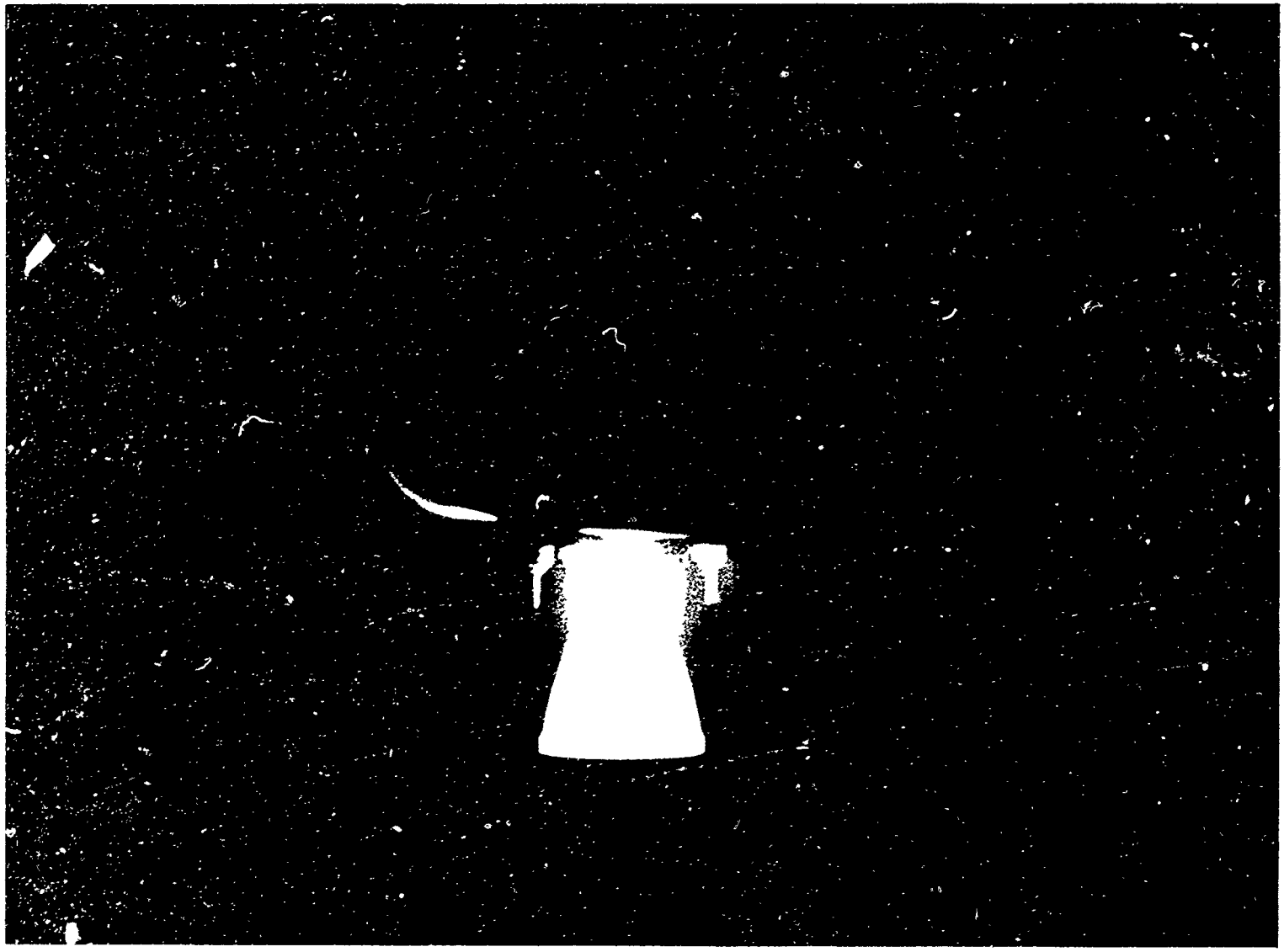

NEG 72-230-9

FIGURE 46. 5 LB_f THRUSTER OPERATING AT 0.25 SEC. ON/0.75 SEC. OFF - 1000 CYCLES

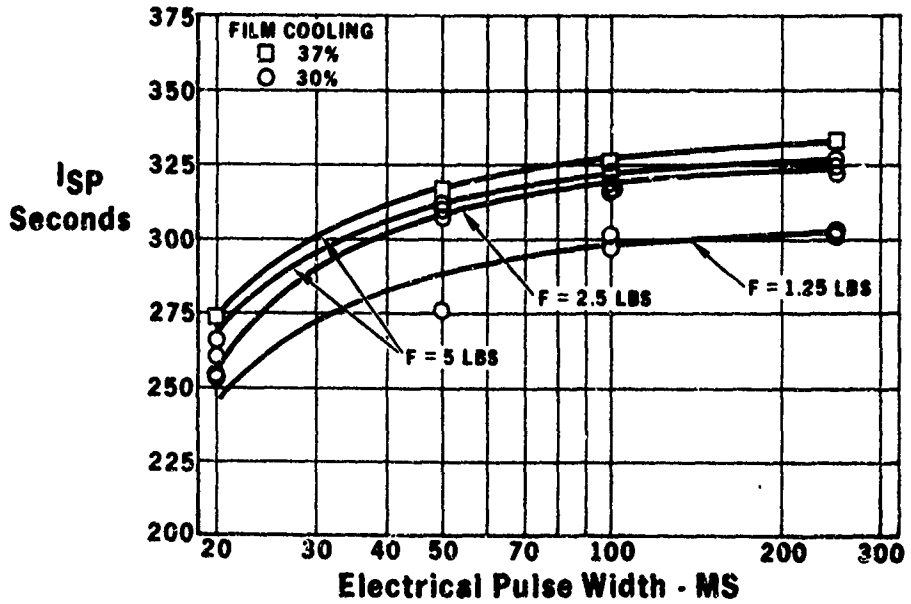

FIGURE 47. SPECIFIC IMPULSE VS ELECTRICAL PULSE WIDTH AT O/F = 8, 5LB_f THRUSTER

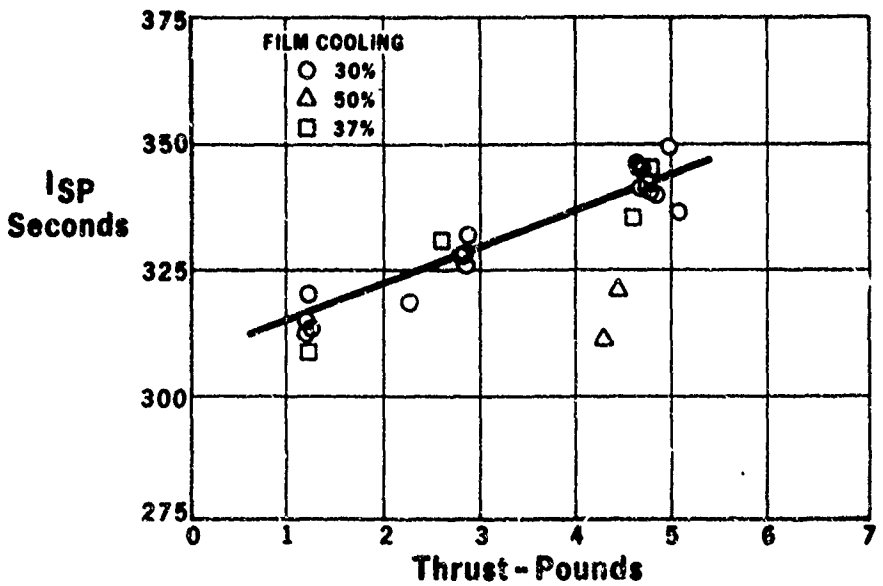

FIGURE 48. SPECIFIC IMPULSE VS THRUST AT O/F = 8, 5 LB_f THRUSTER

TABLE 12. 5 LBF THRUSTER DESIGN CHARACTERISTICS

5 LB THRUST O_2/H_2 ROCKET ENGINE

Design Characteristics

O/F = 8

- 5 Lb Thrust at 50 psia chamber pressure
- Blowdown capability to 16.7 psia (1.67 lb thrust)
- Combustion Chamber - Exit Nozzle
  - Molybdenum Coated with $MoSi_2$
  - Contraction Area Ratio - 10
  - Expansion Area Ratio - 40
- Fuel Film - Radiation - Conduction Cooled
- Nickel Injector
  - 6 Coaxial Elements
  - $VH_2/Vo_2 = 4$
  - FHE 231 Spark Igniter (Champion) Modified to Remove Semiconductor (Shut) Material with Capacitive Discharge Energy Source (450⟶10 Millijoules/Spark at 200 sps)
- Valves
  - 2 R-4D Coaxial Solenoid
  - Capability to Install Latching Type Low Power Valves
- Bolted Construction for Ease of Refurbishment

The engine consists of individual elements which are bolted together. The major elements are:

- Injector
- Combustion Chamber
- Valves
- Igniter

(1) Injector

The 5.0-pound thrust engine injector originally consisted of a series of six coaxial elements with nominal injection velocities of 1000 ft/sec for H_2 and 250 ft/sec O_2. The final design used a premix configuration. The flow rates were controlled by sonic orifices consisting of rounded entrances to the orifice which will discharge through a flat downstream face. The velocity and mass flow of the H_2 coolant are controlled by a subsonic orifice located between the H_2 main manifold and the film cooling manifold. The area of the orifice which controls the film cooling is about 1/4 of the area of the main H_2 orifices. The H_2 film cooling is sized to obtain a film cooling velocity to combustion gas velocity ratio of 1.0.

(2) Spark Plug

The spark plug used in the 5-pound engine is a Champion FHE 231 type with the shunt material removed. The "spark plug" or "igniter" is located in the center of the injector head surrounded by the six elements. A bleed of H_2 gas flows out the small area between the spark plug and injector interface.

(3) Valves

The valves used in the engine are Marquardt R-4D coaxial valves identical to those used on the Apollo 100-pound N_2O_4/MMH engine. The sealing surface is composed of a soft flexible Teflon seal and a metal-to-metal backup. Table 12 lists the characteristics of the valve.

(4) Combustion Chamber

The combustion chamber and exit nozzle are constructed of $MoSi_2$ coated molybdenum. The design incorporates a thick throat section which (a) minimizes the formation of local hot spots due to three-dimensional conduction of the energy away from the surface and (b) increases the outside area of the nozzle for radiation over that of a conventional nozzle, thus increasing the cooling due to thermal radiation.

TABLE 13. R4D VALVE CHARACTERISTICS

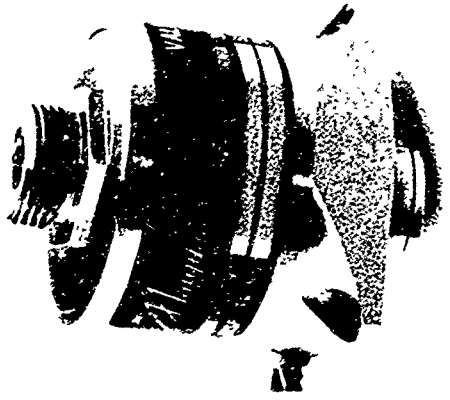

NEG CA6973-1

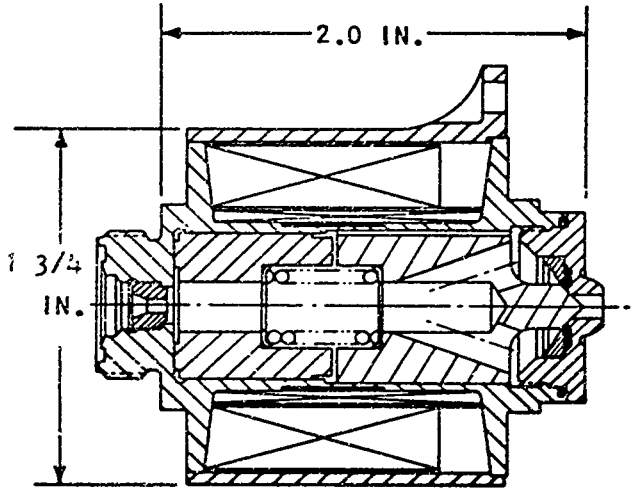

	P/N 228683
Valve Type	Poppet, coaxial flow, normally closed, spring actuated to close.
Operating Fluids	Nitrogen tetroxide, hydrazine, ammonia, oxygen gas, hydrogen gas
Weight	0.98 lbs
Nominal Operating Voltage	27 V. DC
Steady State Current	2.2 amps at 27 V. DC
Pressure Drop	27.5 psi at 0.155 lbs/sec water
Nominal Operating Pressure	180 psig
Proof Pressure	500 psig
Maximum Operating Temperature	200° F
Leakage	Zero Liquid Leakage
Opening Response (Signal "ON" to fully Open)	6.6 ms at 27 V. DC, 181 psig propellant, 70°F
Closing Response (Signal "OFF" to fully Closed)	6.3 ms at 27 V. DC, 0.122 lbs/sec water flowing
Demonstrated Cycle Life	1,000,000 cycles
Response Repeatability	0.2 ms at 27 V. DC, 180 psig propellant, 70°F
Program Application	Lunar Module RCS Engines Lunar Orbiter ΔV Engine Apollo SMRCS Engines MOL RCS Engines
Special Features	Valve contains a second coil for emergency operation. This coil draws only 14 watts at operating conditions. It accounts for 0.25 lbs of the total weight.

(5) General Configuration and Design Criteria

The engine and valves are designed for ease of disassembly. The valves, injector and combustor are connected by bolts and AN fittings while the injector orifices are brazed into place and can be readily removed. The spark plug is installed in the same manner as conventional auto spark plugs.

b. Thermal Analysis

Prior studies had indicated that the cooling of the combustion chamber would be a significant problem. The method proposed was to use a combination of a refractory metal to maximize the temperature limits; radiation cooling, film cooling, and "interegen" type conduction cooling.

The combination of all four of these techniques would result in a metal temperature which was in the 2000 to 3000°F range and would result in a long life capability for the engine. Preliminary thermal analysis using a thermal analyzer computer program resulted in the thermal profile shown in Figure 49. With 25% of the available hydrogen used for cooling the maximum wall temperature was 2300°F, which is well below the structural limits.

c. Performance Estimate

Conventional JANNAF performance estimation methods were used to predict the performance of the 5-pound thrust engine. Only the performance loss due to the hydrogen film cooling was required as an additional parameter. The loss due to film cooling was based on the following equation and resulted in the performance estimate shown on Figure 50.

$$I_{sp} = \frac{I_{sp_{\text{core O/F}}} \cdot W_{\text{core}} + I_{sp_{\text{coolant } H_2}} \cdot W_{\text{coolant } H_2}}{W_{\text{core}} + W_{\text{coolant } H_2}}$$

The predicted performance, based on a 95% C* efficiency, was 354 seconds at 50 psia chamber pressure (5 pounds thrust) and 346 seconds at 16.7 psia (1.67 pounds thrust).

d. Engine Characteristics and Structure

The engine design fabricated for this program is shown in Figure 51. The molybdenum combustor is attached to the nickel 200 injector by four bolts, a split ring and an attach ring (all three are Rene 41). The nickel 200 injector contains the six injector elements, a spark plug holder, and necessary manifolding for the propellants. The manifolding was sized to minimize the amount of propellants contained downstream of the valve to the injector face and was equivalent to approximately 2 to 3 ms of fully

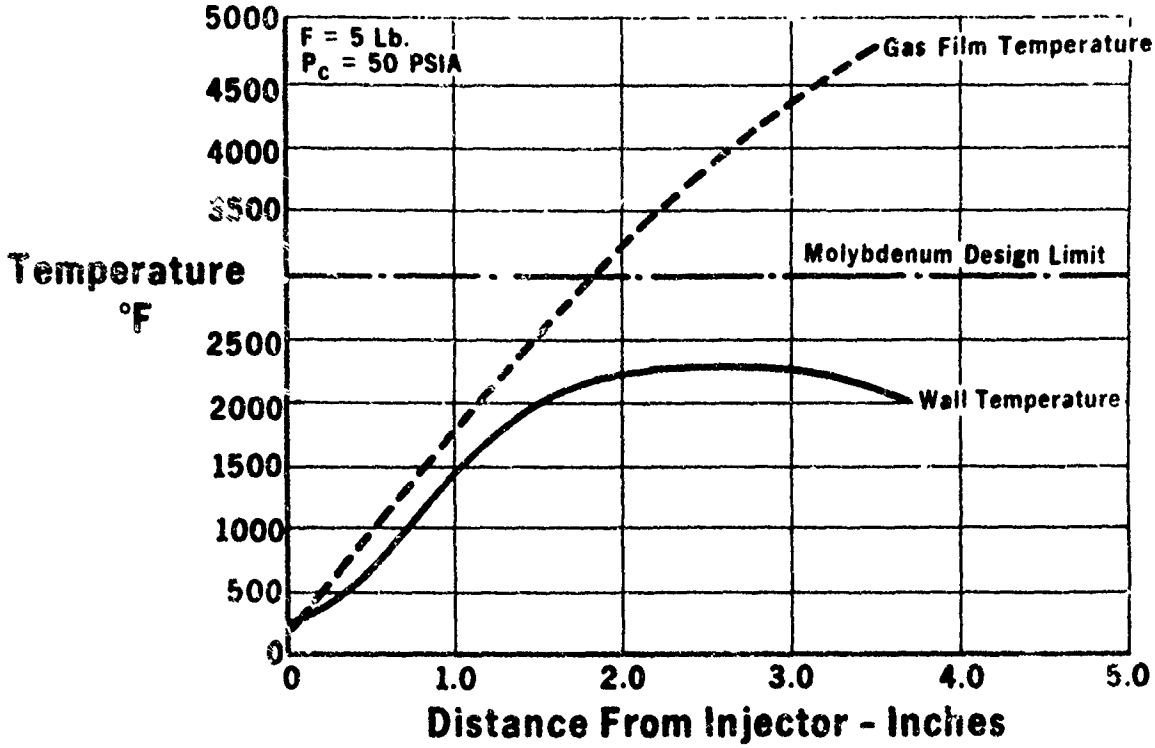

FIGURE 49. 5 LB_f THEORETICAL THRUSTER TEMPERATURE PERFORMANCE

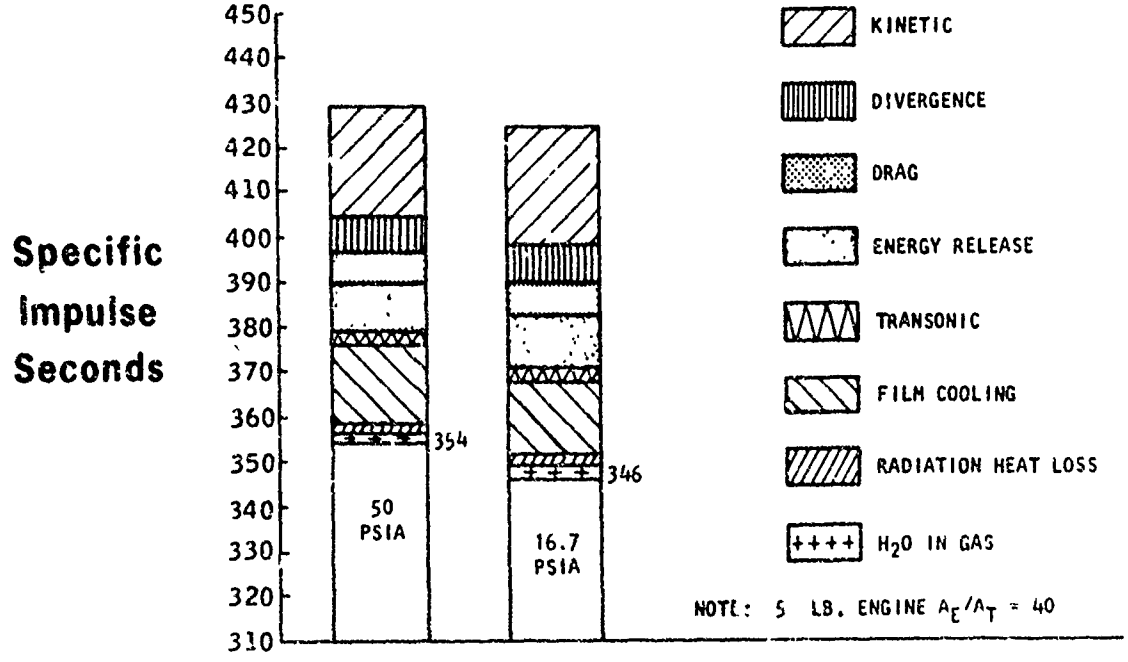

FIGURE 50. 5 LB_f THRUSTER ESTIMATED PERFORMANCE

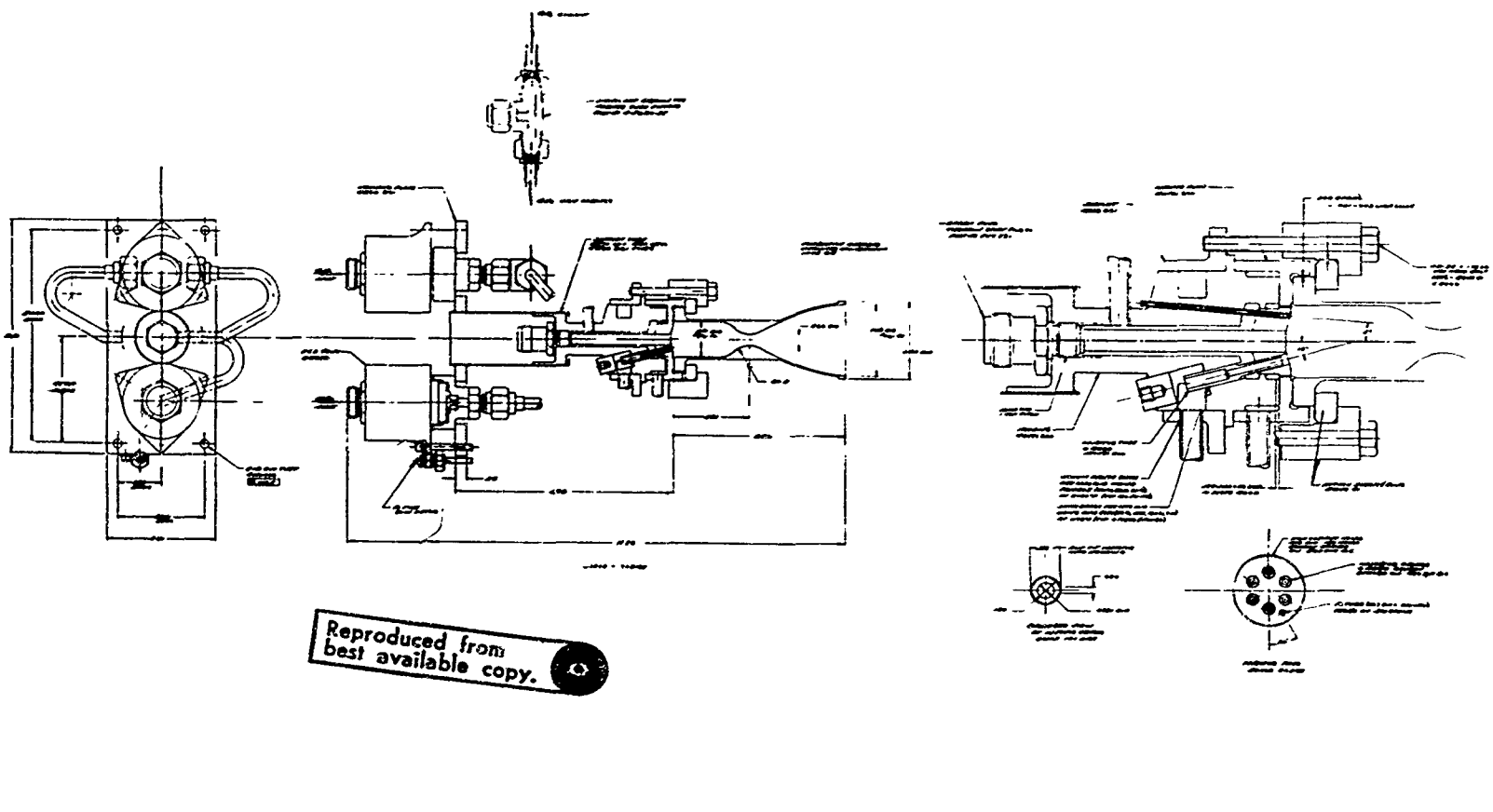

FIGURE 51. 5 LB_f THRUSTER DRAWING L4754

rated flow. The R-4D valves used are thermally isolated from the injector and combustion chamber to insure that the valve temperature does not exceed 250 to 300°F. The flow control (sonic) orifices are located just downstream of the valves, with further control for film cooling split located in the Tee shown in the drawing.

Figures 52, 53, 54 and 55 show the fabricated engine prior to the initial tests. Figure 52 shows the six coaxial ejector elements and the spark plug located in the fore of the injector. The three indentations are for the pressure tap and thermocouples. Located around the periphery of the face are the 35 film cooling holes. Figure 53 is an exploded view of the engine prior to assembly. Attached to the valves are inlet filters which also contain conditioning lines. Figure 54 shows the engine with the flow collection adapter attached. The adjuster was used to collect the gaseous nitrogen during the flow orifice calibrations.

Figure 55 shows the final assembled configuration prior to the initial tests.

3. TEST PROGRAM

a. Test Facility

Marquardt's Test Cell 9 was used for all hot firing tests conducted on the 5-pound thrust engine. The test cell, shown in Figure 56, is a 4000-cubic foot steel sphere, 20 feet in diameter, rated for pressures from 0.0009 to 160 psia. Cell access is through a 90-inch diameter door. A water deluge system is installed for fire control. Vacuum capability in the test cell is continuous and is provided by a five-stage steam ejector system shown schematically in Figure 57. The feed system and engine flow schematic for the 5-pound and 0.1-pound engine tests are shown in Figure 58. The instrumentation was specified according to Marquardt Test Plan MTP 0198.

b. Test Sequence

The tests to be conducted on the 5-pound thrust engine were designed to document the performance of the engine and determine its durability to duty cycle operation. The basic requirements were:

(1) Performance and thermal characterization

(2) Duty cycle capabilities by performing 75,000 pulses which consisted of 25 repetitions of the following cycle.

50 ms on/450 ms off
100 ms on/900 ms off
250 ms on/750 ms off

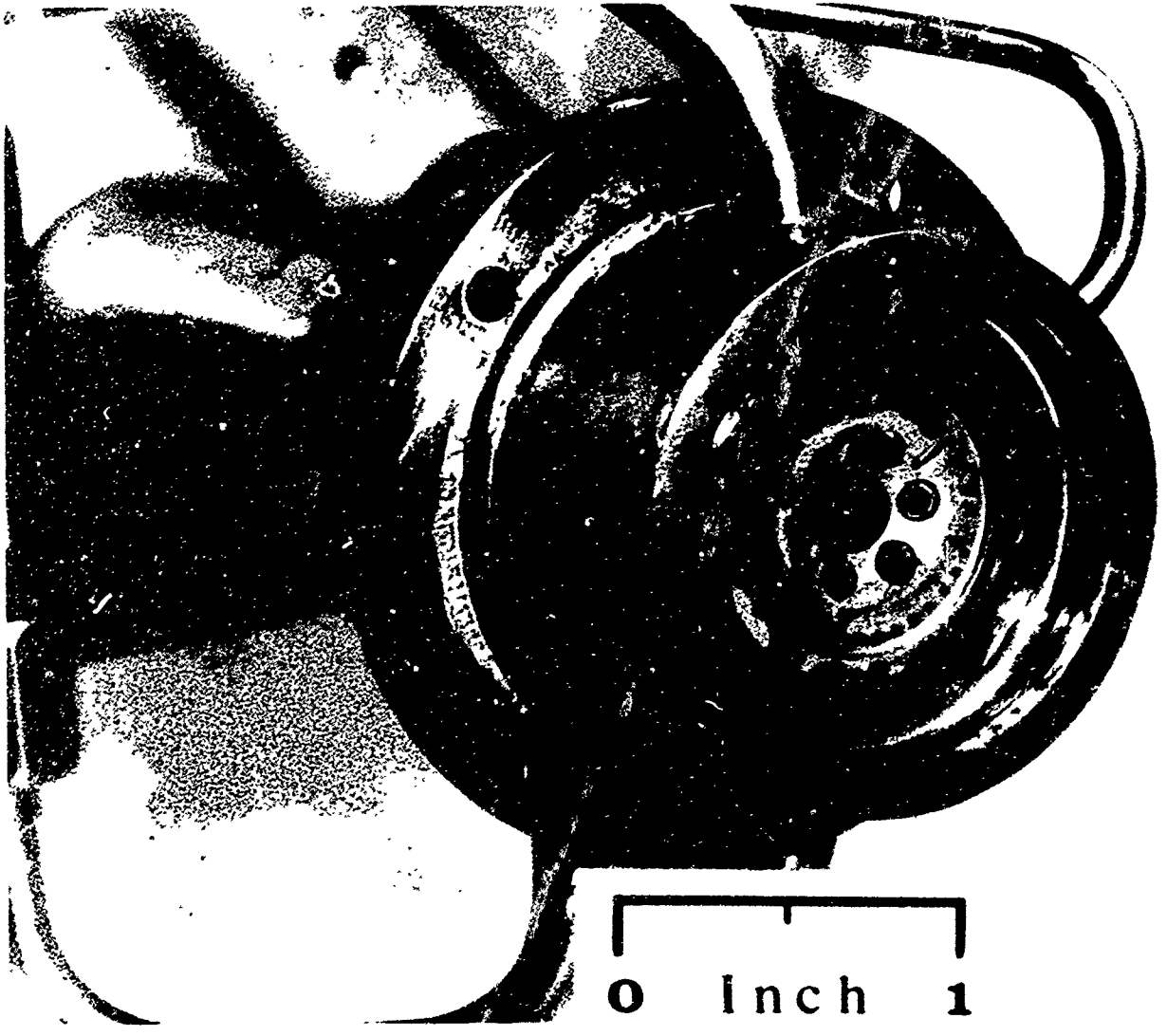

NEG 72-196-7

FIGURE 52. 5 LB_f PROTOTYPE INJECTOR (COAXIAL)

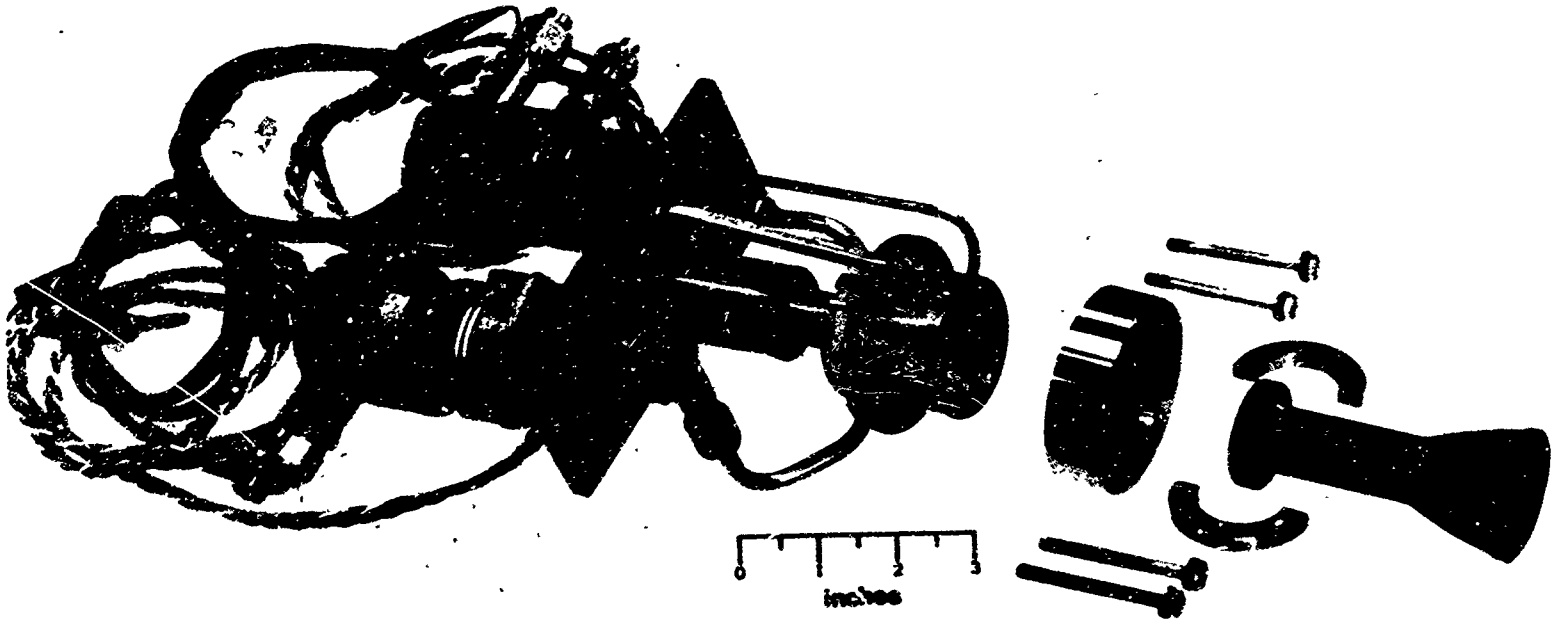

FIGURE 53. PROTOTYPE THRUSTER (EXPLODED VIEW)

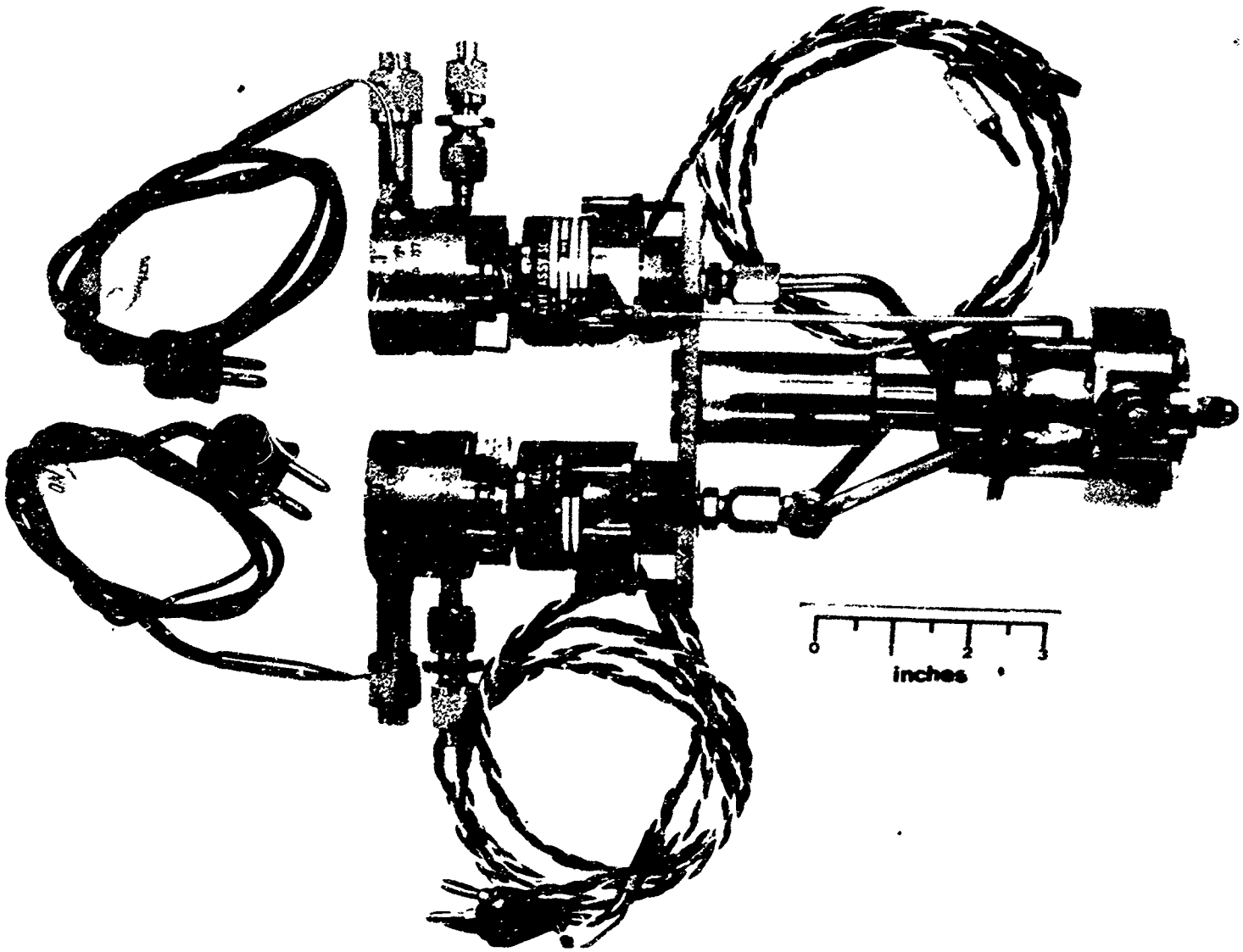

NEG. 72-196-5

FIGURE 54. 5LB$_f$ PROTOTYPE THRUSTER WITH FLOW COLLECTION ADAPTER INSTALLED

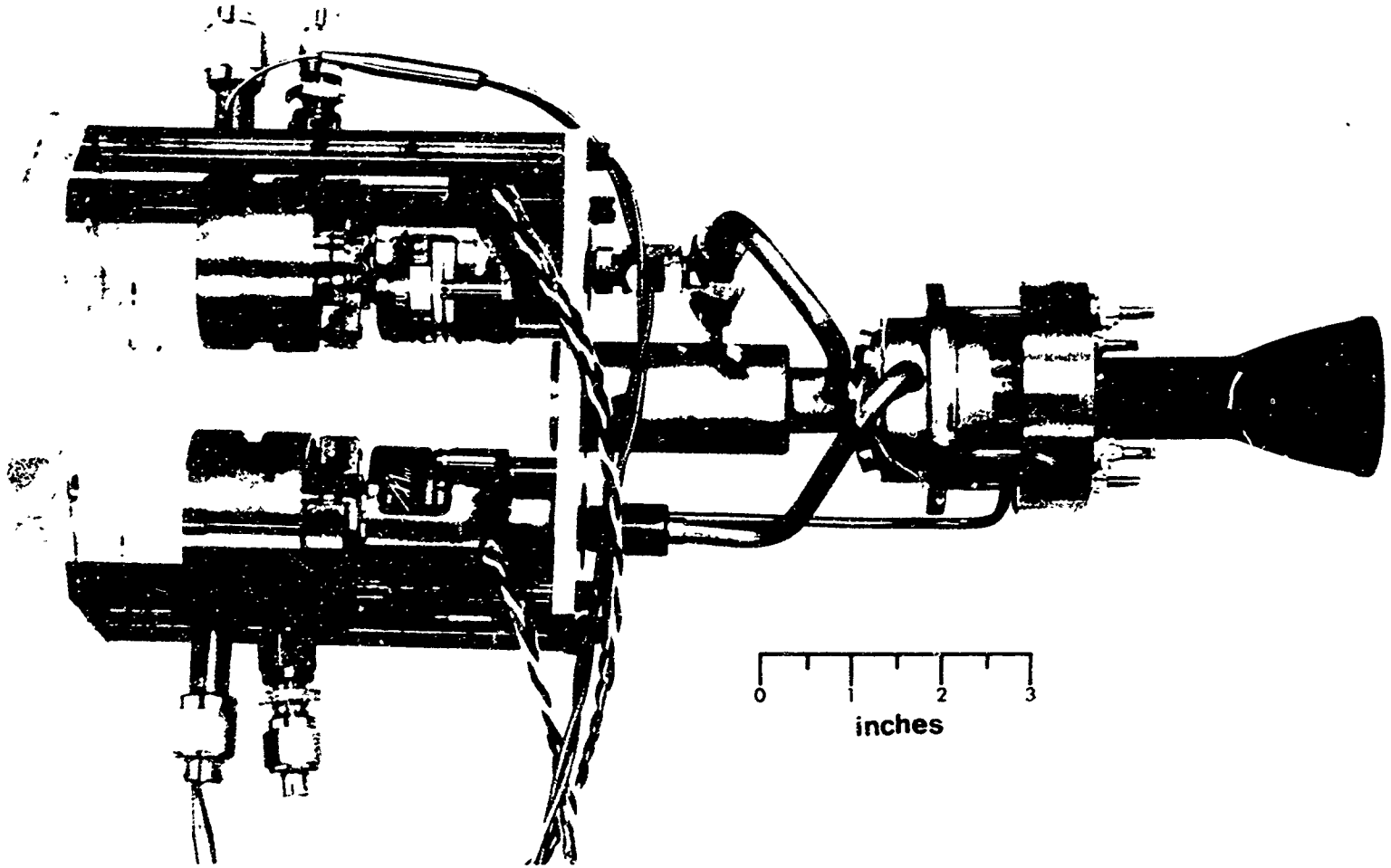

FIGURE 7. 5 POUND THRUST GO_2/GH_2 ROCKET ENGINE (THRUSTER)

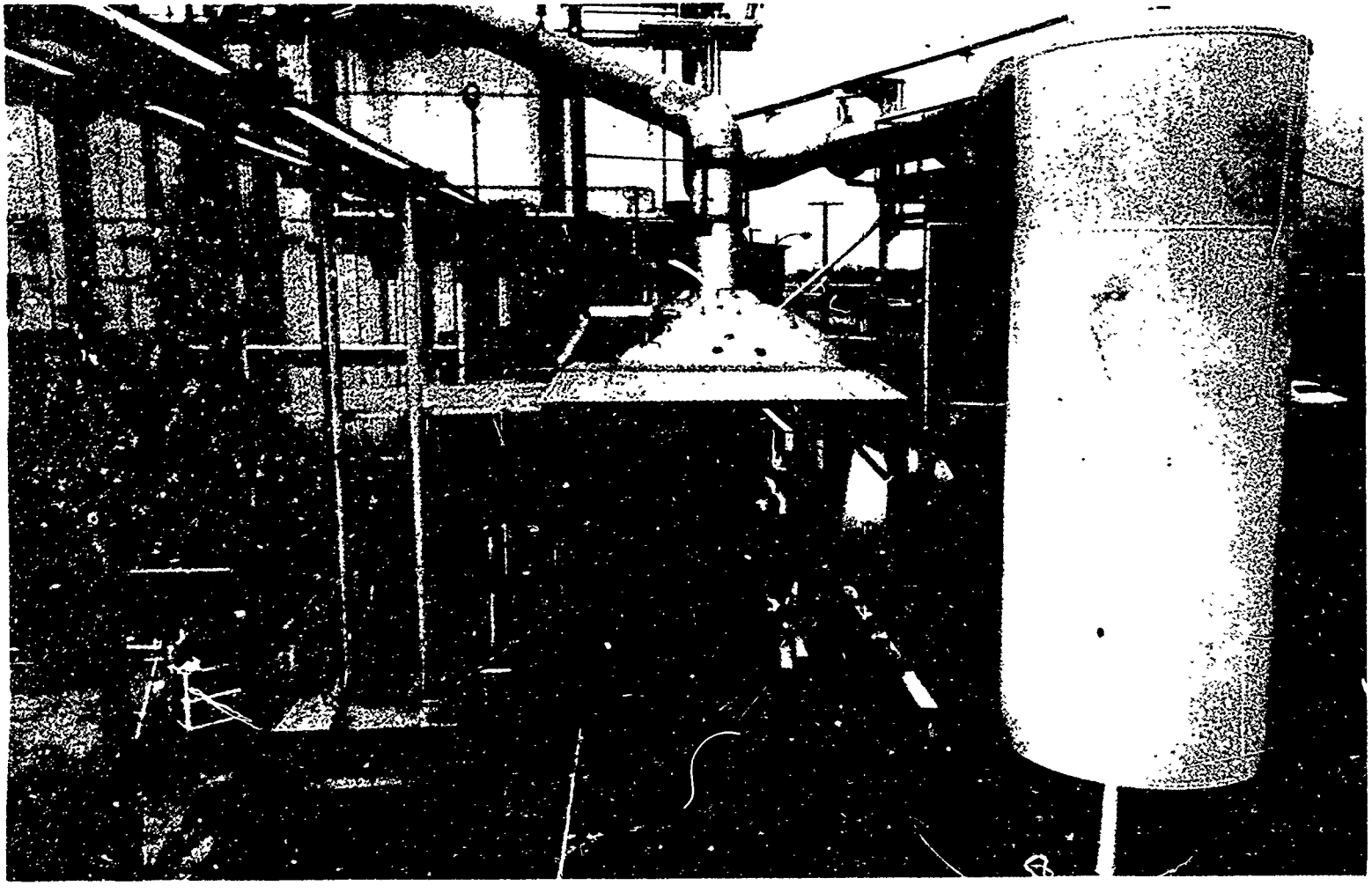

FIGURE 56. CELL 9 TEST FACILITY

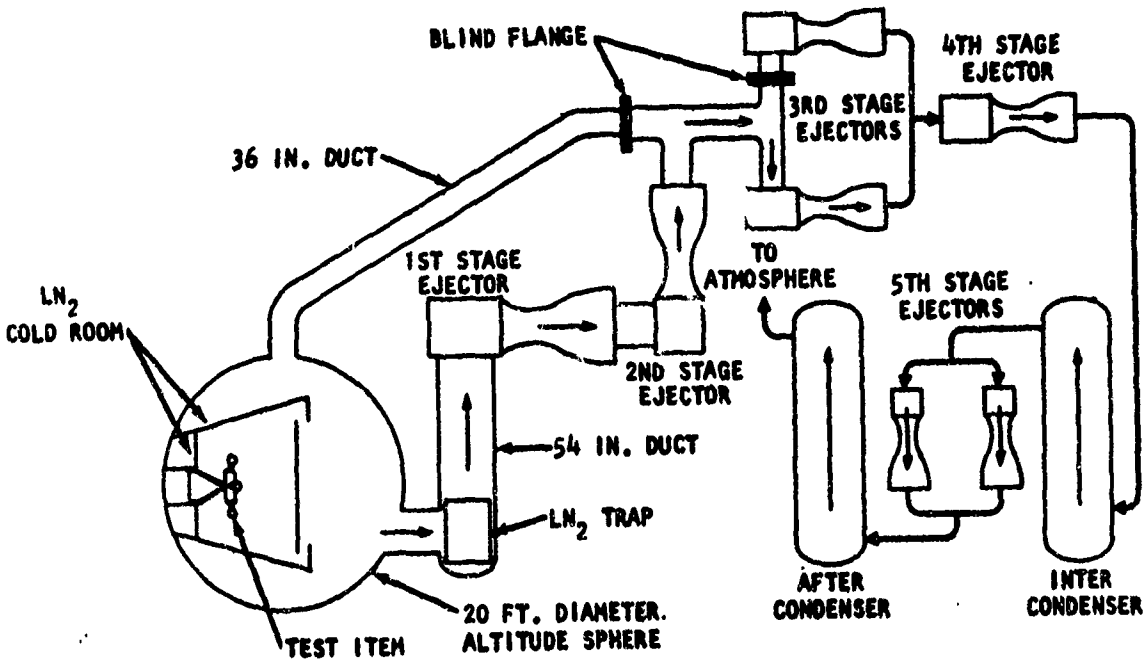

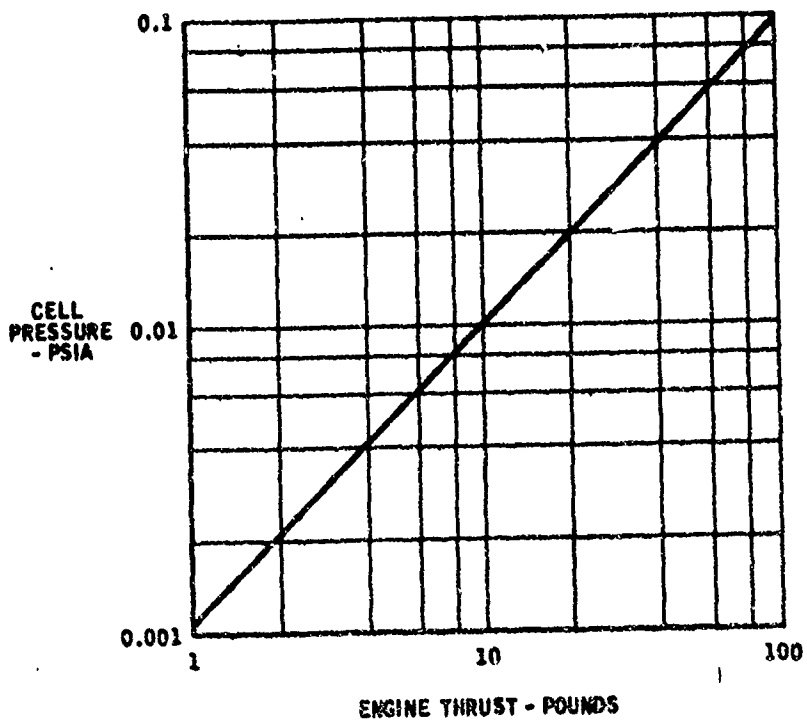

FIGURE 57. CELL 9 VACUUM CELL SCHEMATIC AND ALTITUDE PRESSURE CAPABILITY

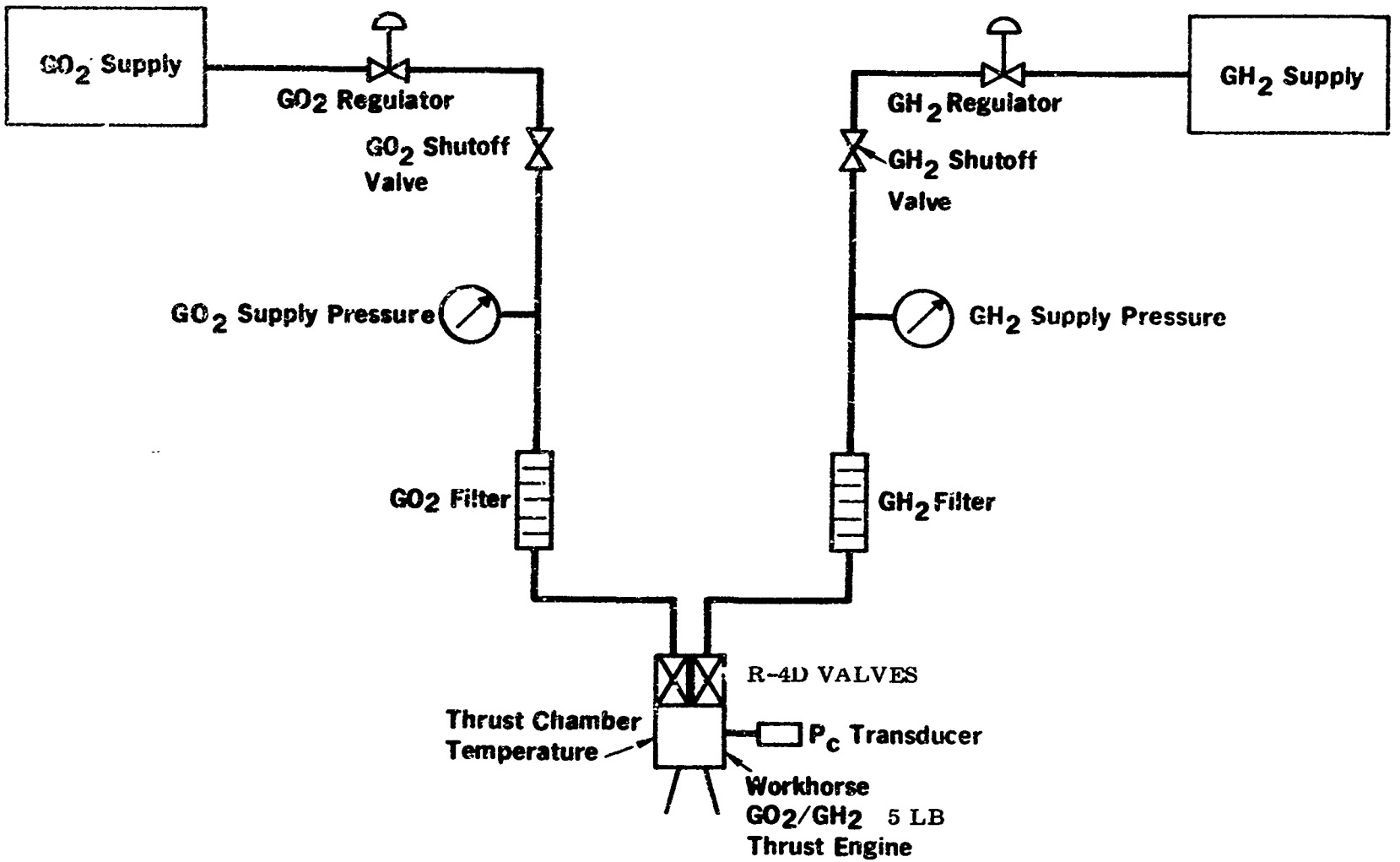

FIGURE 58. ENGINE TEST INSTALLATION SCHEMATIC

(3) Blowdown simulation of electrolysis system.

c. Ignition System

All tests conducted on the 5-pound thrust rocket engine utilized the Bel-Air Laboratories igniter system described in the section on ignition. The ignition energy varied between 35-85 millijoules delivered from the system.

4. TEST RESULTS

a. Initial Tests

Initial tests of the 5-pound engine were disappointing. The configuration designated as 1 on the test configuration summary (Table 14) provided a specific impulse of 272 seconds vs the desired goal of 350 seconds. The results are shown on Table 15 (Runs 1 - 18). In addition, the 2240° F equilibrium temperature reached on Run 17 indicated that the film cooling was also not effective. Configuration no. 2 was tested to determine the effect of the film cooling on performance and, as shown (Runs 19 - 21), an increase of 25 seconds to nearly 300 seconds was attained with 0% film cooling.

b. Revised Configuration Tests

Based on the tests being conducted concurrently on the 0.1-pound thrust engine and the realization that the coaxial element would not provide adequate performanc unless the L* were significantly increased (with the resultant film cooling degradation), a modification in the injecter was made. The six coaxial elements were modified to premix elements. The oxygen posts were machined back approximately 0.2 inch and the machined area was replaced by orifices which resulted in the hydrogen flow being turned 90° into the oxygen stream and mixing in the 0.2-inch long orifice prior to ejection. The configuration modification is shown on Figure 59. The nickel orifices were EB welded to the nickel injector and did not provide a smooth sharp exit for the gases.

The initial test conductions using this configuration (No. 3) were very encouraging, since the performance exceeded the 350 seconds. However, the low film cooling effectiveness resulted in a near burnthrough of the combustor after an 8.7-second run. Examination of the thruster after the test indicated a hot spot on the outside of the combustor as shown in Figure 60. The engine was removed from the test facility and, upon disassembly and examination of the combustor in further detail, two circular areas of erosion were observed and are shown in the section of combustor in Figure 61. Evaluation of the data and combustor indicated that the areas of hot spots were in line with the premix orifices which had no sharp exits.

Since the molybdenum combustor was no longer usable, the decision was made to investigate the effect of both film cooling percent and L* on performance and heat transfer. Two stainless steel combustors of 4.6 and 12.9 L* were fabricated

TABLE 14

5 POUND ENGINE

TEST CONFIGURATION SUMMARY

Configuration No.	Injector	Combustor	Percent H_2 Film Cooling
1	6 element coaxial	Molybdenum L* = 12.9	27
2	6 element coaxial	Molybdenum L* = 12.9	0
3	6 premix elements .012 gap* 0.088 dia x .20 length mixing section	Molybdenum L* = 12.9	27
4	↓	Stainless steel L* = 4.6	52
5	↓	↓	59
6	↓	↓	67
7	↓	Stainless steel L* = 12.9	67
8	↓	↓	27
9	↓	↓	52
10	↓	↓	27
11	6 element coaxial with 0.20 ox post recess	↓	59
12	↓	↓	27
13	6 element premix 0.20 gap 0.110 dia. x .20 length mixing section	↓	27
14	↓	↓	52
15	↓	Stainless steel L* = 4.6	52
16	↓	↓	36
17	↓	↓	27
18	↓	Molybdenum L* = 6.3	52
19	↓	↓	36
20	↓	↓	27

*.020 for runs 57-66

TABLE 15

TEST SUMMARY

6 LB GO_2/GH_2 ROCKET ENGINE

WATER ELECTROLYSIS SATELLITE PROPULSION SYSTEM

Cond.	Date	Run no.	Run time sec.	Number firings	Freq. Hz	Inlet Press. O_2 psia	Inlet Press. H_2 psia	Temp. (Inlet) O_2 °F	Temp. (Inlet) H_2 °F	F lbs	P_c psia	P_o psia	I_{sp} sec	C* ft/sec	C_F	O/F	Max. temp. °F	Comments
1	4/20	1-11	2-10	21	-	86-240	86-240	71-80	68-75	0.3-1.6	1.7-8	.02	62-222	-	-	-	-	Cold flow
1	4/20	12	1	1	-	220	224	68	72	1.15	43	.02	272	—	-	7.7	-	
1	4/21	13	5	1	-	215	212	68	70	1.62	16.2	.02	101	-	-	7.56	-	
		14	1	1	-	215	125	67	69	2.50	41	.02	272	-	-	7.55	275	
		15	5	1	-	215	213	70	72	2.91	41.5	.024	276	-	-	7.77	975	
		16	10	1	-	216	208	72	76	2.88	41.5	.03	277	-	-	8.1	1600	
		17	60	1	-	220	212	-	63	2.62	42	.04	-	-	-	-	2240	
		18	5	1	-	73	67	77	76	1.18	14	.02	246	-	-	8.6	-	
2		19	5	1	-	216	210	74	75	1.48	16.9	.017	161	-	-	7.96	-	
		20	2	1	-	213	210	76	76	4.03	43	.024	243	-	-	7.96	-	
		21	5	1	-	214	211	76	76	4.28	44	.02	290	-	-	7.96	1060	
3	5/2	22-30	10	2	-	(Cold flow)												
		24	2	1	-	208	216	68	71	5.0	51.8	.026	354	6480	1.77	7.80	800	
		25	5	1	-	207	213	72	74	5.03	52.0		355	-	-	-	1900	
		26	8.7	1	-	208	212	75	80	5.16	52.0		357	6370	1.765	8.13	2800	Run cut because of 3000°F reading combustor instrument on Run 26
		27		No P_o response - run terminated														
4	5/14	28-29	10	2	-	212	213	69	61	S	16.3	14.3						
		30	1	1	-			66	61	F	46.3							
		31	2		-			60	66	A	49.3		~336					
5		32	2		-			59	59		-							No ignition
		33	2		-			59	60	L	47.1		~323	Thermal tests				
		34	2		-			59	60	E	47.8							
6		35	2		-			61	61	V	-							No ignition
		36	2		-			61	61	E	44.3		~306					
6	5/24	37	2	1		212	213	61	61	L	44.5	14.3						
7		38	2					62	62	T	47.8							
7		39	2					63	63	E	46.8							
8		40	2					63	63	S	54.3							
8		41	2					64	64	T	54.3							
9		42	2							S	52.3							
10		43	2								52.3							
10		44	2								53.3							
5		45	2				189	65	65		47.3							
5		46	2				213	66	66		46.3							
6		47	2					66	66		46.3			Thermal tests				
11	6/7	48	5	1		211	213	66	66		17.8	14.3						Cold flow
		49	2			210	213	66		S	43.8		~300					Cold flow
		50	5			209	212	66		E	17.8							
		51	2			210	214	66		A	43.8							
12		52	2			209	213	68	66		46.8		~334					
		53	2			210	213	68	69	L	49.8							
		54	2			211	213	70	70	E	18.1							Cold flow
		55	2			209	213	70	70	V	49.3							
		56	4			209	213	70	70	E	49.3							
8	6/20	57	0			214	212			L	17.1		-	2136	-	7.77	-	Cold flow
8		58	0				212				54.3		-	6781	-	7.77	-	
8		59					208				53.8		-	6723	-	8.08	-	
9		60					209				52.8		-	6498	-	7.97	-	
9		61					212				51.8		-	6469	-	7.86	-	
-		-	-	No run														
4	6/22	63	0	1		218	213	70	70		48.7		-	6083	-	7.86	-	
4		64					214				48.8		-	6082	-	7.76	-	
10		65					210				52.3		-	6577	-	7.79	-	
10	6/23	66	0	1	-	215	212	70	70	S	52.3	14.3	-	6660	-	7.76	-	
13		67			-	212	209	75	75	E	17.3		-	2136	-	7.79	-	Cold flow
		68			-	213	210	75	76	A	53.3		-	6712	-	7.76	-	
		69			-	214	209	76	77		53.3		-	6712	-	7.87	-	
14		70			-	215		78	77	L	50.3		-	6290	-	7.89	-	
14		71			-	216		66	69	E	50.3		-	6261	-	7.96	-	
15		72			-	215		64	64	V	47.3		-	5956	-	7.88	-	
15		73	3		-	215					46.8		-	5910	-	7.88	-	
16		74	3		-	214				L	50.8		-	6420	-	7.96	-	
16		75	3		-	215	213				51.3		-	6469	-	7.77	-	
17		76	3		-	215	213				52.5		-	6616	-	7.72	-	
17		77	3		-	215	209				52.5		-	6616	-	7.91	-	
18	6/2	78	5	1	-	213	196	90	90	1.49	18.2	.08	111	1960	1.68	8.27	-	Cold flow
		79	5		-		198			1.58				1984	1.68	8.24	-	
		80	5		-		202			1.56				1967	1.69	8.06	-	
		81	3		-		204			4.31	44.4		213	5400	1.73	8.05	-	
		82	10		-		206			4.48	43.4		211	5500	1.73	8.01	-	
19		83	5		-	211	202			4.88	46.9	.028	326	6048	1.70	7.90	-	
		84	10		-	212	208			1.93	18.4		122	2109	1.67	7.90	-	Cold flow
		85	10		-	215	206			4.79	47.0		342	6179	1.66	7.98	-	
		86	.05		-	215	211			-	-		-	-	-	8.11	-	
		87	.05	10	1	216	214			-	-		-	-	-	8.05	-	Pulser set wrong - no spark
		88	.06	10	1	216	216	88	90	.232	-		317	-	-	8.00	-	
		89	.10	10	1	222	214			.478	-		236	-	-	8.00	-	
		90	.25	10	1	219	208			1.185	-		324	-	-	8.08	-	
		91	.020	10	1	219	224			.0015	-		274	-	-	7.84	-	
		92	5	1		123	130	90	90	0.84	9.6		124	2182	1.89	7.90	-	Cold flow
		93	5			123	121	64	90	2.61	27.6		331	6189	1.78	7.66	-	
		94	5			66	64	96	96	0.62	4.8		137	2211	1.86	8.19	-	Cold flow

TABLE 15 (Cont')

Conf.	Date	Run no.	Run time sec	Number flashes	Freq. (1)	Inlet Press. O_2 psia	Inlet Press. H_2 psia	Temp. (Inlet) O_2 °F	Temp. (Inlet) H_2 °F	F lbs	P_c psia	P_o psia	I_{sp} sec	C^* ft/sec	C_f	O/F	Max. temp. °F	Comments
19	6/3	96	5	1	--	64	87	96	90	1.88	15.4	.080	346	6766	1.78	8.71	-	
		96	30	1	--	213	288	96	90	4.78	47.6	.080	346	6140	1.81	7.65	.23-5400	Steady state attained
20	6/4	97	5	1	--	208	285	96	90	1.46	14.9	.06	118	1889	1.81	7.8	-	Cold flow
		98	5		--	209	288	90	90	1.46	48.2		116	1880	1.81	7.87	-	Cold flow
		99	5		--	209	288	98	98	4.07	48.9		346	6812	1.78	7.81	-	
		100	5		--	208	288			4.06	48.2		346	6806	1.78	7.98	-	
		101	5		--	210	290			4.02	-		345	6170	1.80	7.98	-	
		102	.08	10	2	210	210			.070	-	.007	266	-	-	8.00	-	
		103	.06		-	217	297			.22	-		310	-	-	8.00	-	
		104	.06		-	215	297			.23	-		312	-	-	8.02	-	
		105	.1		-	213	294			.451	-		323	-	-	8.02	-	
		106	.1		-	210	294			.451	-		319	-	-	8.13	-	
		107	.25		1	212	295			1.121	-		325	-	-	7.98	-	
		108	.25		1	211	295			1.121	-		327	-	-	7.94	-	
		109	5	1	-	208	286	90	90	4.06	48.2		341	6812	1.76	7.8	-	
		110	5		-	133	188			1.9	9.9		126	2011	1.86	7.97	-	Cold flow
		111	5		-	133	189			2.05	20	.01	228	6074	1.74	8.08	-	
		112	5		-	134	187			2.06	20	.01	230	6041	1.74	8.15	-	
		113	5	1	-	133	186	90	90	2.05	20	.01	228	6074	1.74	8.05	-	
		114	.08	10	-	137	193	98	98	.0412	-		264	-	-	8.0	-	
		115	.08		2	137	193			.0412	-		264	-	-	8.08	-	
		116	.06			136	189			.137	-		310	-	-	8.06	-	
		117	.06			136	192			.137	-		310	-	-	8.06	-	
		118	.10			133	119			.217	-		310	-	-	7.86	-	
		119	.10			133	133			.277	-		317	-	-	7.81	-	
		120	.25		1	132	186	90	90	.70	-		233	-	-	7.80	-	
		121	.25		1	131	190			.70	-		327	-	-	7.78	-	
		122	5	1	-	132	190			2.06	20.2		328	6170	1.78	7.96	-	
		123	5	1	-	64	92			.61	5.9		198	2837	1.80	7.43	-	
20	6/4	124	5	1	-	89	88	86	84	1.22	13.9	.08	2.0	6041	1.86	9.40	-	
		125	5	1	-	91	88			1.22	13.9		311	6133	1.86	9.83	-	
		126	5	1	-	91	88			1.22	13.8		314	6122	1.86	9.86	-	
		127	.08	10	2	63	65	86	84	.081	-		260	-	-	9.49	-	
		128	.08			66	65			.081	-		264	-	-	9.70	-	
		129	.06			64	66			.066	-		272	-	-	7.97	-	
		130	.06			64	66			.066	-		270	-	-	7.89	-	
		131	.06			64	66			.066	-		270	-	-	7.89	-	
		132	.10			63	64			.110	-		302	-	-	7.82	-	
		133	.10			63	64			.110	-		297	-	-	7.67	-	
		134	.25		1	62	62			.266	-		328	-	-	7.70	-	
		135	.25		1	62	63	86	84	.266	-		300	-	-	7.72	-	
		136	5	1	-	62	63			1.24	12.7		312	5968	1.80	7.63	-	
		137	5	1		111	110			2.05	24.6		310	6011	1.76	7.91	-	
		138	5	1		210	290	86	86	4.78	48.7		340	6832	1.76	7.89	-	
		139	.06	800	2	-	-	-	-	-	-	-	-	-	-	-	-	
		140	.10	800	1												-	
		141	.25	400	1												-	
	6/5	142	5	1	-	227	315	71	91	1.80	16.6	.085	166	1858	1.88	8.05	-	
		143	5	1	-	229	315	72	72	2.07	20.4	.085	230	6146	1.76	8.06	-	
		144	.06	800	2	-	-	-	-	-	-	-	-	-	-	-	-	1490
		145	.10	1000	2												-	1630
		146	.25	1001	1												-	1810
		147	.06	800	2												-	
		148	.10	800	2												-	
	6/5	149	.253	800	1	210											-	
		150	.06	-	2												-	
		151	.10	-	2												-	
		152	.250	-	1												-	
		153	.06	-	2												-	
		154	.10	-	2												-	
20	6/5	155	.250	800	1	229	315	-	-	-	-	-	-	-	-	-	-	
		156	.06		2												-	
		157	.10		2												-	1820
		158	.250		1												-	2000
		159	.06		2												-	
		160	5	1	-	227	315	102	116	4.07	50.2	.085	340	6196	1.78	8.21		
	6/9	161	5	1	-	227	315	98	98	4.06	51.2	.085	338	6864	1.78	8.14		
		162	.1	800	-	-	-	-	-	-	-	-	-	-	-	-	-	
		163	.25		1												-	
		164	.06		2												-	
		165	.10		2												-	
		166	.25		1												-	
		167	.06	-	2												-	Numerous non ignitions
		168	.10	-	2												-	
		169	5	1	-	229	315	86	98	4.06	50.2	.085	338	6868	1.78	8.21	-	Ignition spark quit after
		170	.10	800	2												-	200 ignitions
		171	.25	800	2												-	Replace igniter circuit box
		172	.06		2												-	
		173	.25		1												-	
		174	.06		2												-	
		175	.10		2												-	
		176	.25		1												-	
		177	.06		2												-	
		178	5	1	-	223	315	100	100	4.07	50.2	.085	340	6810	1.78	7.98	-	
	6/10	179	5	1	-	125	189	72	72	.98	9.8	.085	119	1858	1.84	7.89	-	Cold flow
		180	5	1	-	128	189	72	72	2.08	20.8	.083	230	6041	1.78	8.0	-	
		181	.10	800	2												-	
		182	.25		1												-	
		183	.06		2												-	
		184	.10		2												-	

TABLE 15 (Cont')

Conf.	Date	Run no.	Run time sec	Number firings	Freq. Hz	Inlet Press. O_2 psia	Inlet Press. H_2 psia	Temp. Inlet O_2 °F	Temp. Inlet H_2 °F	P psi	P_c psia	P_e psia	I_{sp} sec	O* ft/sec	C_p	O/F	Max. temp. °F	Comments
20	8/10	195	.25	999	1	120	120	-	-	-	-	-	-	-	-	-	-	
		196	.05		2			-	-	-	-	-	-	-	-	-	-	
		197	.1		2			-	-	-	-	-	-	-	-	-	-	
		198	.25		2			-	-	-	-	-	-	-	-	-	-	
		199	.05		2			-	-	-	-	-	-	-	-	-	-	
		200	.1		2	86	85	-	-	-	-	-	-	-	-	-	-	
		201	.1	999	2	110	113	-	-	-	-	-	-	-	-	-	-	
		202	.25		1	90	95	-	-	-	-	-	-	-	-	-	-	
		203	.05		2	90	95	-	-	-	-	-	-	-	-	-	-	
		204	.1		2	84	85	-	-	-	-	-	-	-	-	-	-	
		205	.25		1	71	73	-	-	-	-	-	-	-	-	-	-	
		206	0.	1	-	71	73	117	113	1.46	16.8	.015	207	6883	1.50	-	-	
	8/11	207	0.	1	-	76	71	73	73	.46	8.8		105	1860	1.74	-	-	
		208	0.	1	-	75	73	73	73	1.46	16.8		207	6812	1.68	-	-	
		209	.05	999	2	75	74	-	-	-	-	-	-	-	-	-	-	
		210	.10	150	2	85	84	-	-	-	-	-	-	-	-	-	-	
		211	.10	999	2	224	213	-	-	-	-	-	-	-	-	-	-	
		212	.25		1			-	-	-	-	-	-	-	-	-	-	
		213	.05		2			-	-	-	-	-	-	-	-	-	-	
		214	.10		2			-	-	-	-	-	-	-	-	-	-	
		215	.25		1			-	-	-	-	-	-	-	-	-	-	
		216	0.	1	-	224	214	122	114	4.66	67.6		-	6884	1.65	-	-	
20	8/10	216	0.	1	-	223	213	63	66	1.50	16.8	0.10	-	-	-	-	-	Cold flow
		217	0.	1	-	224	213	63	63	4.66	66.6		-	6868	1.61	-	-	
		218	.05	999	2			-	-	-	-		-	-	-	-	-	
		219	.10	999	2			-	-	-	-		-	-	-	-	-	
		220	.25	999	1			-	-	-	-		-	-	-	-	-	
		221	.05	999	2	224	213	-	-	-	-		-	-	-	-	-	
		222	.10		2			-	-	-	-		-	-	-	-	-	
		223	.25		1			-	-	-	-		-	-	-	-	-	P_c delay indication (65 – 69)
		224	.10		2			-	-	-	-		-	-	-	-	-	
		225	.10		2			-	-	-	-		-	-	-	-	-	
		226	.25		1			-	-	-	-		-	-	-	-	-	
		227	.05	?	2			-	-	-	-		-	-	-	-	-	
		228	.10		2			-	-	-	-		-	-	-	-	2063	
		229	.25	136	1			-	-	-	-		-	-	-	-	2300	Run cut-spark ejected from engine
			10,001	69,746														

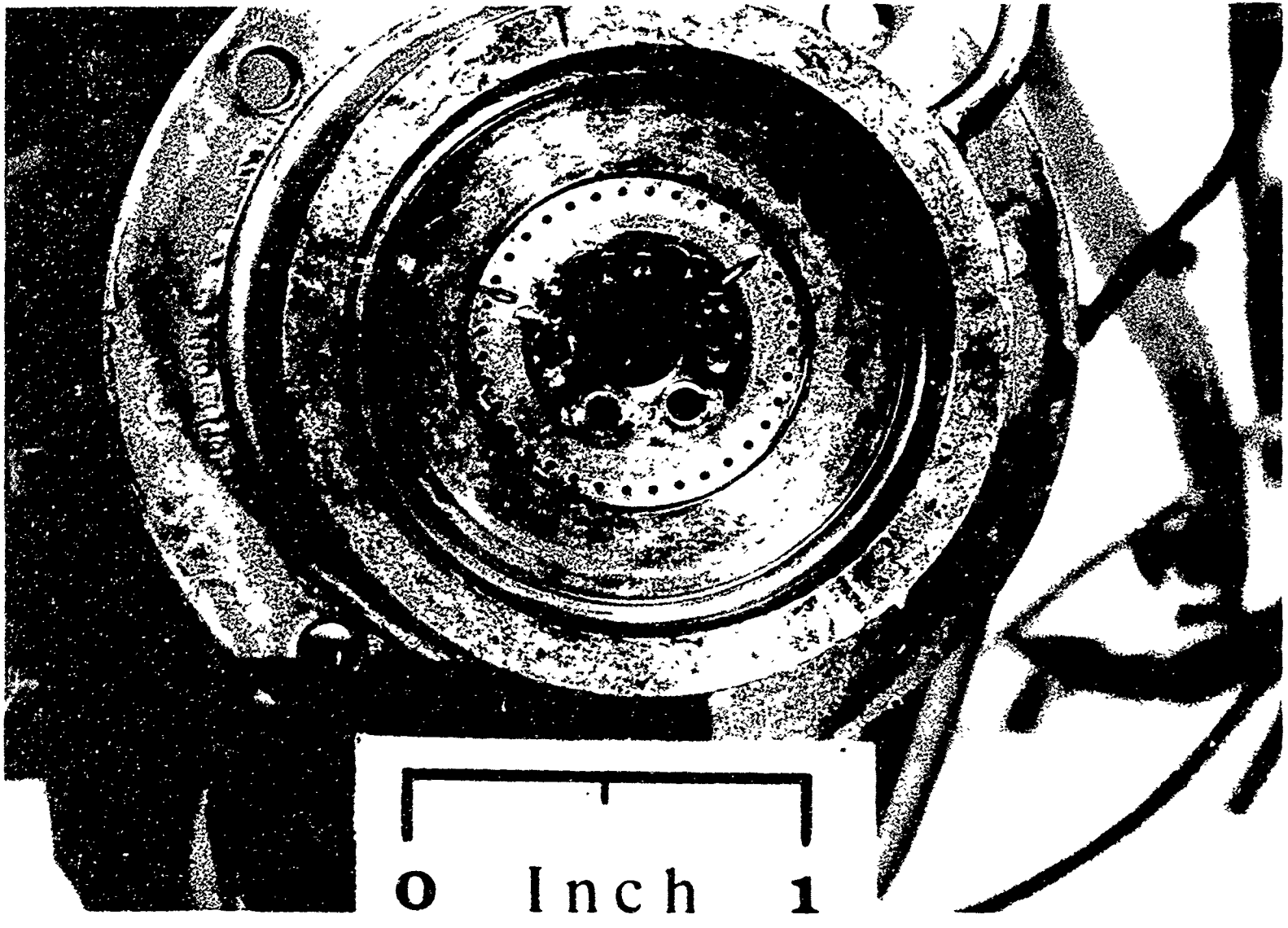

MTG 72-196-15

FIGURE 59. 5 LB_f THRUSTER INJECTER AFTER RUN #28

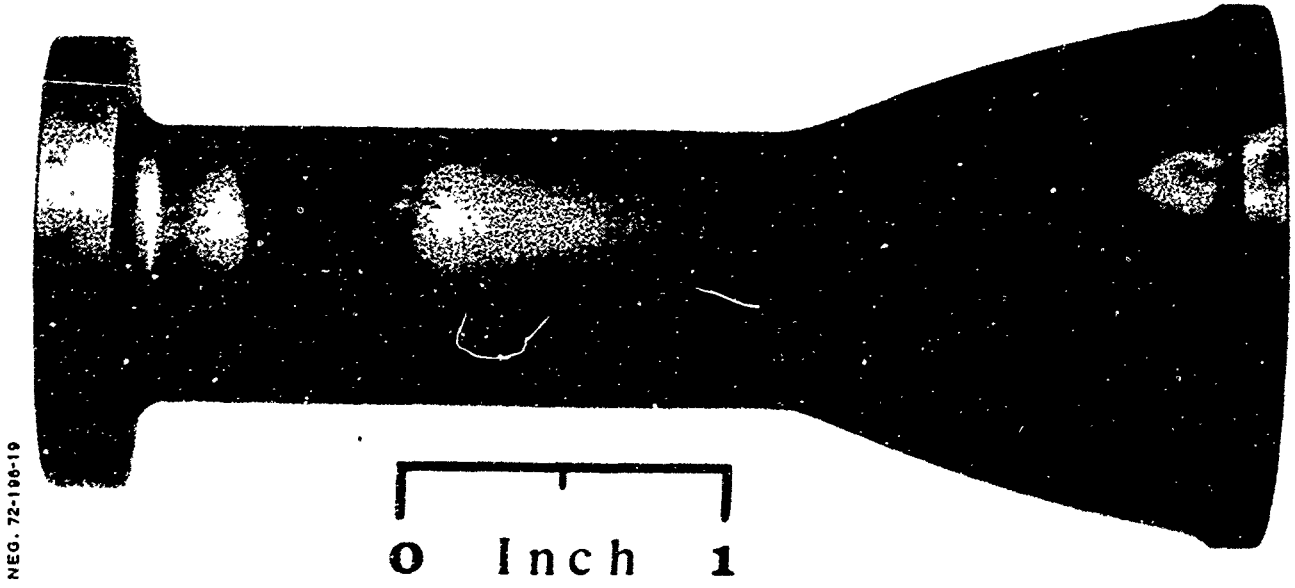

FIGURE 60. 5 LB COMBUSTION CHAMBER AFTER RUN # 28

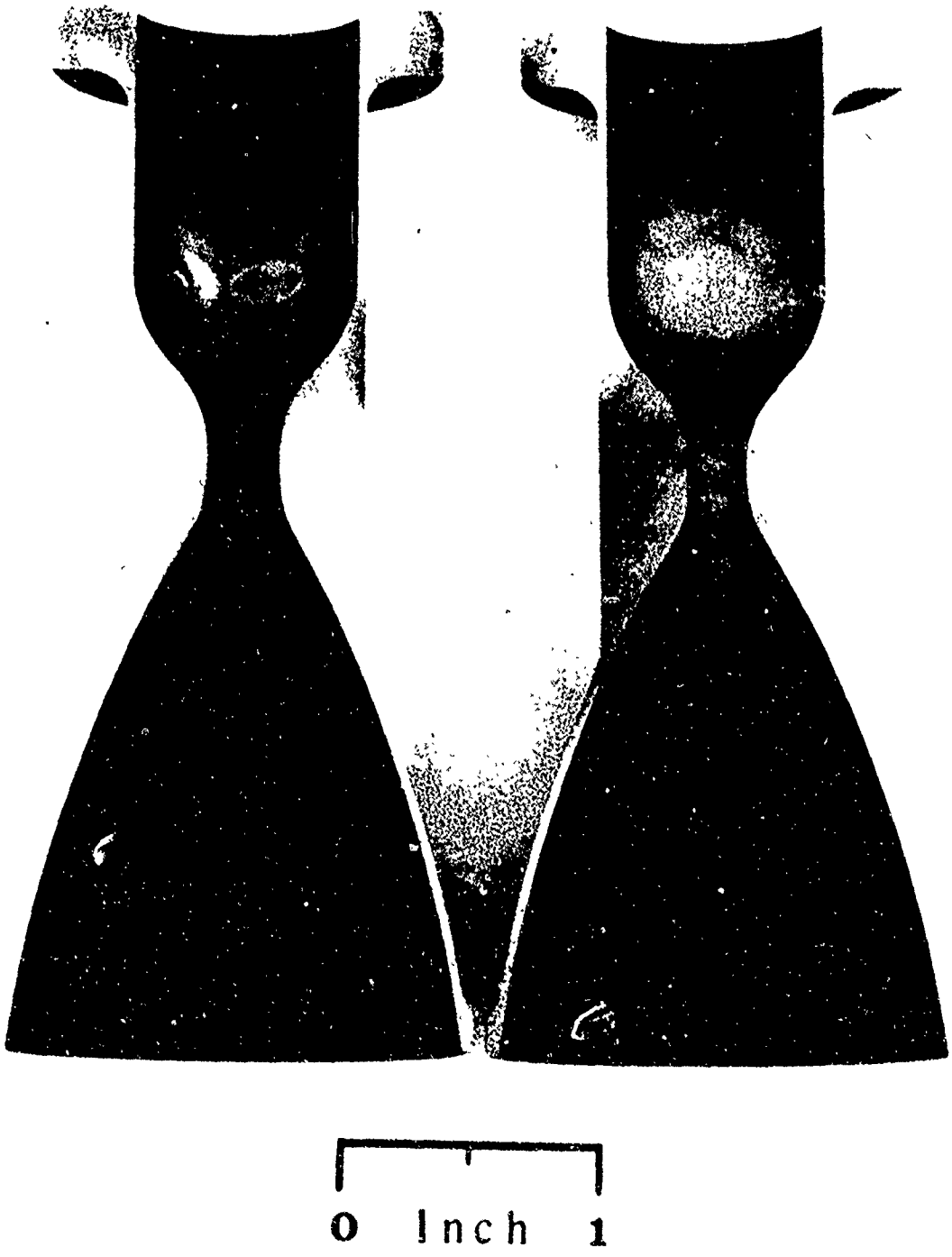

NEG. 72-196-21CN

FIGURE 61. 5 LB_f THRUSTER COMBUSTION CHAMBER FOLLOWING RUN # 28

and tested. Based on the data for chamber pressure (all tests were run at sea level), a decision was made to revise the premix orifices to eliminate the hot spots caused by the nonsharp exit.

Prior to rework of the injector, the engine was tested with the ox post recess (0.2 inch) which indicated that the performance could be improved over the flush post. However, the 300-334 seconds was not adequate.

The premix orifices were replaced and more care was taken to insure sion that the EB weld did not break the sharp edges. In addition, the 0.012 gap was increased to 0.020 and the diameter of the orifice from 0.088 to 0.11. Further tests indicated a significant reduction in the heat flux while performance was near the design goal.

c. Final Configuration Test Results (Runs 83-229)

Based on the results of the tests conducted with the stainless steel combustors, a new molybdenum combustor was fabricated with an L* of 6.3 (one-inch dimension from the injector face). The $MoSi_2$ coating on the combustor, upon examination, indicated that a potential for failure could occur. Due to inadequate cleaning the surface of the combustor in many places was very rough. Figures 62 and 63 show the original combustor that burned out and the second moly combustor for comparison purposes. The obvious roughness of the coating was cause for concern, but dut to the schedule the decision was made, after the combustor was successfully smoke checked, to use it in the tests.

The initial tests of the final engine were encouraging. A specific impulse of 335 - 345 seconds at 37% film cooling, and a 30-second run where the combustor reached a 23-2400° F equilibrium temperature, resulted in the decision to reduce the cooling percent to 25% and perform the characterization and duty cycle tests. It was also decided to delay the thermal tests until completion of the pulsing tests.

(1) Characterization Tests (Runs 97-137)

The engine performance was characterized over a range of pulse widths from 20 ms to 5 seconds, and the results are shown in Figures 47 and 48. The performance at 50 ms (315-320 seconds) exceeds the design goal of 300 seconds, but the 345-second performance at steady state is five seconds below the goal. The repeatability and response of the engine were excellent, with no discernible difference between the first and last pulse in a series. Figures 64 through 69 show some actual oscillograph records of the engine firings at thrust ranges from 5 down to 1.25 pounds. All firings were conducted with gases saturated with water.

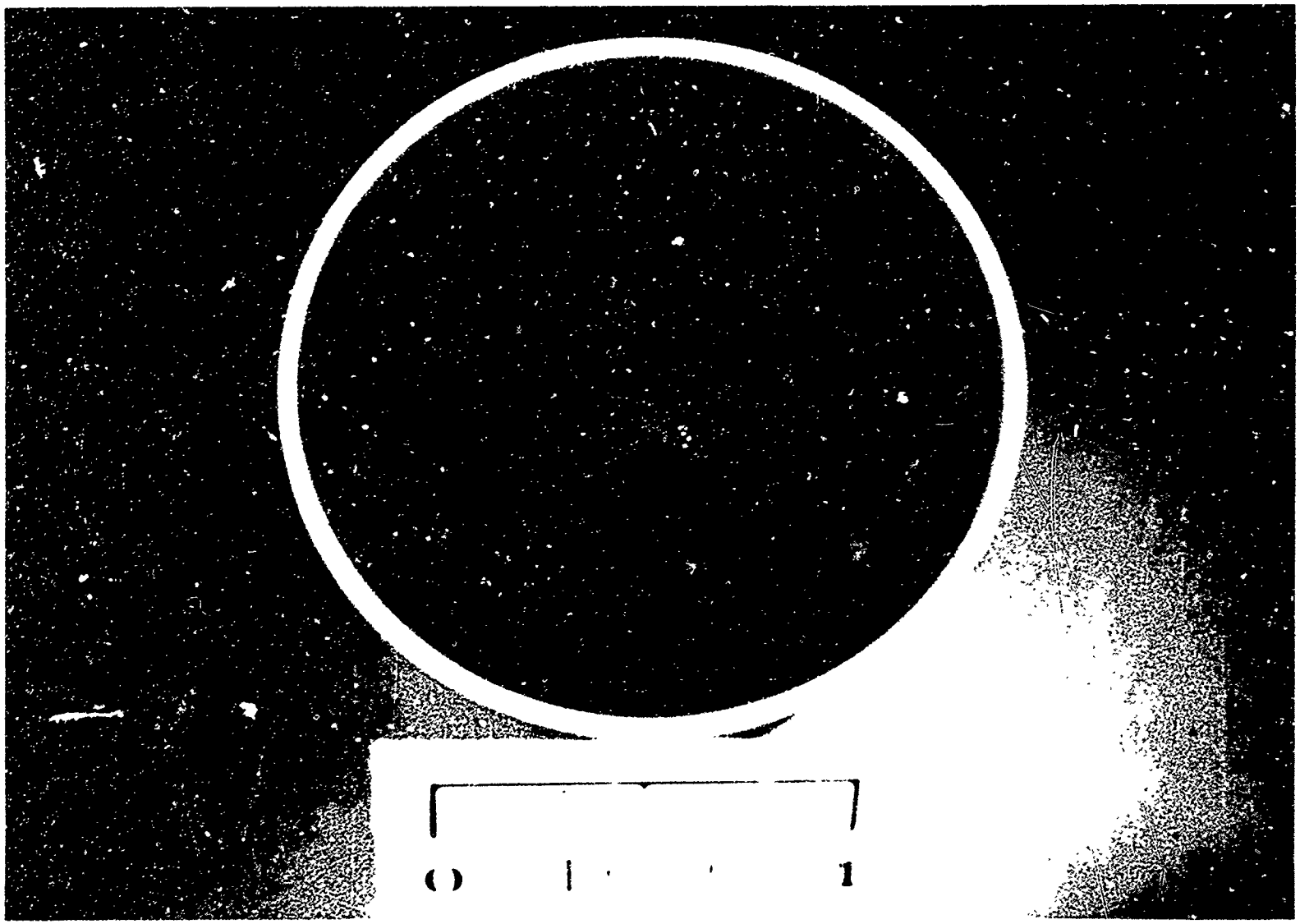

NEG 72-196-11

FIGURE 62. 5 LB_f COMBUSTION CHAMBER, END VIEW PRIOR TO TEST (CONF. # 1)

FIGURE 63. 5 LB_f COMBUSTION CHAMBER, PRETEST (CONF. # 19)

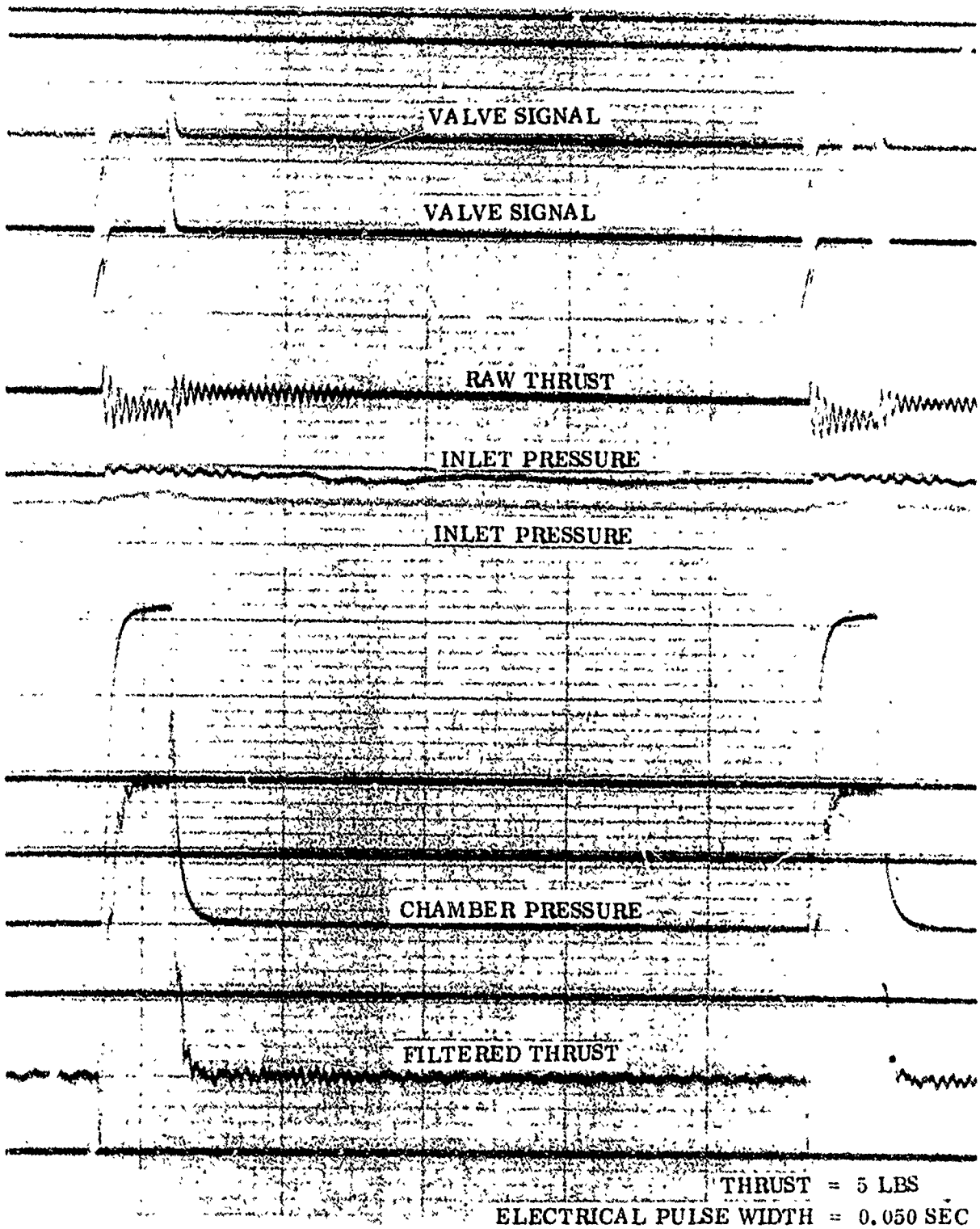

FIGURE 64. GO_2/GH_2 5 POUND THRUST ROCKET ENGINE TEST DATA

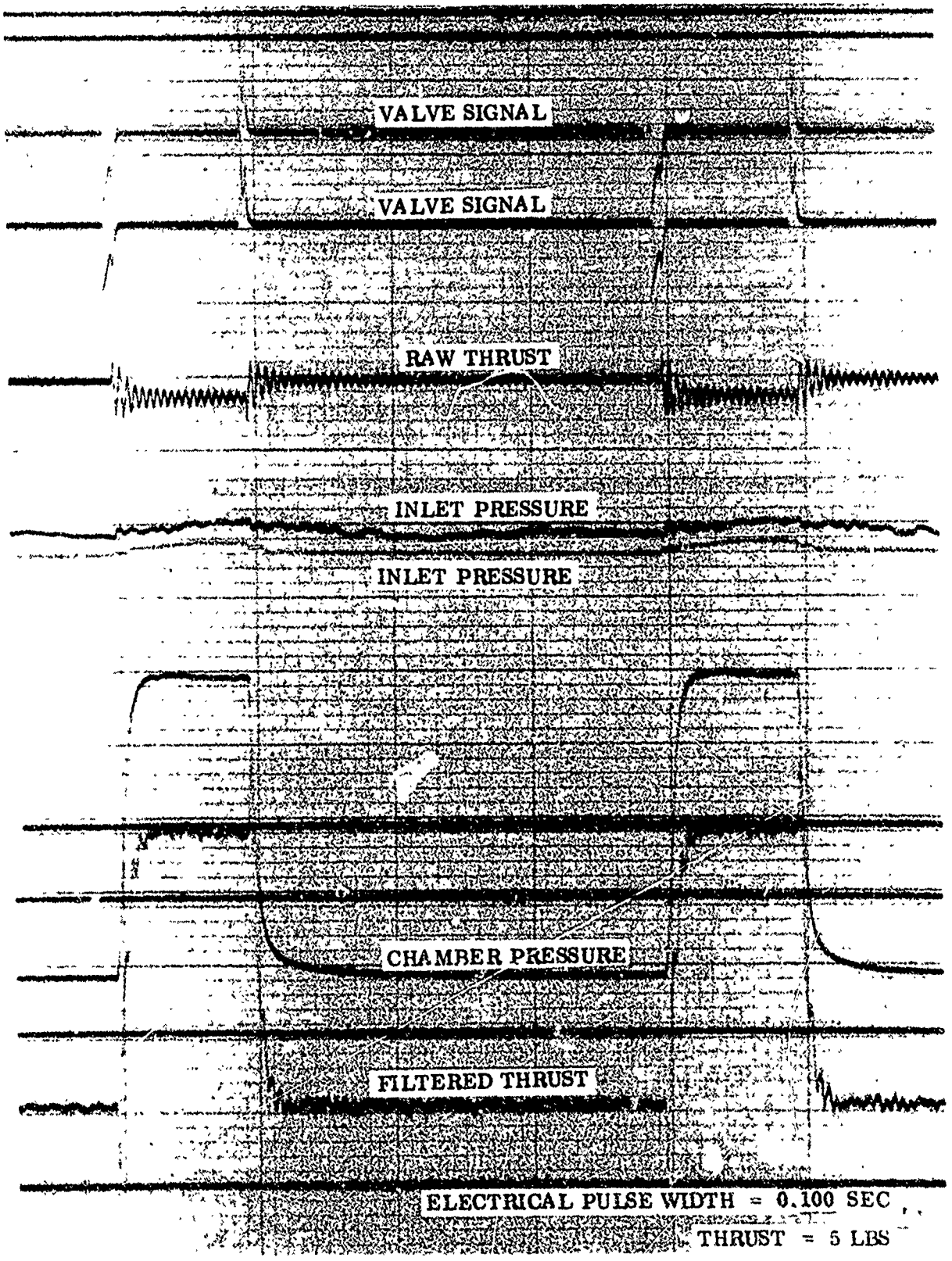

FIGURE 65. GO_2/GH_2 5 POUND THRUST ROCKET ENGINE TEST DATA

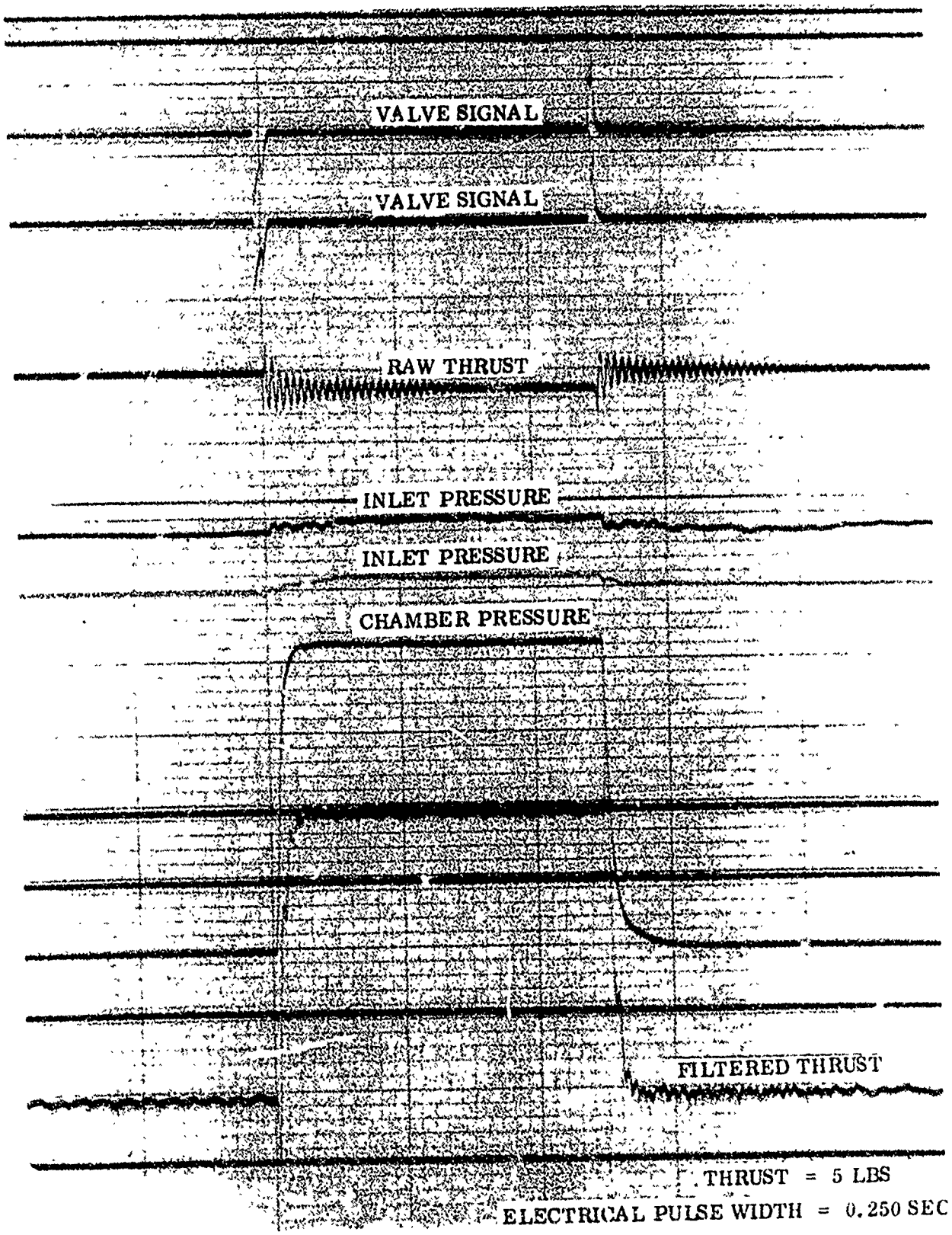

FIGURE 66. GO_2/GH_2 5 POUND THRUST ROCKET ENGINE TEST DATA

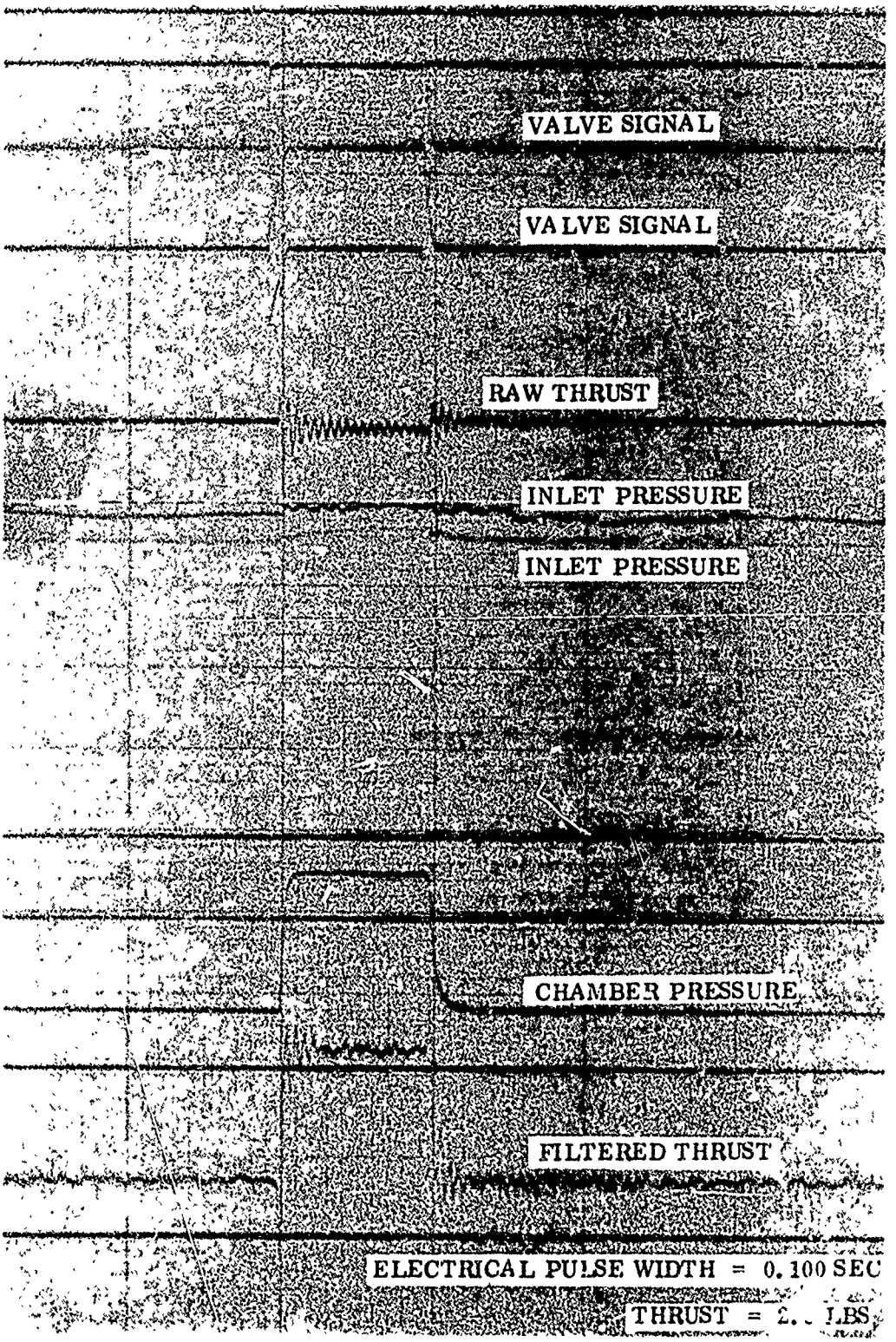

FIGURE 67. GO_2/GH_2 5 POUND THRUST ROCKET ENGINE TEST DATA

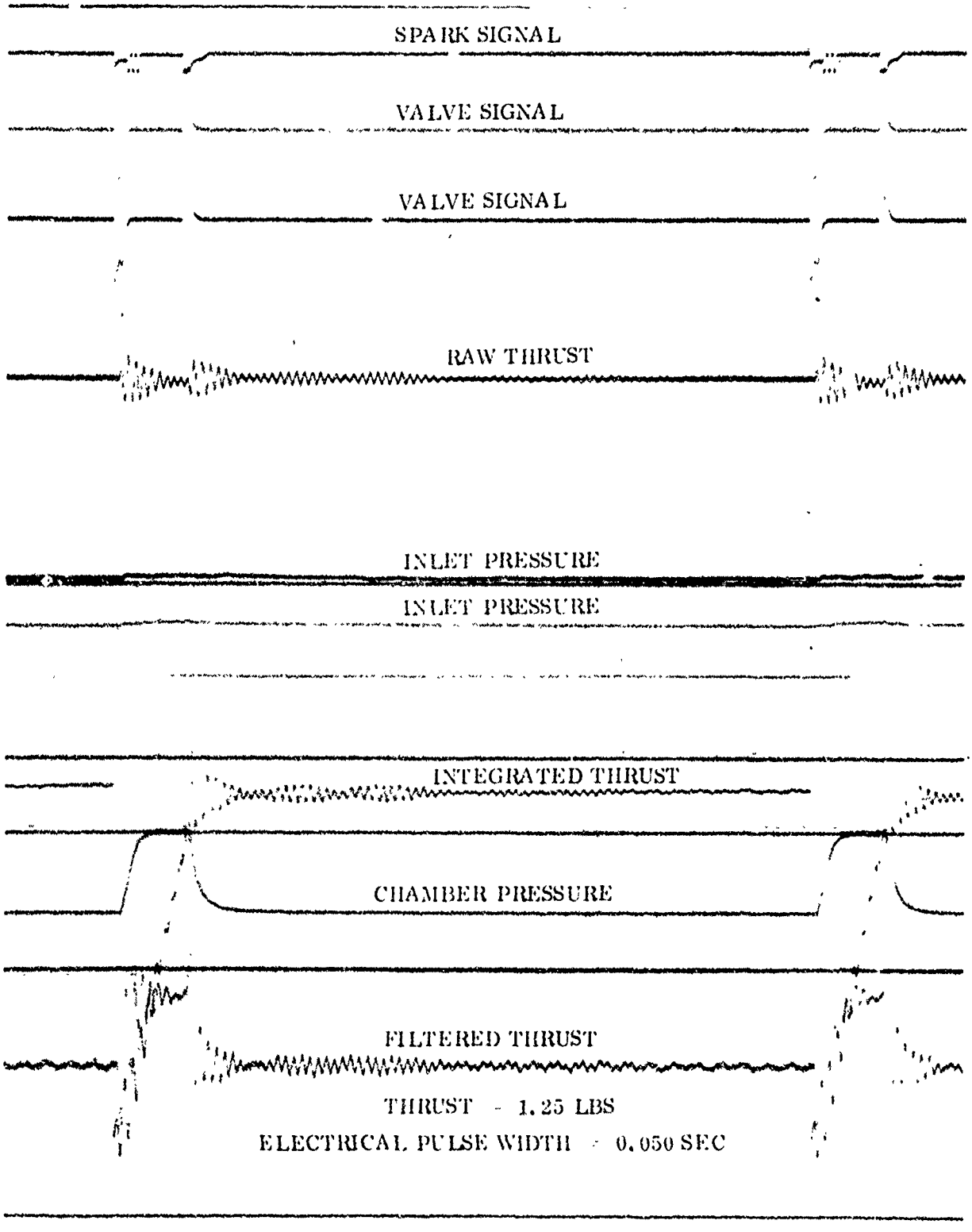

FIGURE 68. GO_2/GH_2 5 POUND THRUST ROCKET ENGINE TEST DATA

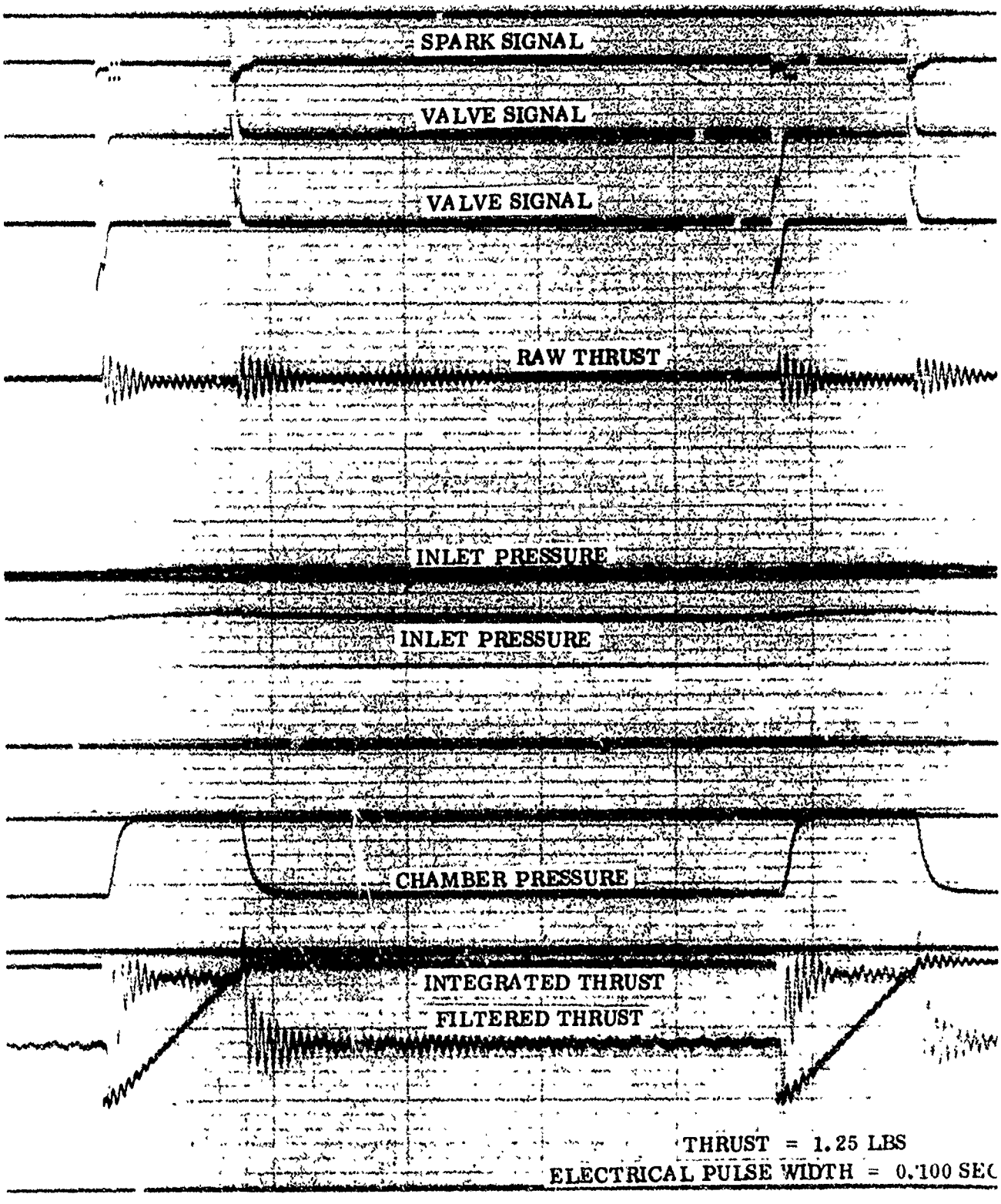

FIGURE 69. GO_2/GH_2 5 POUND THRUST ROCKET ENGINE TEST DATA

(2) Duty Cycle Verification (Runs 138-229)

A series of duty cycle tests were initiated per the requirements of the program to obtain 75,000 ignitions. During the tests the combustor temperature, as well as other parameters, were randomly recorded. The maximum temperature of the engine during the duty cycle occurred during the 250 ms firings wherein the temperature was 1900-2000°F. On Run 167 the engine exhibited numerous nonignitions. Further evaluation indicated that the igniter control circuit had partially failed and was not recharging properly between cycles. The igniter control was replaced by a spare and the testing continued.

Visual examination of the engine on completion of the 8/11 tests, or approximately 58,000 cycles, indicated no anomalies. On Run 223 there was an indication of chamber pressure decay, with no corresponding decay in thrust. Visual observation of the engine and Runs 228 and 229 indicated in increase in combustor temperature, and on Run 229 a few sparks were observed. The testing was terminated and visual examination of the engine indicated erosion of the throat.

Examination of the engine revealed that the combustor throat had partially burned out (see Figures 70 and 70) and the injector face (Figure 72) was severely cracked, and several of the premix orifices had partially slipped out of the injector holes. Also, small pieces of nickel were observed adhering to the combustor walls.

The partial burnout of the combustor, based on the observable data, was hypothesized to be due to failure of the EB weld joints, and the subsequent melting of the nickel orifices due to their partial movement into the area where combustion occurs. The resultant molten nickel impinging on the $MoSi_2$ coating of the combustor resulted in failure of the coating (similar experiences occurred in predevelopment tests with hypergolic engines which used moly combustors). The exposure of the molybdenum to the oxidizing environment caused a gradual erosion of the material as exhibited by a change or decay in chamber pressure. The failure of the weld joints was due to insufficient contact between the orifices and the injector. The temperature differential between the two parts resulted in a thermal fatigue stress failure.

Future designs using the premix concept would not require the use of orifices which are EB welded to the injector, but rather the orifice is part of the injector, thus eliminating this type of failure.

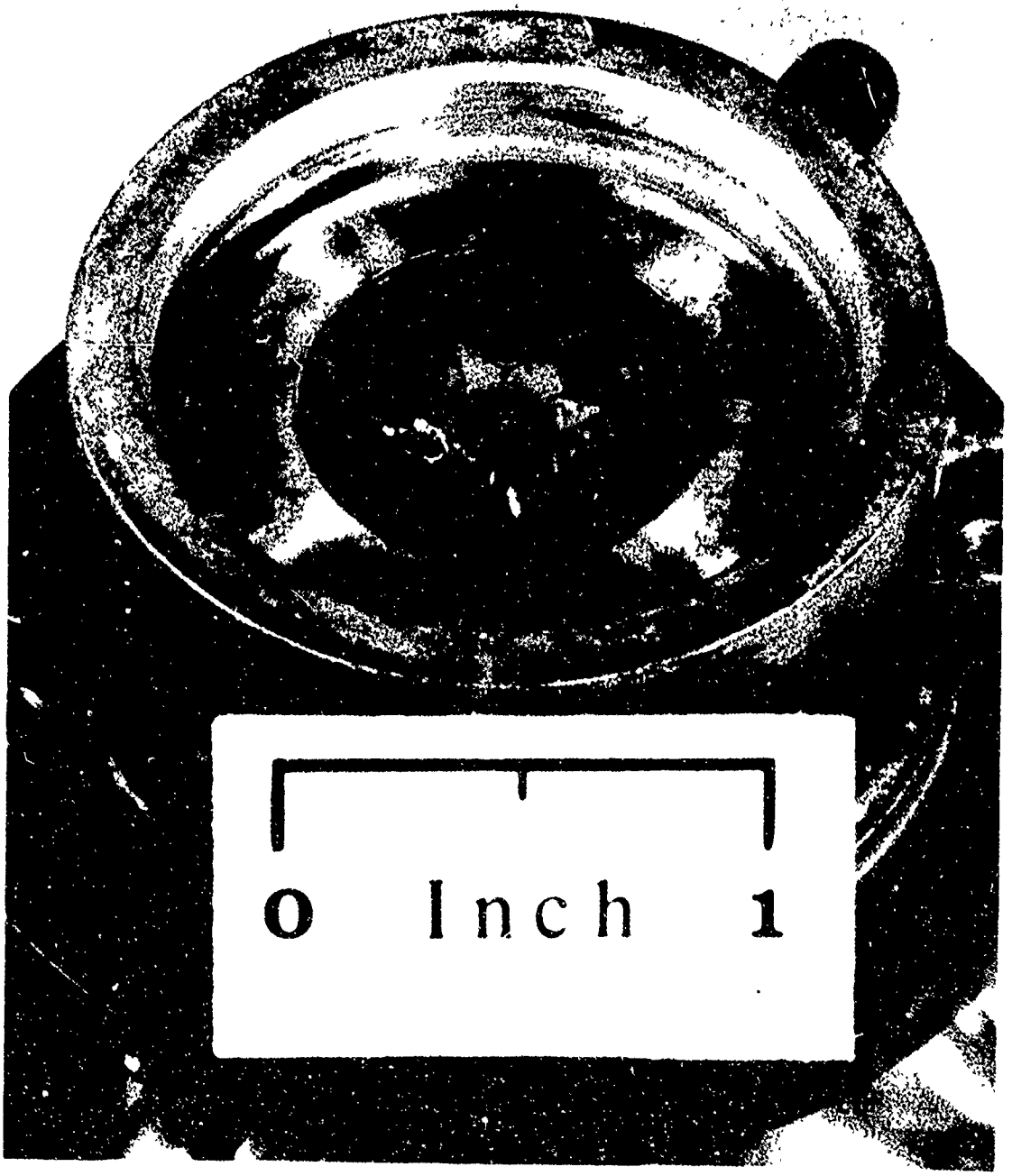

FIGURE 70. 5 LB_f THRUSTER INJECTOR INJECTER (POST TEST)

NEG 72-230-6

FIGURE 71. 5 LB_f THRUSTER
COMBUSTION CHAMBER/EXIT NOZZLE (POSTTEST)

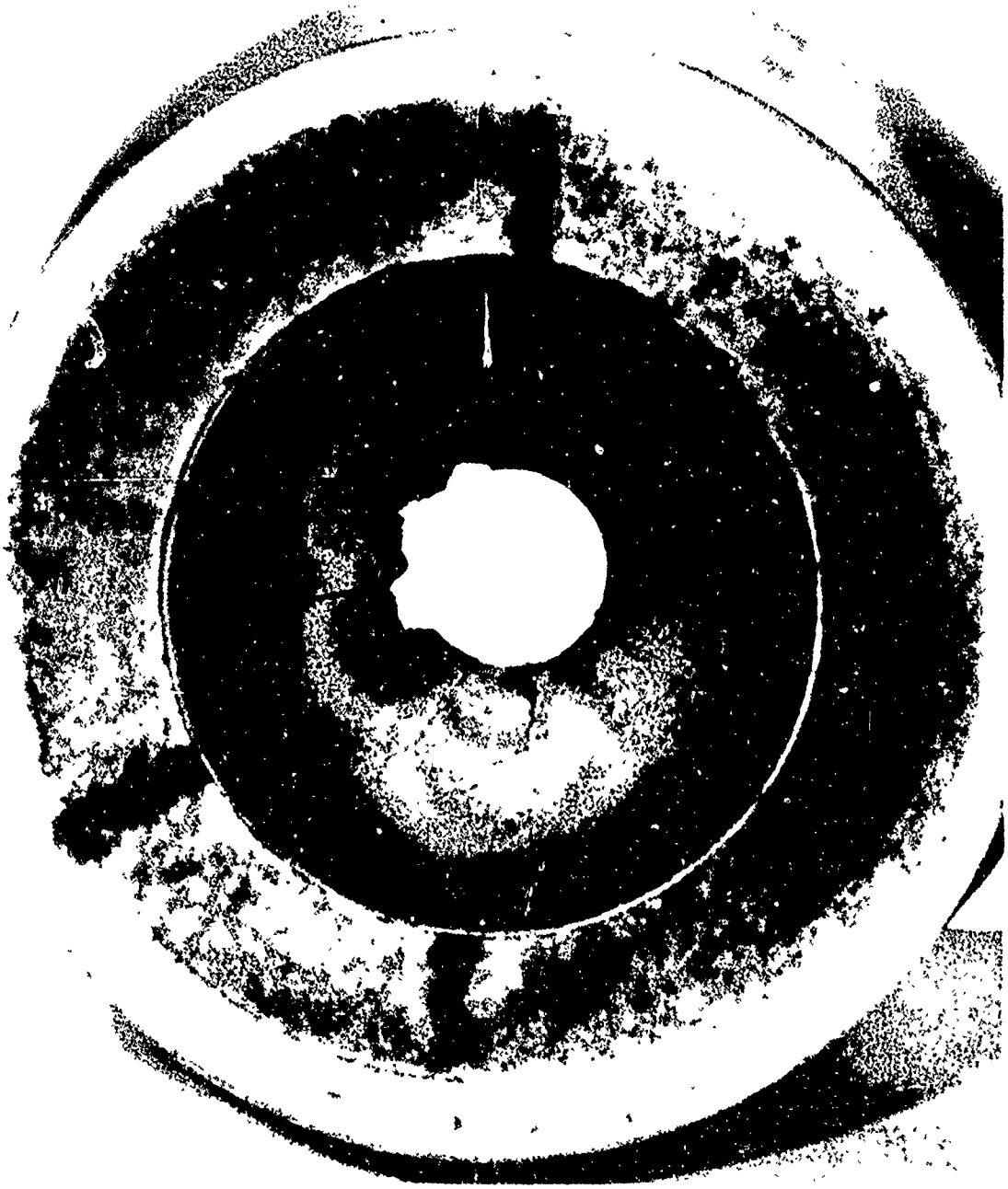

NEG. 72-230-5

FIGURE 72. 5 LB_f THRUSTER COMBUSTION CHAMBER/EXIT NOZZLE (CONFIGURATION NO. 20, POST TEST)

SECTION IV-C

ONE-TENTH POUND THRUST ROCKET ENGINE

The objective of the one-tenth pound thrust rocket engine program was to develop a gaseous oxygen/gaseous hydrogen rocket engine which operates at a mixture ratio of approximately 8 and will ignite 100% of the time. The minimum specific impulse for the engine was specified to be 300 seconds at steady state and 200 seoncds at the minimum impulse bit. In addition, the engine should have the capability to ignite up to 300,000 times and a steady state burn capability in excess of 10 hours.

1. SUMMARY OF RESULTS FROM PROGRAM

During this program 151,263 ignitions and 14,320 seconds of burn time were attained on the 0.1-pound boilerplate engine shown in Figure 73. The majority of the ignitions and burn time was with the molybdenum combustion chamber, but a small portion of the tests used an engine with a nickel combustor to demonstrate its adequacy. The performance of the engine with a 100:1 exit nozzle expansion ratio is 330 seconds at the 0.1-pound thrust level and 300 seconds at approximately 0.03 pounds thrust, as shown in Figure 74. Documentation of the pulsing performance was not possible due to the large pressure port and pressure transducer lines (up to 10 times the combustor volume). Ignition at pulse widths down to 12 ms was verified by the fact that the igniter only operates for 12 ms.

Duty cycle verification tests were conducted at 0.020 second on and 0.480 second off at a rate of 1000 cycles per test. Following the successful completion of this series of 150,000 ignitions, a series of 1000 20 ms firings at a rate of 1/6 Hz (10 seconds off) was conducted to document first pulse capability. At the conclusion of this test, a series of steady state firings ranging up to 60C seconds duration was accomplished.

2. ENGINE DESIGN

The design of the 0.1-pound thrust rocket engine was based on studies and prior experimental work which indicated only that the engine of this size could be ignited and, in a mixed gas situation, exhibit adequate (80 - 100%) combustion efficiencies.

The design of the 0.1-pound engine was divided into two areas:

a. Injection
b. Ignition

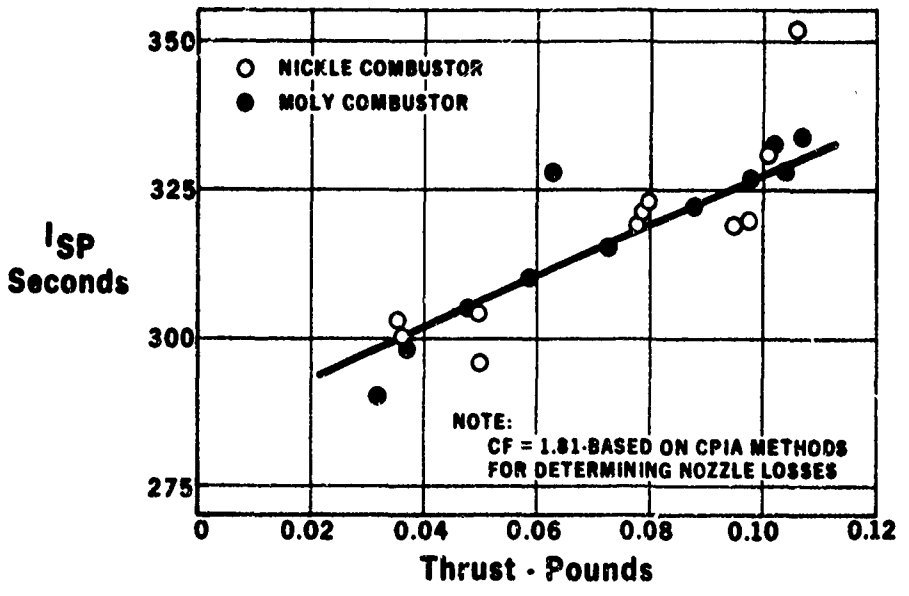

FIGURE 74. 0.1 LB_f THRUSTER PERFORMANCE

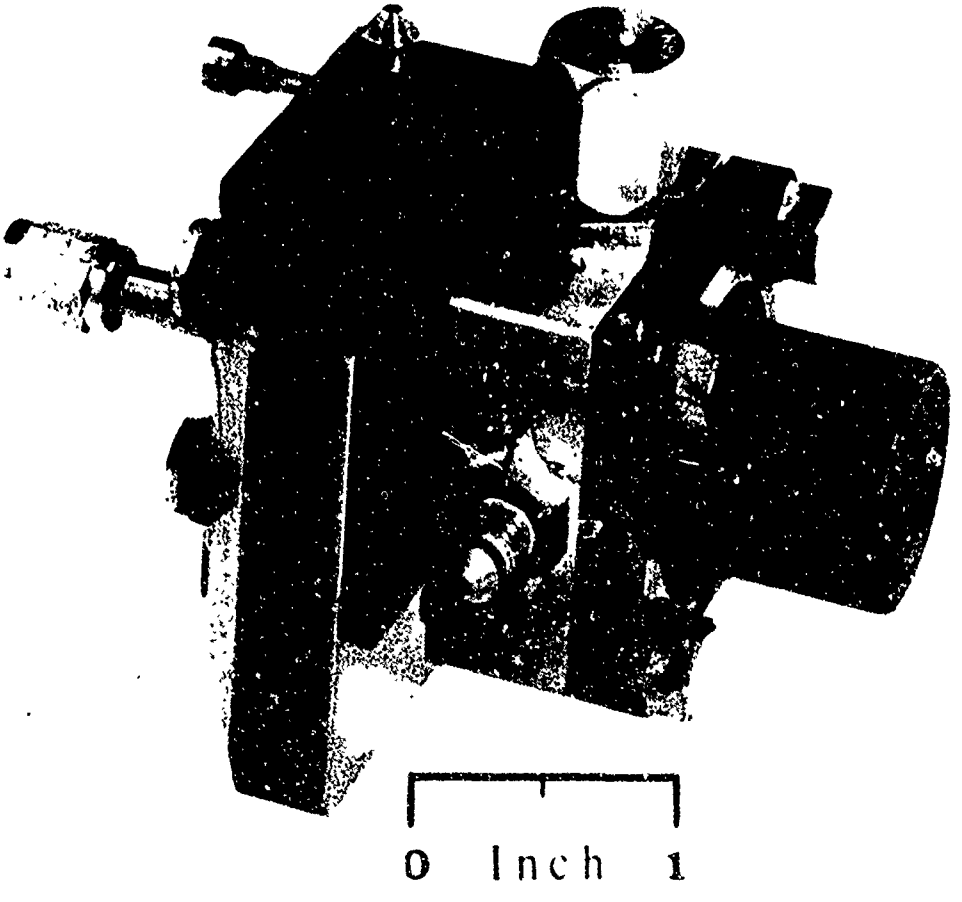

FIGURE 73. 0.1 LB_f THRUSTER

a. Injection (Initial Concepts)

The mixing of gaseous hydrogen and gaseous oxygen has been experimentally and theoretically studied for many years, and in 1971-72 the potential use of this system on the space shuttle resulted in a variety of contractor efforts relating to GO_2/GH_2 combustion. The two candidate injection concepts which, based on prior data, provided the most efficiency were the coaxial and premix concepts. At the initiation of this program, the premix concept was not as developed a method and, as a result, initial efforts in developing an 0.1-pound thrust engine were oriented toward the coaxial element.

Because of the size, only one (1) element could be utilized, and thus the mixing of the two streamswas important since mixing between elements would not be possible. As a result of the design study, the initial injector consisted of a single coaxial element with nominal injection velocities of 500 ft/sec for hydrogen and 125 ft/sec for the oxygen.

b. Ignition (Initial)

The achievement of ignition and long life was a challenging problem because of the small size of the engine. All types of ignition devices were evaluated including catalyst, laser, glow plug, and compression, but the analysis indicated that only spark ignition was potentially the lightest and most reliable. Previous programs using GO_2 and GH_2 had shown its reliability and all that was needed for the concepts' incorporation into the 0.1-pound thrust engine was a plug which was small enough to be compatible with the size of the engine. The spark ignition source and type of ignition would have to be common to both the 5-pound thrust engine and the 0.1-pound engine. The ignition source used is described in a separate section and will not be discussed further other than to indicate that a delivered output from the igniter controller of 50 millijoules or milliwatt seconds was desired.

Success in procurement of a small (0.10-diameter) spark plug was less than desired. The companies contacted either did not desire to fabricate any of that size or were evaluated as not technically capable of providing the adequate plug. As a result, the engine developed in this program used a spark plug which was commercially available.

c. Initial Engine Design

The initial engine tested during this program was boilerplate in nature but incorporated those design criteria and concepts which would be applicable to the future flight design.

The initial engine to be tested was designed to test the effects due to spark location and injector variable for the coaxial concept. Figure 75 shows the

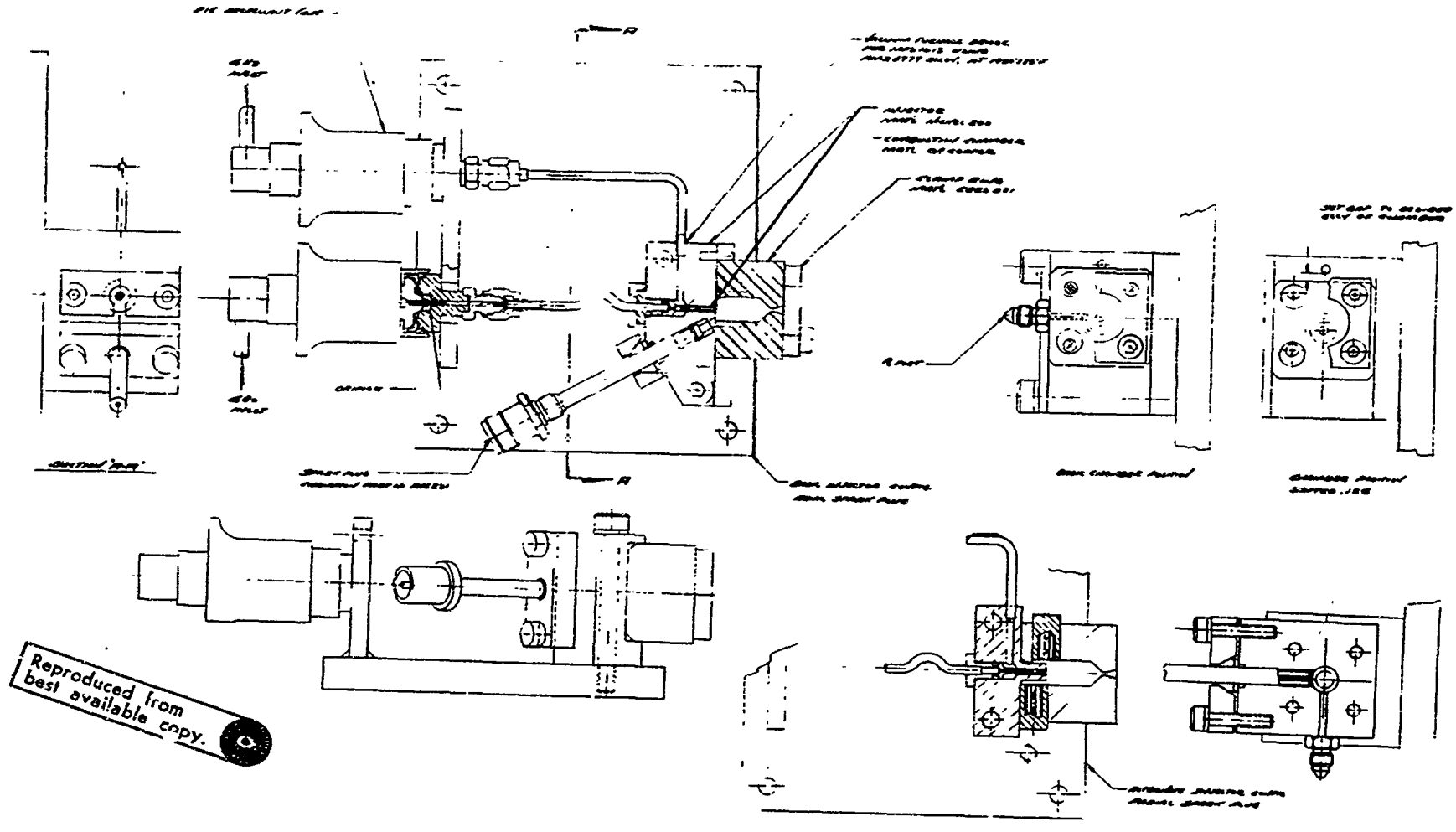

FIGURE 75. 0.1 LB_f THRUSTER DRAWING L-4757

engine design while Figures 76 and 77 show the engine fabricated, exploded (unassembled) and assembled.

The engine consists of two Marquardt R-1E coaxial solenoid valves, a nickel injector, an FHE231 champion spark plug, and a nickel combustion chamber. The engine is mounted on a steel mounting bracket. Flow to the injector is controlled by sonic orifices located downstream of the valves. As shown in Figure 75, the initial configuration could incorporate both side and injector mounted spark plugs.

The engine was designed to deliver 0.1 pound of thrust at a chamber pressure of 50 psia and had the capability to blowdown to a chamber pressure of 16.7 psia. The construction was boilerplate in nature, so that the engine could be run for substantial periods of time and only heat sink cooling would have to be utilized. All parts were bolted together for ease of refurbishment.

(1) Valves

Although R-1E valves, Figure 78, were used in this program, the engine was also designed to incorporate latch type valves shown on Figure 79. The R-1E valves used previously on the birpopellant 22-pound thrust MOL engine consumed more power than desirable, but based on their test history reliability, it was decided early in the program to use them exclusively since the concept was capable of incorporating almost any available valve.

(2) Injector

As described earlier, the injector incorporated a single coaxial element and a FHE 231 spark plug. The oxidizer post shown in Figure 76 was a slip fit with "O" ring seal used to prevent leakage of H_2 to the environment. The spark plug was sealed using a swagelok type arrangement.

(3) Combustion Chamber

The combustion chamber was constructed of nickel with adequate mass to insure a capability for long run times. Seals between elements were by "O" rings.

d. Projected Performance

Prior to tests being conducted, and since no thrust measurement was made, an estimation of what performance losses may be incurred was made based on the JANNAF standard methods. The resulting breakdown is shown in Figure 80 where the predicted performance is approximately 330 seconds. The combustion efficiency was assumed to be 95% excluding heat loss. Heat losses were up to 8-10% of the total heat release due to the small small size, and as a result a projected delivered C* efficiency of 85-90% maximum was expected.

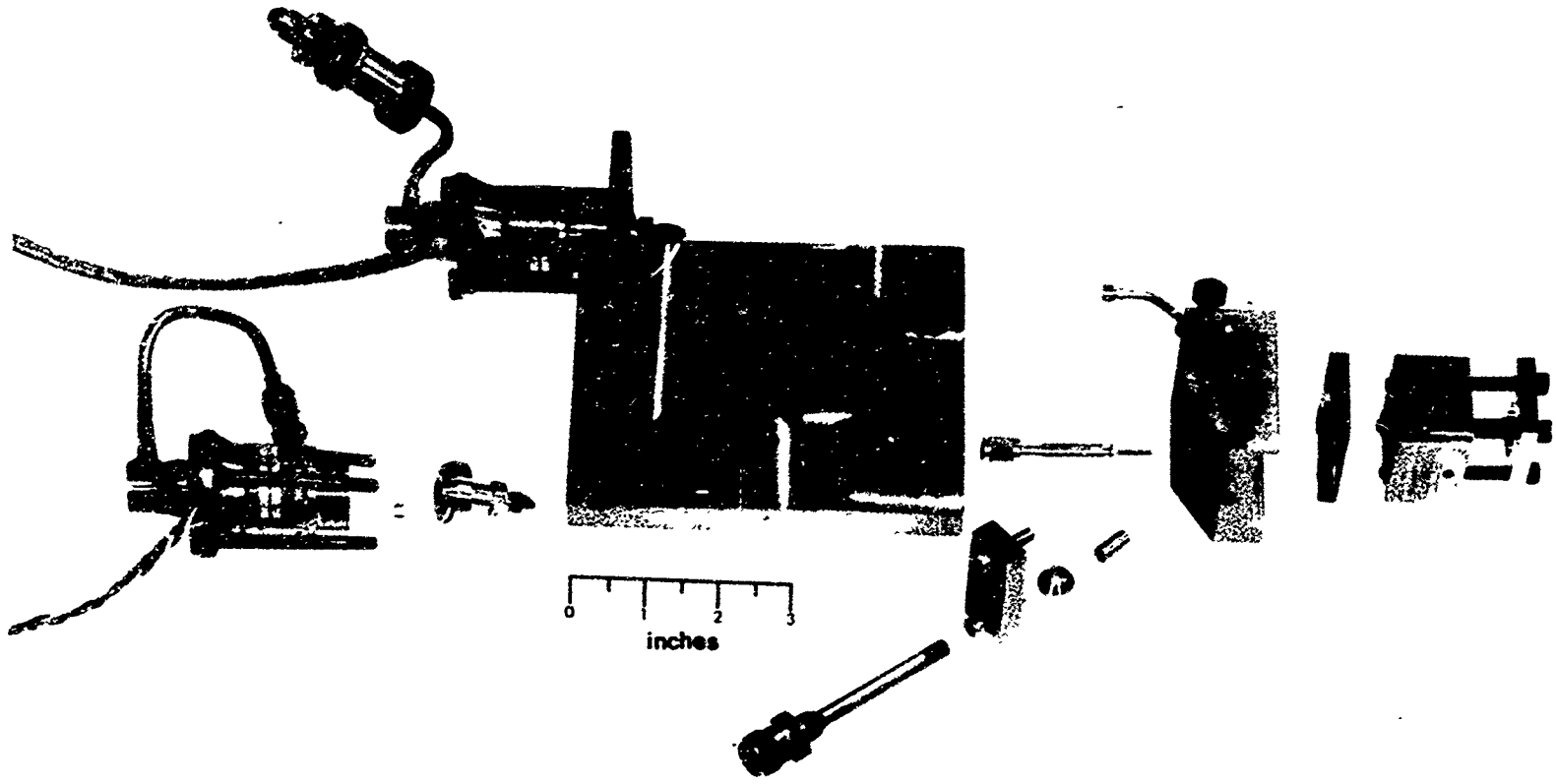

FIGURE 76. 0.1 LB_f THRUSTER (WORKHORSE TYPE - EXPLODED VIEW)

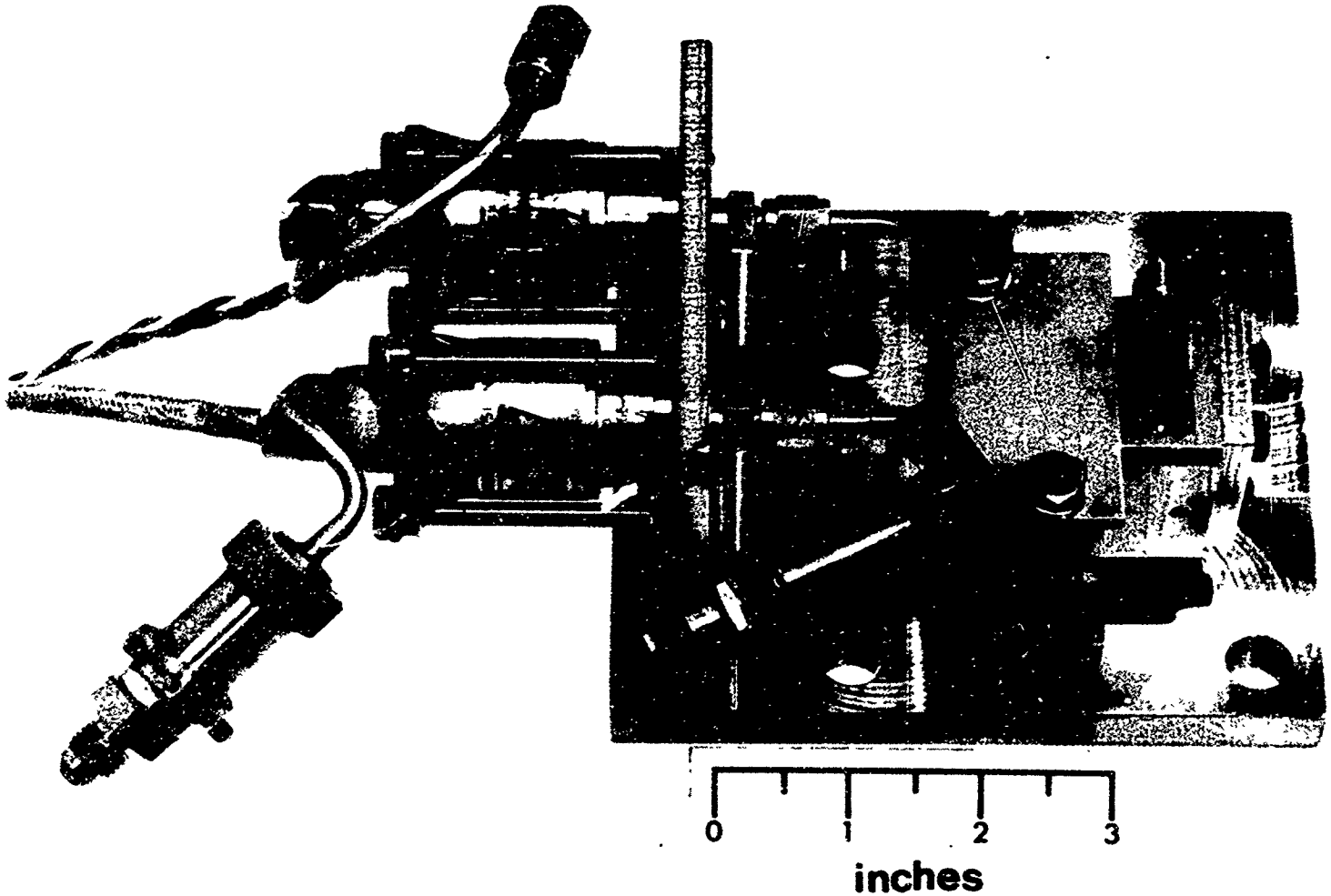

NEG. 71-179-2

FIGURE 77. 0.1 LB_f THRUSTER (WORKHORSE TYPE)

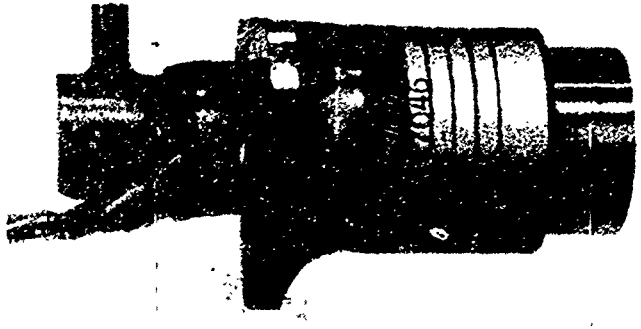

NEG. 9727-2

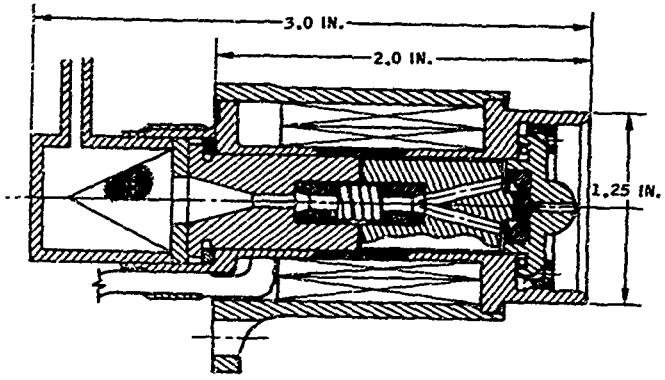

P/N 229068

Valve Type	Poppet, coaxial flow, solenoid actuator
Operating Fluids	Nitrogen tetroxide and MMH
Weight	0.65 lbs.
Nominal Operating Voltage	28 V.DC
Steady State Current	Coil No. 1, 0.56 amps at 25 V.DC and 68°F Coil No. 2, 0.53 amps at 25 V.DC and 68°F
Pressure Drop	25 psi at 0.040 lbs/sec water
Nominal Operating Pressure	200 psia
Maximum Operating Temperature	200° F
Leakage	Zero Liquid Leakage
Opening Response (Signal "ON" to fully OPEN)	8.0 ms at 25 V.DC, 200 psia propellant, 70° F.
Closing Response (Signal "OFF" to fully CLOSED)	5.0 ms at 25 V DC, rated flow of H_2O
Cycle Life	50,000 cycles min.
Program Application	MOL
Special Features	Two (2) actuating coils, integral filter

FIGURE 78. R1E VALVE

P/N X28050

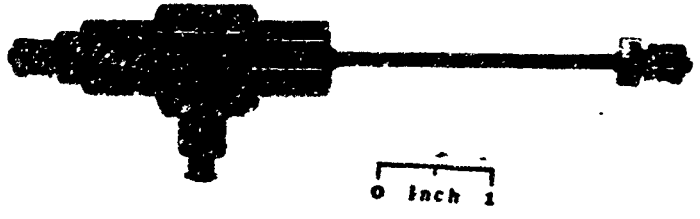

MINIATURE BISTABLE VALVE CROSS SECTION

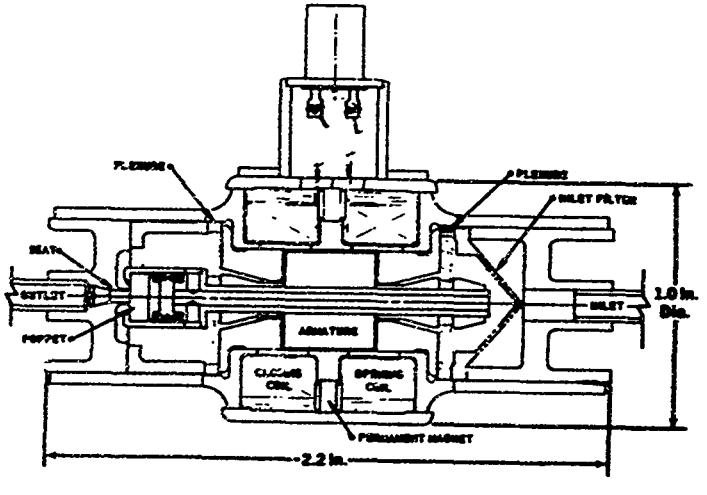

- Valve Type ..... Poppet, Coaxial Flow, Bistable
- Operating Fluids ..... Hydrazine, GN_2, He, H_2O, NH_3, CO_2
- Weight ..... 0.26 LB.
- Operating Voltage ..... 15-32 VDC −40° TO +300°F
- Power ..... 25 Watts Steady State at 30 VDC 70°F
  0.25 Watt Sec. per Cycle
- Pressure Drop ..... < 1 PSI at 0.001 PPS H_2O
- Nominal Operating Pressure .. 0 - 400 PSIA
- Proof Pressure ..... 800 PSIA -MIN.
- Leakage ..... < 1 SCCH He 0 - 400 PSIA
- Opening Response ..... 2.5 MS at 25 VDC, 70°F, 400 PSIA
  (Signal On to Full Open)
- Closing Response ..... 2.5 MS at 25 VDC, 70°F, 400 PSIA
  (Signal On to Full Close)
- Cycle Life ..... >100,000
- Program Application ..... Rugged Resistojet (NASA-Langley)
  0.1 Monopropellant Systems
- Special Features ..... Integral 25 μ Abs. Filter
  No Electrical Power Required
  to Hold Open or Closed.
  Seat Seal of AF-E-102.
  All Welded Construction.
  Flexure Guided—No Sliding Fits.

FIGURE 79. MARQUARDT LATCH VALVE

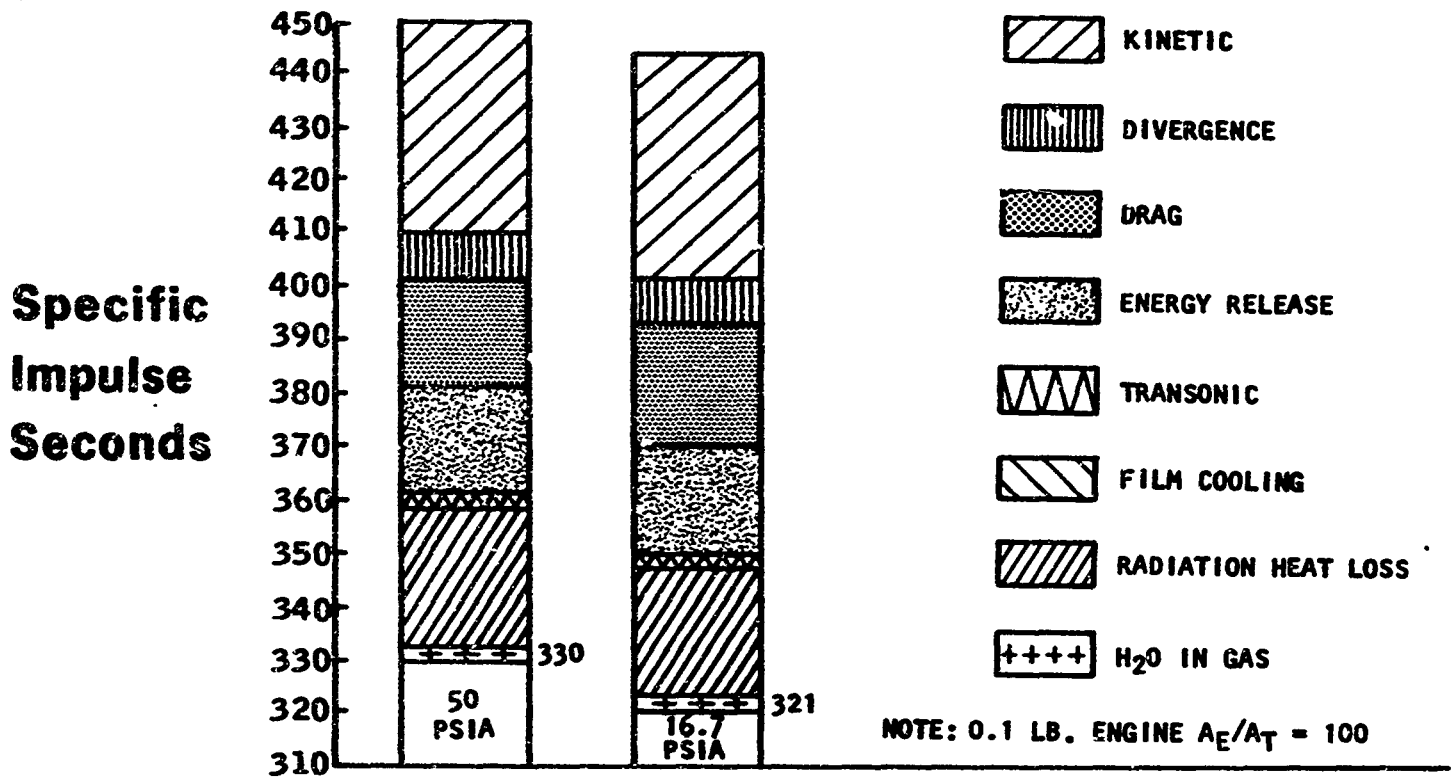

FIGURE 80. 0.1 LB_f THRUSTER PREDICTED PERFORMANCE

3. TEST PROGRAM

The tests on the 0.1-pound GO_2/GH_2 engine were conducted in the Bldg 42 altitude facility shown in Figure 81. The system has a capability of maintaining 235,000-foot altitude pressure (0.0007 psia), although a majority of the tests were conducted approximately 0.009 psia(.5 torr). Instrumentation and test cell setup were according to Marquardt Test Plan MTN 3700. Table 16 and Figure 82 show the instrumentation and test cell schematic for the cell. Data reduction was limited to determination of the delivered C* and the mixture ratio. The gases in the final test series were saturated with water by passing the gases through a column packed with ceramic balls and containing sufficient water to provide 100% saturation.

a. Data Reduction

The characteristic velocity and mixture ratio were determined from measurements of the chamber pressure which was statically located in the combustion chamber and the inlet pressures. The sonic orifices installed in the thruster assembly were, prior to installation in the Bldg 42 test cell, calibrated by volumetrically measuring the amount of gaseous nitrogen which flowed through the engine at various inlet pressures. The calibrations were then corrected to account for changes in the gas constant, isentropic exponent, and type of gas according to standardized ASME methods. No corrections were made in the characteristic velocity for heat loss or static to total pressure. Other data such as valve current, spark number and chamber temperature were recorded for in-cell reference and future thermal and ignition analysis.

b. Ignition System

Initial tests conducted on the 0.1-pound thrust engine incorporated the Marquardt universal spark igniter control system (see section on spark ignition). The unit is a capacitive discharge type with a capability of providing to the spark plug an energy of 0.01 to 0.4 Joules (watt seconds) per spark. The unit can provide sparking at a rate of 200 sparks/second and durations from one spark up to continuous. Delays in initial spark can be up to 85 ms.

c. Test Program (Initial Tests)

The test program for the 0.1-pound thrust was oriented toward establishing a reliable igniting and high performance design. After the initial tests were conducted on the design, it was obvious that performance and ignition are synonymous and that if good mixing is evident, then ignition will be reliable. The evaluation of the final engine design was not the result of several design changes but rather a series of distinct steps in which only one variable was changed. The end result was a high performance/reliable igniting system which can be readily developed into a flightweight system. The next section describes in detail the evolution of the 0.1-pound engine and provides the backhround for the final engine tested in this program

NEG. T11349-6

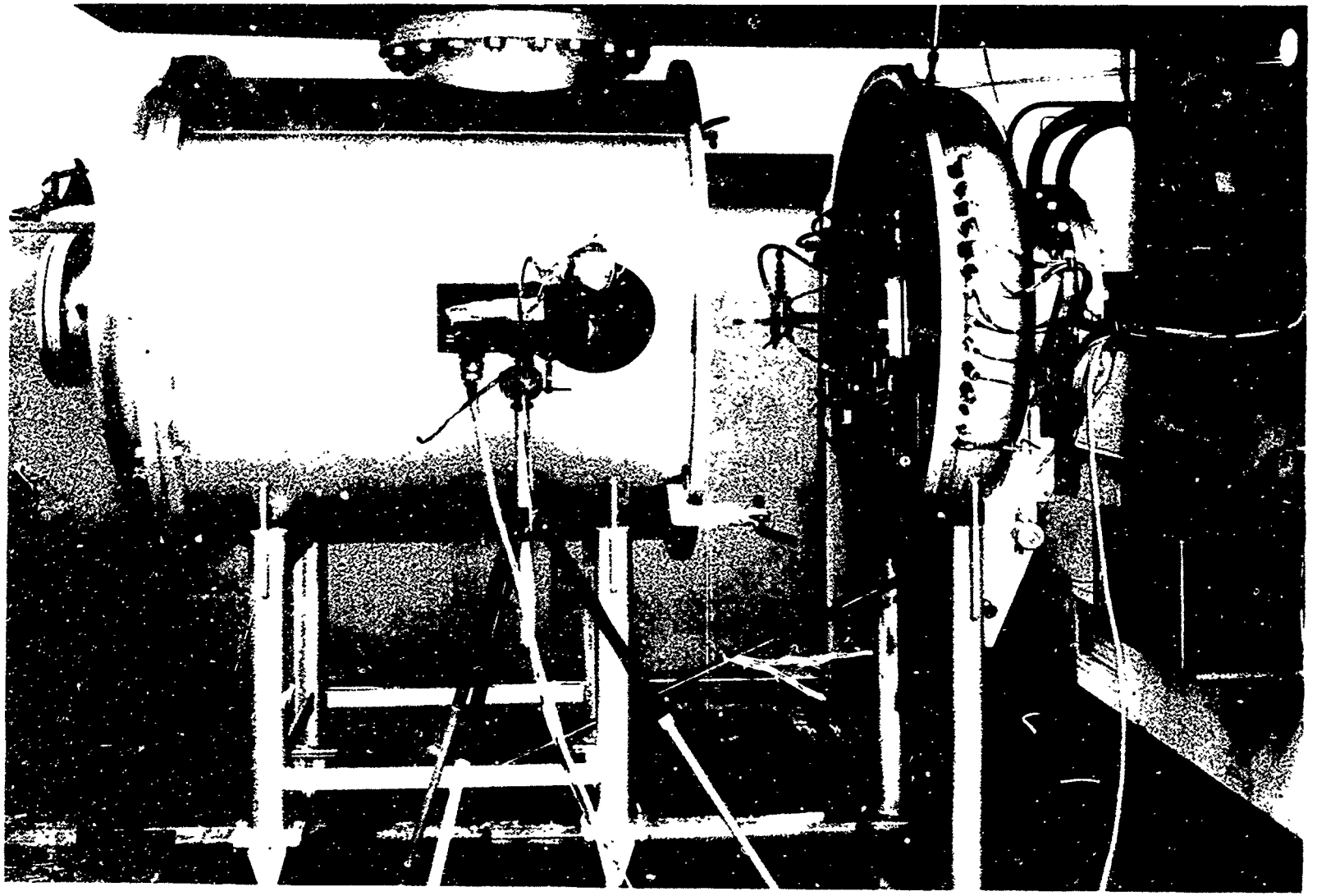

FIGURE 81. BUILDING 42 TEST FACILITY

TABLE 16

INSTRUMENTATION REQUIREMENTS

Parameters	Description	Range of Interest	Readout		
			Digr.	Osc.	Other
P_{O_2}	Oxidizer Inlet Pressure	0-200 psig	-	-	X[1]
P_{H_2}	Hydrogen Inlet Pressure	0-200 psig	-	-	X[1]
P_C	Chamber Pressure	0-100 psia	-	X	-
t	On Time (event marker)	-	X	-	-
i	Valve Current	0-3 amp	-	X[2]	-
E	Valve Voltage	0-40 vdc	-	X[2]	-
T_C	Thrust Chamber Temperature	0-1000°F	X	-	-
N_s	Number of Sparks	0-500 milli-joules	-	X	-

1. Pressure Gage Only

2. Induced Voltage in the passive coil may be measured as an alternate.

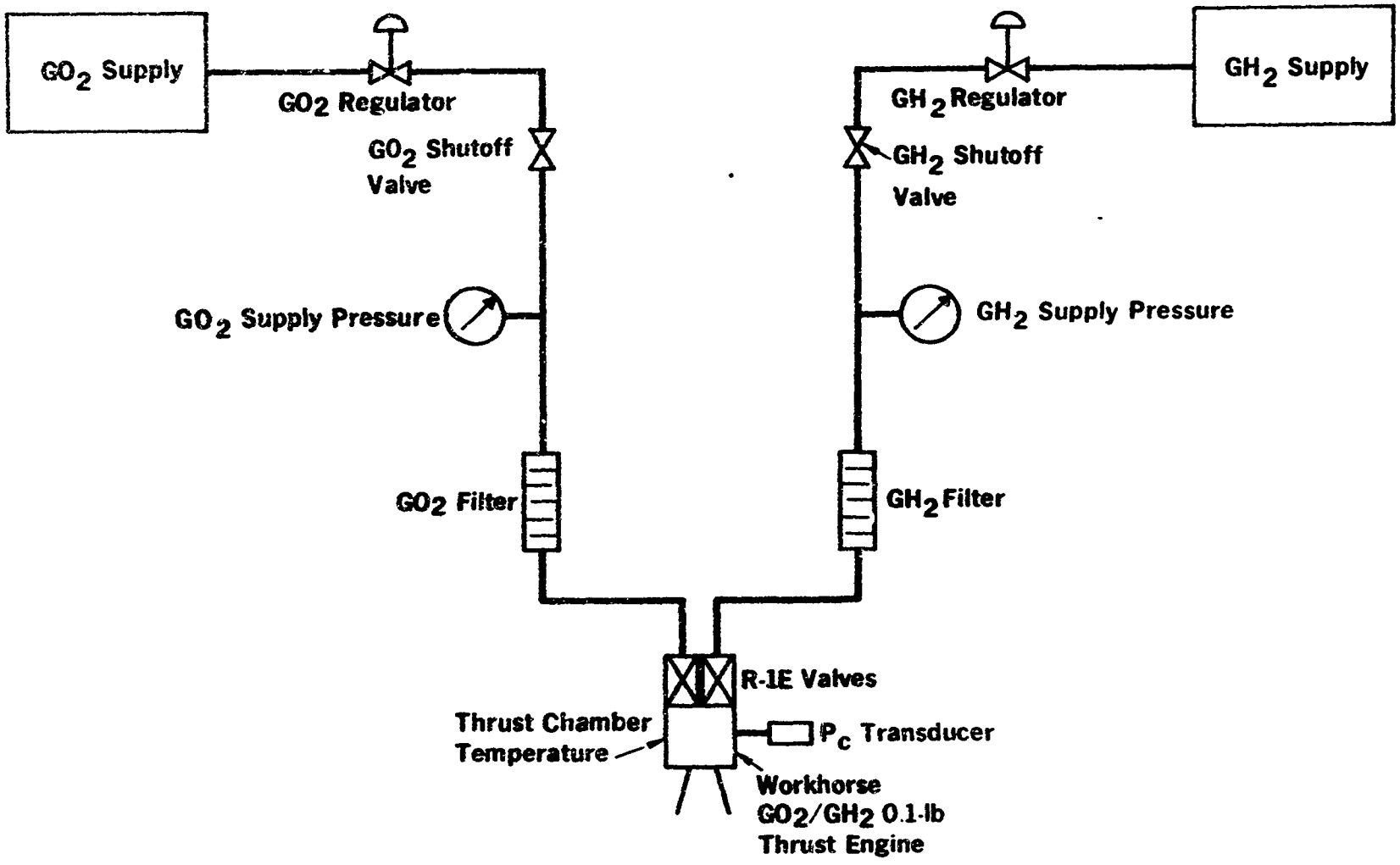

FIGURE 82. 0.1 LB_f THRUSTER TEST INSTALLATION

which successfully accumulated more than 150,000 starts and 10,000 seconds of burn time.

(1) Test Results - Spark Plug in Injector Face

Initial Engine Configuration

The engine configuration tested initially is shown in Figure 83. The injector had a single coaxial element consisting of a central 0.0378-inch oxygen orifice surrounded by five hydrogen orifices in the form of circular segments. At a chamber pressure of 50 psia, the oxygen injection velocity is 125 ft/sec, and the hydrogen velocity is 500 ft/sec.

The initial chamber contraction ratio was 100:1. The spark plug tip was 0.35 inch from the place of the injector face, connected to the combustion chamber through a 1/8-inch hole partially covered by the chamber. A summary of all the tests conducted prior to the final test phase is contained in Table 17.

Runs 1 to 57

A number of runs were made to work out electrical problems in the ignition and pulser circuits. During these runs (1 to 57) some ignitions and short firings were made which revealed that the C* efficiency with the 100:1 chamber was only 55 to 58 percent. It was also found that the spark plug tip had to be moved within 0.10 inch of the injector face.

Runs 58 to 76

An aluminum chamber with a 4:1 contraction was used in the next major configuration change (see Figure 83) and resulted in an increased C* efficiency of 75 percent at a chamber pressure of 50 psia. Ignition was reliable at low spark energy except at low chamber pressures. The rise of chamber pressure was not smooth for chamber pressures of 19 psia and 31 psia. There was also a step in the P_c versus time curve during the first 100 ms, but this was not evident at a chamber pressure of 50 psia.

Runs 77 to 83

A 0.25-inch long copper chamber spacer with a 100:1 ratio was combined with the 4:1 aluminum chamber for Runs 77 to 83. Ignition was reliable at 50 psia but not reliable at low pressures. The step in the P_c response was similar to that observed with the preceding configuration. The C* efficiency had dropped to 69 percent, however.

FIGURE 83.

INITIAL ENGINE CONFIGURATION WITH (100:1) CHAMBER RUNS 1 TO 57 AND (4:1) CHAMBER RUNS 58 TO 76

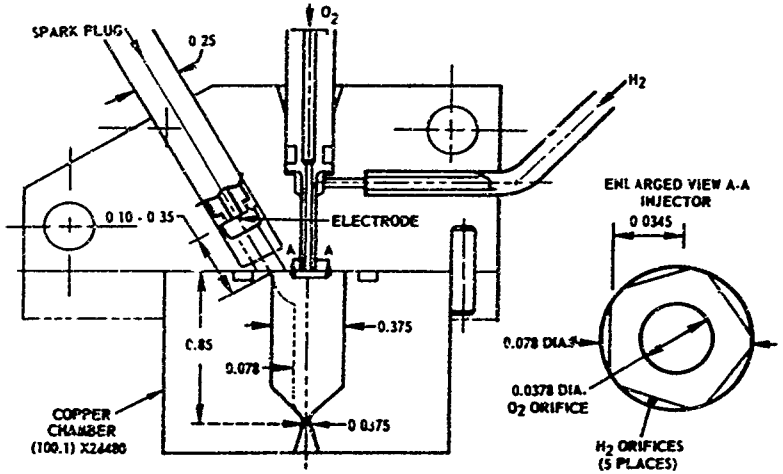

FIGURE 84.

SHORT ALUMINUM CHAMBER (8:1) WITH TWO SPACERS (2:1) RUNS 119 TO 126

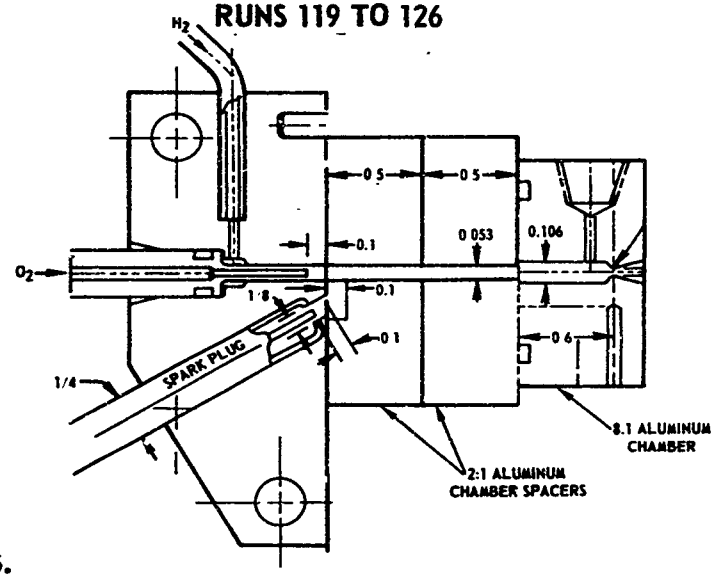

FIGURE 85.

SIDE MOUNTED SPARK PLUG CONFIGURATION RUNS 160 TO 169

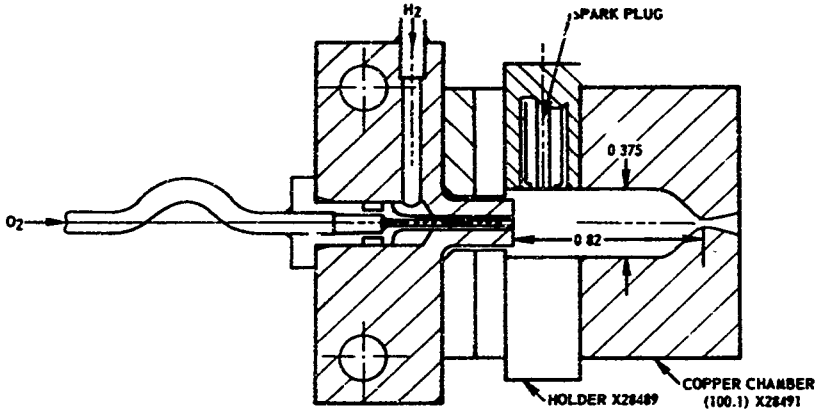

TABLE 17.

SUMMARY OF 0.1-LB TEST FIRINGS

(Boilerplate)

Run No's	Date	Engine Configuration	Chamber	C*Eff.	Ignition Probability	P_c Rise Characteristics
1-2	12-21-71	Coaxial injector, axial plug .35 in. from face	Copper 100:1		Cold Flow Tests Only	
3-15	12-22-71	Coaxial injector, axial plug. 35 in. from face	Copper 100:1	58	Poor	
16-19	1-3-72	Coaxial injector, add .25 in. chamber spacer	Copper 100:1		No Ignition - Spark Circuit Failed	
20	1-3-72	Coaxial injector, no chamber spacer	Copper 100:1		No Ignition - Spark Circuit Failed	
21-57	1-4 to 1-6	Coaxial injector, axial plug .1 in. from face	Copper 100:1	55		
58-76	1-6-72	Coaxial injector, plug bottomed	Aluminum 4:1	75	Good except at low P_c	Good at hi P_c, bad at low P_c
77-83	1-6-72	Coaxial injector, .25 in. chamber spacer	Aluminum 4:1	69	Fair except at low P_c	Good at hi P_c, bad at low P_c
84-93	1-6-72	Coaxial inj. retracted .2 in. no chamber spacer	Aluminum 4:1	69	Very good	Fair
94-111	1-7-72	Coaxial inj. flush, rotated 36°	Aluminum 4:1	69	Poor	Good at hi P_c, bad at low P_c
112-118	1-7-72	Coaxial inj. retracted .1 in.	Aluminum 4:1	66	Good except at low P_c	Good at hi P_c, no tests at low P_c
119-126	1-10-72	Coaxial inj. retracted .1 in., (2) 2:1 chamber spacers	Aluminum 8:1	58	Poor	Slow, smooth

TABLE 17. (CONTINUED)

SUMMARY OF 0.1-LB TEST FIRINGS

Run No's	Date	Engine Configuration	Chamber	C* Eff.	Ignition Probability	P_c Rise Characteristics
127-133	1-11-72	Coaxial inj. retracted .1 in., no chamber spacers	Aluminum 8:1	68	Good at hi P_c	Good at hi P_c, no tests at low P_c
134-159	1-11-72	Coaxial inj. retracted .1 in., (1) 8:1 chamber spacer	Aluminum 8:1	67	Good except at low P_c	Smooth rise
160-169	1-12-72	Coaxial inj. retracted .1 in., side plug, (2) chamber spacers	Aluminum 8:1	68	Good except at low P_c	Bad step
170-178	1-19-72	Radial H_2 inj., axial plug, X28506 deflector plate	Aluminum 8:1	No Ig.	No ignition	No ignition
179-189	1-20-72	Deflected H_2 inj., plug thru injector, X28506 plate	Aluminum 8:1	84	Good at hi P_c	Smooth rise at hi P_c
190-194	1-21-72	Radial H_2 inj., plug thru injector, X28506 plate	Aluminum 8:1	No Ig.	No ignition	No ignition
195-209	1-24-72	Radial H_2 inj., plug thru X28506 plate	Aluminum 8:1	67	Good	Unstable
210-212	1-24-72	Radial H_2 inj., plug thru X28506 plate	Copper 100:1	65	Good at hi P_c no low P_c tests	Smooth rise
213-227	1-24-72	Deflected H_2 inj., X28516-503 plate	Aluminum 8:1	90	Poor	Smooth rise
228-236	1-26-72	Deflected H_2inj., X28516-505 plate	Aluminum 8:1	87	Good	Unstable step
237-248	1-27-72	Deflected H_2 inj., X28516-507 plate	Aluminum 8:1	91.6	Very good	Smooth rise
249-252	1-27-72	Deflected H_2 inj., X28523 plate, 15° cone	Aluminum 8:1	83-85	Good	Bad P_c step

TABLE 17. (CONTINUED)

SUMMARY OF 0.1-LB TEST FIRINGS

Run No's	Date	Engine Configuration	Chamber	C*Eff. @ 50 psia	Ignition Probability	P_c Rise Characteristics
253-259	2-1-72	Deflected H_2 inj., X28526 plate	Aluminum 8:1	85.8	Good	Smooth fast rise
260-263	2-2-72	Deflected H_2 inj., X28526 plate	Aluminum 12:1	75	Poor	Unstable P_c rise
264-269	2-9-72	Deflected H_2 inj., X28516-507 plate, X28528 spacer	Nickel 8:1	No Ig.	No Ignition	No Ignition
270-271	2-10-72	Deflected H_2 inj., X28516-507 plate, X28528 spacer	Nickel 8:1	No Ig.	No Ignition	No Ignition
272-277	2-10-72	Coax. inj. retracted .2", chamber off center, plug in chamber	Copper 100:1	64	Fair	Slow smooth
278-285	2-16-72	Deflected H_2 inj., X28516-507 reworked plate with teflon plug seal, copper ring	Nickel 8:1	84	Good	Slight step
286-295	2-17-72	Same, except use aluminum deflector ring	Nickel 8:1	87	Good	Step, unstable P_c
296-310	2-17-72	Same, except install new teflon plug seal	Nickel 8:1	87	Good	Slight step

TABLE 17. (CONTINUED)

SUMMARY OF 0.1-LB TEST FIRINGS

Run Nos.	Date	Spark Plug Configuration	No. of Pulses	Pulse Duration Sec	Firing Chamber Pressure psia	C* Efficiency %	Spark Energy Millijoules	P_c Rise Characteristics	Ignition Probability %
311-313	3-13-72	Modified	50	1.0	77	88.3	37	Smooth	94
314-317	3-14-72	"	100	1.0	"	89.0	78	Smooth	100
318	"	"	50	1.0	"	89.0	37	Smooth	98
319-321	"	"	50	0.5	47	86.0	78	Smooth	100
322	"	"	50	0.5	"	86.0	37	Smooth	100
323-325	"	"	50	0.5	32	81.5	37	Smooth	94
326	"	"	50	0.5	"	81.5	78	Smooth	98
327-329	"	"	50	0.5	22	77.0	37	Smooth	100
330	"	"	10	0.1	"	77.0	37	Smooth	100
331-333	"	"	50	1.0	15	72.0	37	Uneven	98
334	"	"	49	1.0	"	72.0	78	Uneven	94
335	"	"	50	1.0	"	72.0	210	Uneven	94
336	"	"	200	0.5	40	84.0	37	Smooth	100
337	3-21-72	Standard	1	2.0	77	88.7	37	No Ignition	-
338-339	"	"	32	1.0	"	88.7	210	Some Rough	75
340	"	"	50	0.5	"	88.7	78	Some Rough	100
341	"	"	50	0.5	"	88.7	78	Some Rough	100
342	3-22-72	"	1	2.0	"	88.7	37	No Ignition	-
343	"	"	1	3.5	"	88.7	78	Ignition	-
344	"	"	1	2.0	"	88.7	37	Smooth, Slight Step	-

TABLE 17. (CONTINUED)

SUMMARY OF 0.1-LB TEST FIRINGS

Run Nos	Date	Spark Plug Configuration	No. of Pulses	Pulse Duration Sec	Firing Chamber Pressure psia	C* Efficiency %	Spark Energy Millijoules	P_c Rise Characteristics	Ignition Probability %
345	3-22-72	Standard	1	3.0	37	78.3	37	Smooth, Slight Step	-
346-348	"	"	1	2.0	22	79.3	37	Smooth, Slight Step	-
349-350	"	"	50	1.0	14	71.0	37		98
351-353	"	"	230	0.5	38	79.8	37	Smooth, Slight Step	100
354-356	"	Standard, .5" spacer	3	3.0	72	85.5	37	Step down	-
357-361	"	"	41		77	88.0	37-210	No Ignition	0
362	"	Standard, .25"spacer	10		77	88.0	37	No Ignition	0
363	"	"	3	3.0	77	88.0	210	Ig. 2 of 3	-
364-365		"	18	5.0		86.0	37	Step down	95
366-369	3-23-72	Standard	7	3.0	78	90.0	37	Smooth	100
370	"	"	57	0 Min., then 1 sec.	78	90.0	37	Some Step Down	100
371-373	3-27-72	Modified	10	10.0	77	89.0	37	Some Step Down	100
374	"	"	10 - Cold	10.0	-		-	Smooth	-
375	"	"	7	10.0	77	89.0	37	No Step Down	100

TABLE 17. (CONCLUDED)

SUMMARY OF 0.1-LB TEST FIRINGS

Run Nos.	Date	Chamber Configuration	No. of Pulses	Pulse Duration Sec	Firing Chamber Pressure psia	C* Efficiency %	P_c Rise Characteristics	Notes
376-377	4-3-72	8:1, ℓ = .6 in.	3	10	78.8	87.7	Step down	Two P_c transducers
378	4-3-72	50 psia, 8:1	9	10	50.5		No step down	
379-382	4-6-72	8:1, ℓ = .6 in.	2	10	80.0	91.5	Step down	New Hz orifice
383-384	4-6-72	8:1, ℓ = .6 in.	1	10	63.0	87.0	No step down	Reduced flowrate
385-390	4-12-72	Acceptance tests of spark ignitors No. 1,2						
391-393	4-14-72	8:1, ℓ = 1.1 in.	11	10	78.8	88.0	No step down	.5 in. chamber spacer
394-396	4-18-72	8:1, ℓ = .85 in.	10	10	81.0	91.5	1 step down	.25 in. chamber spacer
397	4-18-72	Acceptance tests of spark ignitor No. 2						
398-399	4-19-72	10:1, ℓ = .6 in.	5	10	77.5	86.3	2 step downs	Enlarged contract ratio
400-404	4-25-72	10:1, ℓ = 1.1 in.	4	.05-.2			100 ms to 90%	Kistler P_c
405-407	4-25-72	10:1, ℓ = .85 in.	20	10	81.0	89.5	No step down	
408	4-25-72	10:1, ℓ = .85 in.	51	Notes	79.5		No step down	150 sec., then 50 pulses, 1 sec. On, 1 sec. Off

Runs 84 to 93

The 100:1 copper chamber spacer was removed for the next engine configuration and the injector was retracted 0.2-inch from the injector face. This in effect gave a 0.078-inch diameter mixing section 0.2 inch long. The C* efficiency was 69 percent, the same as the preceding configuration. This configuration had good ignition probability at low pressures, igniting with 37.5 millijoules spark energy down to chamber pressures of less than 10 psia. However, the rough P_C step early after ignition at intermediate chamber pressures was not improved over that of the preceding configurations.

Runs 94 to 111

The configuration for Runs 94 to 111 was the same as for Runs 58 to 76 except that the injector element was rotated 36 degrees. This placed a land between the hydrogen injector segments in line with the spark plug, whereas in preceding tests the hydrogen segments had been in line with the spark plug. Ignition probability at low spark energy and intermediate chamber pressures was significantly lower for this configuration. It was therefore concluded that the spark plug should be in line with one of the hydrogen injector segments.

Runs 112 to 118

For Runs 112 to 118, the injector was rotated again to place a hydrogen injector segment in line with the spark plug. The injector element was also retracted 0.10-inch behind the injector face. Therefore, the configuration was the same as shown in Figure 83 except for the shorter injector retraction. Ignition characteristics and C* efficiency were similar for either a 0.1-inch or 0.2-inch injector retraction.

Runs 119 to 126

Two aluminum chamber spacers with a 2:1 contraction ratio were used with the aluminum chamber which had been reworked to a shorter length (0.6 inch) and a larger contraction ratio (8:1). The configuration is shown in Figure 84. The combustion gas had access to the spark plug electrode through a 1/8-inch diameter hole about 0.1 inch long in the injector block, adjacent to a slot in the end of the aluminum chamber which was 0.1-inch deep and 0.125-inch wide. This configuration had poor ignition probability and a low C* efficiency of 58 percent.

Runs 127 to 133

The 8:1 aluminum chamber was tested without any chamber spacers on Runs 127 to 133. The C* efficiency was 68 percent, which showed that the engine performance was as good with the 8:1 chamber as it had been with the longer 4:1 chamber used on Runs 84 to 93. Ignition characteristics were good during the tests at 50 psia chamber pressure.

Runs 134 to 159

A 0.5-inch long 8:1 chamber spacer was used with the 8:1 aluminum chamber on Runs 134 to 159. The C* efficienty was 67 percent, indicating no improvement with the longer chamber. The ignition probability was good at 50 psia chamber pressure but was poor at low chamber pressures.

Runs 160 to 169

A different injector with the spark plug mounted on the side of the chamber, as shown in Figure 85, was used for Runs 160 to 169. The combustion chamber had a 100:1 contraction ratio. The C* efficiency was 69 percent. A significant step in chamber pressure rise occurred on all runs at high chamber pressure. No ignition was obtained on two runs at very low chamber pressure. No further testing was done with this configuration because of the undesirable P_c rise characteristics.

Runs 170 to 178

A new injector configuration was used for Runs 170 to 178. The ends of the hydrogen orifices were blocked off by an O-ring and a retainer plate (X28506) as shown in Figure 86. The hydrogen was injected into the oxygen tube through five 0.006-inch diameter holes through the wall of the oxygen injector tube. The oxygen and hydrogen then mixed in a 0.046 diameter section 1/8 inch long before entering the 8:1 aluminum chamber. Ignition could not be obtained with this configuration even with the spark plub bottomed in the injector head port.

Runs 179 to 189

Another injector configuration was tested on Runs 179 to 189, as shown in Figure 87. The hydrogen was deflected radially into the oxygen stream at the exit of the oxygen tube by the deflector plate, X28506. The oxygen injector tube was retracted 0.040 inch, so that the hydrogen from the five hydrogen passages turned inward through the 0.040-inch gap into the oxygen. The C* efficiency was 84 percent. The 1/4-inch diameter hole for the spark plug was drilled all the way through the injector head, and the endge of the spark plug was bottomed against the deflector plate. This placed the electrode 0.22 inch from the slot in the chamber. Ignition probability was good at high chamber pressure but was poor at low chamber pressure.

Runs 190 to 194

The radial hydrogen injection configuration used in Runs 170 to 178 was tested again with the spark plug bottomed against the deflector plate which placed the electrode about 0.22 inch from the chamber slot. Ignition could not be obtained at high chamber pressures, even with high spark energy.

FIGURE 88.

RADIAL HYDROGEN INJECTOR

Runs 195 to 209

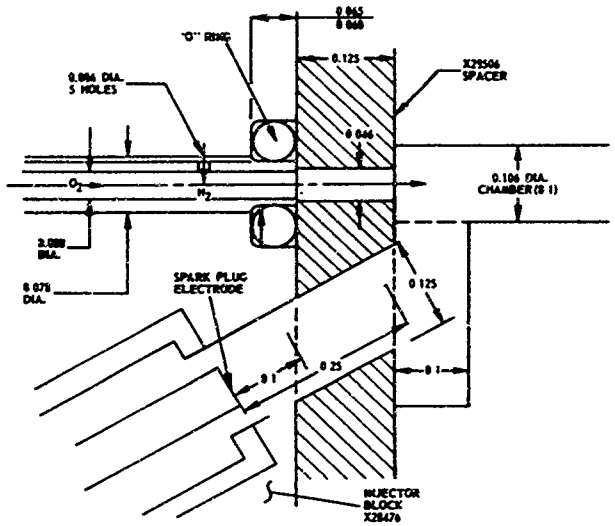

RADIAL HYDROGEN INJECTOR

Runs 170 to 178

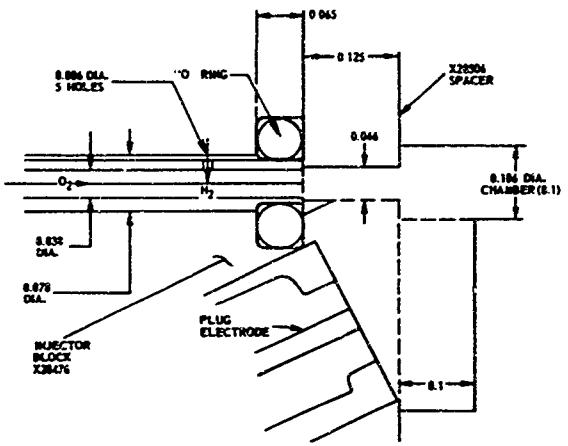

FIGURE 86.

FIGURE 87.

DEFLECTED HYDROGEN INJECTOR

Runs 179 to 189

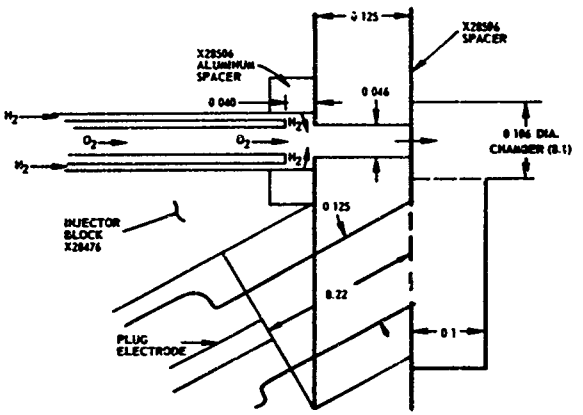

DIMENSIONS OF DEFLECTOR PLATE X28516

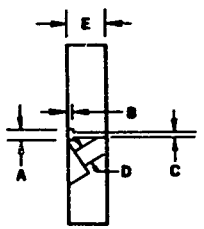

Dash	±.002 A	±.0005 B	±.002 C	±.005 D	±.010 E
501	0	0	0	0.125	0.250
503	0.082	0.002	0.030	0.125	0.250
505	0.082	0.004	0.046	0.125	0.250
507	0.082	0.002	0.030	0.125	0.150

FIGURE 89.

Runs 195 to 209

A 0.275-inch diameter hole was drilled through the deflector plate for Runs 195 to 209 using the radial hydrogen injector, as shown in Figure 88. This produced ignition at high and low chamber pressures with low spark energy, since the plug electrode was now very close to the combustion chamber. However, the mixing section between the tip of the oxygen tube and the spark plug access port was now unsymmetrical because of the hole drilled through one side of the mixing section. Unstable P_c rise characteristics resulted with this configuration. The C* efficiency was 77 percent on the first run at a chamber pressure of 56.3 psia but was only 67 percent on subsequent runs at chamber pressures of 40 psia. The chamber pressure was unstable during these runs, probably due to the unsymmetrical mixing section.

Runs 210 to 212

The radial hydrogen injector was tested with a 100:1 combustion chamber on Runs 210 to 212. The C* efficiency was only 65 percent, although the P_c rise curve was smooth.

Runs 213 to 227

A new deflector plate X28516 (Figure 89) was designed with various dimensional variations for testing the deflected hydrogen injector concept. During Runs 213 to 227, the -503 configuration was tested with the 8:1 aluminum chamber. The distance from the spark plug electrode to the plane of the chamber was 0.2 inch. No ignition was obtained with low spark power (37.5 millijoules) on Run 213, so subsequent runs were made with high spark power of 210 millijoules. The C* efficiency was 91.5, 90, 85, 79 and 74.5 percent for chamber pressures of 66, 52, 38, 25 and 20 psia, respectively.

Runs 228 to 236

The X28516-505 deflector plate was tested with the 8:1 chamber on Runs 228 to 236. The deflector plate had its thickness reduced from 0.25 to 0.15 inch, so the electrode was about 0.1 inch from the plane of the chamber. Ignition probability with low spark energy was good at chamber pressures of 50 psia down to 12 psia, but there was a step in the P_c rise curve. The C* efficiency ranged from 87 percent at 50 psia down to 57 percent at a chamber pressure of 12 psia.

Runs 237 to 248

The X28516-507 deflector plate was tested with the 8:1 chamber on Runs 237 to 248. A smooth ignition with low spark energy was obtained at chamber pressures from 54 psia down to 19 psia. C* efficiency was 91.6 percent at 54 psia,

falling to 70 percent at 19 psia. No ignition was obtained at high chamber pressure and low spark energy on the first two runs but was obtained at those conditions on subsequent runs.

Runs 249 to 252

A deflector plate X28523 similar to X28516 with a conical expansion rather than a sharp step to the 8:1 chamber was tested on Runs 249 to 252. Ignition was obtained with low spark energy at a chamber pressure of 50 psia, but there was a significant step in the P_c rise curve. Ten pulses of 2 seconds on, 2 seconds off were made during Run 251.

A 40-second continuous firing was made on Run 252 with a peak C* efficiency of 91%. Chamber temperature reached 440°F at 40 seconds. Post-test examination of the engine did not reveal any evidence of damage to the engine components.

Runs 253 to 259

A deflector plate (X28526) with a 0.030-inch diameter mixing section of 0.050-inch length was tested during Runs 253 to 259. The deflector plate was similar to the X28516 deflector plate except that the mixing length was shorter. The C* efficiency was about 86 percent, indicating some decrease in performance from the 90 percent level achieved the previous month with the X28516-503 and -507 deflector plates which had 0.030-inch diameter mixing lengths of 0.250 inch and 0.150-inch, respectively. During 20 pulses of 1 second ON, 1 second OFF, at a 50 psia nominal chamber pressure, 17 ignitions were obtained.

Runs 260 to 263

The same engine configuration was used for the next series of tests except that the aluminum chamber contraction ratio was enlarged to 12:1. The C* efficiency dropped even further, to 75 percent, and ignition could not be obtained except when using a high spark energy of 210 millijoules and a long spark duration of 150 milliseconds.

Runs 264 to 271

Runs 264 to 269 were intended to gather more data on ignition reliability with the configuration which had given the best performance in previous tests. An 8:1 nickel chamber was used which would have longer firing capability than the aluminum chamber. No ignitions could be obtained during the test series regardless of the spark energy or spark duration used. A large corona discharge was observed around the spark plug, so a new dielectric coating was applied to the spark plug connector before Runs 270 and 271. The corona discharge was eliminated, but no ignitions could be obtained.

Runs 272 to 277

Exhaustive examination of the spark system did not reveal any reason for failure to achieve ignition. Therefore, a 100:1 chamber displaced to one side to allow insertion of the spark plug into the chamber was used in the next series of tests. Ignition was achieved approximately 80 percent of the time, although C* efficiency was only 65 percent. It was concluded that failure to get ignition on Runs 264 to 271 was not due to electrical problems.

Runs 278 to 285

A study of the engine configuration which had been used on Runs 264 to 271 led to the conclusion that leakage of hydrogen around the aluminum ring filling the volume occupied by the O-ring in the radial hydrogen injector might be bypassing the mixing section and creating a fuel rich mixture ratio at the spark plug. Therefore, the adapter plate was reworked to allow use of a teflon seal at the tip of the spark plug. The aluminum ring was replaced by a somewhat longer copper ring which gave greater sealing pressure against the adapter plate. However, the longer copper ring increased the 0.002-inch hydrogen deflector gap to about 0.005 inch.

Ignition was obtained with fairly good reliability with this configuration, confirming that the bypassed hydrogen flow had been responsible for the earlier failures to ignite. However, the ignition reliability was still not as high as desired. For example, 20 pulses of 3 seconds ON and 3 seconds OFF were attempted on Run 289, but only 14 ignitions were obtained. The C* efficiency was 84 percent, somewhat lower than the 90 percent expected.

Runs 286 to 298

The same engine configuration was used for the next series of tests except that the original aluminum ring was used in an attempt to get higher engine performance. This was accomplished, since the C* efficiency was 87 percent, indicating the importance of holding a narrow gap for radial hydrogen deflection.

Ignition reliability was improved on this series of tests. On Run 289, which was a series of 24 pulses, 23 good ignitions were obtained. Very low ignition probability was obtained after Run 289, and it was concluded that the teflon seal around the spark plug tip had overheated during Run 289, allowing hydrogen bypass to occur again.

Runs 296 to 310

A new teflon spark plug seal was installed before Run 296, and ignition was again obtained at a nominal chamber pressure of 50 psia. The C* efficiency was 87 percent. No ignition could be obtained at chamber pressures below 32

psia (hot firing) and ignition at this pressure was marginal. It was concluded that no further improvement in ignition probability could be obtained with the axial spark plug installation through the injector head without a major rework of the thruster and extensive testing. This configuration had originally been designed to go with a 100:1 contraction ratio chamber, and all possible improvements with 8:1 chambers (found necessary for high combustion efficiency) had been accomplished.

A 10-minute single firing was made on Run 310 to evaluate chamber heat flux, steady state chamber temperatures, and durability of the axial spark plug and deflected hydrogen injector configuration. No damage was found to any of the engine components except the rubber O-rings and teflon plug seal which would not be used in the final engine design. The nickel chamber had essentially reached a steady state temperature of 1060°F at the end of the run, illustrating the high effectiveness of radiation cooling for this very small engine.

(2) Radial Spark Plug Configuration

Based on the previous test results, a new engine configuration was tested which demonstrated excellent ignition probability as well as high combustion efficiency. The new configuration featured a radially mounted spark plug shown in Figure 90 and a combustion chamber pressure of 80 psia. The chamber contraction ratio was 8:1. The deflected hydrogen injector configuration used in earlier tests was also used in the new engine configuration.

An enlarged cross-sectional view of the radial spark plug holder is shown in Figure 91. The spark gap is connected to the 0.083-diameter combustion chamber through a 0.062-inch diameter port with a conical entrance. Two spark plug configurations were used; one was standard spark plug with the shunt material removed (left side of Figure 91). The second spark plug configuration used a modified spark plug (right side of Figure 91) which had a flat tip with the case machined flush with the insulator. The modified spark plug configuration caused sparking to occur from the electrode to the conical wall of the port in the holder, which was made of Nickel 200. The shortest gap from the electrode of the modified plug to the holder wall was 0.030 inch.

The main objective of the modified spark plug design was to minimize the amount of electrode area exposed to convective heating by the combustion gas. In addition the spark would be very close to the combustion chamber, which should maximize ignition probability. The standard spark plug configuration would expose the area on the side of the electrode to convective heating, the amount depending on the depth of the gap between the electrode and the case (ground).

Runs 311 to 313

The modified spark plug configuration was tested with low spark energy of 37 millijoules for 50 pulses of 1 second ON, 1 second OFF, during Runs 311

FIGURE 90.

0.10 LB ENGINE (80 PSIA) WITH RADIAL SPARK PLUG

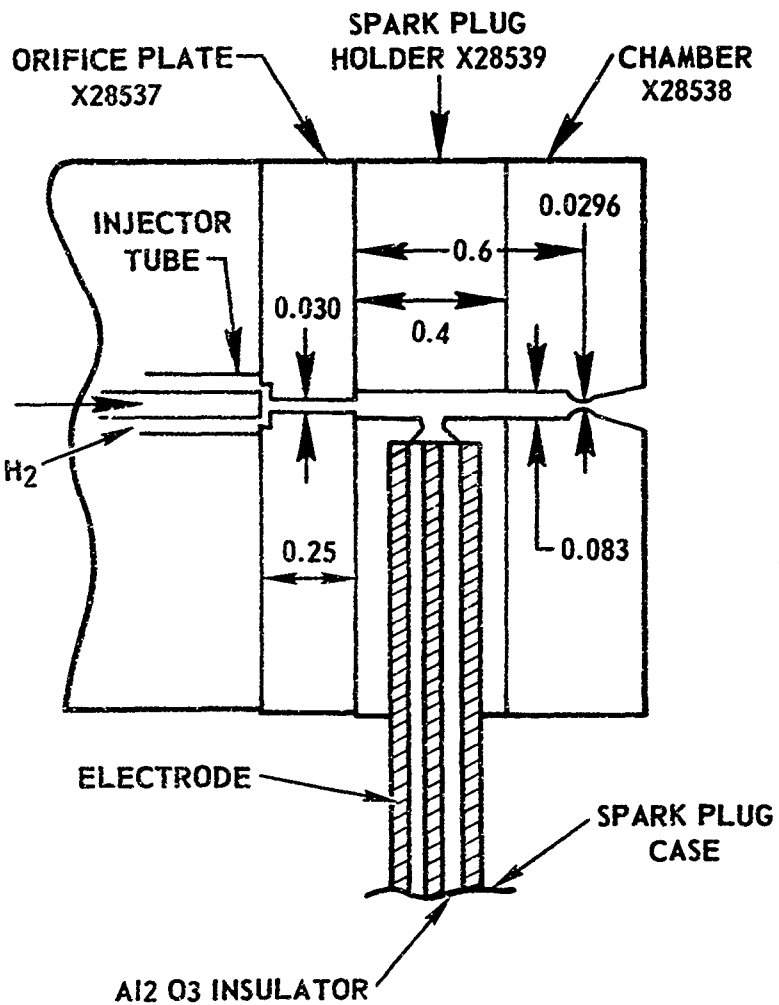

FIGURE 91.

RADIAL SPARK PLUG CONFIGURATIONS

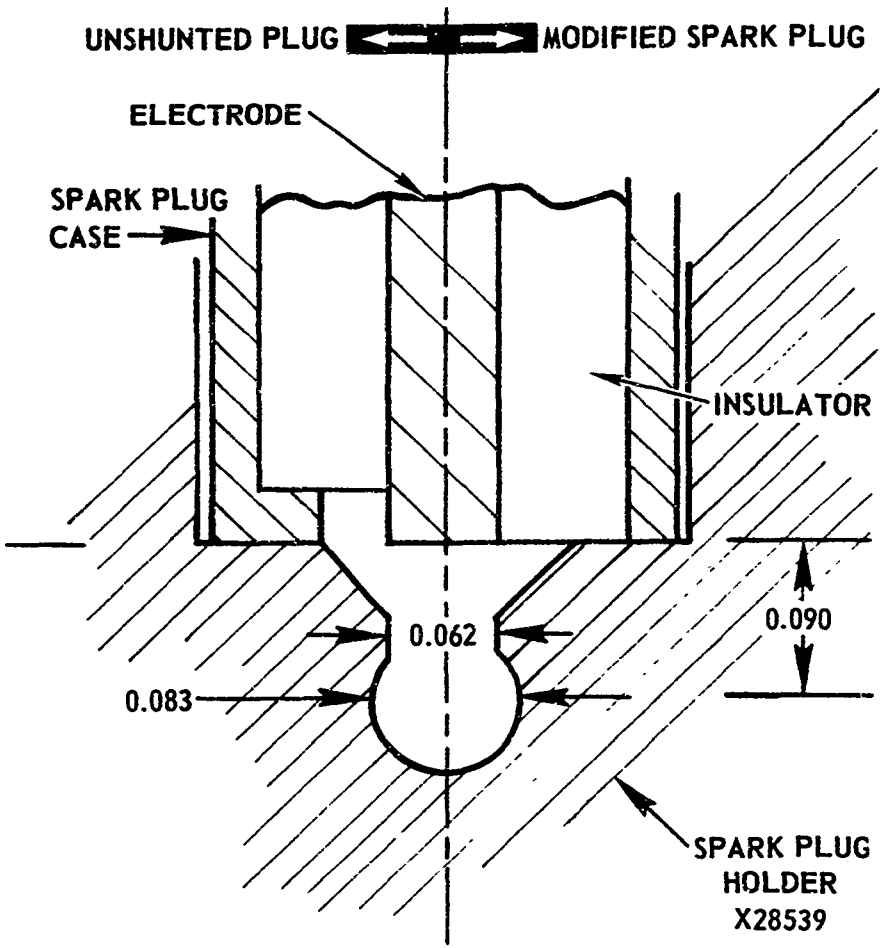

to 313 at the nominal 0.1-pound thrust and chamber pressure of 80 psia. Actual chamber pressure was 77 psia. Ignition was very smooth and occurred on 47 out of 50 pulses.

Runs 314 to 317

During tests with a mdeium spark energy of 78 millikoules, ignition was obtained on all of the 100 pulses.

Run 318

Another 50 pulses with low spark energy of 37 millijoules were made during Run 318, with ignition occurring on 49 of the 50 pulses. This confirmed the results of the previous tests indicating 100% ignition reliability with 78 millijoules, but marginally acceptable ignition reliability with 37 millijoules.

Runs 319 to 322

Testing at reduced flow rates producing a chamber pressure of 47 psia obtained 100 percent ignition during 50 pulses with both low and medium spark energy. The duty cycle during these tests was 0.5 second ON, 0.5 second OFF.

Runs 323 to 326

During 50 pulses of 0.5 second at a chamber pressure of 32 psia, ignition probability was 94 percent with low spark energy and 98 percent with mediura spark energy.

Runs 327 to 330

Ignition probability at a chamber pressure of 22 psia was 100 percent with low spark energy during 50 pulses of 0.5-second duration and 10 pulses of 0.1-second duration.

Runs 331 to 335

Marginal ignition probability between 94 and 98 percent was obtained at a very low flow rate yielding a chamber pressure of 15 psia. The use of a spark energy of 210 millijoules yielded 94 percent ignition during 50 pulses of 1 second ON, 1 second OFF.

Run 336

One hundred percent ignition reliability was obtained during 200 pulses of 0.5 second ON, 0.5 second OFF, at 40 psia.

Runs 337 to 339

Ignition with the standard spark plug at the nominal thrust level (77 psia chamber pressure) was not obtained until the ninth pulse of a 31-pulse train using a high spark energy of 210 millijoules. The chamber pressure fluctuated during pulses 9 to 16, but was smooth on the final 16 pulses.

Runs 340 to 341

Ignition was obtained on all 50 pulses of Run 340 and 50 pulses of Run 341, using medium spark energy of 78 millijoules. However, the chamber pressure fluctuated during portions of the first six pulses of Run 340 and also on Run 341.

Runs 342 to 350

Further tests the following day of the standard spark plug configuration produced ignition at chamber pressures (firing) down to 22 psia, using low spark energy. A pulse train ot 50 pulses was made on Run 350 at low flow rates producing chamber pressure of approximately 14 psia. Ignition was obtained on 49 of 50 pulses. There was no evidence of chamber pressure fluctuations on Runs 342 to 350.

Runs 351 to 353

A pulse train of 230 pulses, 0.5 second ON, 0.5 second OFF, was made at a chamber pressure of 38 psia, using low spark energy. Ignition was obtained on all 230 pulses and was smooth except for a slight step on four of the early pulses.

Runs 354 to 356

Tests with the standard spark plug spaced 0.5-inch up in the plug hole revealed that ignition probability was poor. It was also found during 3-second firings that the chamber pressure would rise smoothly to 71 psia and then drop to 60 psia.

Runs 357 to 361

No ignitions were obtained during 41 pulses at nominal flow rates, including 20 pulses with 210 millijoule spark energy. The engine was leak-checked satisfactorily after Run 361 and a new spark plug was installed. The removed spark plug was found to spark satisfactorily and passed a pressure test of its seal. It was concluded that the only reason for the low ignition probability for the preceding runs was the 1/2-inch spacing of the withdrawn plug.

Runs 362 to 365

Tests with the standard spark plug withdrawn 0.25 inch indicated marginal combustion reliability. Also, a step down in chamber pressure was noted on each of 17 pulses of 5 seconds duration during run 365.

Runs 366 to 369

The standard plug configuration was reinstalled for Runs 366 to 369. Ignition was obtained on each of 7 pulses of 3 seconds duration using low spark energy. No step down of P_c was noted.

Run 370

A long firing of 6 minutes with the chamber temperature reaching 1000°F was immediately followed by 56 pulses of 1 second ON, 1 second OFF, us using low spark energy. Ignition was obtained on all pulses, but step-down of chamber pressure from 77 psia to about 60 psia occurred on 7 of the 56 pulses. The spark plug was examined after Run 370 and appeared to be in good condition. A visual check of the plug sparking was also satisfactory.

Runs 371 to 375

The modified spark plug was reinstalled for Runs 371 to 375. Step-down from 77 to 62 psia occurred on the first three of nine pulses of 10 seconds duration during Run 373. Ten cold flow pulses of 10 seconds duration were made during Run 374, and propellant flow rates were found to be normal. Seven hot firing pulses of 10 seconds duration were made using low spark energy on Run 375. Ignition was obtained on all seven pulses, and no step-down of chamber pressure was observed.

Kuns 376 to 377

Three pulses were made with the 80 psia nickel chamber using a second CEC chamber pressure transducer. Each pulse was 10 seconds ON, 50 seconds OFF. Step-down was recorded on all three pulses with both transducers, which largely eliminated the possibility of transducer or electrical system unreliability being the source of the apparent step-down of chamber pressure.

Run 378

Nine pulses of 10 seconds ON, 50 seconds OFF were made with the 50 psia nickel chamber. No step-down was observed on any of the nine pulses.

Runs 379 to 382

A new hydrogen sonic orifice with a smaller area was installed before Run 379 to eliminate the possibility of unchoked flow at the 80 psia chamber pressure. Two pulses of 10 seconds were made, with step-down occurring on both pulses.

Runs 383 to 384

One 10-second firing was made with reduced flow rate, giving a chamber pressure of 63 psia. No step-down was observed.

Runs 385 to 390

The new spark igniters were given short acceptance test firings during Runs 385 to 390. Successful ignition was demonstrated on Units No. 1 and 2 during 22 pulses over a range of spark energies.

Runs 391 to 393

A 0.5-inch long 8:1 aluminum chamber spacer was added to the 8:1 nickel chamber and tested with 11 firings of 10 seconds duration, with 50 seconds cooldown. No step-down was observed on any firing.

Run 394 to 396

A 0.25-inch long 8:1 aluminum chamber spacer was added to the 8:1 nickel chamber and tested for 10 firings of 10 seconds duration. One step-down of chamber pressure occurred. Spark igniter No. 3 was observed to produce four sparks, with a 12 ms duration and a 9-second delay.

Run 397

Igniter No. 2 was tested with ten 50 ms pulses on Run 397. Three sparks with 9 ms duration and 9 ms delay were observed.

Runs 398 to 399

An enlarged contraction ratio of 10:1 was obtained by reworking the 8:1 nickel chamber and spark plug holder. Five firing tests of 10 seconds were performed. Step-down was observed on the first two pulses.

Runs 400 to 404

A Kistler transducer was close mounted in a 0.5-inch long 10:1 chamber spacer using an installation similar to that of the radial spark plug shown in

last month's report. The tip was covered with RTV to allow longer firing times without overheating. Test firings of 50, 100, 125 and 200 ms were made in an attempt to measure P_c rise time more accurately than is possible with the CED transducers. The basic chamber volume of the 8:1 chamber with a length of 0.6 inch is only 0.00324 in.3, compared to a volume of 0.04096 in.^{3} in the 1/8-inch lines to the CEC transducer, the volume around the transducer head, and clearance around the spark plug. The P_c rise time has generally been recorded by the CEC transducer to be about 15 to 20 ms for cold flow, but 200 to 500 ms during hot firings. The recorded pressure has risen more slowly in hot firings than during cold flow, which cannot be explained at present. The P_c rise time decreases as the chamber gets hotter The only explanation for this at present is that the hot combustion gas entering the P_c line and other branch volumes is quenched and must be replaced by additional hot gas.

The tests with the Kistler transducer wer made with the CED lines capped. The Kistler P_c rise data were handicapped by a zero shift due to heating, but the best indication was that P_c rist time was about 100 to 125 ms. Other techniques of thrust and chamber pressure measurement will be required to more accurately measure P_c rise time.

Runs 405 to 407

A 10:1 aluminum chamber spacer with a length of 0.25 inch was added to the 10:1 nickel chamber for Runs 405 to 407. Twenty pulses of 10 seconds ON, 50 seconds OFF were made without any step-down of chamber pressure. The C* efficiency was 89.5%.

Run 408

The 0.85-inch long 10:1 chamber assembly was tested for 150 seconds, followed by 50 pulses of 1 second ON, 1 second OFF. No step-down was observed.

4. FINAL DESIGN

The substantial testing conducted on the boilerplate engine as documented in the previous section provided the design criteria for the final engine design. Table 18, below, lists the primary design criteria and Figure 92 shows the drawing of the configuration.

The engine assembly is nearly identical to the previously tested configurations, except that the combustion chamber is fabricated of molybdenum with a $MoSi_2$ oxidation resistant coating. The outside diameter of 1 inch provides a substantial indication area (A outside/A combustion chamber) of approximately 12/1. The manifolding of both the hydrogen and oxygen up to the combustion chamber contains the equivalent of 5-6 ms of fuel flow propellant, and the valves can open and shut repeatedly with 1/2 ms of each other.

TABLE 18

DESIGN CHARACTERISTICS

Design Parameter	
Chamber pressure (maximum)	75 psia @ 0.1 lbs thrust
Chamber pressure (minimum)	25 psia @ 0.03 lbs thrust
Contraction area ratio	8:1 (design)
Expansion area ratio	100:1 (design)
L*	9-10 inches
L/D premix	~8
Cooling	Radiation/conduction
Injector	Single element coaxial premix
Valves	R-1E coaxial solenoid
Spark plug	Champion FHE 231A (modified)

The major problem associated with the design of the engine was that the performance of the engine must be measured using apressure transducer. A thrust stand capable of measuring pulse performance was not available and all performance was thus based on C* calculations. In order to measure pressure, it was necessary to install a rather large volume line between the combustor and the transducer surface due to (1) the large size of the transducer and (2) the necessity of keeping the transducer cool.

In the boilerplate engine tests, the same design problem occurred and a series of runs using a Kistler close-mounted transducer (see Runs 400 to 404) indicated that the pressure transducer volume did contribute to the slow pressure rise. However, a phenomena occurred during all of the tests which can only be explained by thermal considerations. Pressurization of the combustor during cold flow tests indicates a fairly fast rise (10-20 ms to 90%) while tests with the same configuration with ignition indicate a delay as long as 500 ms. Besides the long delay, the pressure at the same time period indicated a pressure which was lower than cold flow. The only way in which this can occur is if the gases which are combusted are quenched in the pressure line, and that flow is restricted into the line. Further investigation of this phenomena was not attempted during the program as other considerations such as ignition reliability and combustion efficiency were more important. However, the eventual solution to this phenomena could most likely be the use of a very small-volume transducer for measurement of dynamic thrust .

Ignition of the engine was accomplished with the protytype igniter developed for Marquardt by Bel-Air Laboratories. The igniter, which is described in detail

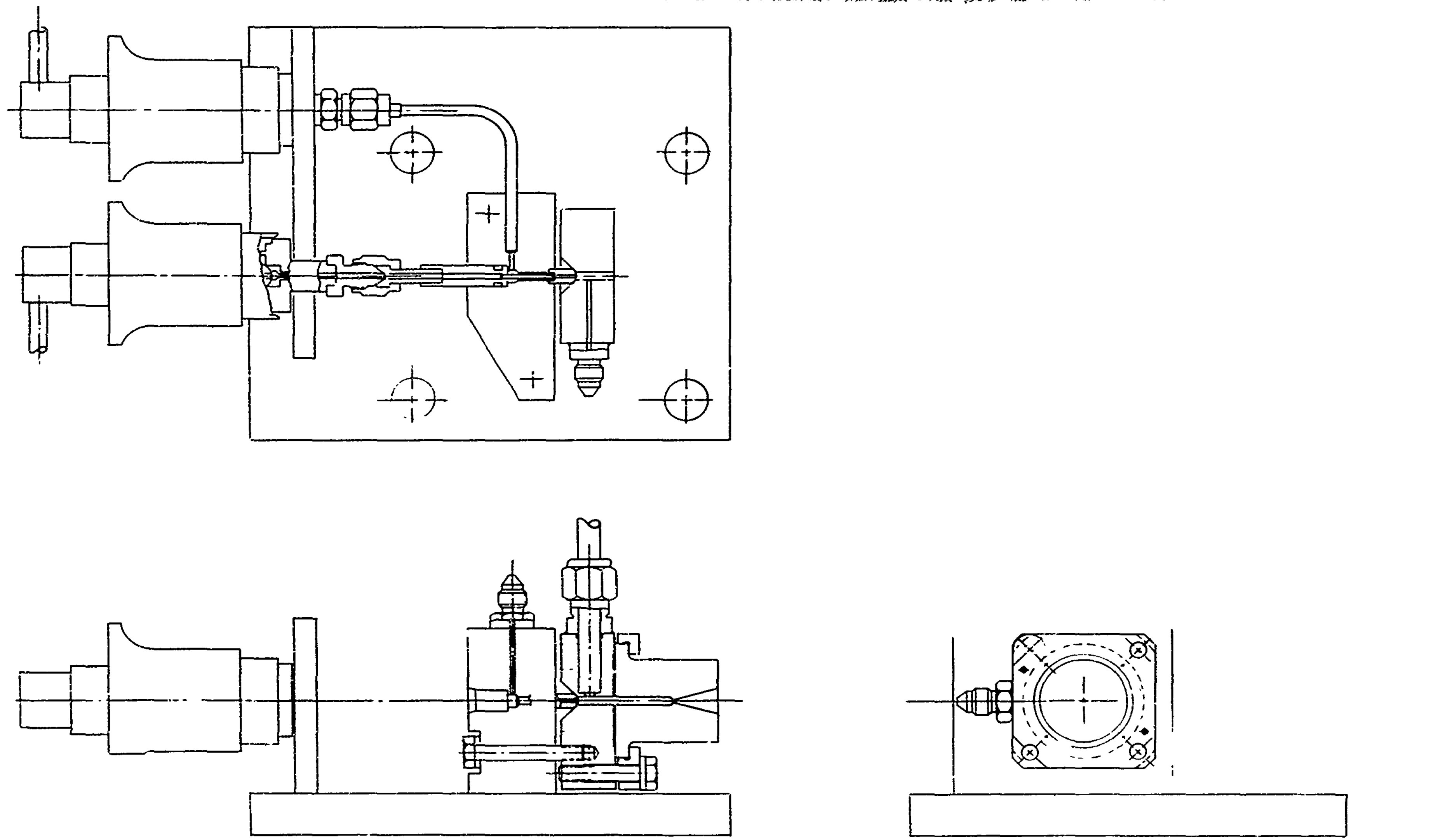

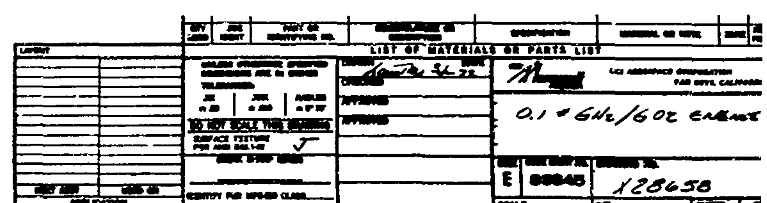

FIGURE [illegible]. 0.1 LBF THRUSTER (FINAL CONFIGURATION)

in the section on ignition, provides 3 to 4 sparks at 3 ms intervals after a specified time from the valve signal. The nominal spark energy provided to the Champion FHE 231 spark plug is 37.5 millijoules at 28 volt dc. The champion plug is produced with a semiconductor (shunt) material between the cathode and anode which is removed before test for use with the capacitance discharge system.

a. Test Program

The final configuration of the 0.1-pound thrust rocket engine shown on Figures 93 was subjected to a series of tests to verify its capabilities to ignite repeatedly and provide satisfactory thermal and performance characteristics. All tests were conducted with water saturated gases simulating the gases from the electrolysis system.

Preliminary tests with the final configuration indicated low performance and a resultant nonreliable ignition even though the configuration was nearly identical to that tested during the previous test series. Examination and retest of the configuration indicated that the cause of the low performance was misalignment of the coaxial oxygen post which had to be bent and resulted in a significant hydrogen slow aberration. Rework and subsequent testing resulted in normal performance and 100% reliable ignition.

The test program was divided into three parts:

- Characterization of performance
- Ignition and cycle life
- Combustor burn time accumulation.

A summary of all tests performed is listed in Table 19

(1) Performance Characterization (Runs 446 to 494)

The performance of the 0.1-pound thrust engine was conducted over a range of inlet pressures to determine the performance at various chamber pressures. Electrical pulse widths from 20 ms up to 10 seconds were documented, although the determination of performance at the short electrical pulse widths was impossible due to the pressure response. Both nickel and molybdenum combustors were used. Table 20 and Figure 74 show the steady state performance of the engine. A nominal I_{sp} of 330 seconds (based on a $C_F = 1.81$) was obtained. The performance at the lower thrust of 0.03 pound is near 300 seconds. A lower limit of ignition at 60 psia inlet pressure (23 psia P_c) was observed. At 50 psia inlet pressure random ignitions were obtained. The cold flow pressure corresponding to this inlet pressure is about 8-9 psia. Previous tests had indicated 4 psia as the lower limit for the 5-pound thrust engine.

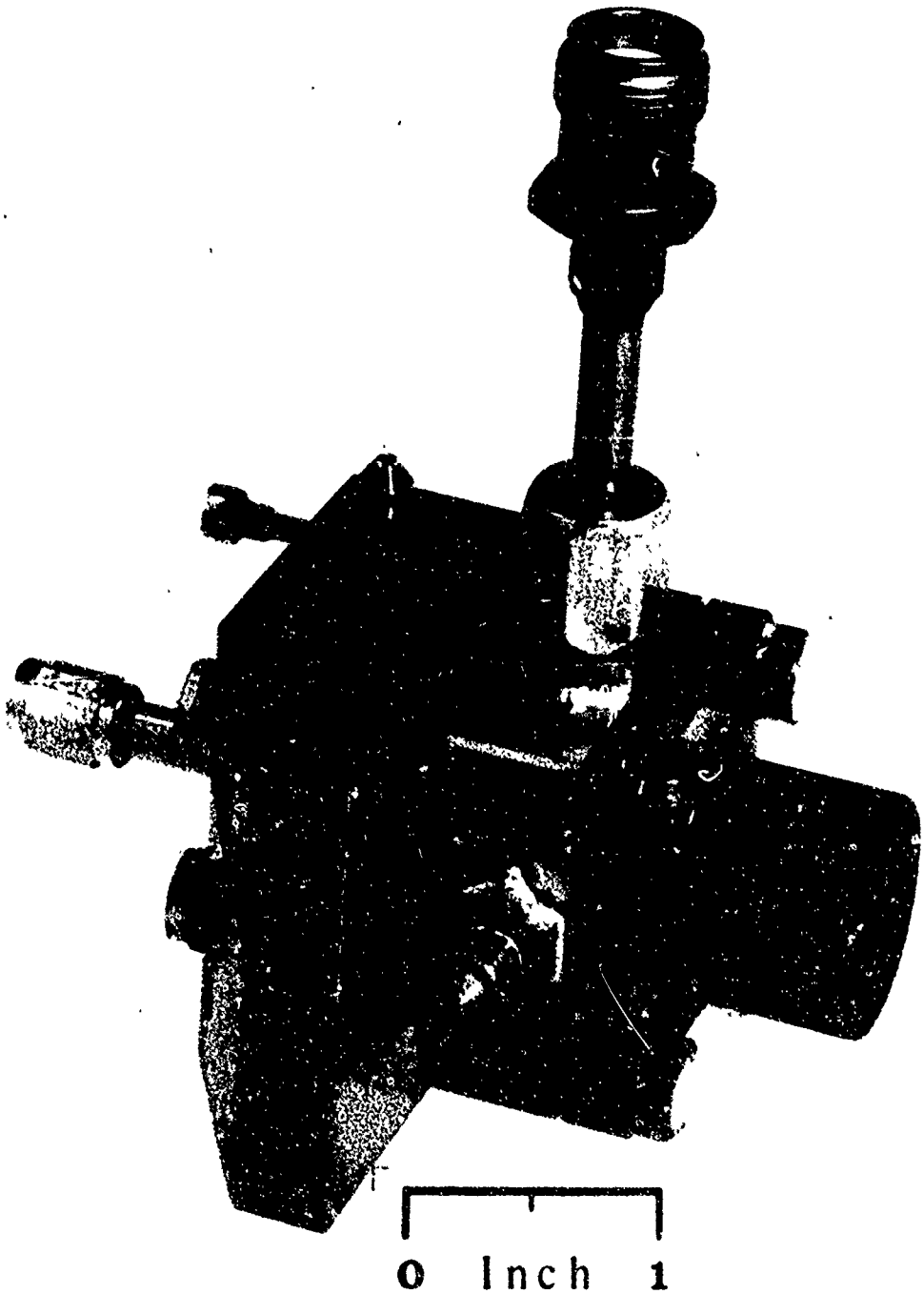

NEG. 72-230-11

FIGURE 93. 0.1 LB_f THRUSTER

TABLE 19

0.1 POUND ENGINE

RUN SUMMARY

FINAL CONFIGURATION
(Data Quick Look)

Date	Run No.	On Time (sec)	No. Pulses	Freq. (Hz)	P_{O_2} (psig)	P_{H_2} (psig)	P_c (psia)	Comments
8/3	445	2	1	-	188	190	75	
	446	1	1	-	↓	↓	73.6	
	447	-	-	-			30.8	Cold flow
	448	-	-	-			30.8	Cold flow
	449	-	-	-			8.9	H_2 cold flow
	450	-	-	-			15.8	O_2 cold flow
	451	2	10	2			78.8	
	452	-	-	-			31.5	Cold flow
	453	4	1		↓	↓		
8/4	454	4	1		182	190	67.4	
	455	-	-		188	190	27.9	Cold flow
	456	10	1		187	190	72.4	
	457	5	10	1	187	190	75.0	
8/7	458	-	-		187	190	27.1	Cold flow
	459	10	1		↓	↓	71.0	
	460	10	20	.0167	↓	↓		
	461	10	1		150	150	58	
	462	-	-		150	150	29.0	Cold flow
	463	10	1		↓	↓	57.4	
	464	10	20	.0167	↓	↓	57.4	
	465	-	-		100	100	15.8	Cold flow
	466	10	1		↓	↓	36.8	
	467	10	20	.0167	↓	↓	37.2	
	468	-	-		67	67	13.1	Cold flow
	469	10	1		↓	↓	25.5	
	470	10	20	.0167	↓	↓	25.5	

TABLE 19 (CONT)

Date	Run No.	On Time (sec)	No. Pulses	Freq. (Hz)	P_{O_2} (psig)	P_{H_2} (psig)	P_c (psia)	Comments
8/7	471	.020		2	67	67		Cold flow
	472	.020	10					Cold flow
	473	.050						Cold flow
	474	.050	10					
	475	.100						Cold flow
	477	.020			187	190		Cold flow
	478	.020	10					
	479	.050						Cold flow
	480	.050	10					
	481	.100						Cold flow
	482	.100	10					
	483	10	1				68.5	
	484	.020	1000	2				
	485							
	486							
	487							
	488							
	489							
	490							
	491							
	492							
	493							
	494	10	1				73.5	
8/10	495	-	-				29.0	Cold flow
	496	10	1				73.6	Start 150,000 cycle test
	497	.020	1000	2				
	498-512	.020	1000	2				
	513	10	1				76.0	
8/11	514	-	-				28.1	Cold flow
	515	10	1				74.2	
	516-545	.020	1000	2				
	546	10	1				73.4	
8/14	547	10	1					

TABLE 19. (CONT)

Date	Run No.	On Time (sec)	No. Pulses	Freq. (Hz)	P_{O_2} (psig)	P_{H_2} (psig)	P_c (psia)	Comments
8/14	548-579	.020	1000	2	187	190		
	580	10	1					
8/15	581	-	1				28.1	Cold flow
	582	10	1				74.7	
	583-590	.020	1000	2				
	591	10	1					
8/16	592	-	-				29	Cold flow
	593	-	-				29	Cold flow
	594	10	1				75.8	
	595-625	.020	1000	2				
	626	10	1				72.3	
8/17	627	-	-				29	Cold flow
	628	-	-				29	Cold flow
	629	10	1				74.69	
	630-654	.020	1000	2				
	655	10	1					
	656	.012						
	657	.012						
	658	.015						
	659	.100						
	660	.200						
	661	.500						
	662	60						
	663	120						
8/18	664	10					75.21	
	665	.02	1					
	666	.202	1000	.167				
	667	10	1				74.69	
8/22	668	-	-				28.	Cold flow
	669	10	1		187	190	72.3	
	670	1	7		52	52		No ignition
	671	1	11		70	70		No ignition
	672	510	1		115	115	45	

TABLE 19. (CONT)

Date	Run No.	On Time (sec)	No. Pulses	Freq. (Hz)	P_{O_2} (psig)	P_{H_2} (psig)	P_c (psia)	Comments
8/31	673	-	-		115	115	18.4	Cold flow
	674	10	1		115	115	34.5	
	675	10			90	90	34.19	
	676	10			70	70		
	677	2			50	50		No ignition
	678	10			60	60	23	
	679	10			140	140		
	680	10			170	170	52	
	681	10			188	190	71	
	682	240						
	683	10					69.8	
	684	300					65.8	
	685	240						
	686	210						
	687	240						
9/1	688	300					70.4	
	689	240						
	690	310						
	691	210						
	692	180						
	693							
	694							
	695							
	696							
	697							
	698							
	699							
	700							
	701							
	702							
	703							
	704							
	705							

TABLE 19. (CONT)

Date	Run No.	On Time (sec)	No. Pulses	Freq. (Hz)	P_{O_2} (psig)	P_{H_2} (psig)	P_c (psia)	Comments
9/1	706	180	1		188	190		
	707	180	↓		↓	↓		
	708	180	↓		↓	190-160	59.2	Lost H_2
9/5	709	180	↓		↓	190	63	
	710	300	↓		↓	↓		
	711	270	↓		↓	↓		
	712	450	↓		140	141	53.5	
	713	180	↓		↓	↓		
	714	180	↓		↓	↓		
	715	180	↓		↓	↓		
	716	180	↓		↓	↓	46.0	
	717	180	↓		↓	↓		
	718	180	↓		↓	↓		
	719	180	↓		↓	↓		
	720	180	↓		↓	↓		
	721	180	↓		↓	↓	47.4	
	722	600	↓		70	70	26.3	
	723	60	↓		↓	↓		
	724	60	↓		↓	↓		
	725	60	↓		↓	↓		
	726	60	↓		↓	↓		
	727	60	↓		↓	↓		
	728	60	↓		↓	↓		
	729	60	↓		↓	↓		
	730	60	↓		↓	↓		
	731	60	↓		↓	↓		
	732	5	↓		181	246	62	
	733	5	↓		185	213	65.7	
	734	5	↓		190	168	70.0	
	735	5	↓		192	151	68.4	
	736	5	↓		188	190	60.5	
	737	10	↓		188	190	60.5	

TABLE 20. 0.1 LB THRUST GO_2/GH_2 ROCKET ENGINE

PERFORMANCE DATA

Run No.	Noz. Mat'l.	T_o °F	T_F °F	P_o psig	P_F psig	P_C psia	WO_2 lb/sec (10-4)	WH_2 lb/sec (10-4)	W_T lb/sec (10-4)	C* ft/sec	O/F	C* Theo	η_c*	Isp sec.	F lbs.
458	Nickel	72	72	188	190	27.5	2.72	.3425	3.062	2193	7.94	-	-	-	-
459		72	72	186	190	71.0	2.72	.3425	3.062	5662	7.94	6740	84.2	320	.095
460		73	72	185	191	73.5	2.687	.3435	3.04	5909	7.832	6740	87.0	331	.101
461		73	73	149.5	151	57.5	2.196	.277	2.473	5682	7.928	6720	84.5	321	.079
462		74	74	150	151	28.7	2.19	.276	2.466	2844	7.934	-	-	-	-
463		74	76	149.5	152	57.0	2.188	.276	2.464	5663	7.937	6700	84.6	319	.078
464		75	78	149.5	152	58.0	2.19	.275	2.465	5750	7.963	6700	85.5	323	.080
465		76	78	100	102	16.	1.51	.191	1.701	2248	7.905	-	-		
466		78	78	100	102	36.5	1.51	.191	1.701	5214	7.905	6650	78.5	296	.05
467		81	81	100	102	37.5	1.51	.191	1.701	5387	7.905	6650	81.0	304	.052
468		82	82	68	68	14.	1.05	.133	1.183	2892	7.884	-	-		
469		83	83	67	67	25.8	1.04	.132	1.172	5379	7.89	6620	81.3	303	.035
470		85	85	69	68	26.5	1.085	.133	1.218	5317	8.157	6620	80.4	300	.036
483		85	85	186	191	69.0	2.647	.340	2.977	5654	7.785	6740	84.0	319	.095
494		85	84	187	189	77.0	2.68	.338	3.028	6224	7.93		92.5	352	.106
496	Moly	63	65	196	200	78.0	2.855	.362	3.217	5935	7.886		88.0	334	.107
513		82	80	195	200	75.0	2.80	.359	3.159	5802	7.739		86.5	328	.104
516		67	68	186	190	74.0	2.75	.343	3.063	5904	8.017		87.7	333	.102
672		78	75	115	115	45	1.7	.216	1.916	5820	7.87	6680	87.1	328	.063
674				115	115	42.5	1.7	.216	1.916	5500	7.87	6680	82.5	310	.059
675				90	90	34.2	1.39	.173	1.563	5420	8.04	6650	815	305	.048
676				70	70	26.5	1.10	.140	1.240	5300	7.86	6620	80.1	298	.037
678				60	60	22.9	.98	.122	1.102	5150	8.03	6610	78.0	290	.032
679				140	140	52	2.05	.257	2.307	5590	7.98	6680	83.6	315	.073
680				170	170	63.7	2.46	.308	2.768	5710	8.0	6710	85.2	322	.088
681				188	190	71.0	2.70	.342	3.042	5790	7.9	6740	85.9	327	.098

1. C_F = 1.81 for 100:1 nozzle
2. A_t = .00076 $in.^2$

(2) Ignition and Cycle Life (Runs 495 to 667)

A series of 150,000 ignitions, composed of 150 individual tests of 0.020 second ON/0.480 second OFF (1000 each test) at the start and end of each test day and at times specified by the development engineer, 10-second runs were conducted to verify performance. Although the slow response of the pressure precluded data reduction for performance value, an evaluation of the 1st pulse and the 150,000th pulse, plus random sampling of the pulse trace between these points, indicated that the engine performance did not degrade and that it was repeatable. Examination of the spark plug at the end of the test series showed no degradation. The thermal data indicated an average temperature of spproximately 300-350°F at steady state for the combustion chamber and spark holder, which is well within the limits of the thermal analysis estimate.

(3) Steady State Burn Tests (Runs 368 to 737)

More than 2-1/2 hours of steady state burn time was accumulated on the 0.1-pound thrust ending during this test phase. A maximum run of 600 seconds was accomplished (Run 722) and steady state temperatures were obtained at chamber pressures down to 25 psia. Figures 94 and 95 show the results of the test. Figure 95 documents the temperature vs time for the various components, while Figure 96 shows the combustion/exit nozzle temperature as a function of chamber pressure. As shown, the combustion chamber temperature is ~1800°F at the nominal 0.1-pound thrust level for the configuration tested. Figure 96 shows a black and white reproduction of a color picture taken at steady state.

The temperature of the combustion chamber was manually recorded using an optical pyrometer, while the spark plug holder and the injector temperatures were recorded using thermocouples. Figure 97 shows the engine at the end of the test series.

b. Evaluation of Engine Durability

Upon completion of the test program, the engine was disassembled and examined for obvious failures or wearout areas. Only two anomalies were observed. All other parts and structure members were satisfactory.

(1) The spark plug and spark plug holder became galled when the spark plug was removed. The spark plug tip was in excellent condition.

(2) The mating surface between the molybdenum combustion chamber and the nickel spark holder exhibited evidence of a leak, and the molybdenum surface was oxidized. (The surface was lapped prior to assembly and all the coating was inadvertently removed-

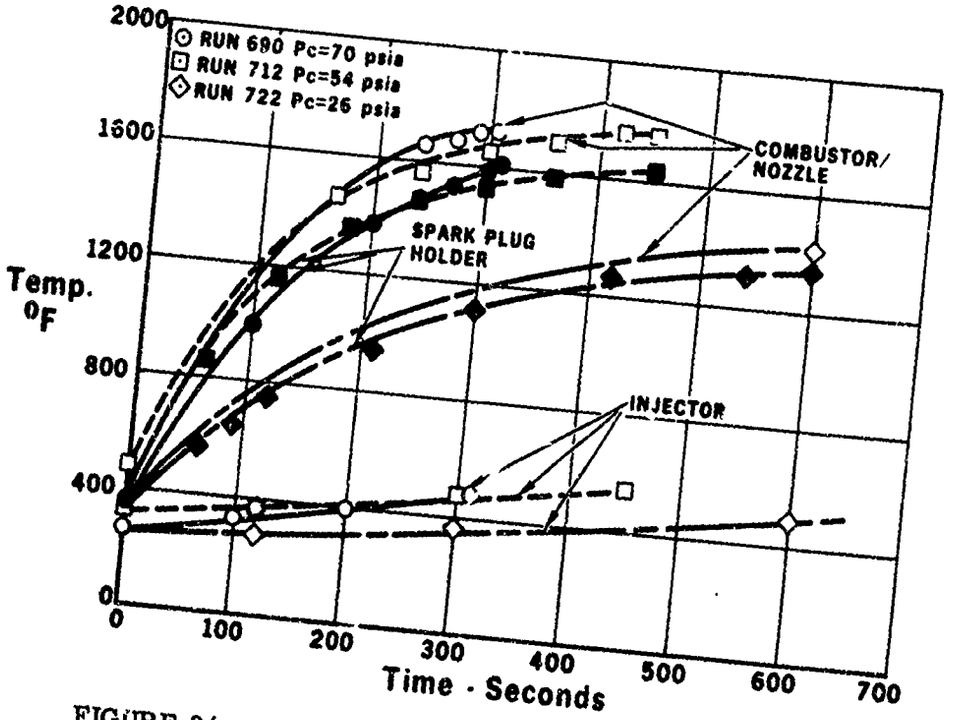

FIGURE 94. 0.1 LB_f THRUSTER TEMPERATURE VS TIME

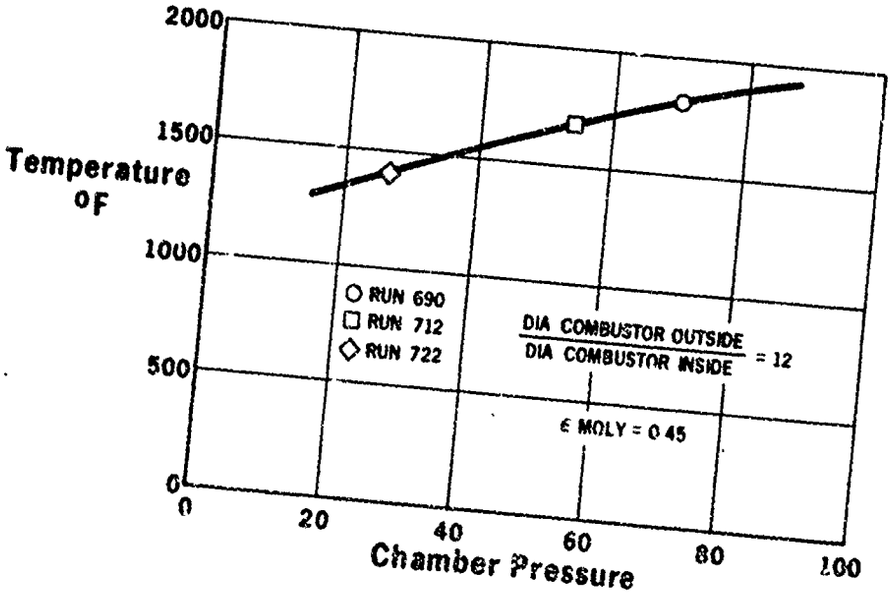

FIGURE 95. 0.1 LB_f THRUSTER EQUILIBRIUM COMBUSTER TEMPERATURE VS THRUST

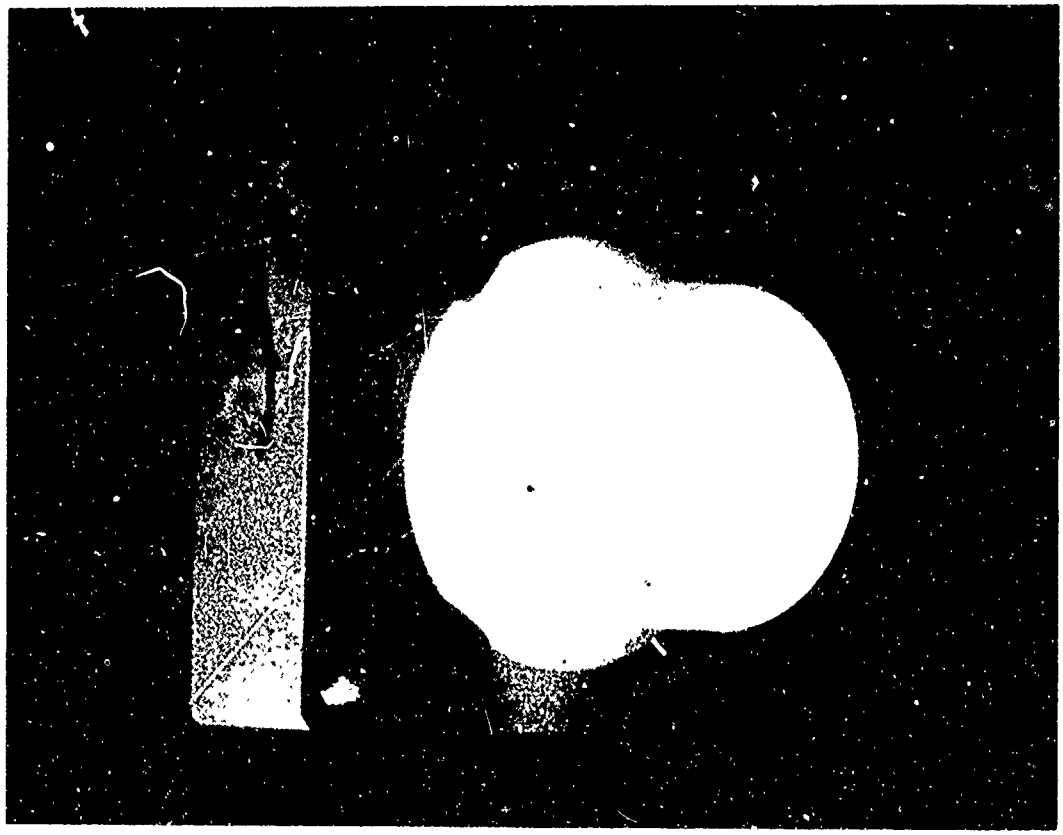

FIGURE 96. 0.1 LB_f THRUSTER DURING STEADY STATE FIRING

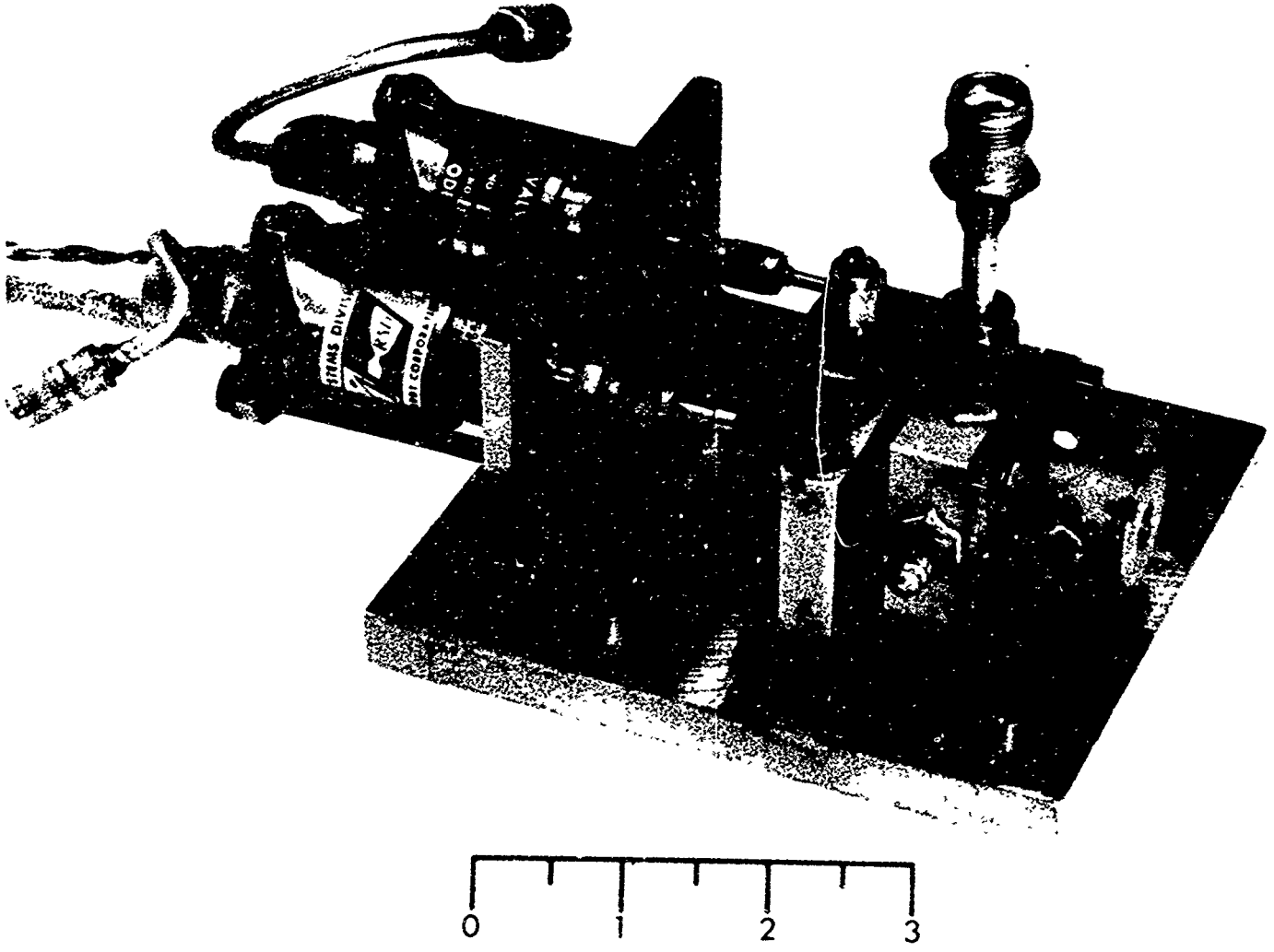

NEG. 72-230-12

FIGURE 97. 0.1 LB_f THRUSTER (AFTER TEST)

since the area would not be in contact with the hot gases, the surface was not recoated.)

The two discrepancies did not affect the performance of the engine, and the engine will be reassembled for use on a future program.

SECTION IV-D

IGNITION/IGNITER SYSTEMS

The ignition of the 5.0-pound thrust and the 0.1-pound thrust engines was accomplished using the energy dissipated from the spark discharge across a Champion FHE 231A spark plug. A detailed schematic of the spark plug is shown on Figure 98. The only modification made by Marquardt is the removal of the semiconductor material between the cathode and the anode.

1. IGNITER CONTROL SYSTEM

The igniter control system provides the spark plug as igniter with a preset quantity of high voltage pulses that are precisely controlled as to time and energy content. Various methods can be incorporated in the design of such a unit and during the program two systems were utilized. The first system was capable of supplying various energy levels and spark rates, delays, etc., while the second was designed to a specified criteria.

a. Variable Energy Igniter Control System

The variable energy igniter control system was used only for the preliminary tests on the 0.1-pound thrust engine. The syste, which was available at the start of the program, was modified to include capabilities for variable energy and rate. Figure 99 shows a photograph of the three units, the power supply, the variable energy supply, and the control circuit.

The engine pulser positive going command signal is applied to the base of an interface transistor whose output saturates, producing a fast fall time used to trigger the digital circuitry. This signal passes to the delay circuit which is a one-shot. It produces a negative going pulse that is coupled to a differentiator stage that produces a negative going output pulse at the trailing edge of the delay pulse. This output drives a dual mode one-shot which is controlled by the mode switch. In the burst mode it is a one-shot whose duration is controlled by the panel burst duration control, while in the continuous mode it is a RS flipflop that is reset by an inverter stage connected to the command switch common. The negative going duration signals are then inverted and control the clock gate so that when both the clock and control inputs are high the clock gate output goes low. The clock is a free-running multivibrator with a 50% duty cycle operating at a frequency of 250 Hz for a cycle interval of 4 milliseconds. The output of the clodk gate drives the firing time one-shot, which is set for 1.9 milliseconds. Its purpose is to assure that the SCR in the ignition unit has turned off prior to turning on the charge transistor, because if both are on at the same time excess input current will flow, which will blow the fuse. The firing time one-shot output goes to the driver chip, directly for the charge control, and inverted for the fire control. The driver controls the 28-volt "charge/fire" circuit by cutting off

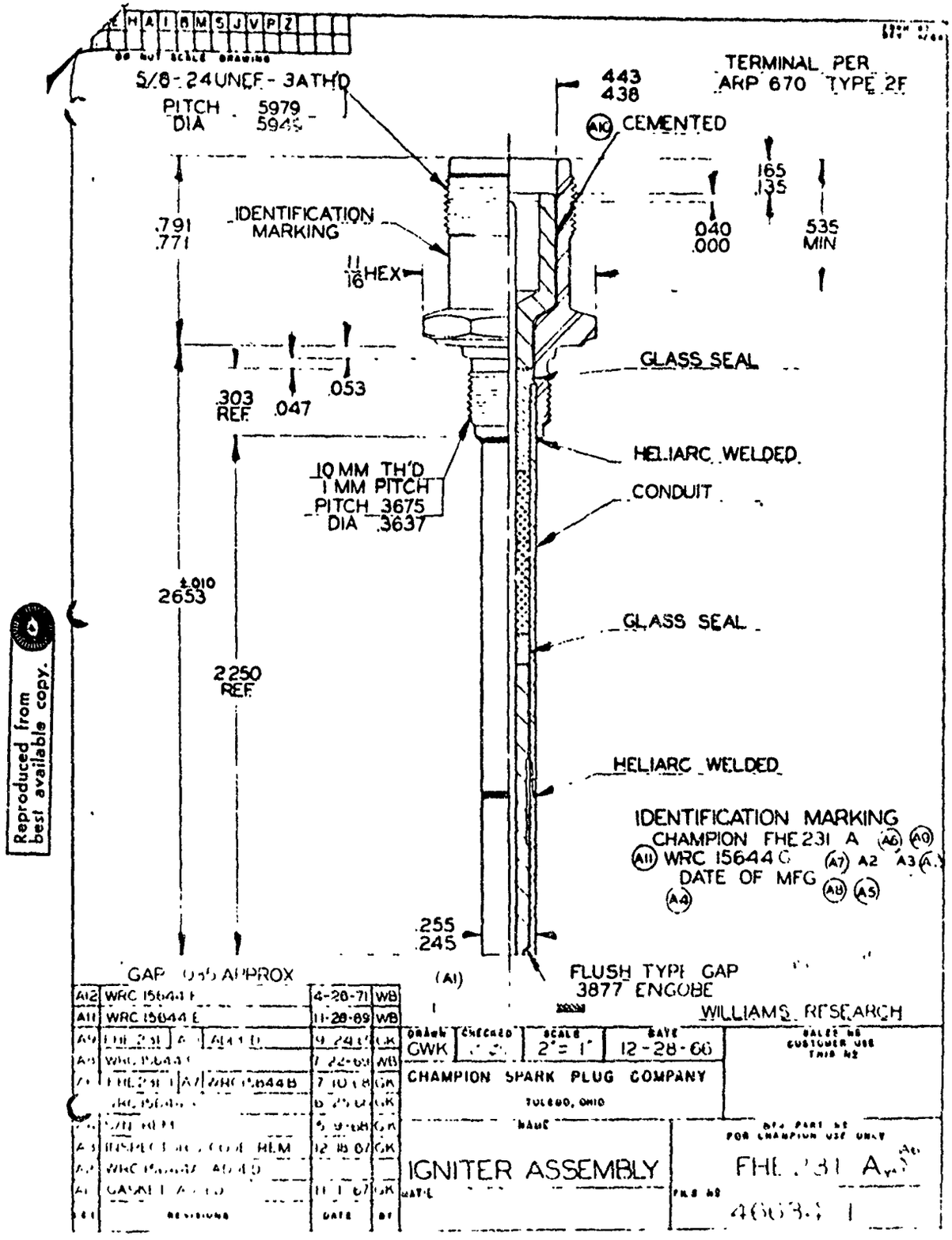

FIGURE 98. 0.1 LB_f and 5 LB_f GO_2/GH_2 THRUSTER SPARK PLUG

NEG. 71-173-1

FIGURE 99. VARIABLE ENERGY SPARK IGNITER SYSTEM

the "charge" driver transistor and allowing the plus 28 voltage to rise for the "fire" command when the firing one-shot output goes low. The SCR is delayed from firing immediately by its gate circuit that is driven from the "charge" transistors until they are cut off.

b. Prototype Igniter Control System

The final tests on both the 5-pound thrust and 0.1-pound thrust engines incorporate a fixed energy igniter control system shown on Figure 100, whose schematics and block diagrams are contained in Figures 101 through 105.

The prototype igniter control system used on the two engines consists of an igniter control unit (ICU) with an integral high voltage cable assembly and the the power input cable. The ICU features a control to adjust the time delay of the first spark from electrical on command. This control is located on the input power end. The adjustment range is from approximately 5 milliseconds in the CCW position to over 10 ms in the CW position, and the setting remains constant over an input voltage range of 26 to 30 vdc. Two power ranges were used: 50 and 100 millijoules. The output power range may be varied in steps by changing the value of the discharge capacitor in each unit and may be varied through the range by connecting the unit as shown in Figure 101 and varying the input voltage to pin A from 21 to 33 vdc. Figure 106 was used to determine the approximate output energy for a given voltage and capacitor size. The command signal to pin D is a positive going pulse starting at zero ±1 volt and have a minimum amplitude of +24 vdc. The driver has a current capacity of 100 ma and a rise and fall time of less than 100 microseconds. Power supply ratings for power to pin A exhibit regulation errors of less than ±5% and a peak current capacity of 25 amperes (10,000 uf capacitor) and an average current rating of 4 to 10 amperes. In operation from batteries, the quiescent current draw through pins A and B is only 200 micro amperes maximum. Power consumption from the driver is approximately 1 watt for a 1-second pulse duration. The minimum pulse duration is 50 milliseconds, and the minimum pulse off time is 50 milliseconds for a minimum engine control pulse time of 100 milliseconds. The maximum power consumed by the ICU is in this 50% duty cycle mode and consumes up to 6 watts/100 mj of rated power. This power consumption reduced to 1.7 watts for a one-second engine pulse. The characteristics of the igniter are as shown in Table 21.

The ICU block diagram and schematic are shown on Figures 102 and 103. The pin B power input is connected to system common, pin A to the positive supply buss, and pin D to a positive going command signal from a driver or pulser. Pins A and D each have a diode for polarity protection and to prevent feeding stored current in the ICU back to the valves that may be connected in parallel with the ICU. The command input pin D contains an RC network to damp transients, a dual Zener regulator to provide the 5-volt power to the computer and 10 volts to the delay timing network. A fast discharge network resets the delay timing capacitor and allows a minimum off time period of 25 ms.

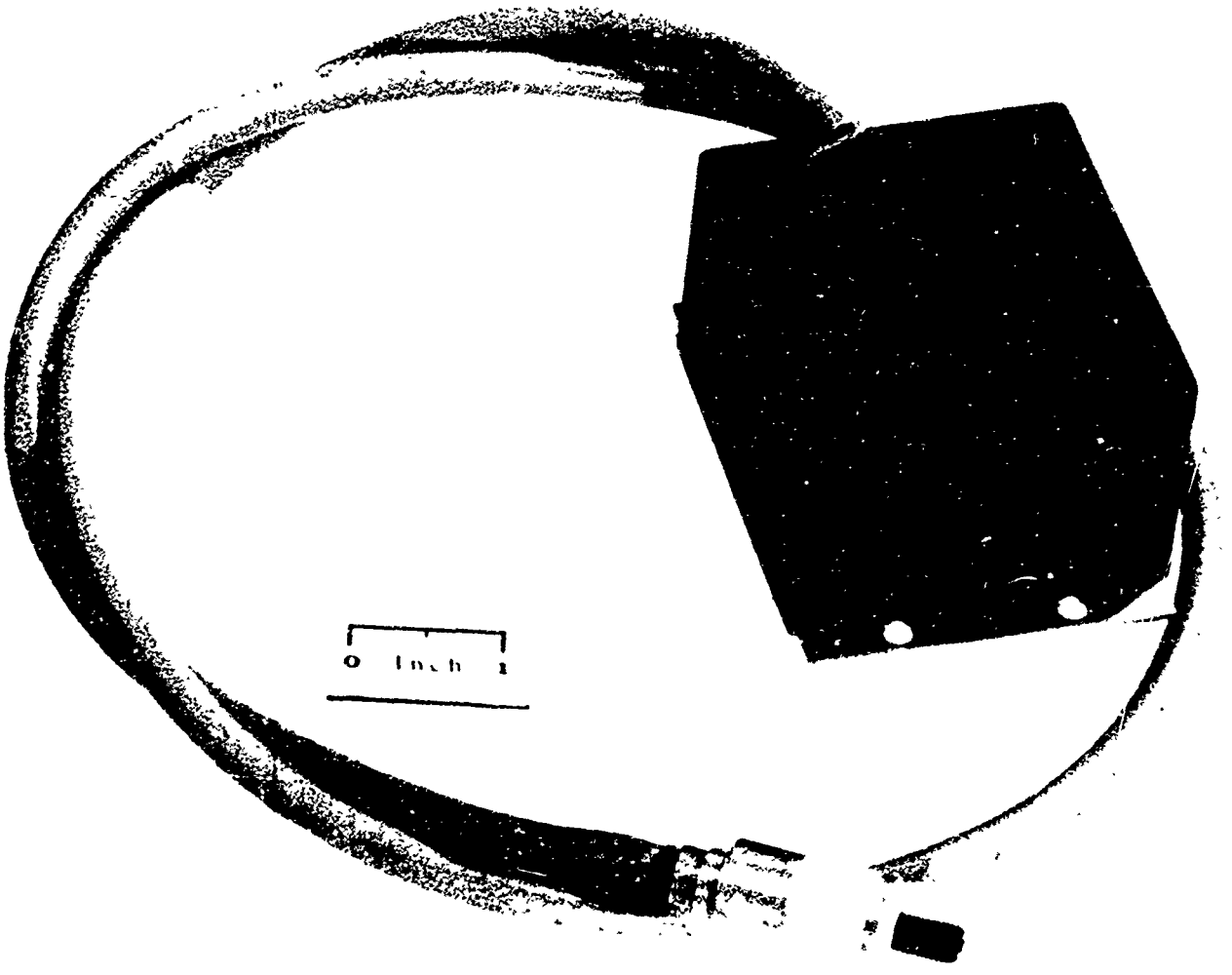

FIGURE 100. SPARK EXCITER SYSTEM (PROTOTYPE)

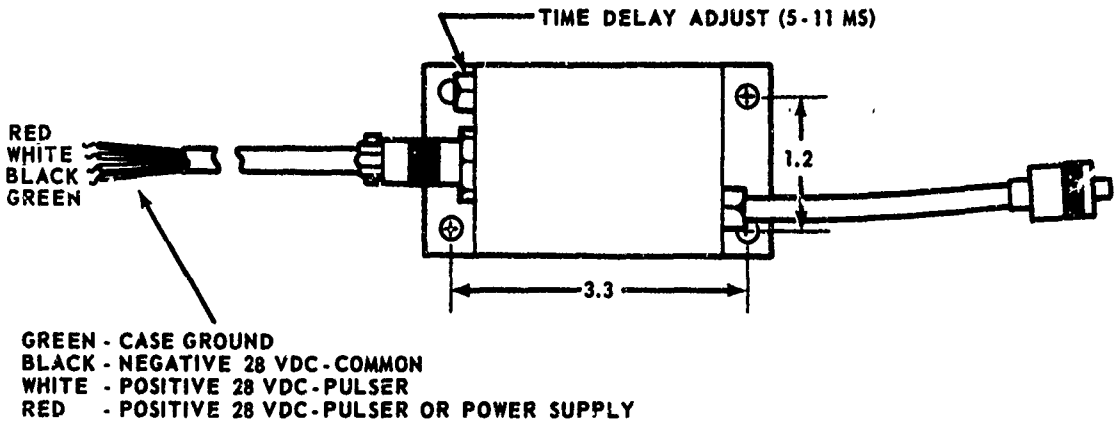

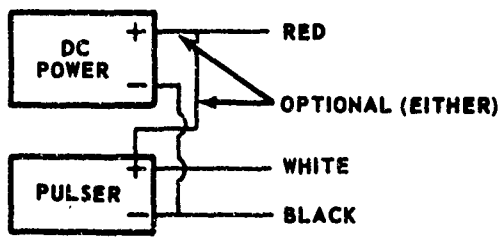

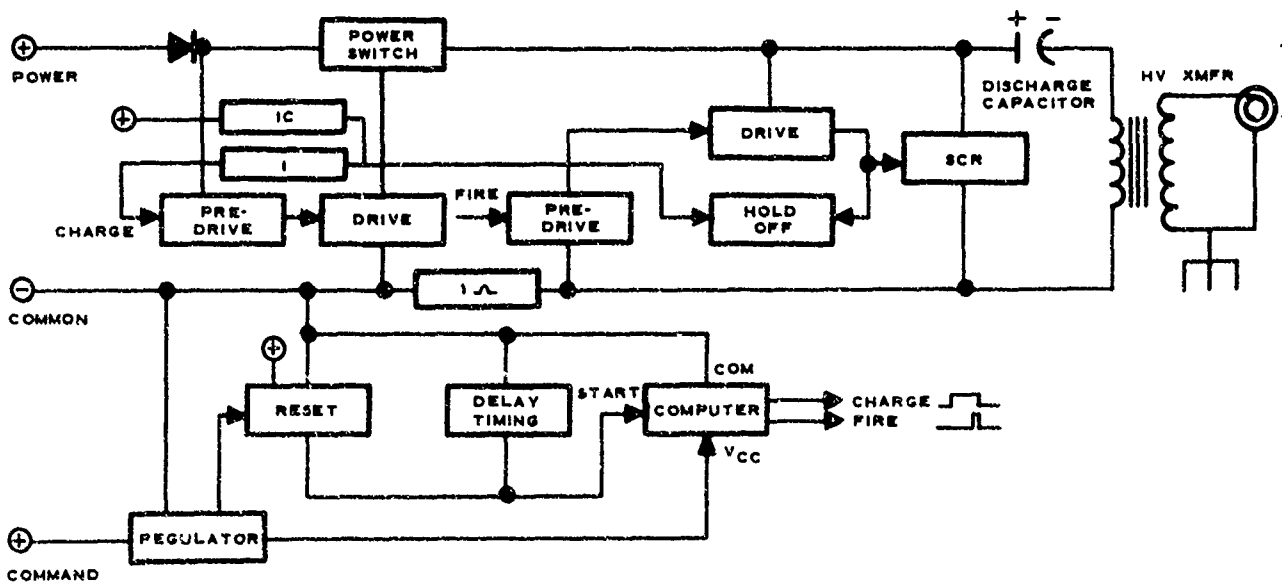

FIGURE 101. IGNITER CONTROL SYSTEM

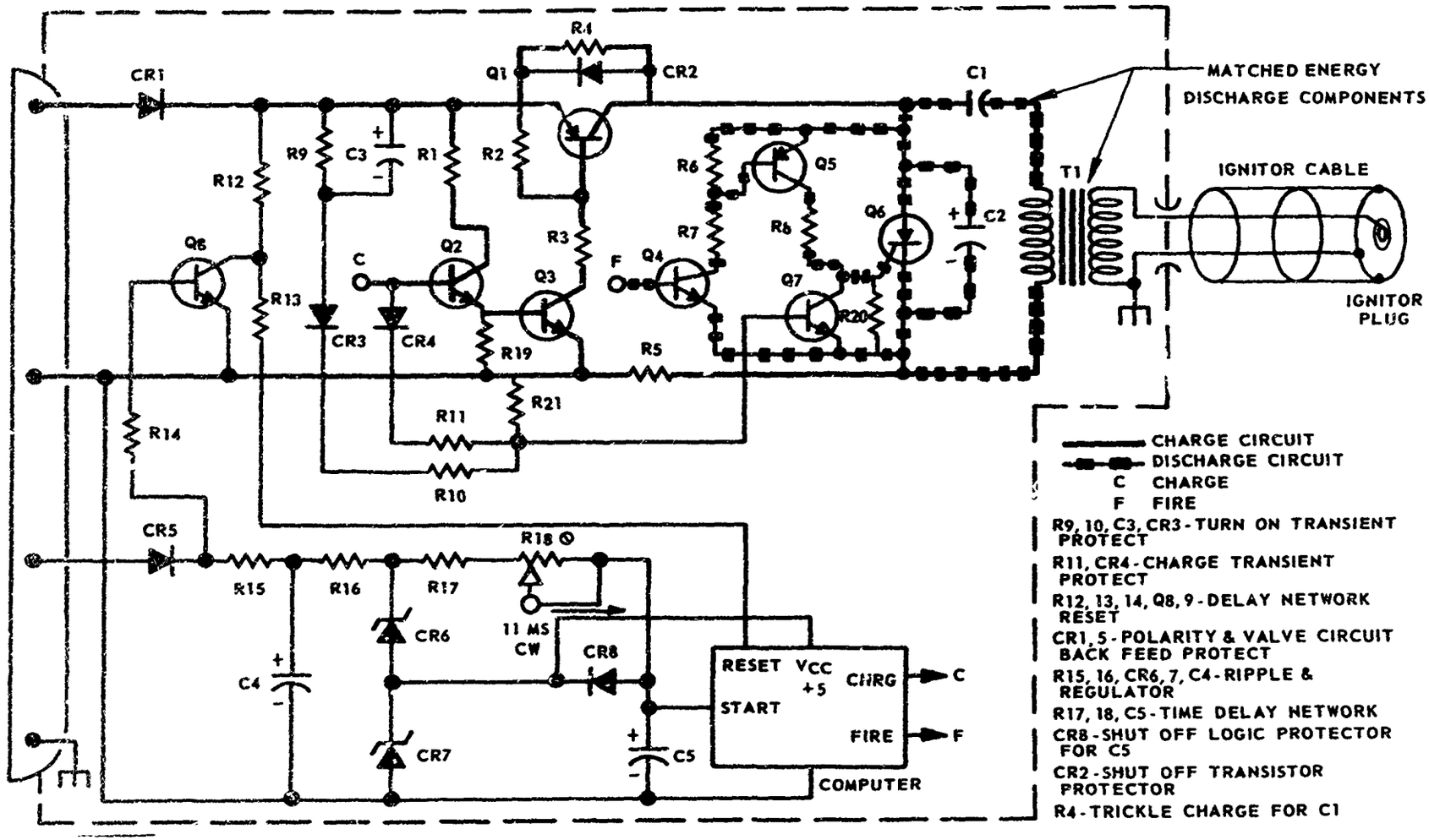

FIGURE 102. IGNITER CONTROL UNIT SCHEMATIC EXCEPT COMPUTER

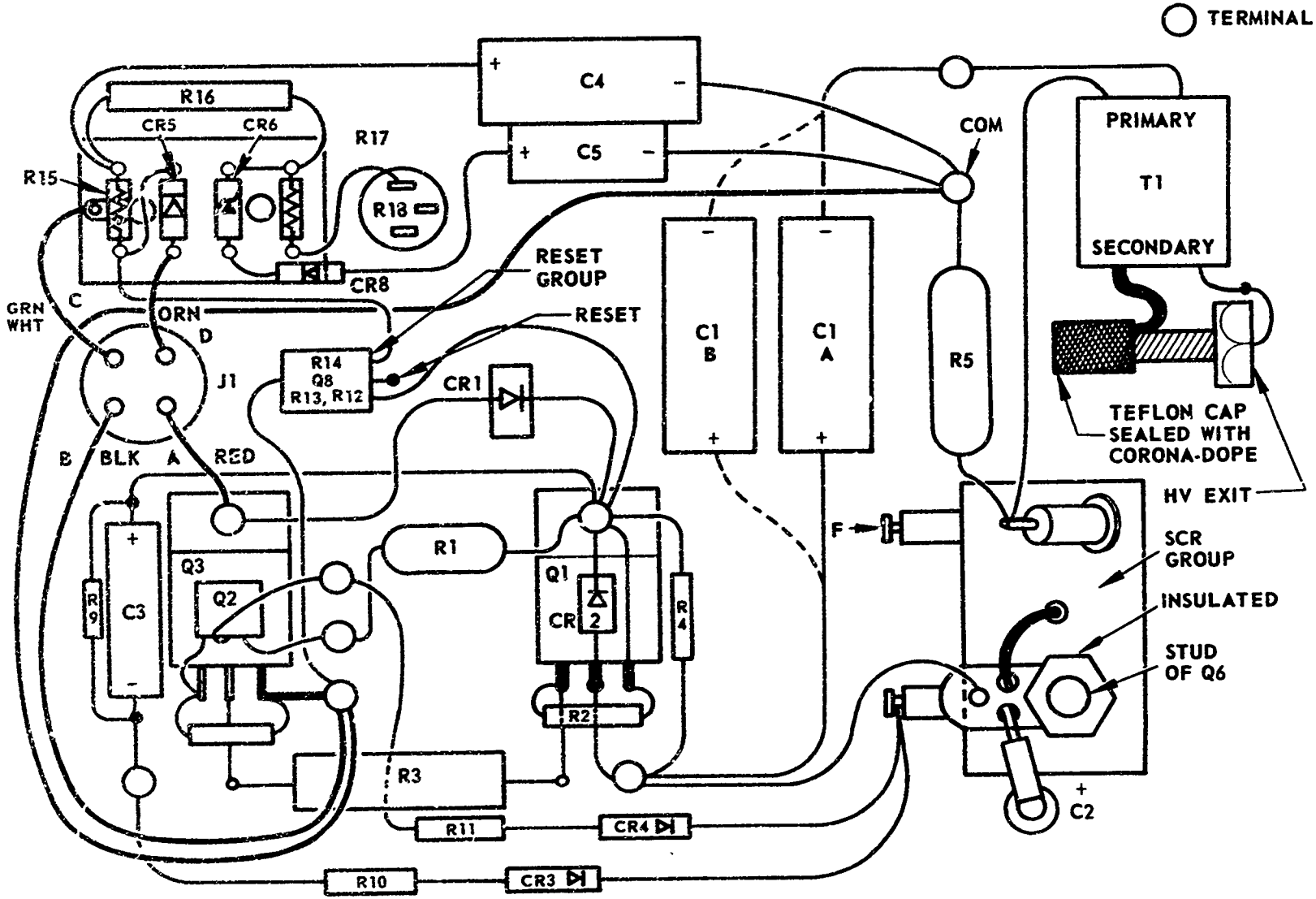

FIGURE 103. IGNITER CONTROL UNIT

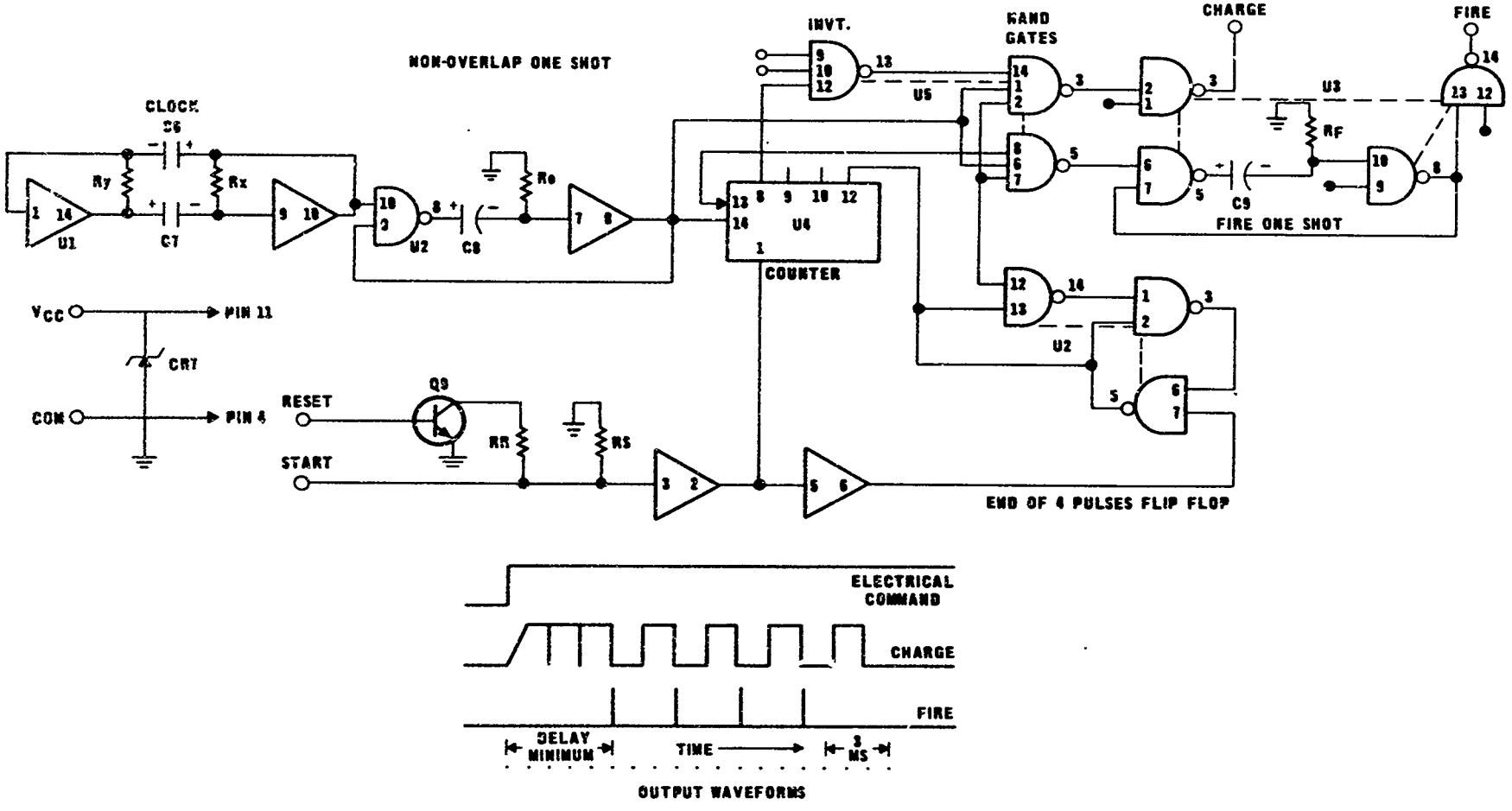

FIGURE 104. COMPUTER CONTROL CONNECTIONS--IGNITER CONTROL UNIT

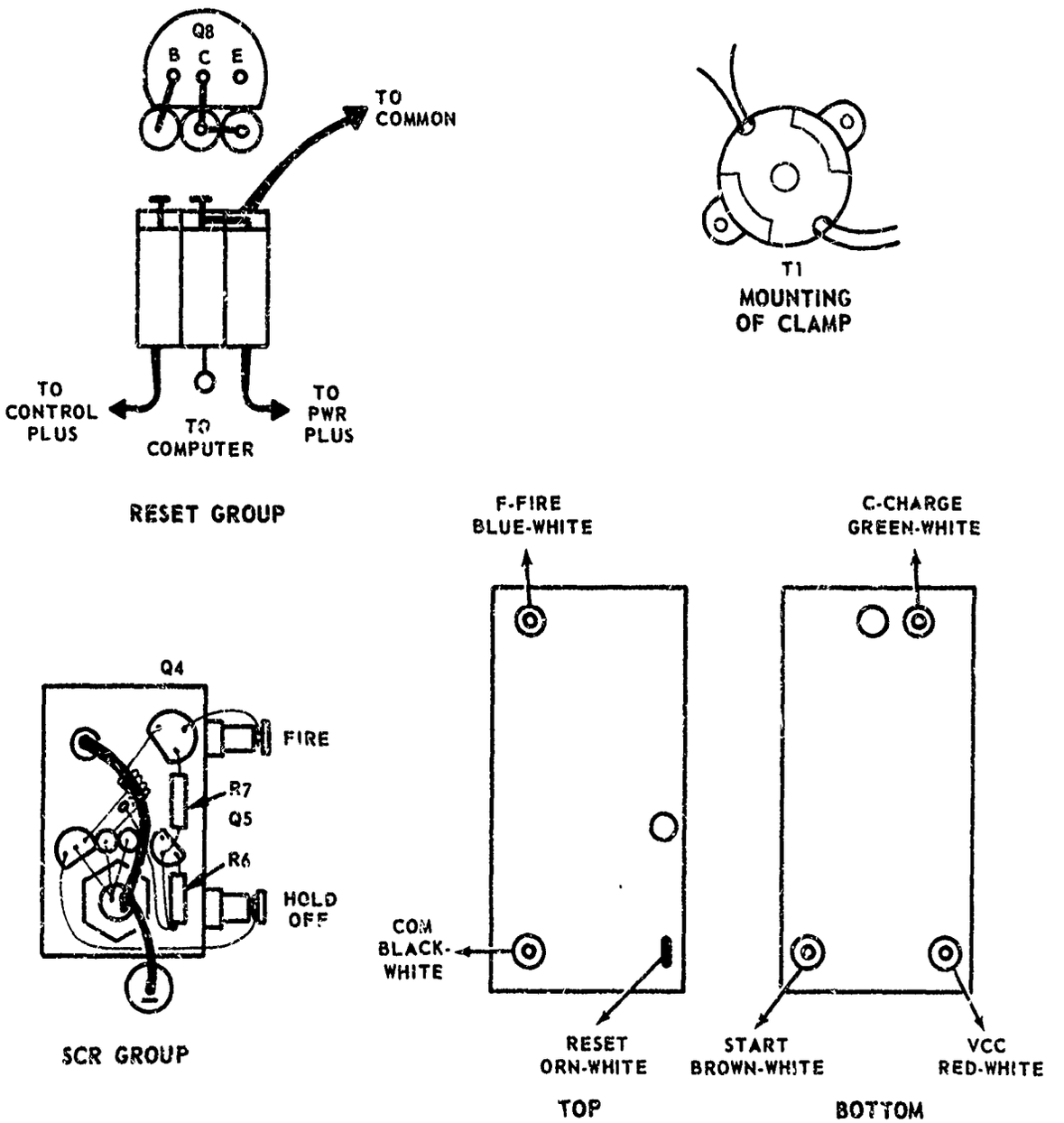

FIGURE 105. COMPUTER CONTROL CONNECTIONS -- IGNITER CONTROL UNIT

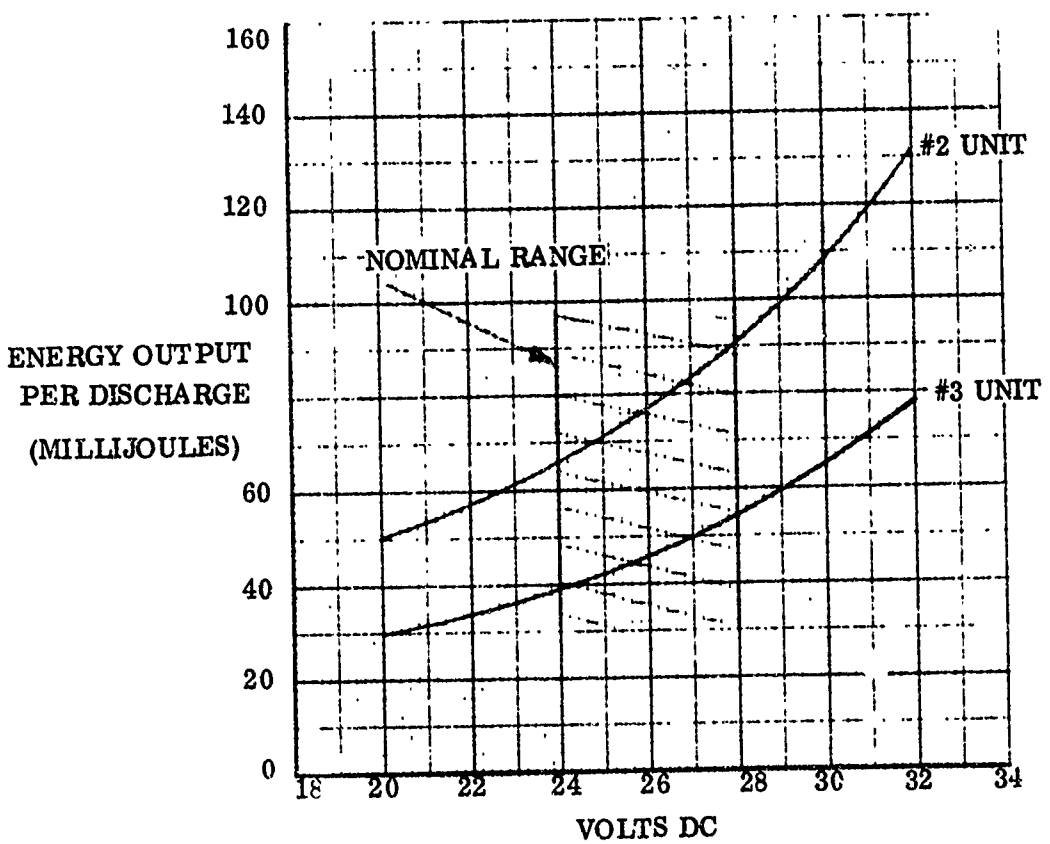

FIGURE 106. IGNITER SYSTEM ENERGY OUTPUT PER DISCHARGE

TABLE 21

IGNITER CHARACTERISTICS

Input Voltage:	Pin B connected to common, Pin A +20 to +33 vdc, Pin D +24 to +30 vdc command pulse
Peak Input Current:	Pin A 25 amperes for 200 us, Pin D 0.3 amperes for 200 us
Design Input Current:	Pin A 3-6 amperes for 16 ms, Pin D 0.05 amperes for duration of pulse
Battery Input Power:	6 watts/100 mj rating for 50 ms on; 50 ms off times (10 pulses/second)
	1.7 watts rating for 950 ms on; 50 ms off times (1 pulse/second)
	1.3 watts rating for 1950 ms on; 50 ms off times (1 pulse/2 seconds)
Delay Time:	5 to 10 ms from electrical on to first spark
Spark Interval:	3 milliseconds between sparks
Spark Burst Duration:	4 complete sparks
Output Voltage:	10 kv minimum peak output voltage
EMI Control:	Sealed box for ICU, integral power line filters, triple shielded high voltage cable, anti-corona cable and terminations
Spark Plug Style:	Open gap, unshunted, 20 to 30 mil gap. Champion FHE
Operation	

c. Igniter Operation

Upon receipt of the command signal the computer outputs the positive charge signal to the charging power switch Q1,2,3. Q1 passes the main current to the energy discharge capacitor, which is limited ty R5 and Q1. Q7 is used to hold off the SCR from firing during the charge and initial turn on cycles. The voltage across the timing capacitor, C5, rises in proportion with time corresponding to the resistance of R18. At a certain level the voltage initiates operation of the computer, which produces alternating charge and discharge pulses, which have equal time periods of 1.5 ms duration and a 150 ms duration fire pulse to the SCR group, nonoverlapping. The SCR, CI, TI, high voltage cable and igniter require a damping time of about 1 ms to unlatch completely. Resistor R4 maintains the working voltage across C1, while its current is less than the holding current of the SCR. Diode CR2 prevents reverse biasing (destruction) of the computer input when the command signal to Pin D goes low. Capacitor C2 assists in blocking currents from C1 and T1 to allow Q6 to turn off quicker, and prevent Di/dt-de/dt breakdown misfiring.

The computer consists of 5 TTL flat pack integrated circuits. These are mounted in cordwood style and are difficult to replace so they are completely tested prior to insertion. Two inverters of U1 are used to form the 666 Hz square wave clock. This clock drives a one-shot that produces a negative going pulse of 120 ms duration used to drive the counter U4 and also produces the blanking pulse to the Nand Gates U5 to prevent overlapping of the charge and fire pulses. Pin 8 of U4 is normally low when the counter is in the reset mode (Pin 1 - H1) and this signal is inverted by 1/3 of U5 and drives the charging Nand Gate. Since all inputs to this gate are basically high, except during the blanking pulse, the gate output is low, which is then inverted by 1/4 of U3 to produce the positive charge signal with negative going blanking pulses. As the voltage across the timing capacitor (re: start input) increases, the first inverter output flips from its H1 state (caused by input resistor RS and VG5) to a low state. This allows the counter to operate, and Pin 8 now goes high and low at 333 Hz alternately selecting the charge and fire Nand gates. A one-shot connected to the fire Nand gate produces a pulse of 120 us duration, which is inverted and used to control the SCR firing network. After 4 firing pulses Pin 12 of the counter goes high and is passed by 1/4 of U2 as a low signal to set a flipflop composed of 1/2 of U2. The FF output goes low, which inhibits operation of further change, fire, or set operations. This FF is reset by a low signal from inverter stage, which means that its input must be high and, therefore, the counter is reset.

SECTION V

FLIGHTWEIGHT SYSTEM

1. FLIGHT SYSTEM DESIGN

The design developed for a flightweight system which uses the water electrolysis scheme for providing gaseous oxygen and gaseous hydrogen to the rocket engine is based on the results of the test program and is constrained by the requirement that there will be no single point failure mode. Based on the reliability analysis and the results of the program, including the various component requirements, a flow schematic for the system was devised based on Design Specification (Table 22), which insures that no single point failure of any component will cause a complete failure of the system. Components such as the tanks and lines were considered in the analysis, but it is obvious that even these components could be made redundant in many cases, but at a larger weight penalty. The schematic for the system shown on Figure 107 specifies that most of the valves, and pressure switches located within the feed system, are quad redundant to account for both fail open and fail close phenomena. The electrolysis unit contains two individual units which provide a capability of 0.1 pounds/day of propellant and 2.3 pounds/day maximum. The two cells which are contained within a single structure can thus provide for all mission objectives which have an inherent redundancy. Table 22 lists the characteristics of the system and Table 23 lists the components chosen for the system. The engines are redundant in that only one of two engines in a system (the one downstream of the isolation valve) operates. If an engine fails, the isolation valve is activated and the engine upstream is activated. This mode accounts for a majority of the failures associated with engine operation. Incorporation of redundant valves, igniters, etc., within a single engine was eliminated due to size and packaging restrictions within each engine. A system which does not use single point failure mode criteria is shown in Figure 108. The total estimated wet weight of the system is approximately 400 pounds. For comparison purposes, the monopropellant system would weigh nearly 550 pounds while the bipropellant system weighs approximately 425 pounds.

a. Electrolysis Unit

Enclosed is the design data material for the flightweight electrolysis module. GE Drawing No. 1076527-969, Figure 109, illustrates the overall envelope of the unit and the internal stacking and component parts of the cells. Various weight tradeoffs were made of the configuration to minimize the weight, including such design parameters as the number of cells, water transport membrane thickness, temperature, end plate weight vs. pressure vessel weights, module material and design operating pressures. The design illustrated in the drawing consists of 13 cells in one stack to provide the high gas rate demand and one additional cell to provide the lower power rate. It was determined during the weight tradeoff study that a savings of 2 lbs could be realized (total

TABLE 22

FLIGHTWEIGHT WATER ELECTROLYSIS SYSTEM

		DESIGN CRITERIA & SPECIFICATION
1.	Total Impulse	100,000 lb-sec
2.	Operating Pressure of Gas Tanks	
	Prior to Blowdown	200 psia
	End of Blowdown	70 psia
3.	Power Requirements	
	Normal	17-20 watts
	Orbit Reposition and Adjust	230 watts
4.	Electrolysis Generation Rate	
	Normal (Unit #1)	0.1 pounds/day
	Orbit Reposition (Unit #2)	2.3 pounds/day
5.	Tank Volumes	
	Water Tank	16,700 in^3 (≈ 10 ft^3)
	H_2 Tank	4 ft^3
	O_2 Tank	2 ft^3
6.	Pressure Control Method H_2O Tank	Blowdown From 400 psia to 200 psia
7.	Electrolysis Unit Control	Pressure Switches
8.	Engine Shutdown at End of Blowdown	Pressure Transducer
9.	Envelope	6 ft dia. x 6 ft height
10.	No Single Point Failure Mode	Redundant Hardware

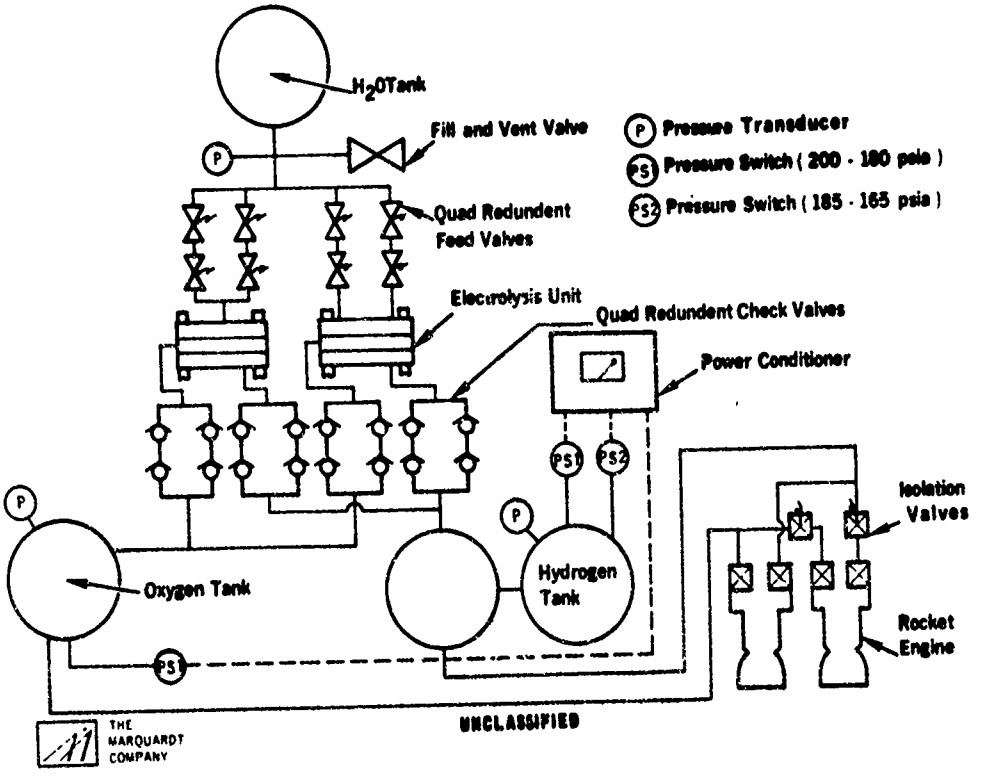

FIGURE 107

FLIGHT SYSTEM SCHEMATIC FOR SYSTEM WITH NO SINGLE POINT FAILURE MODE

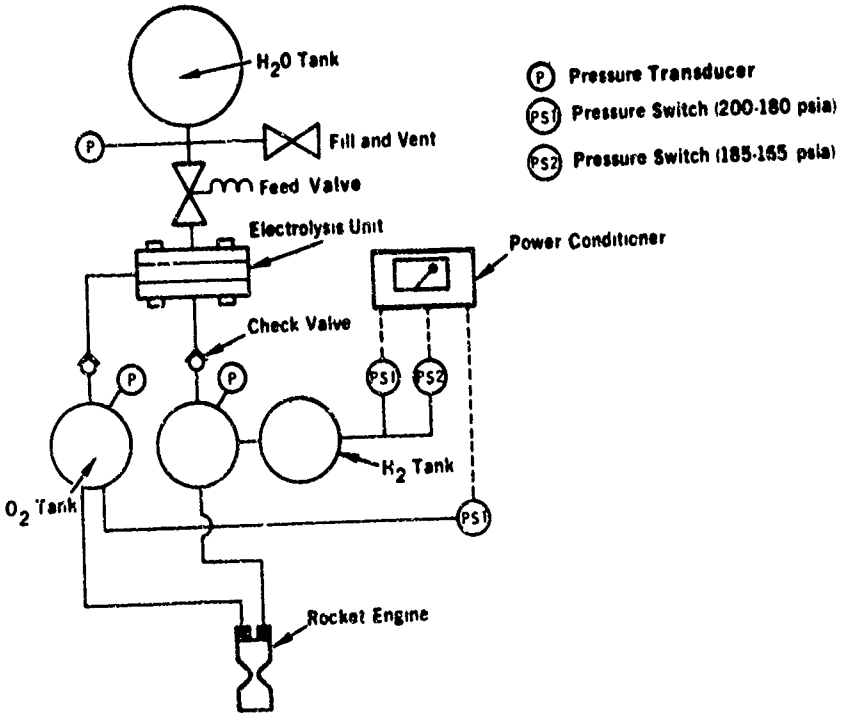

FIGURE 108. FLIGHT SYSTEM SCHEMATIC WITH NO REDUNDENCY

TABLE 23

COMPONENT DESCRIPTION AND WEIGHT SUMMARY

COMPONENT	TYPE	POWER REQUIREMENTS	SIZE	NO.	WT (Lbs)
Water Tank	T.B.D.	-	16,700 in^3	1	28.50 (See Section III)
Pressure Transducer	Statham PA493	10 ma each	-	3	0.93
Fill and Vent	Purolator	-	-	1	0.26
H_2O Isolation Valves	TMC Latch	.25 watt-sec/act	-	8	2.00
Electrolysis Unit	Gen. Elec.	See Table 29	-	1	17.00
Power Conditioner	Gen. Elec.	See Table 30	-	1	5.00
O_2 and H_2 Tanks	T.B.D.	-	3456 in^3	3	18.00
Thruster Isolation Valves	TMC	.25 watt-sec/act	-	TBD	-
Pressure Switches	Custom Components	-	-	12	1.20
Check Valves	Circle Seal 2620T	-	-	16	0.90
Rocket Engine (5 lbf)	TMC	11 watts (firing)	-	TBD	3.50
Rocket Engine (0.1 lbf)	TMC	11 watts (firing)	-	TBD	1.50

Total Estimated Weight Less Thrusters Lines	74.00
Lines @ 10%	8.00
2 5-lb. and 8 0.1-lb Engines	17.50
Total Estimated Weight	100.50
Weight Propellant (includes 2% loss)	300.00
TOTAL SYSTEM WEIGHT	400.50

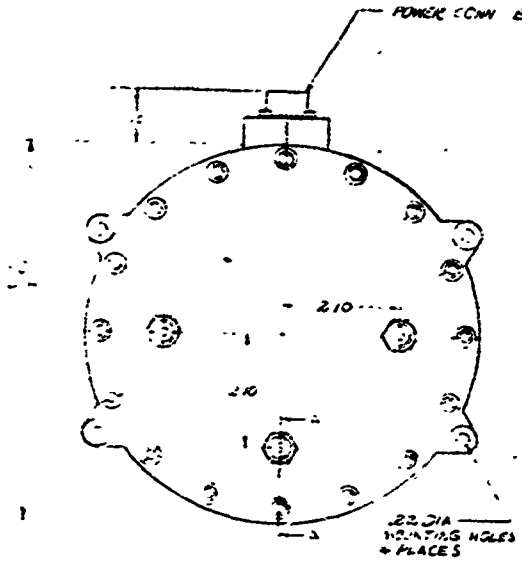

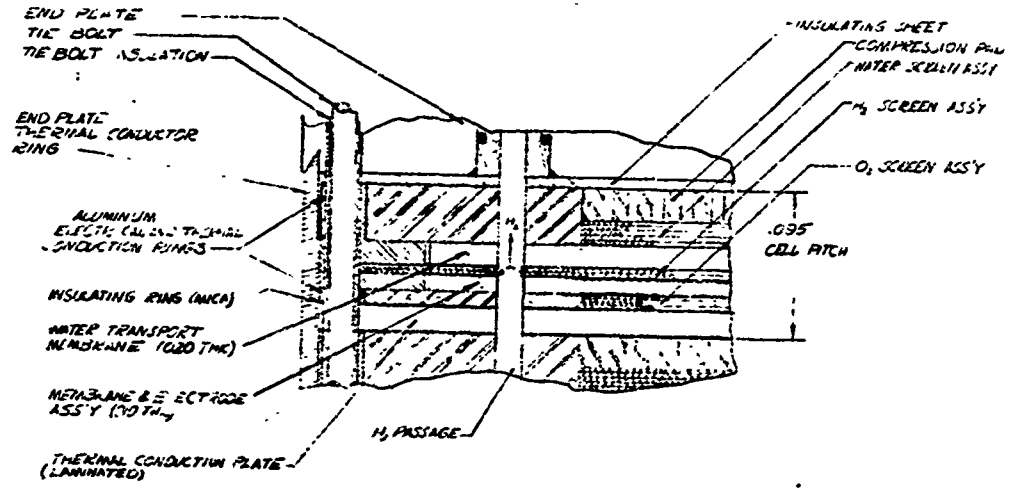

SCHEMATIC OF SECTION AA
VERTICAL SCALE APPROX 20/1
NOT TO SCALE HORIZ

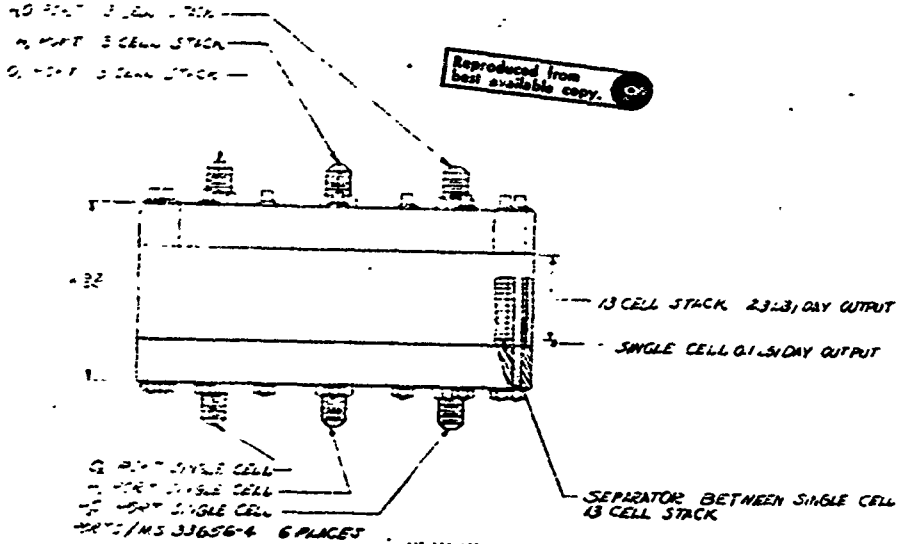

-193, 194-

FIGURE 1. FLIGHT WEIGHT ELECTROLYSIS UNIT (REDUCED SIZE)

ALL DIMENSIONS ✓	GENERAL ELECTRIC	
	WATER ELECTROLYSIS UNIT FLIGHT-WEIGHT DESIGN	
	E 14736	1076527-969

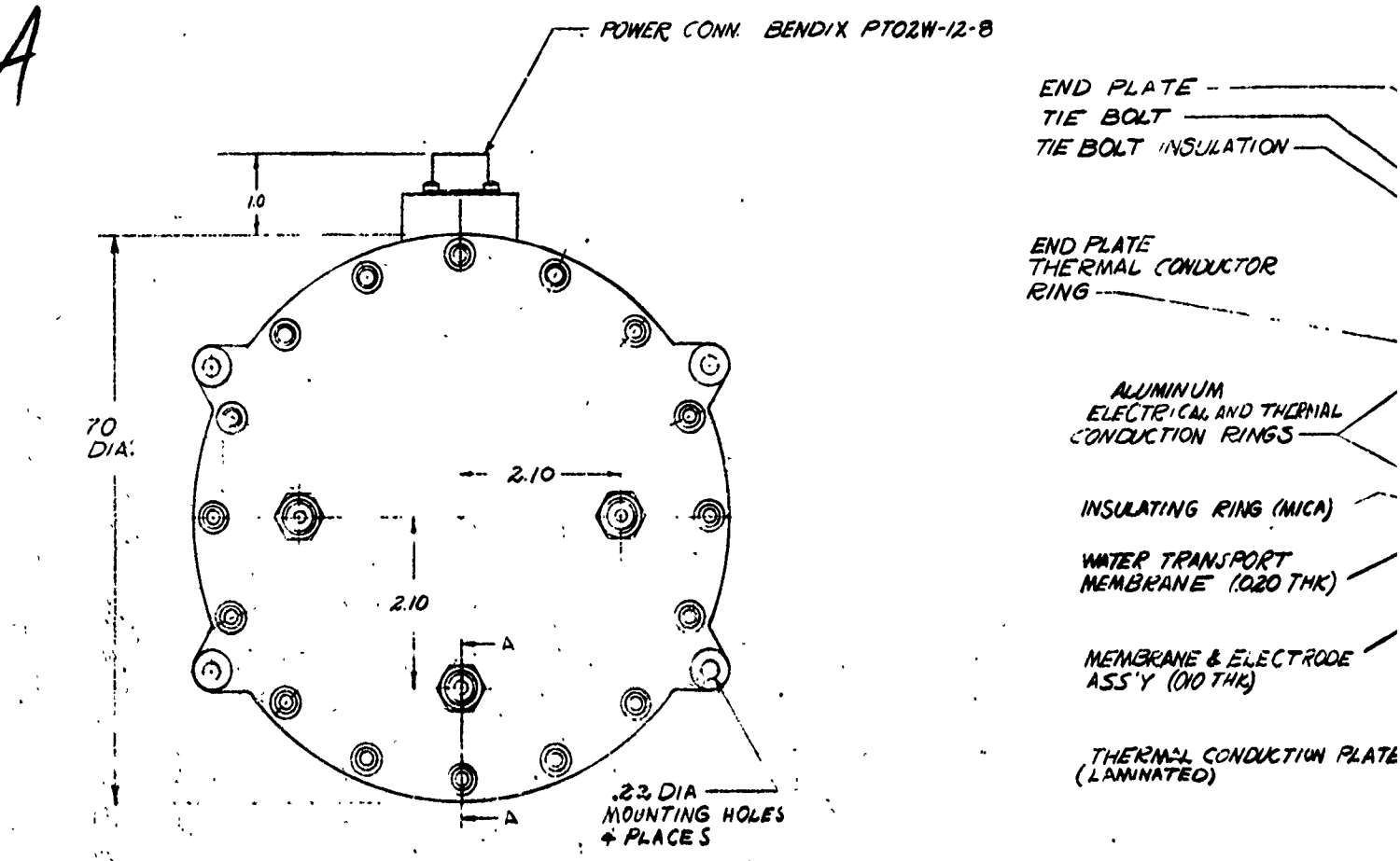

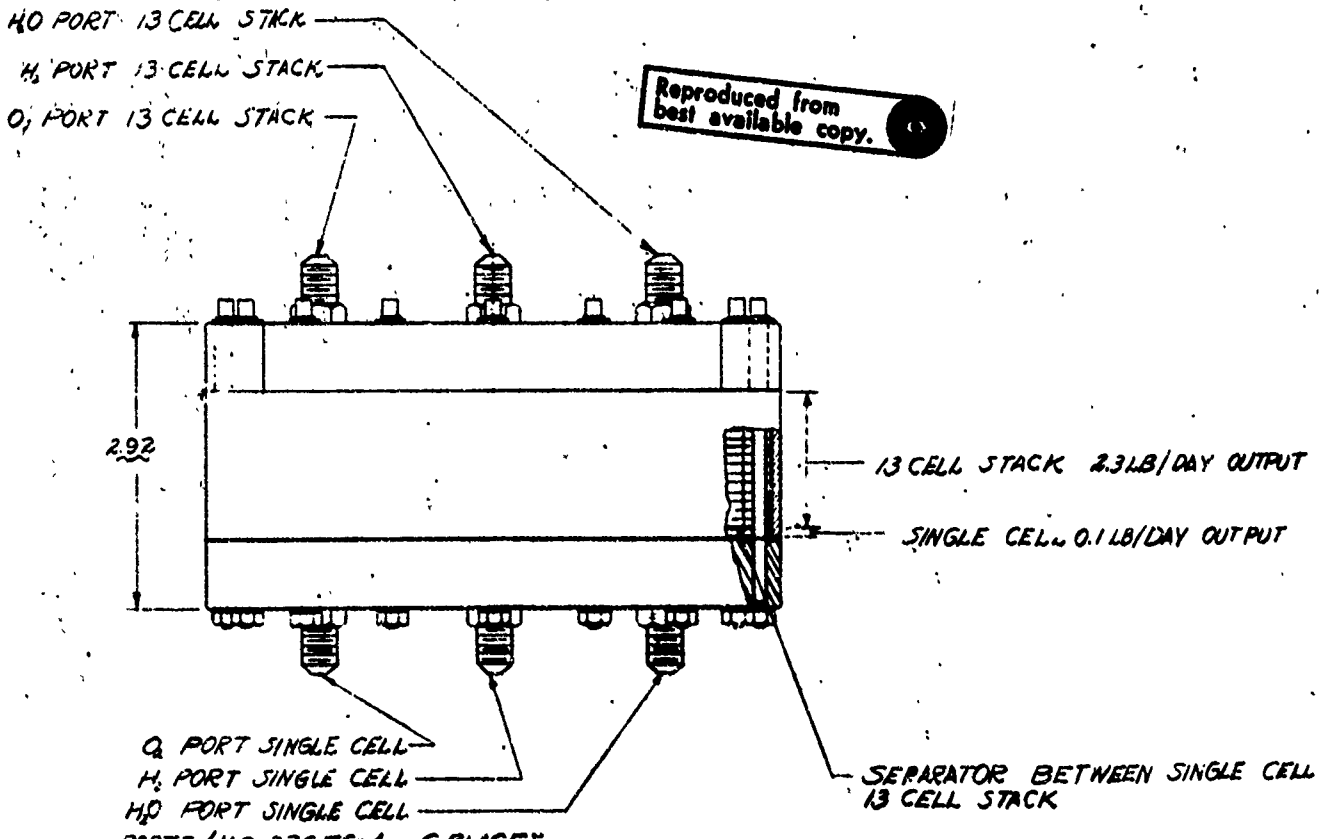

FIGURE 1.1 FLIGHTWEIGHT ELECTROLYSIS UNIT (REDUCED

B

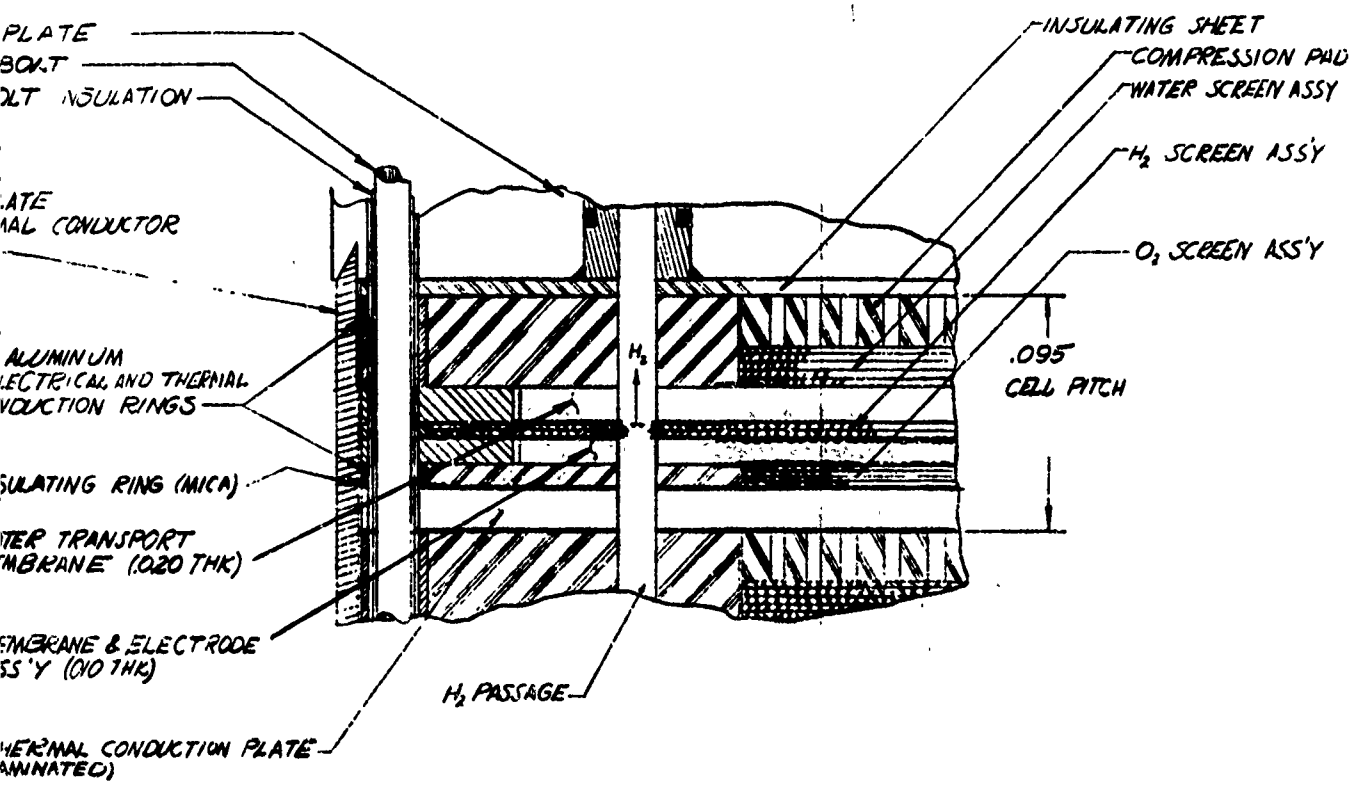

SCHEMATIC OF SECTION AA
VERTICAL SCALE APPROX. 20/1
NOT TO SCALE HORIZ.

AY OUTPUT

OUTPUT

NGLE CELL AND

SIS T IT (REDUND NT T PE)

UNLESS OTHERWISE SPECIFIED DIMENSIONS ARE IN INCHES	SIGNATURES	DATE-DA-YR	GENERAL ELECTRIC DIRECT ENERGY CONVERSION OPERATION LYNN, MASS. U.S.A.
ALL SURFACES ✓		10-19-71	WATER ELECTROLYSIS UNIT FLIGHT-WEIGHT DESIGN
MATL		10-19-71	
FOR G.E. USE ONLY			SIZE E · CODE IDENT NO. 14736 · DWG NO. 1076527-969
SIMILAR TO			SCALE · WT · SHEET 1 OF 1
L/O			
DR			

unit weight of 15 lbs) if the number of cells could be increased to 16. This was not possible due to subsystem input voltage limitations (25 vdc min.). Removal of the hydrogen pressure vessel similar to the current design resulted in a unit weight reduction even though the stack end plates had to be increased in thickness. The proposed configuration also proved to be even lighter than the pressure balanced domes that was previously evaluated.

The end plate material is magnesium and the cell heat conducting rings are aluminum. Both materials are completely isolated from the cells and the fluid passages, thus no contamination problem will exist.

The estimated weight of the total electrolysis module is 17 lbs, and the power conditioner is estimated to weigh approximately 5 lbs. Tables 24 and 25 show the general data for the unit.

b. System

The system design, which is the result of the mission and system analysis, which includes the criteria of no single point failure mode, is shown on Figure 110. The system was located within a given 6' x 6' envelope and was designed to provide 100,000 pounds/seconds of total impulse. The arrangement is such that all components of the electrolysis feed system are arranged within the H_2O tank support area, while the H_2 and O_2 tanks are symmetrical within the structure. The water tank will incorporate either surface tension screens or a integral bladder for feeding the water to the electrolysis unit.

TABLE 24

Water Electrolysis Subsystem

Flight-Weight Design

Significant Design Data

Water Electrolysis Unit Design Parameters

Item No.	Design Parameter	Design Data
1	Water Electrolysis Rate	
	High Rate (13-cell stack)	2.3 lb/day
	Low Rate (single cell)	0.1 lb/day
2	Stack Operating Data at High Rate	
	13-Cell Stack Current	6.5 to 10.0 amps max.
	Single Cell Current	5.6 amps
	Stack Voltage	23.5 VDC max.
	Stack Input Power	235 watts max.
	Stack Heat Loss	149 Btu/hr max.
3	Number of Cells	13 plus 1
4	Compartment Operating Pressures	
	Max. Oxygen	200 psia
	Min. Oxygen at Blowdown	67 psia
	Max. Hydrogen	200 psia
	Min. Hydrogen at Blowdown	67 psia
	Max. Water	400 psia
	Min. Water	200 psia
5	Proof Pressures	
	Container	600 psi
	Water Membrane Differential	400 psid
	Cell Membrane Differential	400 psid

TABLE 24 (CONTINUED)

Item No.	Design Parameter	Design Data
6	Stack (13-cell) Design Parameters	
	Electrode Diameter	4.50 in.
	Active Area/Cell	15.3 $in.^2$
	Current Density	65 to 100 ASF
	Ion Exchange Membrane	GE Spec. A50GN340
	Cell Membrane Nominal Thickness	0.010 in.
	Water Transport Membrane Nom. Thick.	0.020 in.
7	Single Cell Design Parameters	
	Electrode Diameter	4.20 in.
	Active Area	12.4 $in.^2$
	Current Density	65 ASF
	Ion Exchange Membrane	GE Spec. A50GN340
	Cell Membrane Nominal Thickness	0.010 in.
	Water Transport Membrane Nom. Thick.	0.020 in.
8	Water Electrolysis Unit Estimated Weight	17.0 lb
9	Water Electrolysis Unit Envelope	GE Dwg. 1076527-969

TABLE 25

Power Conditioner Design Parameters

Item No.	Design Parameters	Design Data
1	Input Voltage	28 ± 3 VDC
2	Output Voltage	23.5 VDC max.
3	Output Current	2 Output Levels
	High Power Side	6.5 to 10 amps (temp. compensated)
	Low Power Side	5.6 amps.
4	Max. Input Power	270 watts
5	Max. Power Loss	32 watts
6	Max. Heat Loss	108 Btu/hr
7	Power Conditioner Estimated Weight	5.0 lb
8	Power Conditioner Envelope	4.5 x 6.0 x 7.0 (adjustable)

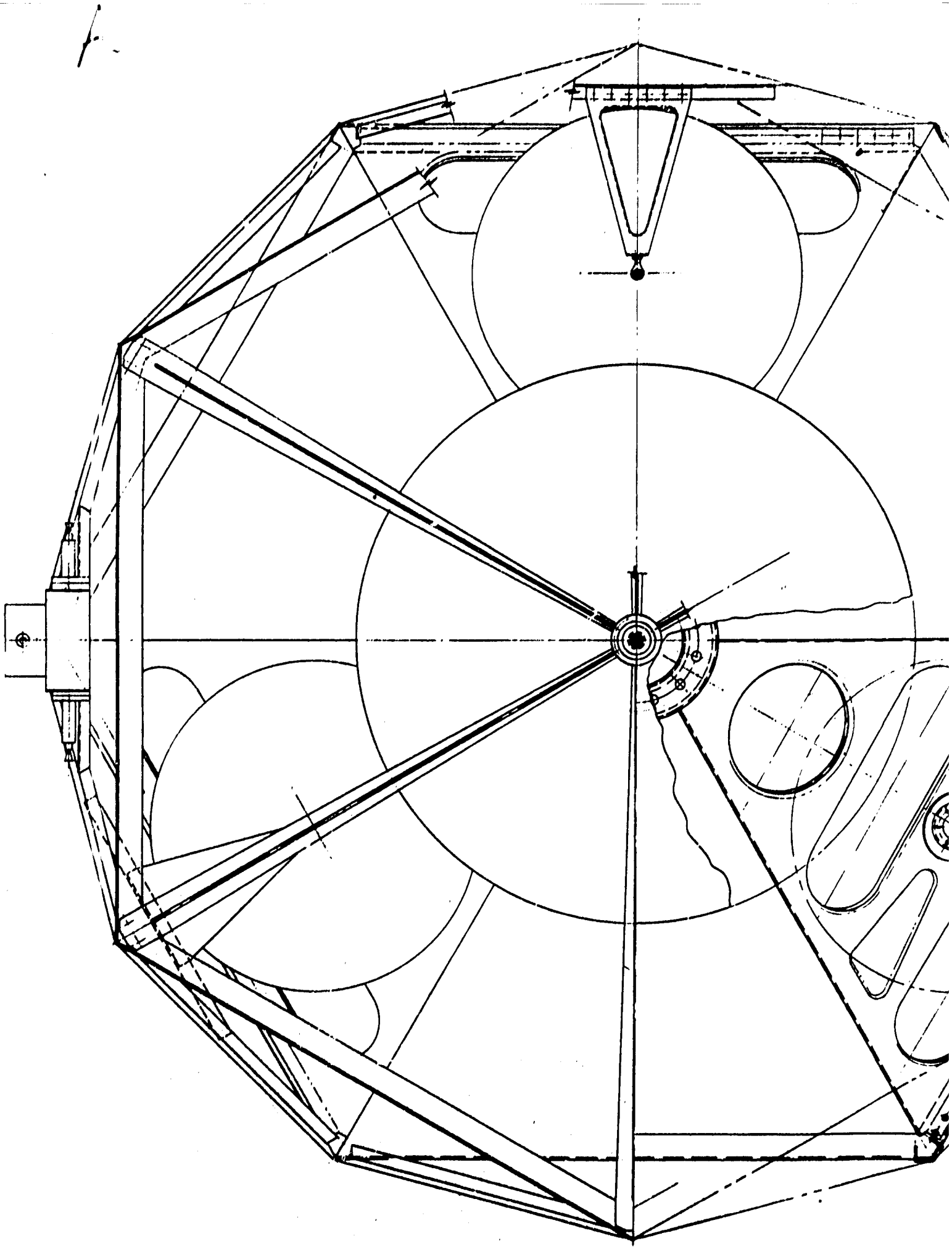

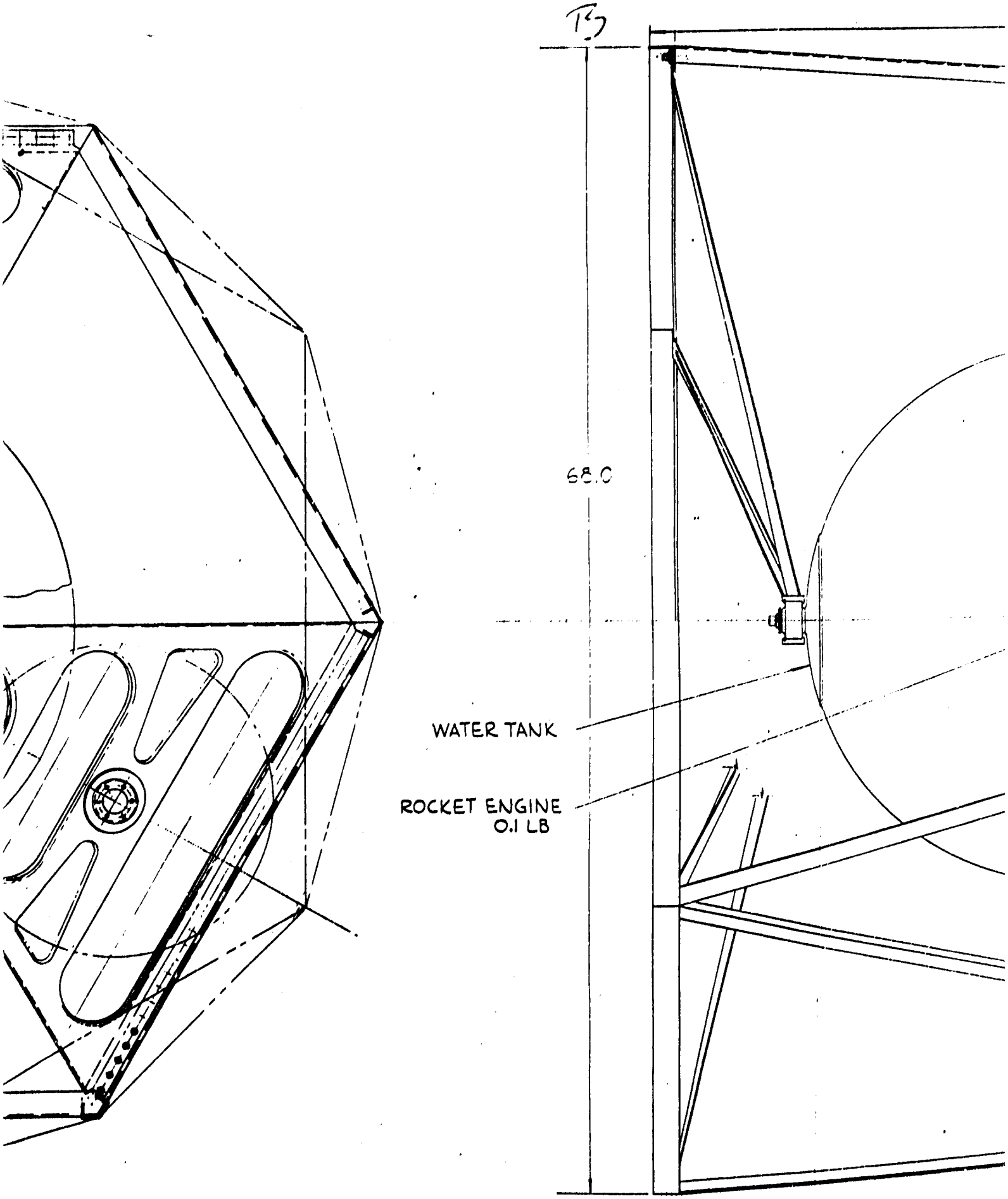
68.0
WATER TANK
ROCKET ENGINE
0.1 LB

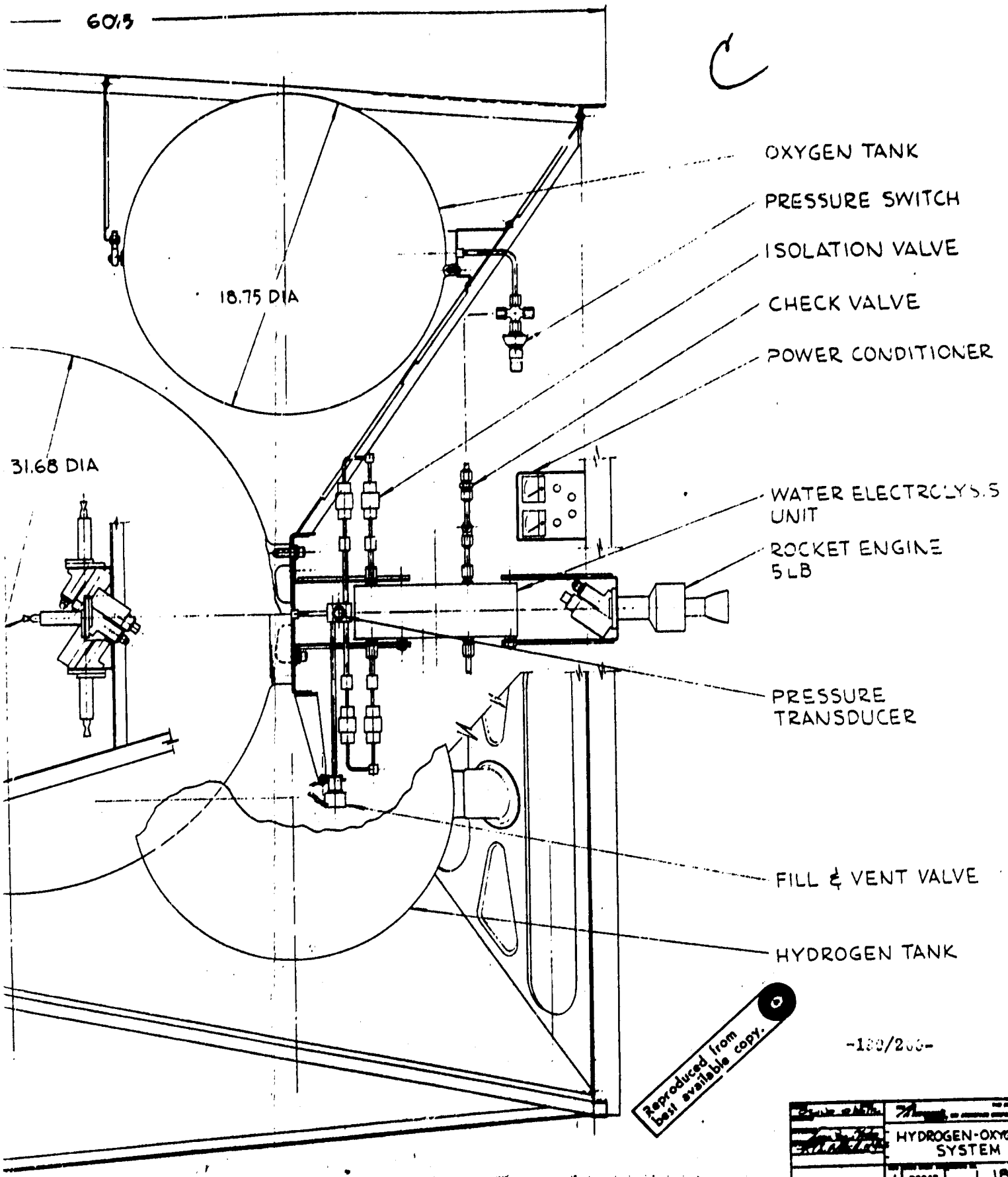

FIGURE 110. FLIGHTWEIGHT PROPULSION SYSTEM (REDUNDANT TYPE)

2. RELIABILITY ANALYSIS

In support of the system and electrolysis unit, a failure modes and effects analysis was accomplished. The Failure Mode and Effects Analysis (FMEA) of the electrolysis defines the potential modes of failure and determines what design features or approaches will eliminate or minimize the probability of occurrence. Figure 111 shows the logic block diagram for the system and the FMEA is cross-referenced to the figures by code numbers.

a. Failure Modes and Effects Analysis (Electrolysis Unit)

A detailed failure modes and effects analysis, given in Table 26, was made for the water electrolysis unit, power conditioner and oxygen cell pressure switch as components of the satellite propulsion system. A configuration consistent with a flight-weight design was assumed and some component changes or redundancy were recommended to eliminate single-point failure conditions. Secondary failure mechanisms were cited which arise from malfunction of other system components. This should aid in a total system FMEA. With the recommendations made, no single point failure condition should result in a catastrophic failure. Several conditions are noted which could result in a gradual degradation of system performance or reduced mission life. A discussion of these items follows.

One failure mode cited is the entrainment of liquid water in either oxygen or hydrogen discharged from the electrolysis unit. As predicted, this could result from the higher permeability of water through the water transport membrane at elevated temperature. Also, a higher rate of condensation could result from higher cell operating temperatures. A probable failure mechanism could be the gradual increase in both electrical and thermal contact resistance, thereby increasing cell operating temperature. Niobium (columbium) with a platinized coating would be used throughout the electrolysis stack assembly to reduce contact resistance and prevent the growth of an oxide layer, although most of these parts reside in a hydrogen atmosphere. Current similar applications and test results using this material selection or plating process show no degradation in performance after one year of continuous operation. Contact pressure would be maintained by Belleville spring washers on the electrolysis stack compression plate.

Minor cross-O_2/H_2 leaks within the electrolysis unit are expected to result in water formation by catalytic reaction at either electrode or by admixed gases of low concentration in the discharge if the catalytic surface is bypassed. Installation of check valves is recommended in both O_2 and H_2 outlet lines from the electrolysis unit to accommodate a cell gross leak condition. The check valves would prevent reverse flow and communication between the oxygen and hydrogen storage tanks through the electrolysis unit. Since the gas volumes of the electrolysis unit are significantly

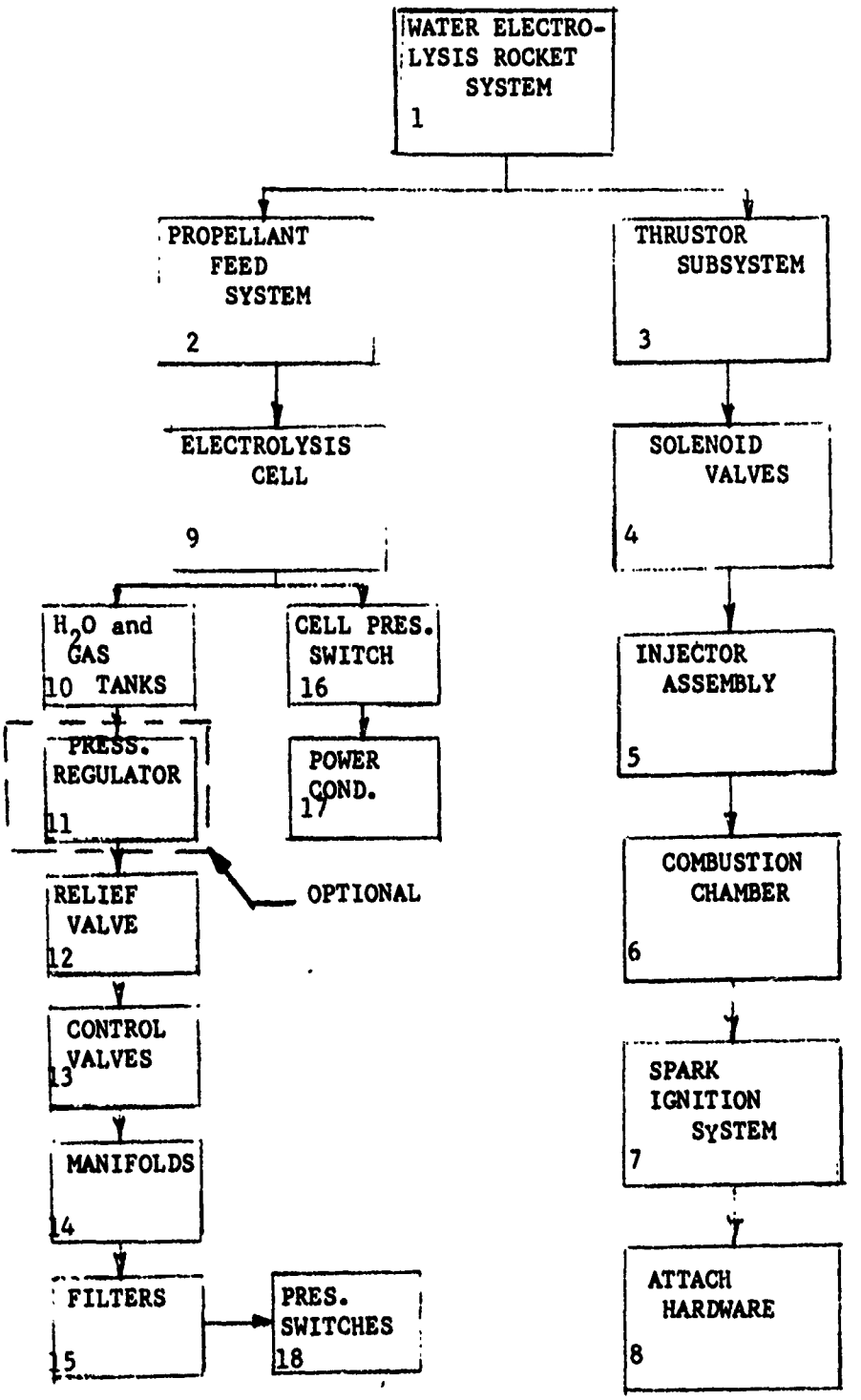

FIGURE 111. LOGIC BLOCK DIAGRAM

TABLE 26

Failure Modes and Effects Analysis

Item	Component	Assumed Failure Mode	Probable Failure Mechanism	Effect on Water Electrolysis Unit or Satellite Propulsion System	Remarks
9.	Water Electrolysis Unit	1.1 Liquid water entrainment in H_2 discharge.	1.1.1. Excessive H_2O permeability thru H_2O membrane due to low current, high (PH_2O-PH_2), high temperature.	Premature expenditure of H_2 desiccant, faulty thruster performance, reduced mission life.	1.1.1 Low current caused by power conditioner malfunction, high ΔP caused by H_2O, H_2 pressure switch malfunction (double failures). High cell temp. caused by high current, high sink or ambient temp. or possible gradual increase in electrical and thermal contact resistance (see 1.5.4.) between metal parts.
			1.1.2. H_2O-to-H_2 leak caused by failure of H_2O cell gasket or H_2O port gasket.		1.1.2. A dual bead will be incorporated in the gasket design to provide a redundant seal.
			1.1.3. Excessive condensation in H_2 enclosure caused by low sink temp. or high cell temp.		1.1.3. High cell temp. same as 1.1.1. low sink temp. Not caused by electrolysis unit.
			1.1.4. O_2-to-H_2 leak (if $PO_2 > PH_2$) caused by failure of O_2 cell gasket or O_2 port gasket. O_2 combines with H_2 on cathode to form water.		1.1.4. Same as 1.1.2.
		1.2 Liquid water entrainment in O_2 discharge.	1.2.1. Excessive decay in O_2 cell pressure during standby mode caused by O_2 cell press. switch malfunction (double failure).	Premature expenditure of O_2 desiccant, faulty thruster performance, reduced mission life.	1.2.1. Water formed on O_2 electrode (anode) in excess of electrolysis rate, will tend to be pumped by electro-osmosis to H_2 electrode (cathode) and H_2 cavity.
			1.2.2. H_2O-to-O_2 leak caused by failure of O_2 cell gasket or H_2O cell gasket.		1.2.2. Same as 1.1.2.
			1.2.3. Excessive condensation in O_2 manifold or outlet line caused by low sink temp. or high cell temp.		1.2.3. Same as 1.1.3.
			1.2.4. H_2-to-O_2 leak (if $PH_2 > PO_2$) caused by failure or O_2 cell gasket or O_2 port gasket. H_2 combines with O_2 on anode to form water.		1.2.4. Same as 1.1.2.
		1.3 Admixed O_2 in H_2 discharge.	1.3.1. O_2-to-H_2 leak (if $PO_2 > PH_2$) which bypasses catalyst on cathode caused by double failure of O_2 cell gasket or O_2 port gasket or O_2 gas dissolved in H_2O feed (minimal).	Some loss in thruster performance for low O_2 concentrations if not consumed by catalytic reactor. Gross leak could lead to flammable mixture formed in H_2 enclosure and eventually in H_2 storage tank.	1.3.1. Same as 1.1.2. Installation of a check valve in O_2 out line would prevent backflow of O_2 from O_2 tank to H_2 tank. Small O_2 cell trapped in H_2 enclosure head. Volume would not yield a flammable mixture.
		1.4 Admixed H_2 in O_2 discharge.	1.4.1. H_2-to-O_2 leak (if $PH_2 > PO_2$ which bypasses catalyst on anode caused by double failure of O_2 port gasket.	Some loss in thruster performance for low H_2 concentrations, if not consumed by catalytic reactor. Gross leak could lead to flammable mixture formed in O_2 cell manifold and eventually in O_2 storage tank.	1.4.1. Same as 1.1.2. O_2 pressurization of water tank would keep O_2 pressure normally greater than H_2 pressure which would preclude this failure mode. Installation of check valve in H_2 out line would prevent backflow of H_2 from H_2 tank to O_2 tank. Volume of H_2 trapped in H_2 enclosure head would not yield a flammable mixture in O_2 storage tank at 70PSID max initial differential before seal failure.

TABLE 26 (CONT')

Failure Modes and Effects Analysis

Item	Component	Assumed Failure	Probable Failure Mechanism	Effect on Water Electrolysis Unit or Satellite Propulsion System	Remarks
		1.5 Reduced gas generation rate.	1.5.1 External H_2 leak thru fitting or O-ring seals in enclosure head or external O_2 leak at fitting.	Reduced performance of satellite propulsion system and mission life.	1.5.1 Dual O-rings will be provided in enclosure head and fittings as redundant seals.
			1.5.2 Water starvation of one or more cells caused by gas blockage of or contamination of H_2O membrane, or, external H_2O leak at fitting.		1.5.2 Any gas blockage is expected to be only temporary and self-clearing with $P_{H_2O} > P_{H_2}$. Same as 1.5.1.
			1.5.3 Short circuit of one or more cells.		1.5.3 Except for effects of local heat generation, short circuit should not interfere with operation of adjacent cells. Short circuit detected during acceptance test, thereafter improbable.
			1.5.4 High electrical impedance caused by cell SPE contamination, loss of cell contact pressure, oxide film on metal parts.		1.5.4 All effects should be very gradual. Selection and verification of materials under current usage show no degradation in performance after one year's continuous operation.

TABLE 26 (CONT')

Failure Modes and Effects Analysis

Item	Component	Assumed Failure Mode	Probable Failure Mechanism	Effect on Water Electrolysis Unit or Satellite Propulsion System	Remarks
16	O_2 Cell Pressure Switch	2.1 Switch contacts remain closed.	2.1.1 Shorted contacts.	Continuous gap generation by electrolysis unit in standby mode, resulting in overpressure of electrolysis unit.	O_2 cell pressure would be limited to a value where parasitic consumption of O_2 by diffusion equals electrolysis rate. Probably less than 2X normal. Check valve in place of O_2 solenoid valve in O_2 outlet line is recommended for limiting O_2 cell pressure.
		2.2 Switch contacts remain open.	2.2.1 Broken linkage or contacts.	Excessive O_2 cell pressure decay during standby mode, resulting in excessive H_2O formation on O_2 side and possible H_2 takeover of O_2 trapped volume.	2.2.1 Redundant pressure switch recommended.
17	Power Conditioner	3.1 Inability to regulate to required value (over high current limit).	Electronic component failure.	3.1 Dependent on mode of operation High Power Mode Excessive water electrolysis operating temp., causing possible H_2O entrainment in H_2 discharge. Excessive power drain on system. Low Power Mode Excessive power drain. Standby Mode Increased cycling frequency of electrolysis unit. Possible premature cyclic failure of O_2 cell pressure switch.	3.1 Electronic component redundancy required as necessary to eliminate single point failures.
		3.2 Inability to regulate current to required value(under low current limit).	Electronic component failure.	3.2 Dependent on mode of operation High Power Mode Excessive time to pump up O_2 and H_2 storage tanks. Probable H_2O entrainment in H_2 discharge. Impaired mission capability. Low Power Mode Possible H_2O entrainment in H_2 discharge. Standby Mode	3.2 Same as 3.1.
		3.3 Zero current output (any mode).	Electronic component failure.	3.3 Gas generation by electrolysis unit, depletion of O_2 and H_2 in storage tanks. Reduced mission life.	3.3 Same as 3.1.
		3.4 Uncontrollable high current output.	Electronic component failure.	3.4 Reduced mission life.	3.4 Same as 3.1. Automatic system protection to remove power conditioner from satellite power supply.

smaller than the tank volumes, any gas mixtures admitted to the storage tanks would be outside the flammability limit. During subsequent sustained electrolysis operation, however, assuming a gross leak caused by failure of the redundant seal, the electrolysis unit would deliver mixed oxygen and hydrogen to the gas storage tank having the lowest pressure. Measuring the temperature increase of a catalytic reactor installed in each gas output line from the electrolysis unit would detect the presence of a gross leak and extensive mixing such that electrolysis operation would be discontinued to preclude an unsafe condition during ground test or attended unit operation.

Within the power conditioner electronics, the elimination of single-point failure mechanisms can be accomplished in flightweight hardware through redundancy of components, subfunction or overall function. The particular method chosen will depend on size, weight and/or power penalty associated with each case involved. Overall simplicity of approach would suggest overall functional redundancy as opposed to the other methods mentioned. In this case, the entire power conditioner function would be duplicated and utilized on a priority basis. Detailed analysis may show, however, that this simplified approach may require significantly greater size and weight than a more subtle subcomponent of subfunction redundancy.

A failure rate of 0.68×10^{-6} failures/hour-cell has been estimated for the electrolysis unit. This is based on fuel cell experience from the Gemini and Biosatellite programs, while the failure rate for the power conditioner is estimated at 5×10^{-6}/hr.

b. Failure Modes and Effects Analysis (Engine)

A detailed failure modes and effects analysis given in Table 27 was made for the engine configuration and associated components. As readily seen, the probable loss or failure of any individual component will result in a subsystem failure, although the probability of such a loss is quite negligible, in most cases.

(1) Thruster Valves

The valves are one of the most critical items for both thrusters since they must provide a positive seal at all times to prevent loss of propellant. As shown in the FMEA, the major items which directly involve reliability are the number of cycles and propellant system cleanliness. The predicted reliability for the valves as experienced by Marquardt is shown on Figure 112.

(2) Spark Ignition

The spark igniter system reliability is presented in Figure 113. The predictions are based on typical direct current design based on a 50 ms operation/start. As described earlier, the actual igniter operation based on the test conducted is about 20 ms; therefore, the number os struts for the abscissa should be multiplied by 2.5 to correct for this variation. Based on the requirements as obtained from the mission

TABLE 27. FAILURE MODES AND EFFECTS ANALYSIS

FAILURE MODE AND EFFECT ANALYSIS — Rocketdyne — Subsystem – Bipropellant O_2/H_2 Thruster — PAGE 1 OF 3

ITEM NAME AND PART NUMBER	BLOCK DIAGRAM REF. NO.	FUNCTION	ASSUMED FAILURE	POSSIBLE CAUSES	EFFECTS AND CONSEQUENCES	METHOD OF DETECTION	INHERENT COMPENSATING PROVISIONS	PROB. OF FAILURE	FAILURE CLASS.
Solenoid Valve	4	Permit propellant flow to injector when coils are energized to open and cease flow when coils are de-energized to closed valve	Failure to open	1. Cold welding of poppet and seat. 2. Electrical open circuit. 3. Electrical short circuit. 4. Contamination entrapped between the armature and stop or between armature and valve body. 5. Structural failure of valve. 6. Structural failure of armature tip. 7. Broken spring causing binding of armature.	Loss of Subsystem Valve failure to open would prevent firing of the engine.	1. Flow sensing device in the propellant line. 2. Chamber pressure transducer. 3. Sensing of anticipated result of expected thrust (i.e. ΔV or reaction control).	Adequate design margins and carefully controlled assembly and processing procedures		
			Failure to close (seat leakage)	1. Contamination entrapped between the poppet and seat or between armature and valve body (sticking the armature). 2. Receded or worn teflon seat such that seal is not effected 360°. Radiation exposure, hard vacuum exposure, and long time compressive loads.)	Probable Loss of Subsystem Depletion of propellant supply. Ignition characteristics may be affected resulting in structural damage.	1. Sensitive flow sensing device in the propellant line. 2. Monitoring of propellant supply.	Adequate contamination control during fabrication and during engine usage.		
			External leakage	Structural failure valve housing on joints at inlet and attachment to injector assembly	Possible Loss of Subsystem Loss of propellant performance degradation	Chamber pressure and temperature transducers could detect significant changes in propellant flow rate or distribution.	Adequate design margins and Quality Control of materials welded inlet and valve attachment would decrease probability of this failure mode.		
Injector Assembly	5	Inject and meter the flow of propellants to effect stable and efficient combustion.	Reduced propellant flow rate or improper flow distribution.	1. Entrapped contamination in the flow passages and/or in the injection ports. 2. External leakage.	Possible Loss of Subsystem Degradation of engine performance. Improper flow distribution may cause unstable burning or excessive heating. Structural damage or combustor burn out may result.	Chamber pressure and temperature transducers could detect significant changes in propellant flow rate or distribution.	Adequate contamination control during fabrication and during engine usage.		

TABLE 27 (CONT')

FAILURE MODE AND EFFECT ANALYSIS — Marquardt — Subsystem – Bipropellant O_2/H_2 Thrustor — PAGE 2 OF 3

ITEM NAME AND PART NUMBER	BLOCK DIAGRAM REF. NO.	FUNCTION	ASSUMED FAILURE	POSSIBLE CAUSES	EFFECTS AND CONSEQUENCES	METHOD OF DETECTION	INHERENT COMPENSATING PROVISIONS	PROB. OF FAILURE	FAILURE CLASS.
		Provide the structural attach surfaces for mounting the valves and combustor and for mounting the engine to the intended system.	Structural failure	Material defects, dimensional discrepancies or fatigue failure.	Probable Loss of Subsystem Component or engine detachment and/or external leakage could result.	1. Chamber pressure transducers. 2. Sensing of anticipated result of expected thrust.	Adequate design margins and Quality Control of materials.		
Combustion Chamber	6	Contains and directs the hot gases developed by combustion of the propellants to produce thrust in a specified direction.	Burn out of the combustion chamber.	1. Defective coating. 2. Repeated cycles of sublimation during combustion chamber cool down at space vacuum conditions. 3. Oxidation and erosion during hot gas firing. 4. Spalling the combustor inside surface or complete wall penetration due to meteroid impact.	Loss of Subsystem Burn out of the combustion chamber would result in performance degradation and loss of thrust vector direction. Possible hot gas impingement on adjacent vehicle hardware may be a significant failure effect.	1. Chamber pressure transducer. 2. Sensing of anticipated result of expected thrust.	Adequate control of coating process and adequate design margin for combustor life in space burning.		
			Structural failure of the combustor	1. Defective material on dimensional discrepancy. 2. Inadvertent damage from external contact.	Loss of Subsystem Inability to generate thrust	1. Chamber pressure transducer. 2. Sensing of anticipated result of expected thrust.	Adequate design margin and adequate Quality Control of materials and critical dimensions.		
Combustor Attach Hardware	8	Provides attachment and sealing between the injector assembly and the combustion chamber.	Structural failure	Defective material or dimensional discrepancy	Possible Loss of Subsystem Hot gas leakage. Possible erosion of seal joint. Possible complete separation of combustor from engine.	Same as above.	Same as above.		
Spark Igniter System	7	Provide ignition spark to combustion chamber as commanded. Ignition spark must be timed to assure combustion ignition then cease to prevent excessive power drain.	1. No spark	1. Circuit component failures. 2. Spark plug failure	Loss of Subsystem Inability to generate thrust.	1. Current or voltage sensing device in output circuit of spark igniter system. 2. Chamber pressure transducer. 3. Sensing of anticipated result of expected thrust.	Use high reliability components with adequate derating to assure high reliability. Spark plug may be a limited life component and require periodic replacement.		
			2. Weak spark	Same as above.	2. Possible Loss of Subsystem Weak spark may not ignite propellants.				

TMC A1771

TABLE 27 (CONT')

FAILURE MODE AND EFFECT ANALYSIS — Marquardt Subsystem — Bipropellant O_2/H_2 Thrustor — PAGE 3 OF 3

ITEM NAME AND PART NUMBER	BLOCK DIAGRAM REF. NO.	FUNCTION	ASSUMED FAILURE	POSSIBLE CAUSES	EFFECTS AND CONSEQUENCES	METHOD OF DETECTION	INHERENT COMPENSATING PROVISIONS	PROB. OF FAILURE	FAILURE CLASS.
			4. Sparks occur too soon.	Component failure or drift in timing delay circuit.	4. Possible Loss of Subsystem Early spark may not ignite propellants.				
			5. Sparks occur too late.	Component failure or drift in timing delay circuit.	5. Possible Loss of Subsystem Late ignition will result in low engine performance. Delayed ignition may cause hard start of engine with possible structural damage.				
			6. Sparks do not cease as required.	Component failure in cutoff circuit.	6. Possible Loss of Subsystem Excessive power drain and possible premature failure of power supply or igniter circuit components.				

TMC A1771

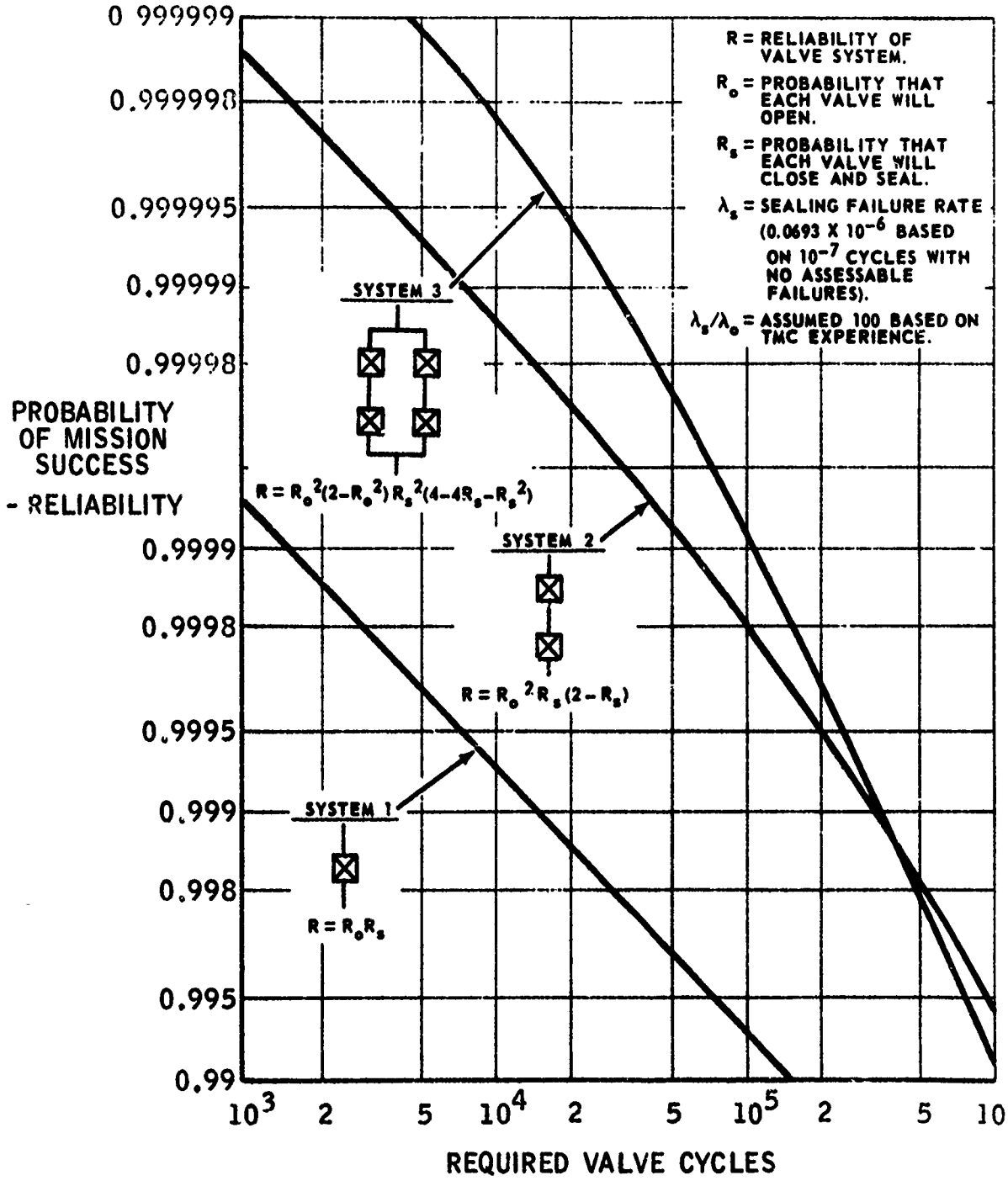

FIGURE 112. ENGINE VALVE RELIABILITY (50% CONFIDENCE LEVEL)

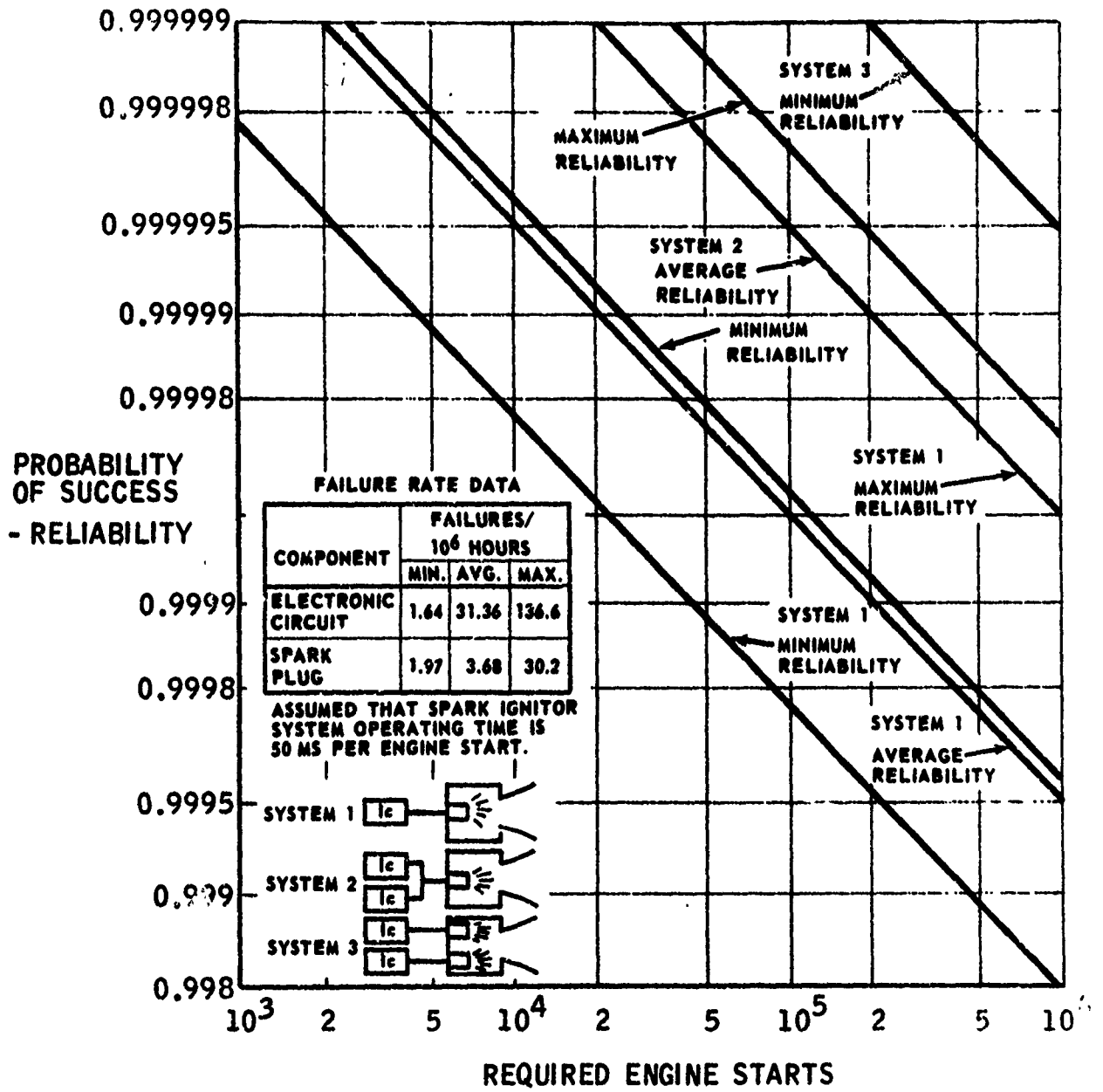

FIGURE 113. SPARK IGNITER SYSTEM RELIABILITY PREDICTION

analysis, the reliability of a single spark/igniter circuit for the 0.1-pound engine is 0.996 and 0.99985 for the 5-pound thrust engine.

(3) Thrustor Combustion Chamber

Because of their high performance capabilities, the GO_2/GH_2 thrusters present a severe thermal environment for the thrust chamber. However, due to the high temperature capabilities of $MoSi_2$ coated molybdenum, large margins of life are available for both the 5-pound and 0.1-pound thrusters. The projected life for the engines, based on a 2500°F wall temperature, is more than 40 hours as compared with the 5-10-hour life requirement.

c. Failure Modes and Effects Analysis System

A failure modes and effects analysis was not conducted on the actual feed system since the exact configuration will not be determined. Rather, an evaluation of the various system components was accomplished, which will provide the guidelines for the eventual design of the system wherein there is no single-point failure.

The following paragraphs present brief discussions of the reliability predictions derived for each basic system component. Actual data was utilized to the maximum extent possible, and in the absence of data conservative estimates were obtained from the failure rate sources listed below.

AVCO - AVCO Corporation Reliability Engineering Data Series, "Failure Rates" dated April 1962

RADC - Rome Air Development Center Report No. RADC-TR-66-828, "RADC Unanalyzed Nonelectronic Part Failure Rate Data" dated December 1966

GAEC - Grumman Aircraft Engineering Corporation, Report No. LED-550-28, "RCS Reliability Ground Rules and Estimates for Success Path Study" dated 25 May 1964

TMC - TMC Report No. RE-3036/3037-6-3, "Reliability Analysis Report for the 100 lb and 22 lb Thrust Engines" dated September 1967.

(1) Structural Elements

All of the system components must maintain their structural integrity while operating within the specified environmental limits; however, the system lines and fittings, and the pressurant tanks perform only as structures and have no nonstructural failure modes (Note: line blockage is an exception; however, the probability of occurrence for this mode is considered negligible). Therefore, the

reliabilities of these components are a function of their design strengths and the stresses to which they are subjected. Stress analyses can define the required strengths for each item, and proper application of inspection techniques can remove defective items prior to use. Consequently, a structural item failure can, in theory, result only if the item is subjected to stresses greater than predicted. In order to reduce the probabilities of such failures, the actual design strength is established at 1.5 times the greatest predicted stress, or higher. Structural item failure probabilities are, therefore, considered to be negligible. However, this assumption is based on the supposition that detailed stress analyses are performed and documented, that the adequacy of inspection methods is verified and that the item is subjected to verification or mission simulation tests prior to the manufacturing of production units.

(2) Plumbing Connections

Although the system lines and fittings are considered as structural elements only, the line determinations and fitting connections do represent potential leak points; hence, must be considered as reliability significant items. The representative failure rate for welded connections obtained from the RADC failure rate source is 0.0023×10^{-6}. A corresponding estimate for brazed connections indicates a failure rate of 0.001×10^{-6}. The connections must contain pressurant and propellant for the entire mission; hence, the applicable operating time is 7 years, or 60,320 hours. The reliabilities for welded and brazed connections are, therefore,

$$\text{Welded:} \quad R_{plc} = e^{-(0.0023 \times 10^{-6})(60,320)} = 0.999861$$

$$\text{Brazed:} \quad R_{plc} = e^{-(0.001 \times 10^{-6})(60,320)} = 0.9999397$$

(3) Check Valve Assembly

The check valve assembly is designed to open at a pressure differential; hence, there is considerable margin of safety in this application, and the estimated probability of failure to open is negligible; i.e., not reliability significant.

(4) Fill Vent Valves

During the mission, the fill vent valves affect system operation only as potential leak points. However, the valves have redundant sealing capability with respect to internal and external leakage. If the probability of leakage is considered equivalent to leakage through a welded connection, then with the redundancy the estimated reliability for one year is > 0.99999999. Therefore, the vill vent valves are not considered to be reliability significant for this analysis.

(5) Burst Disc Relief Valve Assembly

The burst disc relief valve assembly does not affect system reliability during nominal operation unless the disc bursts prematurely, in which case the relief valve represents a likely leakage point.

(6) Filter

The generic failure rate listed in the AVCO source for propellant filters is 0.3×10^{-6}. Since the filter functions only when propellant is flowing; i.e., when engines are firing, the estimated maximum operating requirement for the filter is five hours. The predicted filter reliability is, therefore,

$$R_f = e^{-5 \times 0.3 \times 10^{-6}} = e^{-0.0000015} = 0.9999985$$

(7) Solenoid Actuated Valves

The demonstrated failure rate at Marquardt for latching or coaxial valves is 3.184×10^{-6} cycle. The corresponding predicted reliability is, therefore,

$$R_{sv} = e^{-1 \times 3.184 \times 10^{-6}} = 0.999996816$$

SECTION VI

CONCLUSIONS

The results of the Water Electrolysis Satellite Propulsion System program have demonstrated that a separated gas electrolysis unit which generates gaseous oxygen and hydrogen for use in rocket engines is a safe, cost effective and high performing concept.

The objective of this program, which was to demonstrate the feasibility and capabilities of such a system to meet Air Force objectives, was satisfied.

1. A water electrolysis unit, manufactured by the General Electric Company of Lynn, Massachusetts was tested both at the manufacturer's facility as a separate unit and at Marquardt as a component of the supply system. The results of the tests show that the projected performance of the unit was realized and that no significant operational anomalies were encountered.

2. A propellant supply system consisting of all those components necessary to generate and store the propellants prior to introduction into the rocket engines was fabricated and tested. The tests indicated that the three different types of supply systems - blowdown, repressurized, blowdown, and oxygen repressurized - would supply adequate propellant to meet the specified mission objectives.

3. The 5.0 lb thrust GO_2/GH_2 engine which attained 69,000 firings in a boilerplate version prior to failure demonstrated its capabilities to provide high specific impulse, repeatable impulse bits and 100% ignition reliability at a 3 to 1 blowdown ratio.

4. The 0.1 lb thrust GO_2/GH_2 engine accumulated 150,000 ignitions and the performance data indicated a high specific impulse, repeatable impulse bit, and 100% ignition reliability at a 3 to 1 blowdown ratio.

5. For the mission/system analysis and flightweight system design studies conducted, the water electrolysis system was 27% lighter than the monopropellant system and 6% lighter than the earth storable bipropellant system.

SECTION VII

RECOMMENDATIONS

The following recommendations are based on the premise that the water electrolysis satellite propulsion system will provide the most cost effective and efficient system for use on long life Air Force space missions and thus should be flight tested in the near future.

1. The propellant supply system fabricated during this program should be subjected to the equivalent of 7 years of testing (100,000 lb-sec of equivalent propellant) to demonstrate its reliability.

2. Flightweight 5.0 lb and 0.1 lb thrusters should be developed and tested to the maximum mission requirements.

3. The development of a flightweight water electrolysis unit should be initiated, as soon as the results of the tests conducted on the propellant supply system indicate that the 7 year mission can be met.

4. A small water electrolysis satellite propulsion system consisting of a 0.1 lb/day electrolysis unit and a 0.1 lb_f thrust engine should be flight tested upon completion of the above tasks.

APPENDIX A

ELECTROLYSIS SYSTEM DESCRIPTION AND OPERATION

APPENDIX A

ELECTROLYSIS SYSTEM DESCRIPTION AND OPERATION

1. ELECTROLYSIS SYSTEM DETAILED DESCRIPTION

The system, shown schematically in Figure 114 is assembled on a frame structure and can be transported within the test area by fork lift. Its outer dimensions are about 72 x 34 x 60 inches.

The system has many valves and alternate flow paths provided for ground testing which would not be included in a flight system. The system components are listed in Table 28 and described below.

a. Water Tank

The water tank shown in Figure 115was made by Capital Westward using 321 stainless steel. The cylindrical portion has an inside diameter of 24 inches and a wall thickness of 0.250 inch. The tank was hydrostatically tested at 539 psig for one-half hour with no evidence of deformation or leakage. The volume, including end domes, is 15 ft^3, and the length is about 65 inches. The water tank rests on the bottom plate of the frame. The water exit line is in the bottom tank plug which fills a ~inch diameter port. The tank was cleaned by Astro Park Corp. before being installed in the system. The cleaning steps were as follows:

(1) Vapor degrease

(2) Mild alkaline detergent rinse

(3) Water rinse

(4) Pickle with 15% nitric acid/2% hydrofluoric acid mixture

(5) Water rinse

(6) Passivate with 35% nitric acid

(7) Water rinse

(8) Rinse with deionized water and measurement of particles. The particle count during final rinse was 2 particles of 100 micron collected in 500 cc of water.

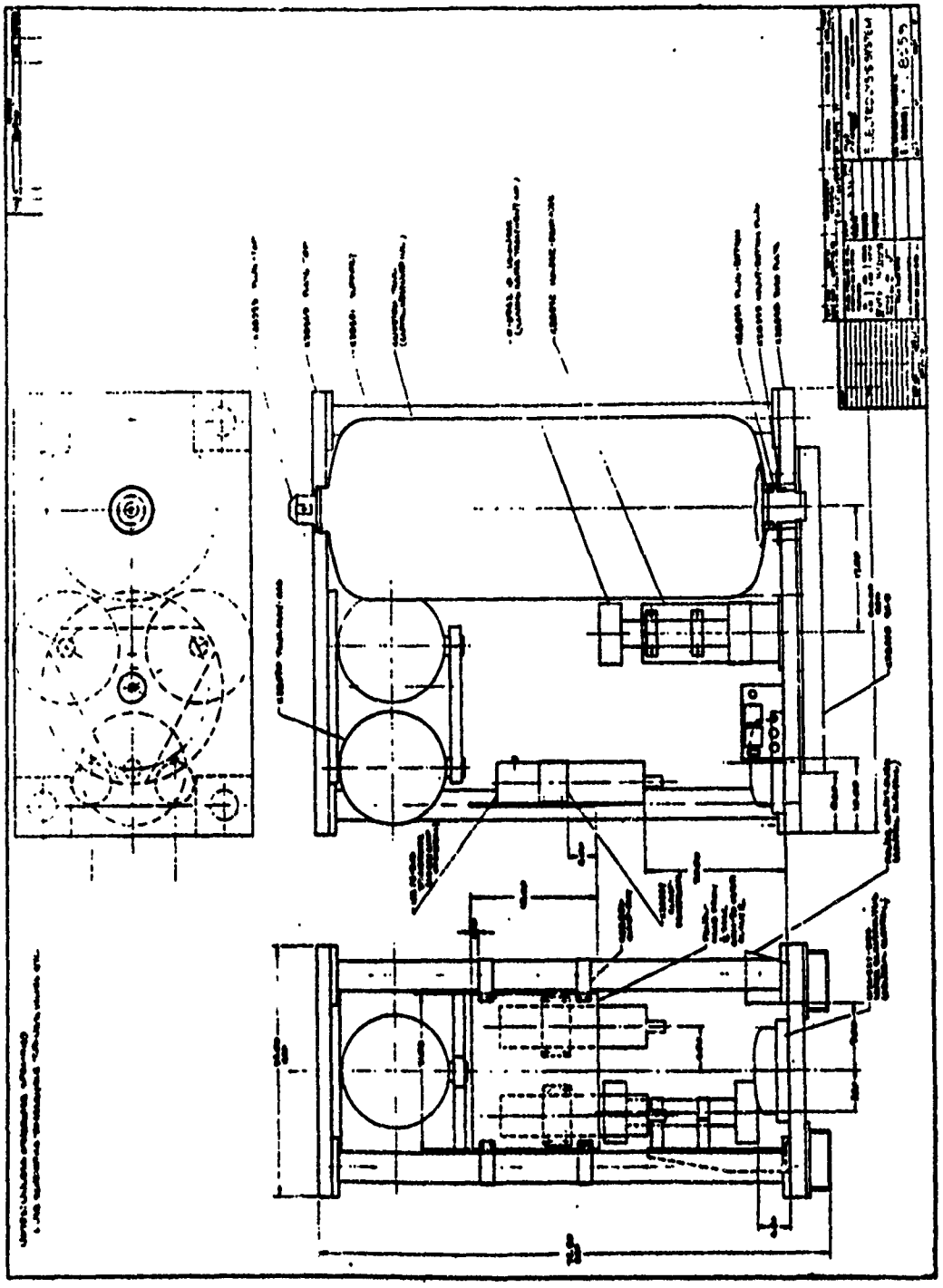

FIGURE 114. ELECTROLYSIS SYSTEM COMPONENT ARRANGMENT

TABLE 28

GROUND TEST SYSTEM COMPONENTS

Component	Manufacturer	Model No.	Description
Water Tank	Capital Westward	CW05706-2	321 S.S., 15 ft^3
Gas Propellant Tanks	Capital Westward	CW05706-1	321 S.S., 1 ft^3
Conductivity Cells	Balsbaugh	900-0.01T-HP	Ti/Pd electrode, 0-18 megohm
Deionizer	Illinois Water Treatment	F-2942.1D	0.06 ft^3 of WT NR-6 resin
Water Filter FW	Millipore Corp.	XX45-047-00	0.45 micron
Desiccant Cartridges	Air Dry Corp.	G-4072	5 lbs Type 4A molecular sieve
Humidity Indicator	Air Dry Corp.	7275	Color change, dew pt. -70° to 60° F
Catalyst Bed	Englehard Industries	Deoxo D-10-2500	Pd alloy catalyst
Water Level Gage	I.T.T. Barton	227	0-50 in. H_2O, 500 psi, 316 S.S.
Hand Valves			
H-1, 2, 10	Nupro	SS-4UW	2000 psi
H-9, 15	Nupro	SS-4BMW	300 psi, metering valve
H-3, 4, 5, 6, 7, 8, 11, 12, 13, 14	Nupro	SS-4BW	300 psi
Solenoid Valves			
S-1	Marquardt	X28050	Latch valve
S-2, 3	Marquardt	R-4D	
S-4, 5, 6, 7, 8	Skinner	V52HDA12501	2500 psi
Check Valves			
C-1, 2, 3	Circle Seal	233T1-4TT-5	5 psi ΔP
C-4	Circle Seal	233T1-4TT-20	20 psi ΔP
Pressure Switches			
PS-1, 2, 3, 5	Meletron	302-6SS-35VA	Single bourdon tube
PS-4	Meletron	542-655-49B	ΔP, 2 bourdon tubes
Burst Discs	Calmec	S3-10	300 psi ΔP
Gas Filters, FG-1, 2, 3, 4	Western	26-1-16510-5	5 micron nom., 18 mocron abs.

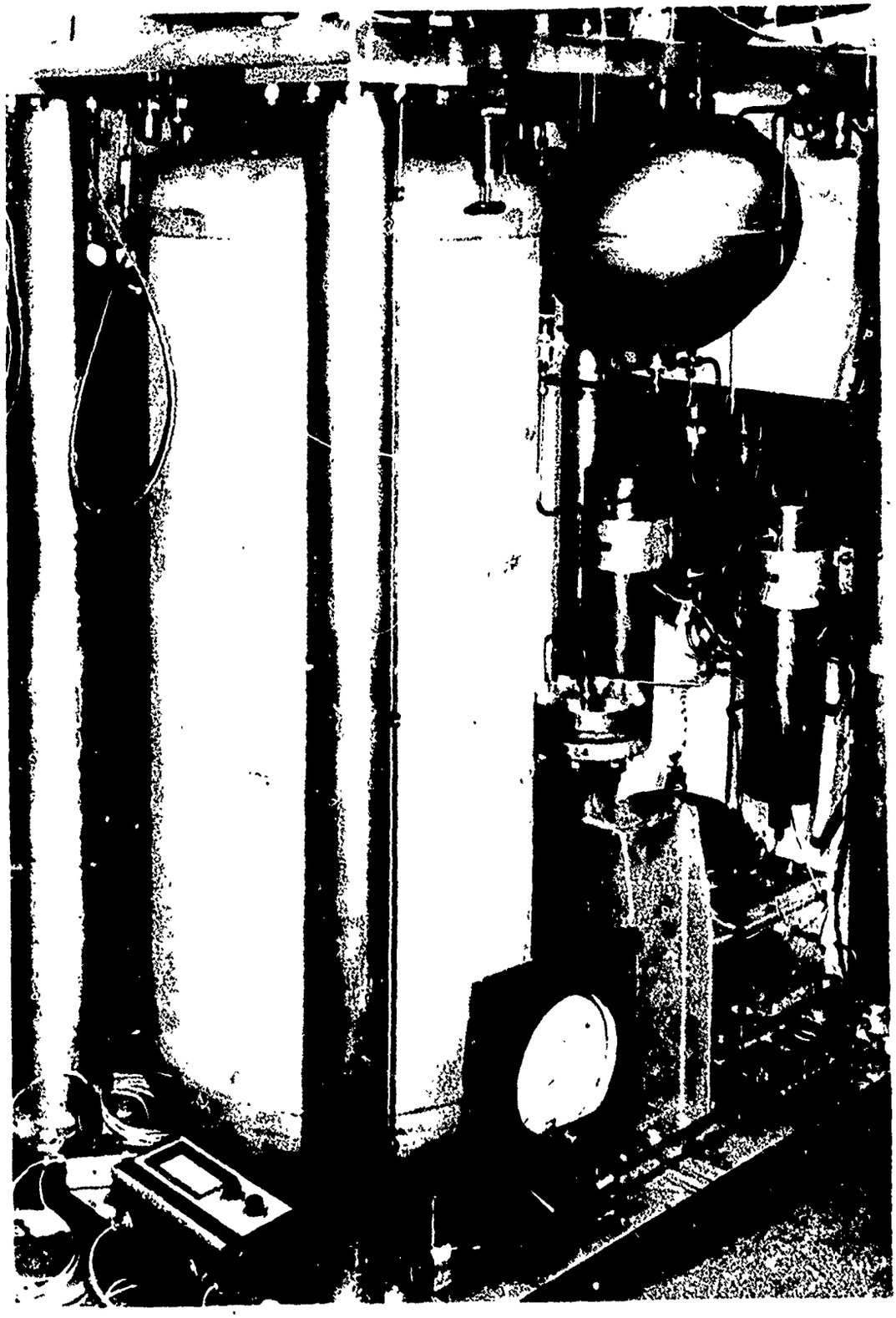

NEG. 72-228-3

FIGURE 115. WATER TANK --- GROUND TEST SYSTEM

(9) Dry tank

(10) Install end plugs and pressurize tank with 5 psig N_2 for shipment to Marquardt.

b. Conductivity Cells

The two conductivity cells are in the water system to measure electrical resistance of the water coming out of the water tank and downstream after passing through the deionizer. The cells were made by Balsbaugh, Model No. 900-.01T-HP, and are designed to withstand 2000 psi and 250°F.

The conductivity cell electrode is made of titanium/palladium. The cell is inserted into a 316 stainless steel holder so that the entering water flows parallel to the electrode. The 316 stainless steel holder so that the entering water flows parallel to the electrode. The electrical resistance of the cells is read visually on a Balsbaugh Monitor No. 900 M-18M-R1 (bottom left, Figure 115).

c. Deionizer

The deionizer shown on the right side of Figure 116 was designed and fabricated by Illinois Water Treatment Co. to meet requirements specified by Marquardt. These requirements included the capability to deionize 300 pounds of water over a period of two years to an outlet resistance of 2 megohms, assuming that 8 megohm water is initially stored in the stainless stell tank. The deionizer contains 0.06 ft^3 of WT NR-6 mixed resins within the steel case which is coated internally with polypropylene to avoid corrosion of the steel case by the resin. A 50 mesh saran screen filter is located on inlet and outlet. The only metal contacted by the water is the 316 stainless end plates and swagelok fittings.

An extensive survey of organizations involved in processing and use of deionized water was made to determine the materials which could be used in the water system while holding the 2 megohm electrical resistance for one year as specified by G.E.

No clear indication of the suitability of stainless steel was obtained from this survey. Therefore, the deionizer unit was included as recommended by General Electric Co. to provide a means of maintaining satisfactorily high electrical resistance of the water if found necessary. However, subsequent water storage tests at Marquardt indicated that water storage in a clean stainless steel system will probably be satisfactory without use of the deionizer. The deionizer can be bypassed in the water flow path, with valves allowing diversion of the water through the deionizer if found necessary.

d. Water Filter

A Millipore Corp. filter, XX45-047-00, is placed in the water system downstream of the deionizer to prevent any particulate matter from reaching the latch

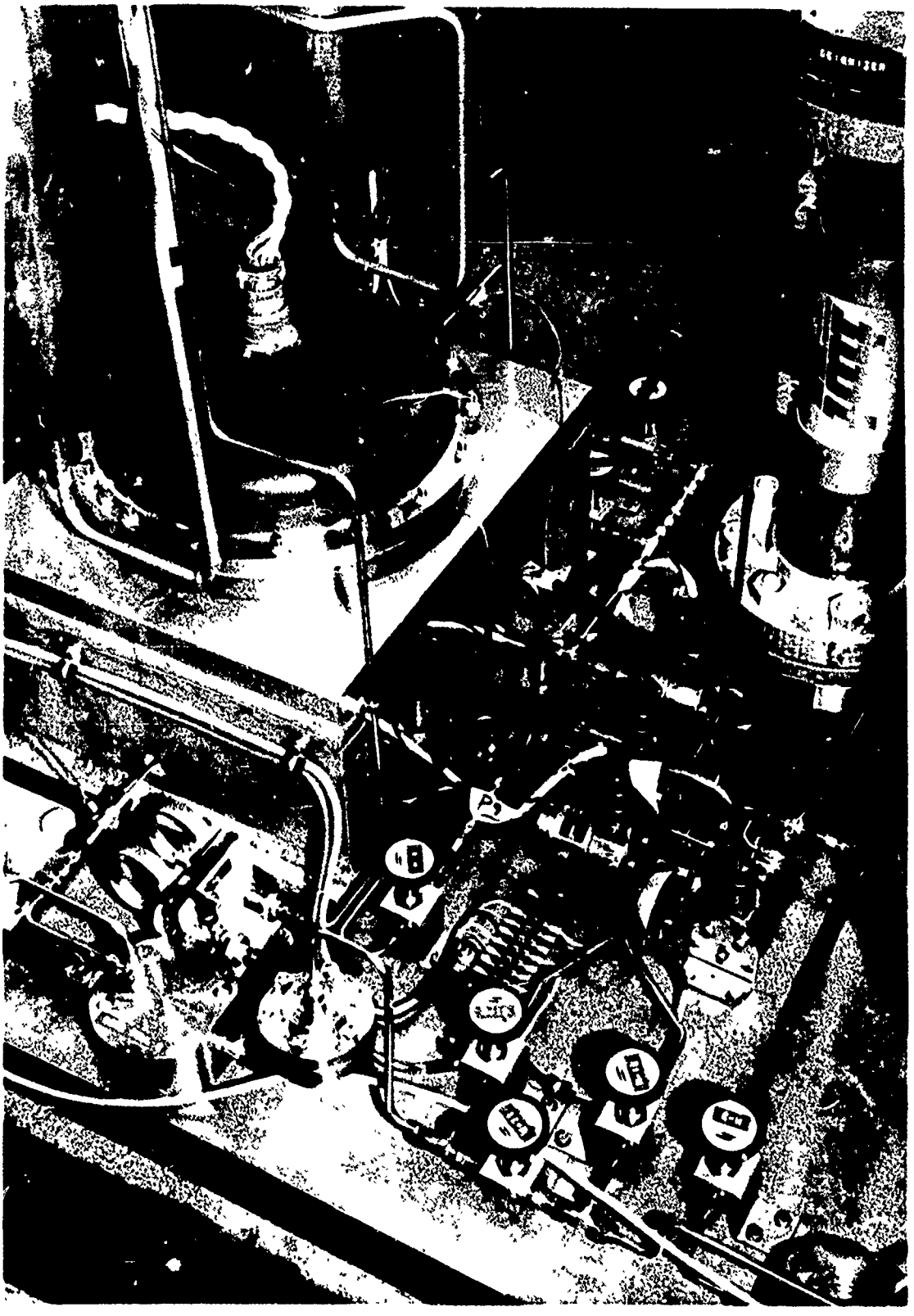

NEG. 72-226-1

FIGURE 116. ASSEMBLY OF GROUND TEST COMPONENTS

valve S-1 which controls water supply to the electrolysis unit. The filter body is made of 316 stainless steel, as are the support and back support screens. A 0.45-micron filter element will be used in the filter.

e. Desiccant

A desiccant unit made by Air Dry Corp. is placed in both the oxygen and hydrogen lines near the exits from the electrolysis unit, as shown in Figure 117. The steel case, Model NR25-5, has a working pressure of 250 psig. A replaceable cartridge, Model G-4072, containing five pounds of Linde, Type 4A, molecular sieve pellets is inserted into the case. The cartridge contains a 10-micron stainless steel woven filter. The molecular sieve pellets can absorb about 20 percent of their weight of water vapor while maintaining a relative humidity of about 8%. As the gas output relative humidity rises, the water absorbing capabilities of the molecular sieve will be exceeded by silica gel or activated alumina. Therefore, a minimum weight desiccant cartridge design would depend on the required relative humidity and temperature of hydrogen or oxygen and might contain two types of desiccants in series, perhaps using activated alumina to absorb most of the water, with the final desiccation to a very low relative humidity provided by the molecular sieve.

During the electrolysis of 300 pounds of water, about 0.8 pounds of water vapor would be transported by the hydrogen if the electrolysis cell were operating at 80°F, rising to 2.69 pounds of water for a cell temperature of 120°F. The corresponding weights of water vapor in the oxygen would be 1.2 pounds at 80°F and 4.02 pounds at 120°F. The required relative humidity will depend on the satellite thermal environment and cannot be specified at the present time. Data on the change of relative humidity of the hydrogen and oxygen will be collected during the system life testing to support the future analysis and design of a flightweight desiccant.

f. Humidity of Gaseous Propellants

The relative humidity of the hydrogen and oxygen generated by the electrolysis unit and then dried by the desiccants will be determined by passing the gases through an Air Dry Corp. Model No. 7275 humidity indicator. The relative humidity is indicated by observing the color change in an indicating desiccant within a 3/4-inch diameter transparent tube. Various models are available to measure dew points from -70°F to 60°F. Either hydrogen, through solenoid valve S-6, or oxygen, through solenoid valve S-7, can be flowed through the humidity indicator and catalyst bed in the ground test system and then vented to atmosphere.

f. Hydrogen/Oxygen Gas Impurities

An Englehard Industries Deoxo gas purifier, Model D-10-2500, will be used to detect the presence of any trace amounts of hydrogen in the oxygen system or oxygen in the hydrogen system. The Deoxo unit is a palladium alloy catalyst which causes chemical reaction between the gases at room temperature. The concentration of impurity is proportional to the measured temperature rise of the gas flowing through

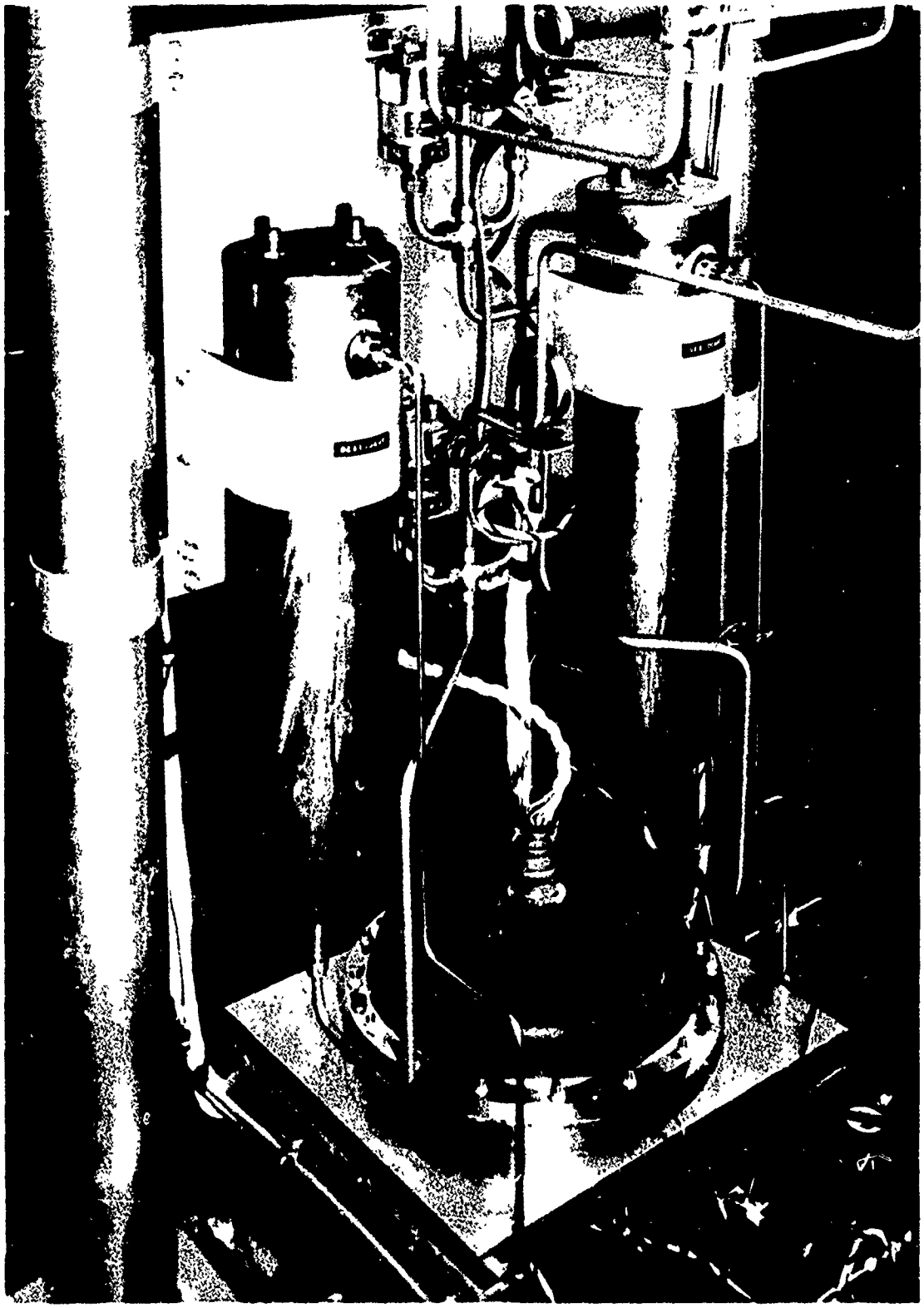

NEG. 72-226-2

FIGURE 117. DESICCANT CYLINDERS AND ELECTROLYSIS UNIT IN GROUND TEST SYSTEM

the catalyst bed. The chemical reaction forms water vapor and a second indication of the amount of impurities could be obtained by subsequently passing the gas through the humidity indicator and comparing the relative humidity with that of the gas when by-passing the catalyst bed.

h. Gaseous Propellant Plenum Tasks

Three identical 1-ft^3 tanks made by Capital Westward, are used as gaseous propellant plenum tanks. Two tanks are used for hydrogen and one is used for oxygen, corresponding to the 2:1 volume ratio of hydrogen to oxygen produced by the electrolysis unit. The tanks were hydrostatically tested to 650 psig without evidence of leakage or deformation.

i. Deionized Water

The water supply for the electrolysis unit should be uncontaminated by any chemical or particulate matter, and dissolved ions of metals or minerals should not be present. The General Electric Co. has specified the electrical resistance requirement for the water as 2 megohm. The need for ultra pure water is dictated by the possibility that the SPE, an ion exchange medium, could be poisoned by absorbing ions of contaminants in the water. The General Electric Co. does not have any data on the degree of SPE degradation which would occur for any level of ion concentration, cell temperature, or water mass electrolyzed. However, the goal of 2 megohms is being maintained for the system life testing, subject to any modifications approved by G. E.

Ultra pure water supplied by Arrowhead Puritas was used. The water is treated by reverse osmosis, then passed through a deionization resin bed, passes through a 25-micron filter, receives ultraviolet sterilization, passes through an 0.45-micron filter, and is loaded in five-gallon plastic containers closed to the atmosphere. Arrowhead Puritas expected the electrical resistance of the water to be at least 8 megohms, but tests at Marquardt have measured about 1.5 megohms, probably caused by dillolved CO_2 from the atmosphere which must have been inadequately sealed off. Pure water will be saturated with CO_2 from the atmosphere in 7-1/2 minutes, falling to an equilibrium resistance of 1 megohm. The electrical resistance of the water was found to be 10 megohms or greater after passing through a deionizer in testing at Marquardt. The deionizer will eliminate CO_2 from the water. A helium system was used to pressurize the plastic bottles, and precautions to eliminate all air from the water system were made during the filling operation.

j. Cleaning

The relationship between electrical resistance of water and the amount of dissolved solids, expressed as parts of $CaCO_3$ per million parts of water, is given in Table 29. The equivalent concentrations of some common metal ions can be obtained by dividing the concentrations of $CaCO_3$ by the conversion factors listed in Table 30.

TABLE 29

ELECTRICAL RESISTANCE OF WATER

Specific Resistance Ohm-cm	Dissolved $CaCO_3$ ppm	Water Quality
26,000,000	0	Theoretical 100% Purity
18,000,000	0.02777	Ultra Pure Water
16,000,000	0.03125	
14,000,000	0.03571	
12,000,000	0.04166	
10,000,000	0.05	
8,000,000	0.0625	
6,000,000	0.08333	
5,000,000	0.1	
4,000,000	0.125	
2,000,000	0.25	
1,000,000	0.5	Good Quality Distilled
500,000	1.	
250,000	2.	
125,000	4.	
100,000	5.	

TABLE 30

CONVERSION FACTOR, PPM $CaCO_3$/PPM METAL ION

Ion	Conversion Factor
Aluminum	5.56
Copper	1.57
Iron (ferrous)	1.8
Iron (ferric)	2.69

All materials in the water system were chosen to minimize contamination by dissolved solids. No comprehensive data could be found on equilibrium ion levels for various metals, although limited information available indicates that the common metal with minimum solubility in water is tin, followed approximately in order by titanium and aluminum. However, the alloying elements of the latter two, particularly aluminum, may be a problem. No data could be located on solubility of stainless steels, although experience with 321 and 316 indicated fairly good resistance to water. Therefore, most of the water system was made of 316 or 321 stainless steel. The only other materials contacting the water en route to the electrolysis unit are teflon, Viton, and possibly the resin beads and saran filter in the deionizar if it is used.

All stainless steel components of the water system were cleaned by the following steps.

(1) Detergent cleaning at 160°F

(2) Passivation in nitric acid bath, one hour at 130°-160°F

(3) Rinse with tap water followed by distilled water

(4) Vapor degrease with hot trichlorethylene

(5) Rinse with distilled water

(6) Ultrasonic cleaning with Bendix detergent and ammonium hydroxide at 140°F for at least three minutes

(7) Rinse with filtered deionized water

(8) Dry and bag.

Teflon and Viton seals were given detergent cleaning and rinsed with deionized water.

2. TEST SYSTEM OPERATION

The ground test system is capable of operating the electrolysis unit automatically by a system of pressure switches which monitor system pressure switches which monitor system pressures and energize various valves and circuit relays as required for any specified mode of water pressurization. The system control logic is shown schematically in Figure 118 and provides the following functions.

a. Maintains water tank pressure between 210 psia and 230 psia by opening or closing the helium solenoid valve (helium repressurized mode only). This function is provided by pressure switch PS-1.

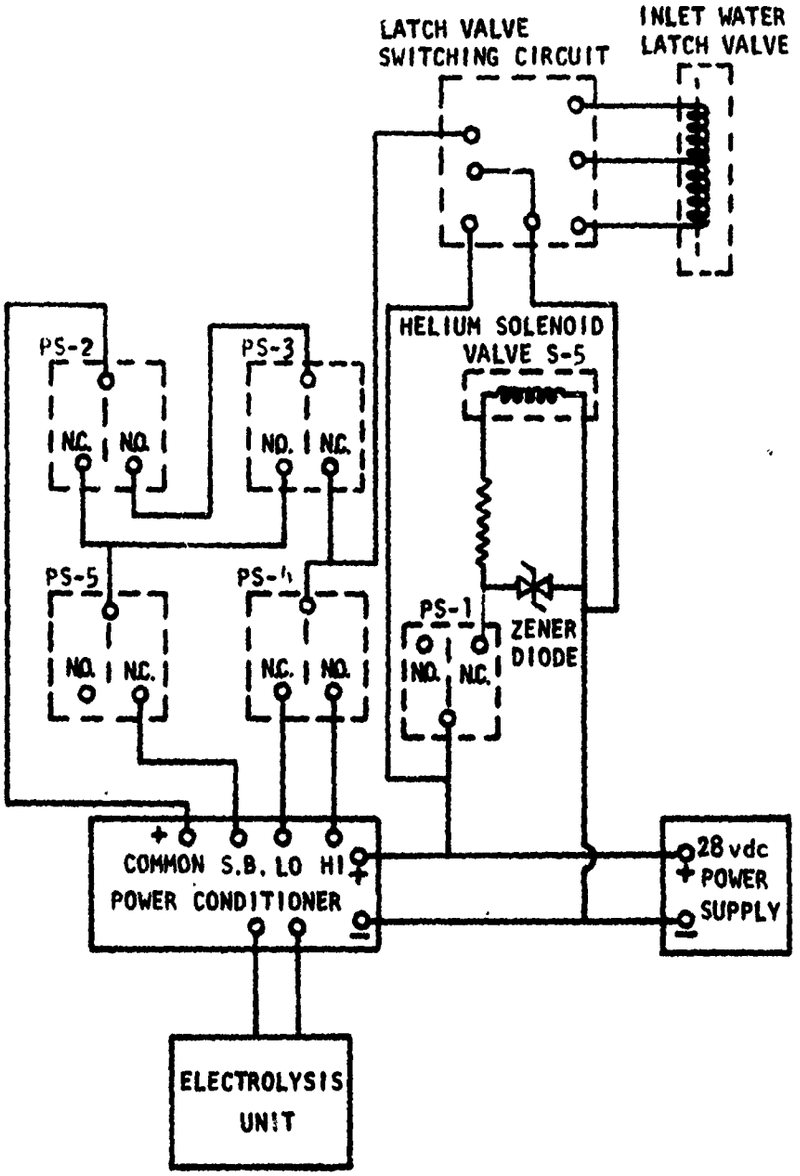

PRESSURE SWITCH	PARAMETER	ELECTRICAL CONTINUITY WHEN	
		N.C.	N.O.
PS-1	H_2O TANK PRESS.	$P_{H_2O} \geq$ 210 PSIA	$P_{H_2O} \geq$ 230 PSIA
PS-2	H_2 TANK PRESS.	$P_{H_2} \leq$ 180 PSIA	$P_{H_2} \geq$ 200 PSIA
PS-3	O_2 TANK PRESS.	$P_{O_2} \leq$ 180 PSIA	$P_{O_2} \geq$ 200 PSIA
PS-4	$P_{H_2O} - P_{H_2}$	$P_{H_2O} - P_{H_2} \leq$ 70 PSIA	$P_{H_2O} - P_{H_2} \geq$ 70 PSIA
PS-5	O_2 CELL PRESS.	$P_{O_2} \leq$ 160 PSIA	$P_{O_2} \geq$ 200 PSIA

FIGURE 118. ELECTROLYSIS SYSTEM CONTROL LOGIC

b. Controls current to the electrolysis unit to any of the following values.

0 amps (off)

1 amp (standby)

6.39 amps (0.6 lb/day water electrolysis)

22 amps (2.3 lb/day water electrolysis)

c. Turns electrolysis unit off when either the hydrogen or oxygen tank pressures reach 200 psia

d. Turns electrolysis unit on when both hydrogen and oxygen tank pressures drop below 180 psia

e. Provides electrolysis unit with 22 amps current whenever P_{H_2O}-P_{H_2} is less than 70 psid. This function is provided by pressure differential switch PS-4. However, no current will be supplied if the tank pressures do not meet the criteria described in c and d above, as measured by pressure switches PS-2 and PS-3. A relay would be placed between pressure switch PS-4 and the power conditioner to allow override selection of the current to high or low power level. This relay is also required during high power operation following blowdown of the gaseous propellants in order to keep the electrolysis unit operating in the high power mode until one of the gas tanks has reached 200 psia.

f. Provides the electrolysis unit with 1-amp standby current whenever the oxygen manifold pressure drops below 160 psia and provides no current for oxygen pressure above 200 psia. This function is provided by pressure switch PS-5. The availability of standby current is required whenever the electrolysis unit would ordinarily be turned off, in order to avoid an initial drop of oxygen cell pressure, followed by eventual diffusion of hydrogen across the SPE to the oxygen manifold during shutdown of the electrolysis unit. This condition of hydrogen take-over is prevented by the trickle current. Therefore, the oxygen manifold pressure slowly oscillates between 160 psia and 200 psia during shutdown. The period of 1-pressure cycle depends on cell temperature but is about four hours.

3. OPERATING PROCEDURES FOR ELECTROLYSIS SYSTEM

The following procedures were established by General Electric for the operation of the electrolysis unit and were used in the testing conducted at Marquardt.

a. Installation

Before installation of the water electrolysis unit into the system, the water inlet port should be inspected while upside down, filled completely with distilled water, if necessary, and recapped. Intimate thermal contact should be provided between the aluminum base plate of the water electrolysis module and a horizontal supporting plate and frame which serve as a heat sink. The water supply line should be completely filled prior to connection to the inlet water fitting of the electrolysis unit to avoid entrapped gas. Pressure in the water compartment of the electrolysis unit should be equalized with the hydrogen and oxygen compartment pressures, except for only short periods when not under load, to avoid flooding the enclosure. Evacuation of the hydrogen and oxygen compartments should not be under the saturation pressure of water vapor (0.96 psia at 100° F) for a period more than five minutes to prevent excessive evaporation of water from the cells and water feed barriers. During this gas side evacuation the water pressure should be maintained approximately at atmospheric pressure to prevent outgassing of dissolved gas in the water compartment. Once primed with water and with helium or nitrogen in the hydrogen and oxygen compartments, the pressures should be equalized if maintained for an extended period (greater than one hour) in this condition. Removal of the inert gas in the hydrogen and oxygen compartment should be accomplished by evacuation and only immediately prior to commencing electrolysis operation. This will minimize inert gases entrained in the generated gases, particularly on the hydrogen side, because of the relatively large volume of the enclosure.

Leakage tests were conducted on the electrolysis module as part of unit acceptance tests. The following conditions, procedures, and limits were established.

b. Cross Membrane Leakage Test, H_2O and $O_2 > H_2$

This test verifies the integrity of both the water feed membranes and cell membranes as well as the gasket seals between the water and the hydrogen and oxygen compartments. Minimum "leakage" is actually the normal permeation rate of gas through the membranes. With the module inverted, the hydrogen outlet port is connected to an inverted water graduate or burette at atmospheric pressure to capture and measure the gas discharge rate. The water inlet and oxygen outlet ports are connected in common and are pressurized with helium to 200 psig. All water in the water compartment must be driven into the enclosure before a reliable and steady gas diffusion rate is measured, usually taking 30 minutes or more. An acceptable diffusion rate at 70° F is 30 scc/min of helium gas. After completion, water should be drained from the enclosure.

c. Cell Cross Membrane Leakage Test, H_2O and $H_2 > O_2$

This test verifies the integrity of the cell membranes and gasket seals between the oxygen and the water and hydrogen compartments. As before, minimum "leakage" is actually the normal diffusion of gas through the cell membranes as distinct from the previous test which included the water feed membranes. With the oxygen outlet connected to a burette, the water and hydrogen compartments are pressurized in common with helium to a pressure of 75 psig. An acceptable diffusion rate at 70° F is 7 scc/min of helium gas.

d. External Leakage Test

This test verifies the integrity of the enclosure and fluid seals at the bolted flange, fluid fittings and electrical connector. The water, hydrogen, and oxygen compartments are connected in common and pressurized to 250 psig with helium or nitrogen with the entire electrolysis unit submerged in water. No external leakage is acceptable as evidenced by any continuous discharge of gas bubbles.

e. Startup From an Inert Discharged Condition

This condition is represented by the electrolysis unit water compartment filled with water and both the hydrogen and oxygen compartments filled with inert gas, all compartments approximately at 1 atmosphere pressure and electrically discharged with essentially no residual voltage on the cells.

After completing electrical connections, and only immediately prior to energization of the power conditioner/water electrolysis module, the water compartment should be pressurized to approximately 25 psig (to establish positive water feed) and the hydrogen and oxygen compartments evacuated in common to water saturation pressure to remove inert gas. With 28 vdc supplied to the power conditioner, power is supplied to the electrolysis unit by energizing the "on" and "reset" buttons of the power conditioner. A low-power mode current will be established by the pressure switches from this start condition. Current can be manually adjusted (range 1 to 25 amp) to a desired setting by the "current adjust" knob on the front panel of the power conditioner.

The volumetric generation rate of hydrogen is twice that of oxygen. However, because of the very small oxygen volume in the cells, the oxygen pressure will rise much more rapidly than hydrogen pressure when isolated from the storage tanks. For this reason it will be necessary to discharge oxygen from the cells to the oxygen storage tank as the electrolysis unit is pumped up to keep oxygen pressure under hydrogen pressure within the unit. Water pressure should be maintained at at pressure greater than internal gas pressures during this period. A pressure differential ($P_{H_2O} - P_{H_2}$) greater than 70 psid will energize the power conditioner to the

to the high power mode of 23 amps. This current will provide the maximum gas generation rate and reduce pump-up time. The high-power mode will also generate the most heat, increase cell operating temperatures, and will tend to increase the amount of condensation on relatively colder hardware surfaces. During electrolysis operation, module pressurization with either hydrogen valve H-8 or oxygen valve H-6 closed should be closely monitored to avoid overpressurization since the electrolysis unit is isolated from the controlling pressure switches PS-2 and PS-3.

f. Low-Power-Mode Operation

The power conditioner and water electrolysis unit are energized in the low power mode in accordance with the control logic indicated by Figure 118. This maintains hydrogen and oxygen tank pressures between 180 and 200 psia and water supply pressure between 210 and 250 psia. Electrolysis current in this mode can be manually adjusted between 1 - 25 amps by the "current adjust" knob on the front of the power conditioner. For electrolysis module operation at an ambient temperature of 70-80° F and maximum ($P_{H_2O} - P_{H_2}$) pressure differential of 70 psid, a current setting of 6.5 amperes is required to obtain a water electrolysis rate of 0.6 lb H_2O/day sufficient to exceed the water feed barrier hydraulic permeability rate according to Figure 15. At a cell operating temperature of 100° F the current must be increased to approximately 8.5 amperes to avoid water carry-over to the hydrogen side.

g. High-Power-Mode Operation

High-power-mode operation results when the water to hydrogen (P_{H_2O}-P_{H_2}) differential pressure exceeds 70 psid. The power conditioner has an internal potentiometer setting for a regulated current output of approximately 23 amperes. It is possible to manually adjust this potentiometer with a small screw driver inserted through the capped hole designated "Hi" on the right front of the power conditioner. This high current condition would occur during blowdown of the hydrogen tank or excessive pressurization of the water supply. Maximum cell voltage and maximum cell heat generation occur during this high-current operating mode. The anode (oxygen side) of the cells runs drier than the low power mode, thereby increasing cell voltage. More heat is generated which elevates the cell operating temperature which improves water transport capability. At a given current an equilibrium operating temperature is established after a warm-up period depending on the thermal capacity of the electrolysis module and heat sink. A stable cell operating voltage may not be obtained in this high power mode of 23 amperes at cell operating temperatures under 80-85° F. The operating current should be reduced if cell voltage continues increasing with time and exceeds 1.9 vdc.

h. Standby-Mode Operation

Standby occurs when the hydrogen and/or oxygen tanks are topped off at 200 psia and no net gas generation is required by the electrolysis unit. When input power to the electrolysis module is removed, the diffusion of gas across the cell membranes results in a gradual pressure decay in the hydrogen and oxygen compartments as these gases are consumed by recombination at the catalyst to form water. There is no gas-phase mixing during this period since hydrogen molecules are immediately combined with adsorbed oxygen on the anode catalyst. Oxygen molecules diffusing across the cell membrane are similarly combined with adsorbed hydrogen on the cathode. Since the oxygen compartment volume is much smaller than the hydrogen enclosure, the oxygen pressure will fall more rapidly than hydrogen pressure. Check valves in the gas outlet lines from the electrolysis unit allow this pressure decay as oxygen tank pressure is retained. When oxygen compartment pressure falls to approximately 160 psia, power is reapplied to the electrolysis module at a regulated current of approximately one ampere, thereby repressurizing the oxygen compartment. This current level is slightly greater than the parasitic current (about 0.7 ampere, depending upon cell pressures and temperature) where electrolysis rate equals gas diffusion rate. Power will again be removed when oxygen compartment pressure reaches approximately 200 psia. The values of minimum oxygen pressure and current were selected to provide feasible operation with a minimum number of cycles during the standby period.

If power is removed from an activated electrolysis module over a period of several hours, oxygen pressure will continue reducing until all oxygen has been consumed in the oxygen compartment leaving only water vapor at saturation conditions. Because of the larger hydrogen volume, hydrogen will continue diffusing to the oxygen compartment until a complete "hydrogen takeover" occurs with equal hydrogen pressures in both the hydrogen and oxygen compartments. Cell voltages will also decay to essentially zero as this process occurs. Reapplication of power to the electrolysis module will first pump essentially all hydrogen from the oxygen compartment to the hydrogen compartment, pulling the oxygen compartment pressure down to water vapor pressure consistent with cell temperature. Since there may be lower temperatures in external lines of the oxygen compartment (where water vapor pressure is lower) a small amount of hydrogen may remain. The rate of hydrogen pumping is proportional to current, and this process occurs at a cell voltage less than 0.1 vdc. Continued application of current will result in a sharp rise in cell voltage and commence electrolysis at 1.46 vdc with oxygen being generated in the oxygen compartment. A hydrogen takeover does not cause any harm to the electrolysis unit except for possible excessive cell pressure differentials. It is to be avoided to prevent potential residual hydrogen in the oxygen lines which may be eventually discharged to the oxygen tank. For this reason, the standby mode of operation is utilized. If a standby condition cannot be maintained on the electrolysis unit, the unit should be deactivated according to procedures for extended shutdown.

Regulated current for standby operation can be manually adjusted with a small screw driver inserted through the capped hole designaged "Lo" on the top of the power conditioner. Since the parasitic current is proportional to gas pressure, this adjustment should not be changed during electrolysis operation at low pressures.

i. Shutdown of Electrolysis Module

For short intervals of less than one hour, power can be removed from the power conditioner/electrolysis unit provided oxygen pressure is closely monitored to avoid excessive depressurization of the oxygen compartment. The effect of this condition is more fully discussed under Standby-Mode operation. If unattended for short or long periods, it is more desirable to maintain the unit in the standby mode if power is available to the power conditioner.

For a shutdown period exceeding an hour where a standby mode cannot be maintained, it is necessary to depressurize and deactivate the electrolysis module to prevent a hydrogen takeover. The hydrogen, oxygen, and water compartments of the electrolysis module should be gradually depressurized to approximately one atmosphere pressure. It is desirable, if possible, to maintain low power mode operation during depressurization with ($P_{H_2O} - P_{H_2}$) less than 70 psid. With power removed, the hydrogen enclosure should be purged with inert gas as prepared for storage conditions. With the hydrogen and oxygen compartments vented to atmosphere and valves H-8, H-6 closed, and with the water compartment pressure also at one atmosphere and at essentially zero water head, the unit should be allowed to electrically discharge itself to under 1.0 vdc stack voltage, or for several hours, before recapping the hydrogen and oxygen ports. A startup procedure from a storage condition should be followed for reactivation of the electrolysis unit.

j. Storage Conditions

Preparation for storage following electrolysis operation includes, for safety, the replacement of residual hydrogen in the enclosure with helium or nitrogen gas. The water compartment (approximately 60 cc capacity to inlet "H_2O" fitting) should remain filled or be filled with distilled water having a specific resistance of 1.5 megohm-cm or greater. Purging of the enclosure can be accomplished by utilizing the hydrogen outlet and case drain fittings with a through-put of 1 standard cubic foot of inert gas at approximately atmospheric pressure. Following this purge, the unit should be allowed to discharge itself electrically with hydrogen, oxygen and water (filled) ports vented to atmosphere. The unit is considered in an electrical discharged condition when stack terminal voltage is under 2 vdc and maximum individual cell voltage is 0.5 vdc. A cell voltage greater than 0.1 volt indicates the presence of hydorgen and oxygen absorbed on the catalyst and exposure to air will consume residual hydrogen, thereby reducing the voltage and deactivating the unit. All ports must be securely capped thereafter to maintain a 100 percent relative humidity condition within the enclosure and cells. The enclosure may be drained of excess water by venting both hydrogen and drain ports to atmosphere.

Ambient pressure is not important during storage provided all four fittings are securely capped. However, ambient and internal temperatures must be maintained above 32° F and under 160° F to prevent deleterious conditions on the cells. Because both the electrolysis unit and power conditioner are breadboard designs, shock and vibration conditions during handling and transport of these units should be minimized.

k. Potential Failure Modes and Troubleshooting

It is extremely important that the water content of the cell and water feed SPE membranes be maintained at all times. Therefore, the electrolysis unit is stored with the water compartment filled and with all fluid ports capped to eliminate moisture loss. Providing a sufficient supply of water to all cells during electrolysis operation is even more critical because of continuous water dissociation to gas. If a cell is deprived of a water supply to sustain its normal water content during electrolysis, its electrical resistance will increase, thereby affecting performance. So-called "water starvation" of a cell during electrolysis operation is detected by a sharp increase in cell voltage to 2.0 vdc or more. This condition could be caused by any of several failure modes which interfere with the water supply to a cell such as (1) loss of water tank pressure; (2) gas blocking of the water compartment by $P_{H_2} > P_{H_2O}$; (3) plugging of a water feedline or of the internal water manifold or feed ports to one or more cells, which might be caused by corrosive deposits or biological growth during long-term operation. The power conditioner is equipped with an output overvoltage cut out to prevent damage to the electrolysis unit in the event of water starvation. This is set at 15 vdc output. Normal electrolysis operation is under 11.5 vdc. Power supplied to the electrolysis unit is automatically cut off by the power conditioner when stack terminal voltage reaches 15.0 vdc. Contribution to the excessive voltage may be by one or more cells. Overvoltage caused by an insufficient water supply is, of course, aggravated by a high electrolysis current. Internal plugging of one or more water feed ports would be evidenced by cell performance (cell voltage) being sensitive to water pressure or ($P_{H_2O} - P_{H_2}$) differential, particularly at the high-power mode.

Internal water leakage caused by loss of a water gasket seal or by perforation of a water feed membrane would be evidenced by excessive water discharged with generated hydrogen or oxygen (oxygen manifold seal). Some water may be discharged due to condensation primarily occurring at high cell operating temperature. Leakage would be suspected if water accumulation or discharge would increase at high ($P_{H_2O} - P_{H_2}$) or ($P_{H_2O} - P_{O_2}$) differentials and occur even at low operating current and temperature. This failure could be further verified by performance of cross-membrane leakage tests conducted with helium as previously discussed.

Internal gas leakage caused by loss of a gasket seal or by perforation of a cell membrane may demonstrate the following phenomena. Cell performance may actually improve (i.e., lower cell voltage) owing to the local release of heat by combination of H_2 and O_2 gases which elevates cell temperature. During standby operation at 1 amp current, voltage of the failed cell may fall significantly below (0.1 volt or

more) the others. Similarly, at open circuit the voltage of this cell would decay much more rapidly than the others. These effects would be aggravated by increased pressure differential across the hydrogen and oxygen compartments of the cells. If a cell failure is suspected, this pressure differential should be minimized as discussed previously and P_{H_2} P_{O_2} pressure differential is preferred. At low P_{H_2}/P_{O_2} operating differentials, the discharge of mixed gases by a failed cell may not be detectable because the cell electrodes contain efficient catalyst for hydrogen and oxygen combination.

If a cell fails due to suspected cross-membrane leakage, the electrolysis unit should be slowly depressurized to atmospheric pressure maintaining hydrogen pressure only slightly greater than oxygen pressure. The hydrogen enclosure should be immediately purged with inert gas and with all cells allowed to be electrically discharged by consuming adsorbed hydrogen on the catalyst with air through the uncapped ports as with normal deactivation for storage. A cell cross-membrane leakage test H_2O and H_2 O_2 can be performed as previously described on the unit to verify cause of cell failure.

Cell failure by gradual contamination with metal ions will cause a gradual increase in cell resistance and loss of performance; i.e., increase in voltage. Because the water feed membrane is an ion exchange material, it will sacrificially protect the SPE cells from contaminated feed water. Its loss in ion exchange capacity would result in reduced water transport properties. This mode of failure would be a gradual cell water starvation with gradual loss in performance (increased cell voltage).